Quantitative and qualitative description of iodine and selenium cycles in forest ecosystems : the influence of tree species, climate and physicochemical conditions of the soils.

Paulina Pisarek

THÈSE

UNIVERSITE DE PAU ET DES PAYS DE L'ADOUR

École doctorale des sciences exactes et de leurs applications

Présentée et soutenue le 9 juillet 2021

par **Paulina Pisarek**

pour obtenir le grade de docteur
de l'Université de Pau et des Pays de l'Adour
Spécialité : Chimie Analytique et Environnement

QUANTITATIVE AND QUALITATIVE DESCRIPTION OF IODINE AND SELENIUM CYCLES IN FOREST ECOSYSTEMS: THE INFLUENCE OF TREE SPECIES, CLIMATE AND PHYSICOCHEMICAL CONDITIONS OF THE SOILS

MEMBRES DU JURY

CO-DIRECTEURS
- Hervé GALLARD — Professeur / Université de Poitiers
- Isabelle LE HECHO — Maîtres de conférence / Université de Pau et des Pays de l'Adour

CO-ENCADRANTE
- Maïté BUENO — Maîtres de conférence / Université de Pau et des Pays de l'Adour

RAPPORTEURS
- Anne PROBST — Directrice de recherche/ CNRS, EcoLab
- Pascal REILLER — Directeur de recherche / CEA

EXAMINATEURS
- Brice BOUYSSIERE — Professeur / Université de Pau et des Pays de l'Adour
- Arnaud LEGOUT — Chercheur / INRAE
- Yves THIRY — Chercheur / Andra

Acknowledgment

This dissertation is the culmination of a work financed by French National Agency of Radioactive wastes management (Andra) and performed at The Institute of Analytical Sciences and Physico-Chemistry for Environment and Materials (IPREM). I would like to thank all those who made the realization of this thesis possible.

I would like to thank the rapporteurs for this thesis, Anne Probst and Pascal Reiller, for their keen interest in my work and the time devoted to evaluating it. I associate with these thanks Brice Bouyssiere, Arnaud Legout and Yves Thiry for having accepted to be the part of the jury.

I am grateful to my supervisors, Isabelle LeHecho and Hervé Gallard for all the advice that allowed me to overcome the obstacles and the motivation that you installed in me during the thesis. I would like to express my gratitude to Maite Bueno for the availability, the time dedicated to improving my work and guiding me through these four years. To Yves Thiry, whose perspective on the subject have helped me to see things clearly and allowed me to go further. I also acknowledge Laurent Grasset, who introduced me to organic chemistry and Arnaud Legout and Manuel Nicolas for providing the samples, data collection and accurate comments.

Many thanks my colleagues from IPREM: Javier, Kasia B., Andrea, Maroussia, Stephane, Fran, Nagore, Iza, Simon, Lucile, Madga, Sebastiano, Ahmed, Youn, with whom I shared good times in the laboratory and outside. My sincere gratitude to Joanna Szpunar, who believed in my potential and gave me the opportunity to grown on professional and personal fields.

All my sympathy to Ghaya, Kasia K. and Alexandre for their unwavering support that brought me to the end. Finally, to my parents, who gave me the courage and the desire to continue my growth.

Abstract

The long-lived radioisotopes of selenium (^{79}Se, $t_{1/2}$ = 3.3× 10^5 years) and iodine (^{129}I, $t_{1/2}$ =1.6 × 10^7 years) were identified as high priority in the safety assessment of the biosphere towards potential contaminations from nuclear power plants activity, waste repositories and nuclear weapon tests. Selenium and iodine are essential micronutrients indispensable for proper functioning of mammalian life. Once ^{79}Se and ^{129}I enter into the ecosystem, they may be easily incorporated into stable Se and I cycles. The understanding of their biogeochemical cycling is thus necessary to properly evaluate the harmful consequences after anthropogenic radiocontamination events. In this study, the forest ecosystem attracted attention as a place of enlarged interception surface formed by tree canopy.

Climate, environmental and geochemical conditions were examined in order to discriminate important factors regarding the distribution and accumulation of Se in French forests. Selenium concentrations in litterfall were strongly and positively correlated with those in precipitations and, were significantly higher under oceanic compared to transition and mountain climates. Selenium stocks in humus decreased in the order: mor > moder > mull. The highest Se concentrations in soil were determined in mountain climate in Douglas and beech forests, where soils were acidic and rich in organic matter and Fe/Al oxides.

The monitoring of monospecific stands (Douglas, spruce, pine, beech, oak) with identical geogenic material and climate allowed specifying the impact of tree species on inventories and fluxes of selenium and iodine. Tree canopies interacted with atmospheric inputs leading to element enrichment in throughfall, especially for conifers. Tree species showed divergent Se and I requirement, uptake and return fluxes in the forest soils. For both elements, the amount of elements stored in aboveground tree parts were marginal compared to soil stocks. Humus showed positive Se and I accumulation rates and continuous enrichment from fresh to humified organic material. The water-soluble fraction of the elements represented only ~1.1% of their total content in soil, while the largest proportion was soluble in NaOH (51-72% of Se and 84-100% of I content). Only inorganic species (SeO_4^{2-} or SeO_3^{2-}, I^- and IO_3^-) were detected in water and NaOH extracts, accounting for ~1-52% of total element contents in extracts. A significant proportion of Se and I remained unidentified and was supposed to be in dissolved and/or colloidal organic forms. Selenium content in soil was controlled by its strong affinity with organic matter and Fe minerals, while specific I “enrichment-depletion profile” in soil column might be due to iodination of organic matter and association of this iodinated organic matter with Al minerals.

Keywords: selenium, iodine, forest, tree species, humus, speciation

Résumé

Les radio-isotopes à vie longue du sélénium (^{79}Se, $t_{1/2} = 3,3 \times 10^5$ ans) et de l'iode (^{129}I, $t_{1/2} = 1,6 \times 10^7$ ans) sont reconnus comme hautement prioritaires dans l'évaluation de la sécurité de la biosphère face aux contaminations potentielles issues de l'activité des centrales nucléaires, l'enfouissement de déchets et les essais d'armes nucléaires. Dans les écosystèmes, ces radio-isotopes se comportent comme leurs isotopes stables. La compréhension de leur cycle et de leur bioaccumulation est donc cruciale afin d'évaluer les conséquences d'une radiocontamination. Dans cette étude, l'écosystème forestier a été plus particulièrement étudié car la canopée constitue une surface d'interception importante des dépôts atmosphériques.

Dans une première partie, les échantillons de litières, humus et sols issus de 51 sites forestiers ont été analysés afin d'évaluer l'importance du climat, des conditions environnementales et géochimiques dans la distribution et l'accumulation du sélénium dans les forêts françaises. Les concentrations de Se dans les litières sont positivement corrélées avec celles dans les pluies et sont supérieures en climat océanique par rapport aux climats montagnard et de transition. Les stocks de sélénium dans l'humus diminuent dans l'ordre: mor > moder > mull. Les concentrations les plus élevées de Se dans le sol sont observées pour des sols acides, riches en matière organique et en oxydes de Fe/Al sous Douglas et hêtre en climat de montagne.

Dans une seconde partie, le suivi de peuplements monospécifiques (Douglas, épicéa, pin, hêtre, chêne) pour un même climat et des conditions édaphiques identiques a permis de préciser l'impact des espèces d'arbre sur les inventaires et les flux de sélénium et d'iode. Un enrichissement des pluviolessivats plus important a été observé pour les conifères. Des flux différents de Se et I entre biomasse aérienne, humus et sols ont été déterminés en fonction des espèces d'arbres. Pour les deux éléments, la quantité d'éléments stockés dans les parties aériennes des arbres apparait marginale par rapport aux stocks du sol. Un enrichissement continu en élément de la litière fraîche aux couches les plus profondes de l'humus a été observé. En complément des mesures totales, la spéciation de Se et I dans les fractions aqueuses et NaOH d'humus et de sol a été réalisée. Les fractions hydrosolubles ne représentent que ~1,1 % des teneurs totales en Se et I dans le sol tandis que de plus grandes proportions (51 à 72 % de Se et 84 à 100 % de I) sont extraites à l'aide de NaOH. Seules les espèces inorganiques (SeO_4^{2-} ou SeO_3^{2-}, I^- et IO_3^-), représentant ~1 à 52% des teneurs totales dans les extraits, ont été détectées. Une large proportion reste donc non identifiée, vraisemblablement sous des formes organiques dissoutes ou colloidales. La teneur en sélénium dans le sol apparait principalement contrôlée par sa forte affinité avec la matière organique et les oxydes de Fe, tandis que le profil particulier de l'iode dans la colonne de sol, de type "enrichissement-depletion", semble lié à des réactions entre l'iode et les matières organiques dissoutes puis une adsorption de cette matière organique sur les oxydes de Al.

Mots-clés : sélénium, iode, forêt, arbre, humus, spéciation

Table of content

List of figures

Chapter 1

Chapter 2

Chapter 3

List of tables

Chapter 1

Chapter 2

Chapter 3

Abbreviations

-A-

Andra – French National Agency of Radioactive wastes management (fr. *L'Agence nationale pour la gestion des déchets radioactifs*)

-C-

CRMs – Certified Reference Materials

-D-

Da – Dalton (unified atomic mass unit)
DMSe – dimethyl selenide
DMDSe – dimethyl diselenide
DW – dry weight

-F-

FA – fulvic acid

-H-

HA – humic acid
HAc – acetic acid
HLW – High-level waste
HMW – high molecular weight

-I-

ICP – MS – inductively coupled plasma mass spectrometry
IDD – Iodine Deficiency Disorders
INRAE – National Institute of Agricultural Research (fr. *Institut National de la Recherche en Agriculture, Alimentation et Environnement*)
INAA- Instrumental Neutron Activation Analysis
IPREM – The Institute of Analytical Sciences and Physico-Chemistry for Environment and Materials (fr. *L'Institut des sciences analytiques et de physico-chimie pour l'environnement et les matériaux*)

-K-

Kd – distribution coefficient

-L-

LC – liquid chromatography
LMW – low molecular weight
LOD – limit of detection

-M-

MIC – microwave-induced combustion
MQ – Milli-Q water

-N-

Nd – not detailed
NMR – nuclear magnetic resonance

-O-

OA – organic acid
OAs – organic acids
OM – organic matter
ONF – French National Forestry Office (fr. *L'Office national des forêts*)
Oln – organic horizon code: organic, litter, new
Olv – organic horizon code: organic, litter, old
Of – organic horizon code: organic, fragmented
Oh – organic horizon code: organic, humified

-R-

RENECOFOR – French National Network for Long-term FOrest ECOsystem Monitoring (fr. *Réseau National de suivi à long terme des ECOsystèmes FORestiers*)
RF – rainfall flux
RPC – reversed-phase chromatography

-S-

SEC – size exclusion chromatography
SF – stemflow flux
SOM – soil organic matter
SSA – specific surface area
SRHA – Suwannee River humic acid

-T-

TF – throughfall
TMAH – Tetra methyl ammonium hydroxide

-U-

UP – University of Poitiers (fr. *Université de Poitiers*)
UPPA – University of Pau and the Adour Region (fr. *L'université de Pau et des pays de l'Adour*)

-W-

WHO – World Health Organization

-X-

XANES – X-ray absorption near-edge structure

General introduction

Selenium and iodine are crucial elements in mammalian body, with Se being incorporated in seleno proteins and I controlling production of thyroid hormones. Although they occur naturally in trace levels, they are ubiquitous in all compartments of the ecosystem. In the environment they exist in different oxidation states (selenium: −II, −I, 0, IV, VI; iodine: −I, 0, I, III, V, VII) as inorganic and organic compounds, in gaseous, solid or in dissolved forms. The behavior of these elements is complex and depends on their physical and chemical properties, on natural conditions and human activities.

The long-living radioisotopes, ^{79}Se and ^{129}I, both of anthropogenic origin, are present in High-level wastes (HLW) from nuclear power plants. The main issue concerning ^{79}Se and ^{129}I is their long half-lives (^{79}Se, $t_{1/2}$ = 3.3 × 10^5 years, ^{129}I, $t_{1/2}$ =1.6 × 10^7 years), during which they can integrate natural biogeochemical cycles of selenium and iodine. Thus, it is essential to understand their circulation in the atmosphere, hydrosphere, biosphere and lithosphere to predict their fate.

Modelling of elements in forests is challenging due to the spatially heterogeneous nature of the biota and a high biodiversity, from tree species to microorganisms. Forest ecosystems are known to be efficient receptors of atmospheric contaminants due to enlarged surface area of tree canopies. Moreover, forest soils have a layered structure with a gradient of degraded plant material in humus, a topsoil rich in organic matter and a mineral subsoil. Organic matter and Fe/Al oxides are well known to absorb Se and I. In this context, soil can accumulate ^{79}Se and ^{129}I in case of potential contamination of the ecosystem. The aim of this work is to improve the quantitative and qualitative description of Se and I cycles in forest ecosystems, in order to refine radio-ecotoxicological prediction models.

Chapter 1 contains a literature review of the biogeochemical cycles of stable selenium and iodine and their radioisotopes including their sources and distribution in water, atmosphere, soil and plants. Particular attention is given to the fate of elements in soil, detailing their organic and inorganic forms, their interactions with soil mineral phases and Soil Organic Matter (SOM) mediated by biotic and abiotic mechanisms. Specific knowledge on the fate of elements in forest and model allowing a description of their cycle are presented. Analytical techniques including sample preparation, determination of total element content and speciation methods used to

study the mobility and persistence of the elements in the environment have been reviewed. The scientific problematic and objectives of the thesis are discussed at the end of the chapter.

Chapter 2 is a comprehensive study on the influence of environmental and edaphic conditions on Se distribution in French forest ecosystems. Selenium concentrations were determined in litterfall, humus and soils from 51 sites of the RENECOFOR network handled by ONF (French National Forest Office). Sample collection represents a wide variety in types of trees, soils and climates. Fluxes and stocks of Se in forest compartments were estimated as well as time-scale involved in Se retention in humus and soil.

Chapter 3 presents the study of Se and I distribution and cycle in five monospecific forest plantations located under identical climatic and edaphic conditions in the forest of Breuil-Chenue (Nièvre, France). In the first part, the concentrations of Se and I were quantified in the aboveground tree compartments, litterfall, humus and soil horizons for the five tree species in order to identify the differences between tree species in terms of element fluxes and distribution in soil profile. In the second part, focused on two of the tree species, a monthly monitoring was conducted in rainfall, throughfall, stemflow and soil solutions over one year to quantify element inputs by atmospheric deposition, outputs from the canopies and by drainage. The fractionation and speciation of selenium and iodine and their relation with soil organic matter constituents was thoroughly examined in the forest soil profile.

Chapter 4 presents the conclusions and perspectives of the research work.

This work was scientifically supported and financed by French National Agency of Radioactive wastes management (ANDRA). The research was carried out in two laboratories: The Institute of Analytical Sciences and Physico-Chemistry for the Environment and Materials (IPREM) and The Institute of Chemistry of Materials and Media of Poitiers (IC2MP), which are joint interdisciplinary research units of CNRS and University of Pau and the Adour Region (UPPA) and CNRS and University of Poitiers (UP), respectively. The samples and the data collection were provided by the French National Forestry Office (ONF) and the National Institute of Agricultural Research and Environment (INRAE).

Chapter 1. Bibliographic synthesis and objectives of the thesis

Part A. The biogeochemical cycles of selenium and iodine

1. Selenium and iodine in human health

The major role of Se in physiology is associated with its presence in amino acids as selenocysteine (SeCys) and selenomethionine (SeMet), which are part of important proteins (Rayman, 2000). Examples of known selenoproteins are glutathione peroxidases and thioredoxin reductases, which are involved in protection against oxidative damages, regulation of thyroid hormone and intracellular redox state. The range of appropriate Se intake level for human is narrow: dose < 30 μg day^{-1} is insufficient for humans, whereas intake > 900 μg day^{-1} may be toxic (Fairweather-Tait et al., 2011). The deficiency of Se in human diet is more widespread over the world than its excess and, generally linked to its low content in soil (Winkel et al., 2015). Insufficient Se intake was reported to lead to Keshan and Kashin-Beck diseases. Moreover, Se supplementation would reduce the progression of HIV and mortality due to AIDS (Brigelius-Flohé, 2018; Stone et al., 2010).

Iodine is necessary for the production of thyroid hormones that control important physiological processes in the body. All symptoms caused by iodine deficiency are called Iodine Deficiency Disorders (IDD). Around 35% of world's population was affected by IDD in 1996, making it a worldwide health problem (Nutrition Unit, 1996). IDD symptoms have not only clinical, but also social and intellectual consequences. Insufficient amount of iodine, especially in critical periods of human growth may cause goiter, hypothyroidism, cretinism, retarded physical and mental developments (Saikat et al., 2004). Iodine fortification in the diet is one of the strategies to combat IDD (for example food products like milk, bread, water and salt). The most common over the past century was salt (Universal Salt Iodization (USI) program adopted by the World Health Assembly in 1990). Another strategy for IDD suppression is plant fertilization, which requires a thorough understanding of I biogeochemistry including its interactions with different soil components and its bioavailability for plant uptake (Dai et al., 2004).

Selenium and iodine are essential elements for the healthy growth and functioning of human and animal organisms. In this context, absorption of their radioisotopes by inhalation from the atmosphere or indirectly through the food chain can result in serious consequences.

2. The importance of the radionuclides ^{79}Se and ^{129}I

Selenium and iodine have numerous stable[1] and radioactive isotopes (**Table chap.1 – 1**). The most abundant selenium isotopes are ^{74}Se, ^{76}Se, ^{77}Se, ^{78}Se, ^{80}Se, ^{82}Se .^{79}Se and ^{82}Se are not stable isotopes with half-lives of 3.27×10^{5} and 1.08×10^{20} years, respectively. Natural isotopic composition of iodine consists of one stable isotope ^{127}I, but there are 37 known radioisotopes (Wu et al., 2018). Some of them such as ^{123}I, ^{124}I, ^{125}I, ^{131}I, ^{135}I, have half-lives ranging from hours to a few dozen days. The radioisotope ^{129}I, with a half-life of 1.57×10^{7} years, is the longest-lived isotope (**Table chap.1 – 1**; Lin and Chao, 2009).

Table chap.1 – 1 Main isotopes of selenium and iodine

Isotope	**Abundance**	**Half-life**	Ref.
		Selenium	
^{74}Se	0.86%	Stable	
^{76}Se	9.22%	Stable	
^{77}Se	7.6%	Stable	
^{78}Se	23.7%	Stable	Meija et al., 2016
^{79}Se	trace amount	3.27×10^{5} y	
^{80}Se	49.8%	Stable	
^{82}Se	8.82%	1.08×10^{20} y	
		Iodine	
^{123}I	Synthetic	13 h	
^{124}I	Synthetic	4.18 d	
^{125}I	Synthetic	60.1 d	
^{127}I	100%	Stable	Lin and Chao, 2009
^{129}I	trace amount	1.57×10^{7} y	
^{131}I	synthetic	8.02 d	
^{135}I	synthetic	6.61 h	

The two long-lived radionuclides ^{79}Se and ^{129}I originate mainly from nuclear accidents, nuclear waste leakages at disposal sites, mining industry and nuclear weapons (**Table chap.1 – 2**; Bienvenu et al., 2007; Hansen et al., 2011). Beside anthropogenic origin, ^{129}I also has natural sources. Its contribution to the hydrosphere and lithosphere was estimated at 250 kg in steady state inventory (Hou et al., 2009). Approximately 5645 kg of ^{129}I were released by the reprocessing plants at La Hague (France) and Sellafield (UK) until 2007, 1.3 – 6 kg during the Chernobyl accident, 0.8 – 1.4 kg during the Fukushima accident and 50 – 150 kg during nuclear weapon tests (Aldahan et al., 2007; Hou et al., 2009; Kaplan et al., 2014; Raisbeck and Yiou,

[1] "Stable isotopes are non-radioactive forms of atoms."(IAEA, 2016)

1999; Yeager et al., 2017). To our knowledge there is no similar estimation for ^{79}Se in the literature.

Table chap.1 – 2 Natural and anthropogenic sources of the radionuclides ^{79}Se and ^{129}I (Bienvenu et al., 2007; Hansen et al., 2011).

Natural source	Anthropogenic
^{79}Se	
–	♦ in nuclear reactors as product of spontaneous fission of ^{235}U
^{129}I	
♦ cosmic-ray radiation spallation of Xe in the upper atmosphere ♦ spontaneous fission of ^{238}U ♦ neutron bombardment of Te in the geosphere ♦ thermal neutron induced fission of ^{235}U in the lithosphere	♦ fission product of uranium and plutonium ♦ fallouts from reactor accidents or nuclear explosions ♦ nuclear weapons testing and accidents associated with nuclear power plants.

Selenium and iodine radioisotopes were emitted into the environment during the deadliest nuclear reactor explosion in Chernobyl, Ukrainian Soviet Socialist Republic, in 1986. The numerous damages caused to human health (i.e. increased morbidity associated with thyroid cancer among the children, Kazakov et al., 1992), pollution of the surrounding terrains and the danger of radioactive clouds have led to a re-assessment of the safety of nuclear power plants around the world. Both isotopes were classified into the Top (^{129}I) and High (^{79}Se) priority radioisotopes, which needed to be surveyed in the biosphere surrounding the waste repositories and nuclear power plant in Olkiluoto, Finland (**Table chap.1 – 3**; Hjerpe and Broed 2010).

Table chap.1 – 3 Classification of key radionuclides in biosphere assessment (Hjerpe and Broed, 2010).

Key set of radionuclides	
Top priority	^{14}C, ^{36}Cl, **^{129}I**
High priority (I)	^{93}Mo, ^{94}Nb, ^{135}Cs
High priority (II)	^{59}Ni, **^{79}Se**, ^{90}Sr
High priority (III)	^{107}Pd, ^{126}Sn

Although the levels of radioisotope ^{131}I were much higher than ^{129}I after nuclear plant accidents, as observed after Fukushima Daiichi nuclear catastrophe in 2011, its fate in the environment can be monitored during only few weeks after the accident because of its short half-life of 8 days (**Table chap.1 – 1**). For this reason, ^{129}I has been used to reconstruct the content and fate

of iodine radioisotopes in soils, plants and atmosphere after nuclear accidents, but also to monitor diffuse contaminations in the surrounding environment of nuclear power plants (Michel et al., 2005; Miyake et al., 2012; Ohno et al., 2013).

3. The environmental risk of radioactive contamination in forest ecosystem

The long-lived radioisotopes (half-lives > 10 years) have great predisposition to integrate ecosystems via the cycle of the corresponding stable isotope. Forests cover around 33% of land in Europe and this value is continuously increasing (Alberdi et al., 2015). Forests play an important role in macro and micro climates and in the balance of water and element cycling. Exposition to increased radiological levels in forests can occur directly during work and recreational activities (foresters, hunters, lumberjack, berry and mushroom pickers) and also via products originating from forest (use of wood, consumption of mushrooms, berries, wild animal meat and use of fur) (Calmon et al., 2009; Gwynn et al., 2013). Secondary contamination can occur as a result of unexpected natural events such as forest fire, when radiocontaminants are mobilized through ashes and fumes, but also during floods, when radionuclides are transported from deep layers of soil to the surface (Monte et al., 2006; Zhou et al., 2016). Furthermore, wood from radiocontaminated forests used for industrial and/or domestic purposes, such as paper production, building construction, heat generation in power plant and fireplace, is an additional source of radiation by external exposure and inhalation (Charro et al., 2013).

Contamination of forest ecosystems by radionuclides occurs mainly through wet or dry deposition (**Figure chap.1 – 1**). Forests, compared to other ecosystems such as grasslands and arable lands, has a large interception surface made by the canopy. The interception of dry and wet deposits depends on the species and the population density of trees, season of the year and meteorological conditions. Interactions with the canopy can alter the speciation and the fate of the elements due to direct foliar absorption, flushing from the leaf surface (i.e. throughfall) or retention and subsequent wash-off of dry deposits (Lovett and Lindberg, 1984).

The cycle of the elements is strongly linked to climatological seasons, rainfall and also natural organic matter cycle including periodical growth, decline and decomposition of living organisms. Bergman (1994) specified three periods within cycle: “the early phase”, “the medium phase” and “the long term phase”, which, according to Shaw (2007), correspond to the Shcheglow’s periods:

1. fast weathering from the canopy to the soil (e.g. by runoff) (~1-3 months),
2. biological decontamination of the canopy (e.g. by leaves fall, growth dilution) and the rise of substantial root uptake of radionuclides (~2-3 years),
3. root uptake and equilibrium maintenance (~3-10 years).

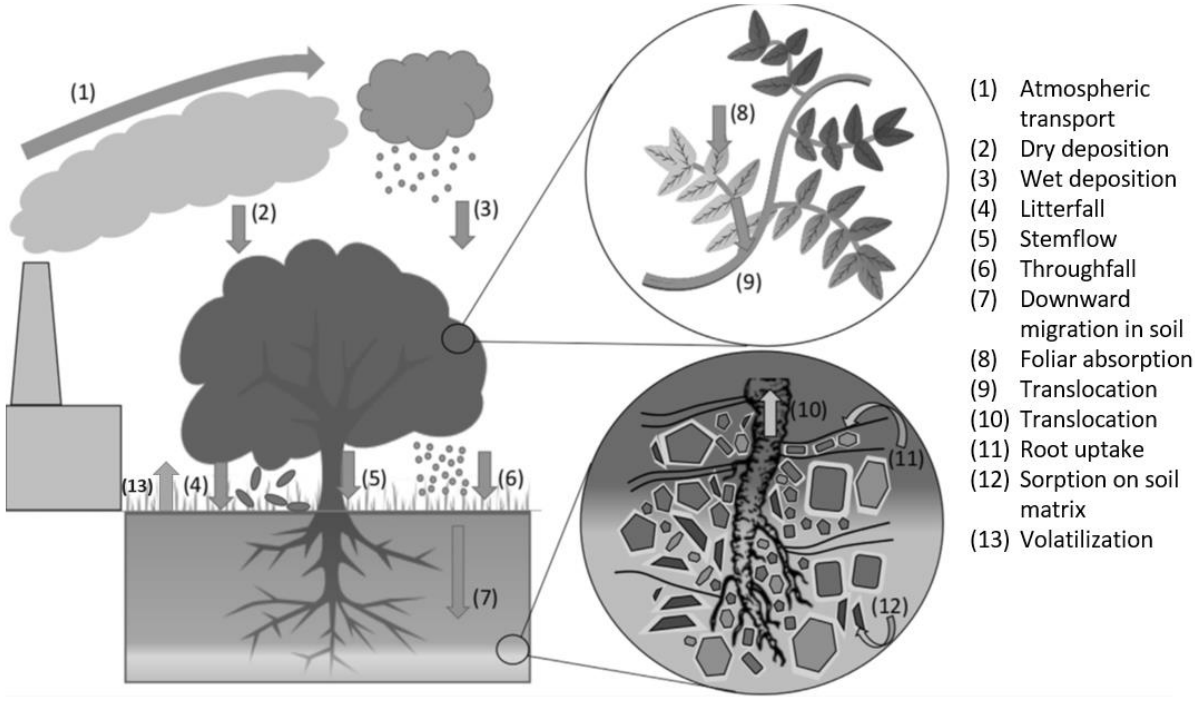

Figure chap.1 – 1 Main processes of radionuclides cycle in forests (modified from Diener et al., 2017).

In the early phase of deposition, exposure to pollutants is very high. Radiocontaminants can be absorbed directly by leaves or needles and translocated into branches and stem, or they are loosen from the surface of the canopy by wind or rainfall and penetrate the soil surface (**Figure chap.1 – 1**).

In the medium phase, radionuclides are weathered from the canopy as a result of litterfall, throughfall and stemflow. Due to the decomposition of organic matter, radionuclides can be released into the soil, where they can be adsorbed by the mineral phase, bound to OM, leached into the deeper layer of lithosphere or reintegrated to the cycle by the plant roots.

The “long term phase” concerns long-lived radionuclides. The time required to reach equilibrium depends on organic matter decomposition time (e.g. humus residence time) when contaminants are released into the soil solution and are being associated with soil constituents, leached to groundwater, volatilized or taken up by living organisms.

3.1 Soil and humus characteristics

Soil is defined as a porous media generated at the earth surface by the weathering processes induced by hydrological, biological and geological phenomena. Soil can be considered as a complex, open biogeochemical system composed of gas, solid and liquid phases (Sposito, 2008). The pores of the soil are filled with the same gas composition as the atmosphere: N_2, O_2, Ar, CO_2. In addition to the gases naturally present in the atmosphere, the soil gas phase also contains: H_2, NH_3, NO, N_2O, H_2S whose productions are mediated by microbial activity under low oxygen content (Sposito, 2008). The CO_2 content has a great impact on soil acidity. In deeper layers and under special conditions, the gas phase composition may differ. The content of CO_2 increases after rain, while O_2 content can achieve lower values after rainfall or irrigation and near plant roots. Water reaches the soil through precipitation and irrigation, and is eliminated by evaporation and drainage. Since water in soil acts as reservoir for dissolved gases and solids, it is considered as a 'soil solution'. The major elements present as soluble forms in soil solution are: C (HCO_3^-), N (NO_3^-), Na (Na^+), Mg (Mg^{2+}), Si ($[Si(OH)_4]$), S (SO_4^{2-}), Cl (Cl^-), K (K^+), Ca (Ca^{2+}) (Sposito, 2008). Half to two thirds of the soil consists of solids containing variable proportions of organic matter. Primary minerals are those arisen directly from parent material (e.g. quartz, mica) while secondary minerals result from the weathering of primary minerals (e.g. gypsum, calcite). Mineral particles are classified by their size: stone and gravel (>2 mm), sands (2mm - 50µm), silts (50 µm – 2 µm) and fine fraction (< 2 µm) (Duchaufour, 1998). The main mineral oxides of Si, Fe, Al, Mn and Ti are present in soil in more or less hydrated forms, hydroxides and oxyhydroxides (Hillel, 2005).

Soil organic matter (SOM) includes all decomposing plant and animal matters transformed by two processes: humification and mineralization. Mineralization is a conversion of organic matter into inorganic constituents mostly by microbial activity. Humification is a process of degradation of organic residues and their conversion into humic substances (Guggenberger, 2005). 'Humus' is a broad conceptual term, as it is associated with the mineral phase of soil and with the undecomposed organic material, which is difficult to separate physically (Shcheglov and Tsvetnova, 2001). Litter deposition is the main input of fresh organic material to soil. Their decomposition can be used to classify humus horizons (**Table chap.1 – 4**, modified from Andreetta et al., 2011).

Table chap.1 – 4 Humus organic horizons (adapted from Andreetta et al., 2011).

Code	Explication	Definition
oln	Organic, litter, new	Fresh or hardly fragmented plant remains
olv	Organic, litter, old	Fragmented, discolored, compressed plant remains
of	Organic, fragmented	Fragmented, but still recognizable plant remains
oh	Organic, humified	Strongly fragmented plant remains

The factors limiting biological (e.g. earthworm, fungi and microbes) decomposition are mainly climate and stability of the soil parent material. Faunal activities have then been used as criteria to classify humus types (**Figure chap.1 – 2**) in terrestrial environment (Zanella et al., 2018):

- Mor – biological activity is not notable, it is limited by atmospheric (cold) or soil (acidity) conditions (Humimor, hemimor, Eumor)
- Moder – faunal activity is fairly limited by soil acidity or low temperatures (Hemimoder, Dysmoder, Eumoder)
- Mull – faunal activity is poorly limited by environmental conditions
- Amphi – because of seasonal climate alteration showing the features of Mull; and Moder – phases of low and high biological activities (Eumacroamphi, Pachyamphi, Eumesoamphi, Leptoamphi)
- Tangel – biological activity strongly restricted by mountain climate and hard calcareous rock surface (Eutangel, Leptotangel, Pachytangel)

Figure chap.1 – 2 The main terrestrial humus types in temperate ecosystems (Ponge et al., 2010).

The origin of organic acids (OAs) is mainly related to organic matter decomposition and to plant and microbial activities. Plants, bacteria and fungi excrete OAs as stress-induced reaction, to maintain internal equilibrium and to facilitate the bioavailability of poorly soluble nutrients.

Soil OAs are able to dissolve insoluble minerals by three principal mechanisms: chelation, acidification, exchange reactions (Adeleke et al., 2017). OAs are classified as low molecular weight organic acids (LMWOAs), with mass range from 46 Da to a few 100 Da and, high molecular weight organic acids (HMWOAs), from a few hundreds to a million Da (Adeleke et al., 2017). Fulvic (FA) and humic acids (HA), belonging to HMWOAs, form the colloidal organic fraction in humus. Depending on the degree of humification and the origin of organic matter, they contain both aliphatic chains and aromatic ring functional groups in variable proportions (Bowley et al., 2016). Humic substances constitute up to 70-80% of the SOM. Citric, maleic, malonic, malic, succinic, and oxalic acids are included into the LMWOAs groups. Generally, LMWOAs have from one to three carboxylic groups and are more soluble in water than HMWOAs.

3.2 Modelling of radioactive contamination in forest ecosystem

Because forest ecosystems are complex and highly diverse, modelling of element cycling and prediction of the mobilization and immobilization of radioisotopes are challenging (Shaw, 2007). There are two main strategies to describe the element cycles: empirical approach and the process-based modelling approach (Diener et al., 2017). Process-based modelling approach is based on a well-detailed representation of key processes characterized by mathematical equations. With an appropriate number of parameters, it has a high predictive potential when applied to different ecosystems. Vives i Batlle et al. (2014) published the process-based model of ^{36}Cl built on an array of physical properties (e.g. stand density, characteristics of the vegetation, hydraulic properties of the soil) represented by 66 parameters. The empirical approach is based on data measured in laboratory or on experiments conducted with real ecosystems. The empirically obtained parameters characterize well the corresponding sites, but they should be applied with great caution to the description of other sites. Two parameters are usually used in empirical approach i) aggregated transfer factors (Tag) (Howard et al., 1995), which describe radionuclides transfer from soil to plant, and ii) the solid-liquid partition coefficient Kd (Whicker et al., 2007).

3.3 Distribution coefficient – Kd

The distribution coefficient, Kd is defined as the ratio between the residual concentration of the contaminant in solid phase to the equilibrium concentration of soluble contaminant (Eq. 1).

$$K_d = \frac{[X]_{\text{soil residual}}}{[X]_{\text{soluble}}} \qquad (1)$$

$[X]_{\text{soil residual}}$ - total residual concentration of element X in the solid phase (μg kg^{-1})

$[X]_{soluble}$ - total soluble concentration of element X in solution (μg L^{-1})

Conventional methods for Kd determination are batch, column and lysimeter tests (Pathak et al., 2014). Kd value can be determined either in sorption experiments when mixing different concentrations of element species with the soil, or in desorption experiments, when extraction is carried out with unspiked soil. Kd is not a feature of a contaminant, its value depends on numerous factors such as temperature, pH of water solution, liquid phase to solid phase ratio, ionic strength, micro-biological activity, size of geomaterial particles, OM content, redox conditions, incubation time. It is thus difficult to extrapolate the results from one soil system to another. These variations are caused by specific soil characteristics, but also a lack of unified methodology for Kd values determination. Values of Kd coefficients reported for iodine and selenium are presented in **Table chap.1 – 5**.

Table chap.1 – 5 Kd coefficient values in soils for selenium and iodine.

Soil		Experimental procedure	Kd value	Reference
Selenium				
Different types		Sorption experiment	4-2130	IAEA, 2010
Different types		Desorption experiment	10-140	Sheppard et al., 2009
Forest soils			512-1198	Tolu et al., 2014
	Topsoil		90-789	Almahayni et al., 2017
	Subsoil		4-161	Almahayni et al., 2017
Agricultural			332-868	Tolu et al., 2014
	topsoil		103-252	Almahayni et al., 2017
	subsoil		59-169	Almahayni et al., 2017
Grassland			335-1156	Tolu et al., 2014
Iodine				
Different types		Sorption experiment	0.01-580	IAEA, 2010
Different types		Desorption experiment	60-1600	Sheppard et al., 2009
Forest soils				
	humus		106	Roulier et al., 2018
	topsoil		329	Roulier et al., 2018
			4-281	Almahayni et al., 2017
	subsoil		1031	Roulier et al., 2018
			1-318	Almahayni et al., 2017
Agricultural	topsoil		5-176	Almahayni et al., 2017
	subsoil		9-32	Almahayni et al., 2017

The compilation of reported Kd values were higher for Se than those for I (IAEA, 2010). When Kd values were determined both in sorption and desorption experiments, the latter resulted in

higher values (Sheppard et al., 2009). Kd values assessed for forest and agricultural soils decreased with incubation time and a 4-week period was sufficient to reach a plateau for Se and I (Almahayni et al., 2017). Almahayni et al. (2017) observed that Kd values tended to be higher in topsoils than in subsoils for both elements, while Roulier et al. (2018) reported the opposite for iodine. The coefficients Kd obtained in sorption experiments describe the ability of the soil to sorb a specific form of the element. Since the concentrations of added form are higher than in the natural soil solution, this method is preferably chosen to observe the impact of different conditions (effect of soil pH, mineralogy, microbial activity, temperature) on its immobilization on soil (Söderlund et al., 2017, 2016).

Importance and fate of selenium and iodine elements - summary

- Selenium and iodine are necessary elements for the body
- Deficiency and excess of Se cause damages for human health, while I deficiency is fatal and demands fortification
- Long-living radionuclides ^{79}Se and ^{129}I are of major health and ecological concern due to their biophilic properties
- Forests are able to absorb radiocontaminants by tree canopies, recycle them from the soil and accumulate them in their biomass
- Humus and soil are complex earth surface compartments consisting of biota, organic matter and mineral phase
- The distribution coefficient Kd is an empirical parameter describing mobility of contaminants in soil, however there is no unified methodology for its determination

4. Selenium

4.1 Chemistry of selenium

Selenium with the atomic mass 78.971 exists in the environment on the following oxidation states: −II (Se^{2-} - selenide), −I (Se_2^{2-} - diselenide), 0 (Se^0 - elemental selenium), IV (SeO_3^{2-} - selenite), VI (SeO_4^{2-} - selenate). The speciation of inorganic selenium in soils is highly influenced by redox potential and pH (**Figure chap.1 – 3**). The main Se species under strong oxidizing conditions in natural water is SeO_4^{2-}, while $HSeO_3^-$ and SeO_3^{2-} are more prevalent in mild oxidizing conditions. Elemental Se and volatile H_2Se occur under strong reducing conditions, while HSe^- exists at pH > 4 (Sharma et al., 2015).

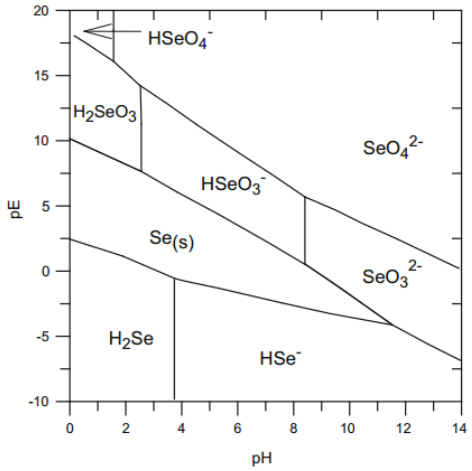

Figure chap.1 – 3 Selenium pE-pH diagram at 25°C, 1 bar pressure, and zero ionic strength for Se activity of 10^{-10} mol L^{-1} (Sharma et al., 2015).

4.2 Selenium in the environment

Environmental selenium contents are in the range of 0.06–10 ng m^{-3} in the atmosphere, 0.018–2.5 µg L^{-1} in hydrosphere, 0.05 mg kg^{-1} in rocks and 0.01–2 mg kg^{-1} in soil (**Table chap.1 – 6**).

Table chap.1 – 6 Selenium concentrations in the environment.

Environmental compartment	[Se] range	Reference
Hydrosphere		
rainwater	0.018-0.22 µg L^{-1}	Conde and Sanz Alaejos, 1997
fresh water	0.02-0.4 µg L^{-1}	Fernández-Martínez and Charlet, 2009
sea water	0.2-2.5 µg L^{-1}	Conde and Sanz Alaejos, 1997
Atmosphere	0.06-10 ng m^{-3}	El-Ramady et al., 2015
Earth crust	0.05 mg kg^{-1}	Shahid et al., 2018
Soils	0.01-2 mg kg^{-1}	Fernández-Martínez and Charlet, 2009
Igneous rocks	0.35 mg kg^{-1}	Fernández-Martínez and Charlet, 2009
granite	0.025 mg kg^{-1}	Shahid et al., 2018
Sedimentary rocks		
limestone	0.03–0.08 mg kg^{-1}	Fernández-Martínez and Charlet, 2009
sandstone	0.05 mg kg^{-1}	Shahid et al., 2018
clay	0.17 mg kg^{-1}	Shahid et al., 2018
coal	300 mg kg^{-1}	Shahid et al., 2018
shales	≥0.6 mg kg^{-1}	Shahid et al., 2018
phosphatic rocks	≥300 mg kg^{-1}	Sharma et al., 2015
Volcanic rocks	0.35 mg kg^{-1}	Fernández-Martínez and Charlet, 2009

Sources of selenium can be classified according to two criteria: the distribution scale (local or regional) and their origin (anthropogenic or natural). Natural sources include forest fires, volcanic eruptions, soil erosion, plant growth, oxidation processes in oceans and soils. Anthropogenic sources contribute almost 35-65% of total Se emission (**Figure chap.1 – 4**; Feinberg et al., 2020; Shahid et al., 2018). Significant anthropogenic Se contaminations come from dust released during coal or petroleum combustion and agricultural activities (Shahid et al., 2018).

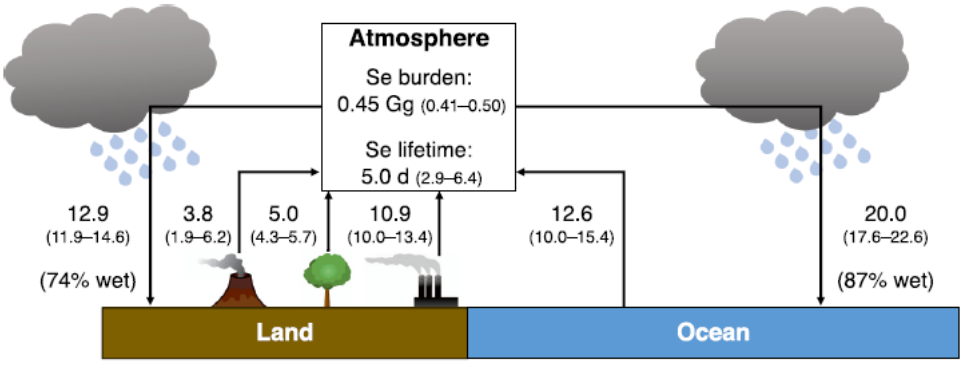

Figure chap.1 – 4 Global modelling of atmospheric Se fluxes (Gg Se yr^{-1}) for the period 2000−2015 (Feinberg et al., 2020).

Most data about atmospheric Se deposition are from local collection of precipitation and aerosol samples (Winkel et al., 2015). Roulier et al. (2021a) assessed Se atmospheric inputs into French forests to be in the range of 0.25-2.01 g Se ha^{-1} yr^{-1}. In the region between 30°N to 90°N, Ross (1985) estimated wet and dry deposition as 3.6–10 and 0.55–2.6 Gg Se yr^{-1}, respectively. Feinberg et al. (2020) highlighted the crucial role of atmospheric transport in Se budget with annual flux of 29−36 Gg Se yr^{-1}. Ocean appears both as a dominant source of naturally emitted atmospheric Se (32−50% of total production) and a net sink for atmospheric Se (Feinberg et al., 2020). Increasing Se content in seawater over last decades may come from anthropogenic activities (Mason et al., 2018). The dominant forms in the ocean are inorganic Se (IV) (predominantly as $HSeO_3^-$) and Se (VI) (as SeO_4^{2-}) (Sherrard et al., 2004). Microorganisms absorb dissolved Se and transform it into gaseous forms (Amouroux et al., 2001). The main volatile organo-Se compounds are CH_3SeCH_3 (dimethyl selenide, DMSe), CH_3SeSCH_3 (dimethyl selenenyl sulfide, DMSeS), $CH_3SeSeCH_3$ (dimethyl diselenide, DMDSe). The inorganic volatile compounds are H_2Se and SeO_2. They are released to the atmosphere as products of biomethylation by microorganisms and organic matter decomposition in soils and oceans (Paikaray, 2016) (**Figure chap.1 – 5**). The flux of Se emission to the atmosphere from

global wetland area was estimated as 0.19–0.37 Gg Se yr^{-1} (Vriens et al., 2014). In the atmosphere, ozone, nitrate and hydroxyl radicals, produced by UV exposure leads to degradation of DMSe and DMDSe to inorganic SeO_2 and SeO_3 (**Figure chap.1 – 5**) (Wen and Carignan, 2007).

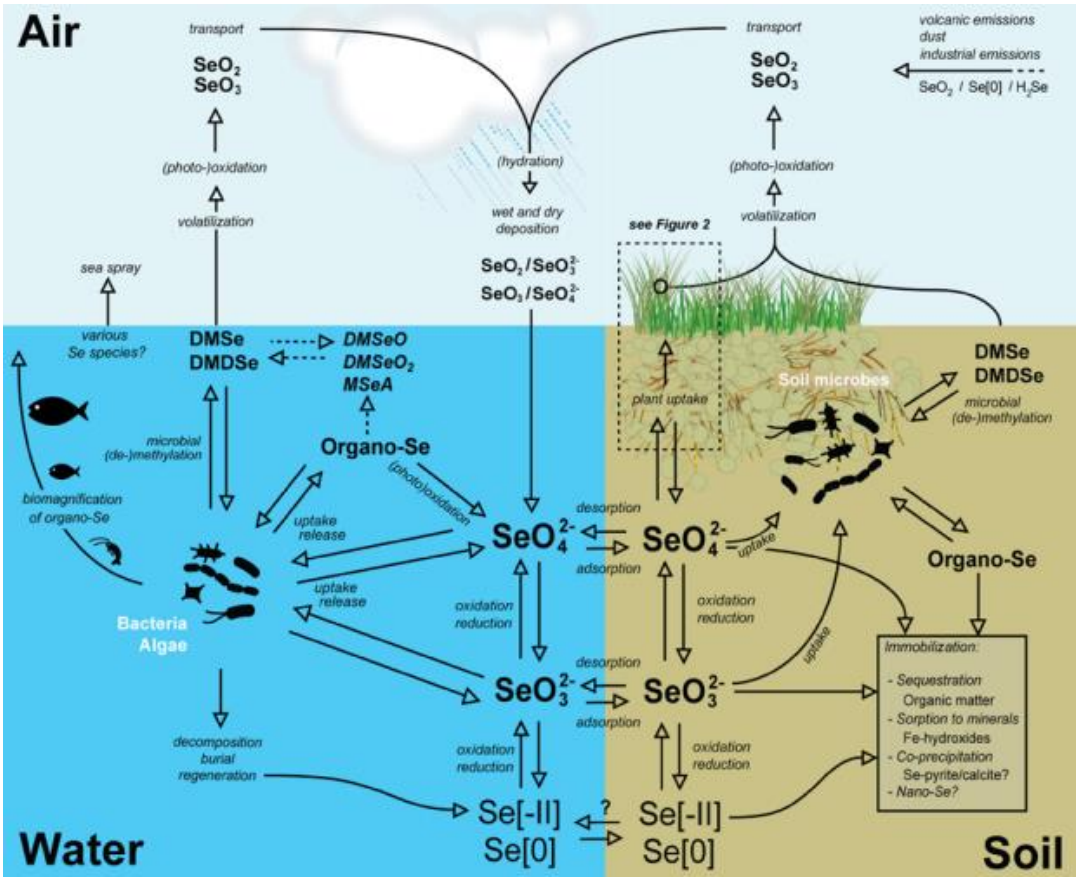

Figure chap.1 – 5 Se cycle in the environment (Winkel et al., 2015).

Selenium is not homogenously spread all over the earth crust. Igneous rocks (0.35 mg Se kg^{-1}) are generally viewed as poorer in Se than sedimentary rocks. Sedimentary rocks are however characterized by wide variety of Se levels: 0.03–0.08 mg kg^{-1} in limestone, 0.17 mg kg^{-1} in clay, ≥ 600 mg kg^{-1} in black shales, 300 mg kg^{-1} in coal (**Table chap.1 – 6**). Rock weathering was thought to be the main local natural source of Se in soil, but this factor alone cannot account for the large-scale distribution of Se (Blazina et al., 2014; Sun et al., 2019). High concentration of Se was observed in areas where black shales with high carbon and metal content are prevalent: Ireland (up to 1250 mg kg^{-1}), Yutangba, China (8590 mg kg^{-1}), the Colorado River Basin, USA: (3.3 g kg^{-1}) (Tuttle et al., 2014; Winkel et al., 2015). The world mean Se concentration in soil is 0.4 mg kg^{-1} (Shahid et al., 2018). In areas where bedrocks are poor in selenium, Se concentrations in soils appear to be influenced by atmospheric deposition (Blazina

et al., 2014). Wet and dry depositions (40–160 μg m^{-2} yr^{-1}) and volatilisation (100–200 μg m^{-2} yr^{-1}, mostly driven by soil microorganisms) were two key factors regulating Se partitioning in Chinese terrestrial environment (Sun et al., 2019). Increased deposition with proximity to the sea resulted in higher Se content in coastal area (Låg and Steinnes, 1978).

Selenium in the environment – summary

- Ocean is a dominant natural source of atmospheric Se and a net sink for atmospheric Se due to its large surface
- Anthropogenic activities result in emission of considerable pool of Se into the atmosphere
- UV exposure in the atmosphere results in degradation of volatile organic compounds into inorganic species
- Wet and dry depositions are an important source of selenium for the soil
- Main volatile organic compounds are organic: DMSe, DMSeS, DMDSe and inorganic: H_2Se and SeO_2
- Higher Se content was observed in the nearest ocean soils
- Biomethylation is driven by microorganisms and OM decomposition in oceans and soils
- Igneous rocks are generally poorer in Se than sedimentary rocks.

4.3 Selenium in soil

Selenium occurs in soil in soluble forms, adsorbed on mineral phases, complexed with OM or as organo-mineral colloids (Winkel et al., 2015) (**Figure chap.1 – 5**). Under common environmental conditions, selenium oxyanions are present in deprotonatedforms as selenite Se(IV): SeO_3^{2-} and $HSeO_3^-$ (selenous acid: H_2SeO_3, pK_{a1} = 2.62, pK_{a2} = 8.3) and selenate Se(VI): SeO_4^{2-} (selenic acid: H_2SeO_4, pK_{a1} = - 2.01, pK_{a2} = 1.91) (Adriano, 2001; Séby et al., 2001). Se (-II) exists as metallic selenide (e.g., FeSe, iron selenide), organic selenide (R-Se-R') and volatile compounds (H_2Se, DMSe) (Winkel et al., 2015). Elemental selenium (also as (nano)-sized Se(0) form) may be a product of bacterial and fungal reduction of selenate and selenite (Eszenyi et al., 2011; Ponce de León et al., 2003). Metallic selenides and elemental Se are water insoluble and cannot be assimilated by plants even in colloidal form (White, 2016), although selenite and selenate are frequently used in agricultural biofortification in areas with low soil Se content. Selenium (IV) and Se (VI) are water soluble, but Se (VI) shows lower

retention on soil consituents and therefore higher availability for plants in soil solution (Sharma et al., 2015).

4.3.1 Selenium and organic matter

OM-bound Se fraction includes organic Se compounds and inorganic Se compounds adsorbed on soil organic matter (Li et al., 2017). Its proportion can vary according to the soils in the range of 14-91% (**Table chap.1 – 7**).

Table chap.1 – 7 Proportion of organic Se fraction (org-Se) in soils.

org-Se %	Soil type	Soil site	Reference
82-90 68-91 82	sand clay peat	Netherlands	Supriatin et al., 2015
32-51	-	China	Qin et al., 2012
19-58	-	Soil CRMs	Tolu et al., 2011
14-35	sandy loam	Shaanxi Province, China	Wang et al., 2012

Tolu et al. (2011) found out that around 80% of OM-bound Se extracted from Rothamsted soil was in inorganic Se(IV) form. This proportion varied from 20 to 100 % in 26 soils including forest, arable land and grassland (Tolu et al., 2014). Specific organic compounds MetSeOOH and SeMet were detected only in 3 of the grassland soil water extracts (Tolu et al., 2014). It can be attributed to limitation of the analytical instruments and low content of detected species for which a standard solution is commercially available (SeMet, MetSeOOH, $SeCys_2$, $TMSe^+$) and emphasized the need of sample preparation and detection method improvements. The lack of commercially available standards is also a limiting factor (Tolu et al., 2011). Another explanation of the lack or low abundance of organo-Se species may be their fast mineralization in soil. SeMet and SeCys were shown to rapidly disappear in soil after few days by decomposition or volatilization (Martens and Suarez, 1997). Organo-Se species (selenomethionine Se oxide and unidentified species) were formed in soil extracts after hydrogen peroxide addition (Stroud et al., 2012).

Undoubtedly, soil organic matter influences Se retention in soil, but mechanisms are still unclear. The type and strength of binding determines whether Se is mobilized (e.g., through release from complexes by change of pH) or immobilized (e.g. through covalent binding to the OM). As summed up by Winkel et al. (2015), three hypotheses of Se immobilization by OM are discussed in the literature: (I) OM increases soil sorption surface, which favors direct Se complexation, (II) possibility of indirect Se binding by OM-metal complexes, (III) biotic (microbial and fungal) reduction and incorporation into organic compounds: proteins, amino

acids and natural organic matter. Li et al. (2017) added a fourth mechanism: facilitation of Se reduction and immobilization by OM in anoxic zones (**Figure chap.1 – 6**). Moreover, they concluded that biotic mechanism of OM-Se interaction has been extensively studied and is better understood than the abiotic one. Abiotic mechanism is hidden by the strong influence of biotic mechanism, making it difficult to study.

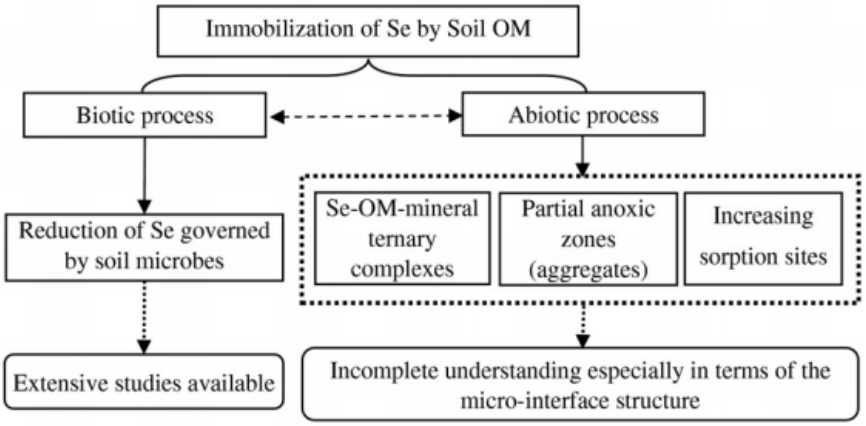

Figure chap.1 – 6 Mechanisms of Se immobilization by soil OM (Li et al., 2017).

Selenium in forest soil was shown to be preferentially incorporated into low-molecular-weight humic substances (Gustafsson and Johnsson, 1994) with formation of organic selenium compounds or adsorption into OM. Literature pointed out two hypotheses to explain Se-OAs complexation: 1) direct complexation, 2) presence of ternary complexes.

According to direct complexation mechanism, FA and HA are able to form direct chemical bond with Se(IV) oxyanions. The interaction could be possible only in presence of positively charged groups in HMW organic acids (Maes and Bruggeman, 2010). A possible functional group with positive charge is amine moiety from amino acid chain or products of peptide degradation (Dinh et al., 2017). In the concept of ternary complexes (**Figure chap.1 – 7)**, metallic cation plays the role of bridge between negatively charged Se anion and negatively charged FA and HA functional groups (e.g. CO_2H, OH, NH_2 (Chen et al., 2002)). Ternary complexes of Se(IV) have been identified for Fe(III) and Cr(III)-loaded humic acids from the Suwannee River by showing coelution of Se, Fe or Cr and HA using chromatographic monitoring and ICP-MS and UV detections (Martin et al., 2017). Se(VI), unlike Se(IV), did not show a tendency to form ternary complexes in presence of metallic cations and HMW organic acids nor a direct complex with dissolved humic substances fraction (Bruggeman et al., 2007; Martin et al., 2017). However, in real soil extracts, coeluting Fe and Se signals were very low.

This was interpreted as unstable interaction and prevailing presence of Se(VI) which does not form such complexes (Peel et al., 2017).

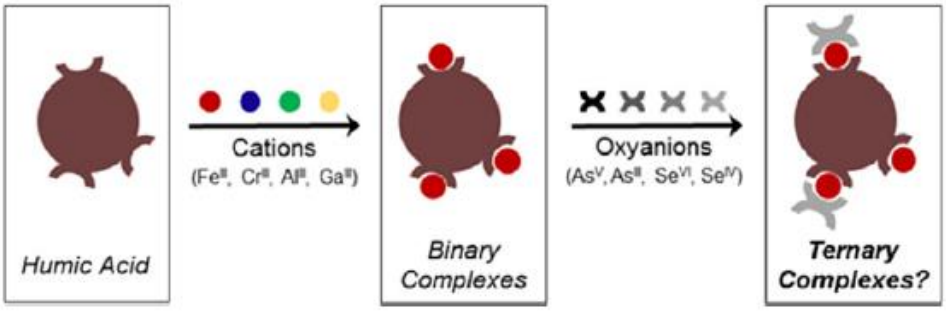

Figure chap.1 – 7 Scheme of ternary complexes formation mechanism between HA, metallic cations and oxyanions (edited from Martin et al., 2017).

4.3.2 The microbial influence

Selenate and selenite can be used by bacteria as the terminal electron acceptors in some metabolic pathways (dissimilatory reduction) or be reduced and incorporated in organic compounds (assimilatory reduction) (Wessjohann et al., 2007). Some microorganisms use reducible Se(VI) (terminal electron acceptor) and organic acids (electron donors) to support their growth in anoxic and anaerobic conditions according to the following reactions (Nancharaiah and Lens, 2015):

$$CH_3COO^- + 4{SeO_4}^{2-} + H^+_{aq} \rightarrow 2CO_2 + 4{SeO_3}^{2-} + 2H_2O$$

$$C_2H_4OHCOO^- + 2{SeO_4}^{2-} \rightarrow CH_3COO^- + 2{SeO_3}^{2-} + {HCO_3}^- + H^+_{aq}$$

$$C_2H_4OHCOO^- + {SeO_3}^{2-} + H^+_{aq} \rightarrow CH_3COO^- + Se^0 + {HCO_3}^- + H_2O$$

Further, Se(0) can be biotically reduced to Se(-II) :

$$C_2H_4OHCOO^- + 2Se^0 + 2H_2O \rightarrow CH_3COO^- + 2HSe^- + {HCO_3}^- + 3H^+_{aq}$$

The resulting inorganic forms of oxyanions reduction are elemental selenium (including nanoscale elemental selenium) or metallic selenide (Li et al., 2017). The oxidation of Se(0) yields both SeO_4^{2-} and SeO_3^{2-} as terminal products with low rates (3-4 times lower than those in the reductive part of Se transformation cycle) (Dowdle and Oremland, 1998; Nancharaiah and Lens, 2015).

The gaseous products of microbial activity are H_2Se, which is a result of selenoaminoacids metabolism, and DMSe and DMDSe, formed in the biomethylation process. Due to their volatile properties, they can be released to the atmosphere, or be microbiologically oxidized to elemental selenium (Wessjohann et al., 2007).

4.3.3 Selenium and soil mineral phase

The redox potential and pH of soil solution influence the sorption behavior of selenium on Fe, Mn and Al oxyhydroxides (Sharma et al., 2015; Torres et al., 2010). Selenite and selenate adsorption was investigated on kaolinite, goethite, sodium bentonite and calcareous soil in the pH range of 2-9 (Goldberg and Glaubig, 2002). Maximum adsorption of selenite occurred in the range of pH 3-4, decreasing with increasing pH with a minimal value for pH > 8. Adsorption of selenate was not influenced by pH changes in the range of 2-9 on calcareous and montmorillonite containing soils (Goldberg and Glaubig, 2002). Some sorption on goethite was noticed for a very high initial concentration of selenate (> 30 mg L^{-1}) (Balistrieri and Chao, 1987).

Selenite and selenate are immobilized by outer-sphere complexation (an ion exchange mechanism; **Figure chap.1 – 8**), while selenite is also able to form inner-sphere monodentate, bidentate mononuclear or binuclear surface complexes with Fe and Al atoms in hydrous aluminum oxide, hematite, goethite and magnetite (Kwon et al., 2015; Martínez et al., 2006; Söderlund et al., 2016). Moreover, the presence of Fe(II) in biotite ($K(Fe(II),Mg)_3(Si_3Al)$ increased sorption of selenite by reduction to elemental selenium or by the formation of FeSe (Charlet et al., 2007; Scheinost et al., 2008; Söderlund et al., 2016).

Limited leaching potential of selenite from minerals makes this form unavailable for plants at the pH of the soils (pH ≈ 5 to 9), while selenate weakly sorbed to soil minerals by electrostatic attraction is more bioavailable (Sharma et al., 2015).

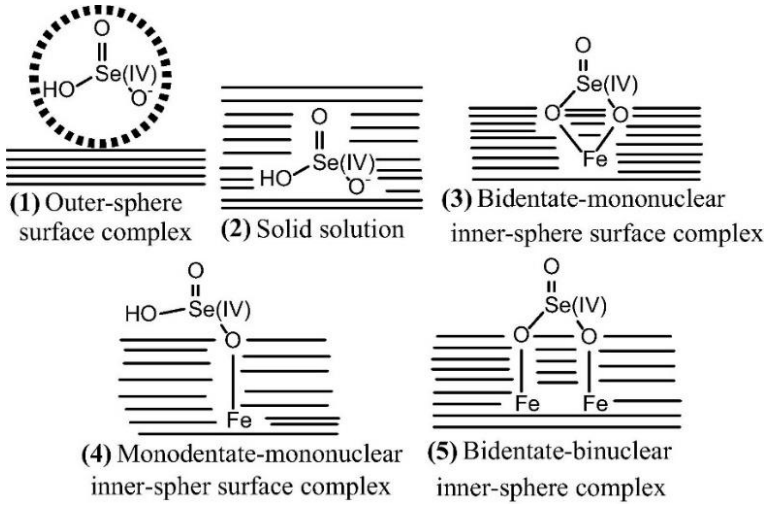

Figure chap.1 – 8 Complexes of Se(IV) adsorbed onto magnetite surface in soil solution: (1) an outer-sphere complex (dotted area - first hydration sphere), (2) a solid solution of Se(IV) in the oxide phase, and (3–5) inner-sphere complexes (adapted from Kwon et al., 2015).

Selenium in soil - summary

- Se concentrations in different soil types are in the range of 0.01 - 2 mg kg^{-1}
- 14-82% of Se are associated with organic fraction in soil
- Organo-Se species in soil are still little known and need more investigation
- Biotic and abiotic mechanisms of selenium-OM associations are still unclear
- Few abiotic mechanisms of Se bonding with OM have been proposed: Se-OM-mineral ternary complexation, sorption, aggregation
- The ternary complex between oxyanion Se(VI), cations (Fe(III)) and HMW OAs has been observed in a model study, but in real soil samples its occurrence was not clear
- To our knowledge, soil mineral phase has not been shown to directly transform inorganic Se to organic Se. It is able to reduce Se(VI) and Se(IV) to inorganic Se(-II) and Se(0)
- SeO_4^{2-} is less adsorbed on soil mineral phase than SeO_3^{2-}
- Retention on Fe/Al oxides depends on pH of soil solution
- SeO_4^{2-} and SeO_3^{2-} are microbially reduced to Se^0 and Se^{2-}, which can be released to the atmosphere as H_2Se or be incorporated into biomass (e.g. proteins, amino acids, OM)
- Microbial Se(0) oxidation occurs on much lower level than its reduction
- Microbial activity increases Se retention in soil

4.4 Selenium in plants

Selenium accumulation level has been a criteria for classifying plants into non-Se accumulators (< 100 mg kg^{-1}), Se-accumulators (100-1000 mg kg^{-1}) and Se hyperaccumulators (> 1000 mg kg^{-1}) (Valdez Barillas et al., 2011). Se hyperaccumulators are plants adapted to seleniferous soils, which can accumulate Se 100 times higher than other plants (up to 15 000 mg kg^{-1} DW). Selenium is not an essential nutrient for higher plants, however some positive effects were observed, especially in hyperaccumulators plants for which Se supplementation increased biomass production (Winkel et al., 2015). For all plants, other benefits exist as: protection against pathogens and herbivores, allelopathic reduction of competition with other plants (negative effect on the growth of Se-sensitive plant species) and enhanced growth (El Mehdawi and Pilon-Smits, 2012).

Plants take up Se species differently, which influences Se redistribution in the environment. Both organic and inorganic Se species are taken up via active membrane transport (**Figure chap.1 – 9**); simple diffusion has lower importance. The active transport of Se does not seem to depend on Se selective transporters but on shared transporters (proteins). SeMet and $SeCys_2$ species have been shown to be absorbed at a greater rate (20–100 fold) than inorganic Se species, suggesting the importance of amino acid transporters (Kikkert and Berkelaar, 2013). Selenate is actively internalized via sulfate transporters, whereas phosphate transporters and Si-transporters are involved in the case of selenite (Terry et al., 2000; Zhao et al., 2010). When sulfate and phosphate are present in soil solution, uptake of inorganic Se is reduced. In the opposite case, i.e. when the Se concentration is high and the S and P contents in soil are low, Se is more readily absorbed, leading to enhanced gene expression of sulfate and phosphate transporters to compensate for their low availability. However, in the absence of S and P, this strategy leads to higher Se uptake. No Se-specific uptake mechanism is known, however it has been hypothesized for hyperaccumulative plants, where selenite uptake is less inhibited by the presence of sulfate. Selenite is converted to organic forms in roots (SeMet, SeMet-oxide, Se-methyl-SeCys and other unidentified Se species, detected in roots of Se(IV) treated plants) with limited translocation to shoots (Li et al., 2008).

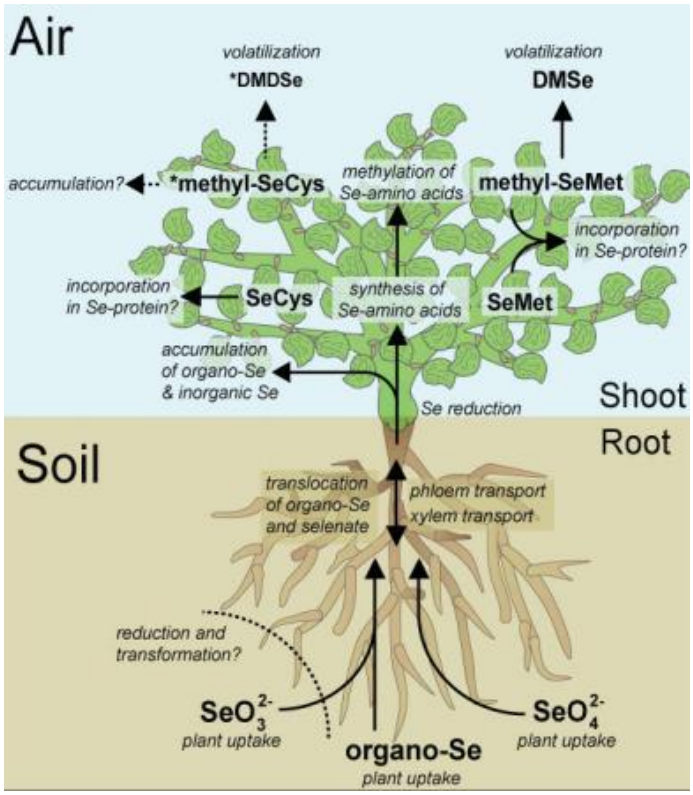

Figure chap.1 – 9 Se uptake and transformation at soil-plant-atmosphere system (Winkel et al., 2015).

Inorganic Se applied directly to leaf surface has been shown to be more bioavailable than soil applied Se (Drahoňovský et al., 2016; Kápolna et al., 2009). Foliar application, avoiding or limiting translocation from root to shoot, appears thus to be a promising strategy of biofortification. Moreover, inorganic ^{77}Se(IV) spiked by foliar application was taken up and transformed in onion and carrot leaves and bulb/root into organic species (^{77}SeMet, Me^{77}SeCys, γ-glutamyl-Me^{77}SeCys) that are more bioavailable for humans and animals (Kápolna et al., 2012).

Selenium in plants – summary

- Selenium is not an essential element for plant, but it has some beneficial effects especially for Se hyperaccumulators.
- Selenium can be absorbed by the roots by active transport (transporters shared with another elements) and simple diffusion has limited importance
- Selenium specific transporters are not known, but their existence is suspected, especially in Se hyperaccumulators
- Organic Se species are much more readily absorbed by plants than inorganic species.

4.5 Selenium in forest ecosystem

Very few studies focused on Se distribution in forest ecosystems. Roulier et al. (2021b) found that rainfall interactions with tree canopy resulted in twofold enrichment of Se in throughfall compared to rainfall, mostly due to dry deposition. Moreover, the inorganic Se species present in rainfall were almost totally transformed into unidentified organo-Se species in throughfall (Roulier et al., 2021a). Negative below canopy flux (- 0.34 ± 0.07 g ha^{-1} yr^{-1}) suggested element absorption from atmospheric deposits by beech leaves (Di Tullo, 2015). **Table chap.1 – 8** shows the total selenium concentrations reported in the different compartments of forest ecosystems. Branches, bark and foliage of beech trees were characterized by similar low Se values of 7-30 µg kg^{-1} (Di Tullo, 2015). Higher content in tree leaves (< 100-400 µg kg^{-1}) were found in birch and willow leaves (Reimann et al., 2015). The high content in fine beech roots (264 µg kg^{-1}) and much lower in large roots and wood stem (5 µg kg^{-1}) suggest that roots act as a barrier for Se, which is not an essential element for plant and thus Se translocation is negligible. Wood compartment stored 43% of total stock of Se in aerial tree because of its great biomass and despite low concentration in wood (Di Tullo, 2015). Detoxification mechanism

was also hypothesized in aerial part, as Se content in litterfall (59 µg kg^{-1}) was about twice as high as in the leaves, suggesting a translocation of Se from leaving to senescing leaves.

Selenium content was shown to increase during decomposition from 112 µg kg^{-1} in litterfall to 261 µg kg^{-1} in one-year leaf litter and to 650 µg kg^{-1} in O-horizon (Tyler, 2005). O-horizon enrichment in Se suggests deposition as an important source of this element. The vegetation had a minor contribution to humus and soil reserves compared to atmospheric deposition (Di Tullo, 2015). Elevated concentration of Se in some fungi (up to 1260 µg kg^{-1}) may be a result of its mobilization from lower soil horizons and cause Se enrichment in upper layer (Tyler, 2005).

Table chap.1 – 8 Total selenium concentrations in forests.

	Tree species	**Total Se (µg kg^{-1})**	Reference
Fungi		22 - 1260	Tyler, 2005
		160-4780	Di Tullo, 2015
Forest floor			
Litterfall (leaves)	beech	261	Tyler, 2005
		59 ± 11	Di Tullo, 2015
Humus		650	Tyler, 2005
		151	Di Tullo, 2015
Tree parts			
	willow	<100-400	Reimann et al., 2015
	birch	<100-300	
Tree foliage	beech	112	Tyler, 2005
		30	Di Tullo, 2015
Branches		7 - 13	Di Tullo, 2015
Bark		28	Di Tullo, 2015
Wood		5	Di Tullo, 2015
Coarse roots		5	Di Tullo, 2015
Fine roots		264	

The positive input-output budget in beech forest suggests that soil acts as a sink for Se (Di Tullo, 2015). However, there is no data about Se residence time in humus and soil inventories. Very limited studies concerned Se content in forest soil. The mean concentration of Se in soil decreased in the order: grassland (323 – 1119 µg kg^{-1}) > forest (172 – 1041 µg kg^{-1}) > culture (198-815 µg kg^{-1}) (Tolu et al., 2014). Kd values showed that Se water solubility was the lowest in forest soils (mean values : 715 L kg^{-1} for forest, 689 L kg^{-1} for grassland and 614 L kg^{-1} for culture soils). In average, 67% of total Se in forest soils was found in the NaOH fraction

containing dissolved OM, while it was 35% and 55% in culture and grassland soils respectively. Di Tullo (2015) did not remark fluctuations in Se concentration down the soil column, whereas Almahayni et al. (2017) measured significant difference between topsoil (330 µg kg^{-1}) and subsoil (100 µg kg^{-1}; **Table chap.1 – 9**). Similarly, Reimann et al. (2015) reported higher median Se concentrations of 2000 µg kg^{-1} in organic O-horizon compared to 450 µg kg^{-1} in mineral C-horizon of Norwegian forests.

Table chap.1 – 9 Total selenium concentrations reported in forest soils.

Region	Forest type	Depth	[Se] (µg kg^{-1})	Reference
UK	deciduous	0 - 10 cm	330	Almahayni et al., 2017
		40 - 50 cm	100	
France	deciduous	0 - 5 cm	465 ± 42	Di Tullo, 2015
		5 - 15 cm	496 ± 37	
		15 - 30 cm	483 ± 52	
		30 - 45 cm	483 ± 47	
		45 - 60 cm	431 ± 44	
Norway	-	O-horizon	400-6300	Reimann et al., 2015
		20-80 cm	100-2700	
France	-	0 - 30 cm	172 – 1041	Tolu et al., 2014

Selenium in forest – summary

- The lower Se concentration in above-ground tree biomass and its increase during decomposition from leaf litter to O-horizon organic soil layer, suggest that atmospheric deposition is more important Se input for soil than vegetation
- Low concentrations of Se in large roots and wood stem compared to fine roots prove poor transport into aerial parts
- Se cycle in forest ecosystem is not sufficiently documented, available data mainly concerns beech stands, the effect of tree species remains unknown
- Se fate in forest ecosystem is not well established and there is still a need of more data on complex Se cycle

5. Iodine

5.1 Chemistry of iodine

Iodine, with atomic number 53 and standard atomic weight 126.90, belongs to the halogen group. It occurs naturally in a variety of oxidation states: −I (iodide), 0 (I_2 - elementary iodine), I (HOI - hypoiodous acid; IX - iodine monohalides, where X = F, Cl are halides lighter than iodine), III (IX_3– iodine trihalides, where X = F, Cl), V (IO_3^- - iodate), VII (IO_4^-- periodate). Iodide has the widest range of thermodynamic stability in typical range of pH and Eh for natural soil-water systems (**Figure chap.1 – 10**). Iodide can be oxidized to I_2 in oxidizing acidic surface soil medium.

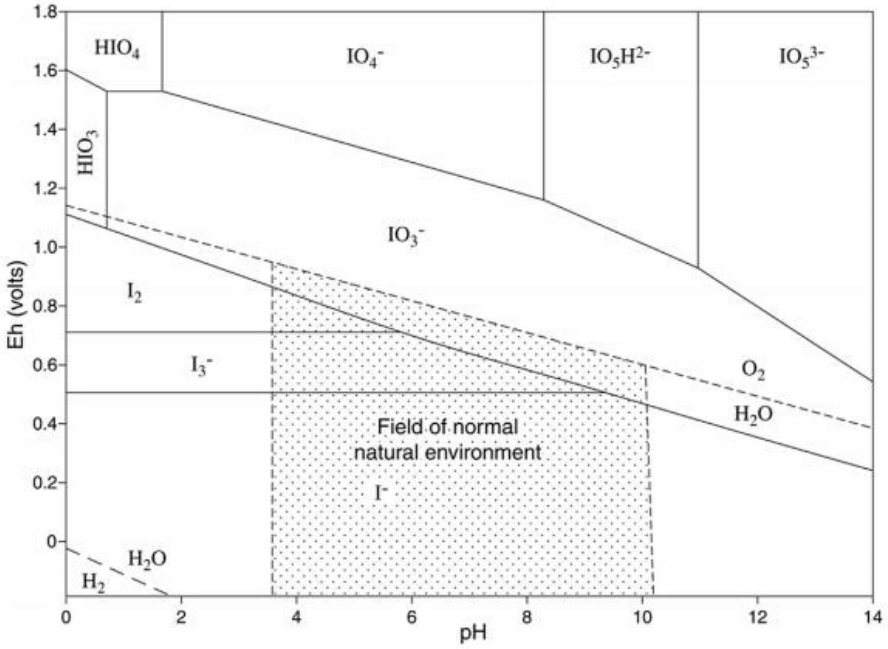

Figure chap.1 – 10 Iodine Eh/pH diagram at 25°C (Fuge and Johnson, 2015).

5.2 Iodine in the environment

The ranges of iodine concentrations in the environment are gathered in **Table chap.1 – 10**. The average iodine concentration is approximately 0.5-60 µg L^{-1} in hydrosphere, 0.1-3 mg kg^{-1} in rocks, 1-5 mg kg^{-1} in soil and 10 - 20 ng m^{-3} in the atmosphere (Moreda-Piñeiro et al., 2011a; Yeager et al., 2017).

Approximately 70% of total I on the Earth's surface is stored in the oceans. Iodate IO_3^- and iodide I^- are the most widespread and stable forms under weakly alkaline and oxidizing conditions of seawater (Fuge and Johnson, 2015).

Table chap.1 – 10 Iodine concentrations in the environment.

Environmental compartment	[I] range	Reference
Hydrosphere		Yeager et al., 2017
Rainwater	0.5 – 10 µg L^{-1}	
Fresh water	2 –10 µg L^{-1}	
Sea water	45 – 60 µg L^{-1}	
Atmosphere	10 – 20 ng m^{-3}	Moreda-Piñeiro et al., 2011a
Earth crust	0.1–3 mg kg^{-1}	Yeager et al., 2017
Soils	1–5 mg kg^{-1}	Yeager et al., 2017
Peat	0.2–98	Fuge and Johnson, 2015
Igneous rocks		Fuge and Johnson, 2015
Granite	0.25 mg kg^{-1}	
Basalts	0.22 mg kg^{-1}	
Volcanic glasses	0.52 mg kg^{-1}	
Sedimentary rocks		Fuge and Johnson, 2015
Limestone	1 – 76 mg kg^{-1}	
Sand	0.08 – 58 mg kg^{-1}	
Silt	0.1–135 mg kg^{-1}	
Clay	0.1 – 69 mg kg^{-1}	
Shale	2.3 mg kg^{-1}	Fuge and Johnson, 2015
Organic-rich shales	16.7 mg kg^{-1}	Fuge and Johnson, 2015

The most important I fluxes are volatilization from the ocean to the atmosphere and transfer to the terrestrial environment (**Figure chap.1 – 11**). Volatile compounds are mostly small organic compounds such as iodomethane (CH_3I), diiodomethane (CH_2I_2) and chloroiodomethane (CH_2ClI), but also inorganic compounds such as I_2 and HOI (Fuge and Johnson, 2015). Annual global marine production of CH_3I was estimated as 1 - 4 10^{11} g yr^{-1} (Moore and Groszko, 1999). Microalgae play the main role with estimated annual values of 1.2 to 38 10^9 g yr^{-1}. Many studies have shown that iodine volatile compounds have biotic origin, however there is also evidence of abiotic origin by photochemical reactions. Sea-vaporized iodine is transported in the gas and aerosol phases and deposited on the soil surface with dry and wet depositions. Geochemical maps of the distribution of I in soils in Europe show that soils near the sea are generally richer in iodine compared to those away from the sea (Fuge and Johnson, 2015; Rawlins et al., 2012). Iodine concentrations in topsoils were higher in the proximity of the coast and on the natural barriers like hills in west coast of Ireland (Fuge, 2007).

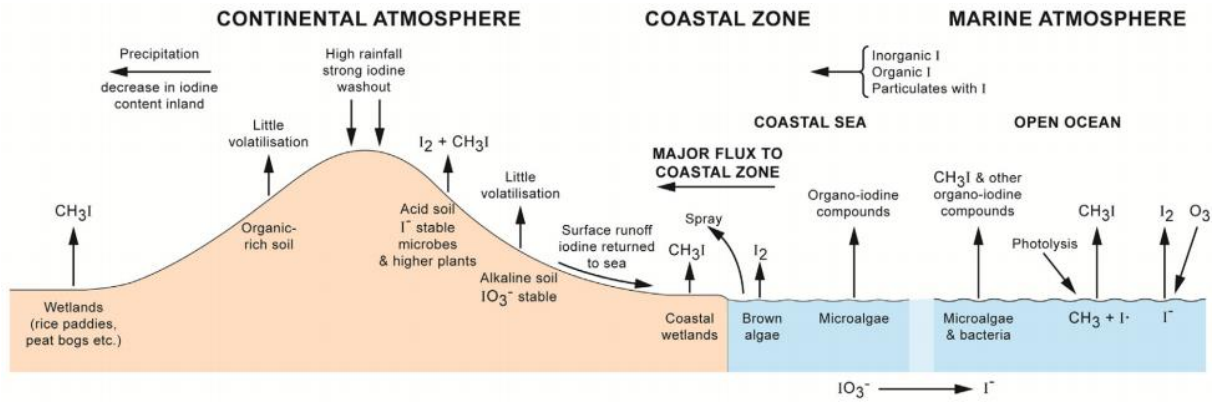

Figure chap.1 – 11 Iodine cycle in the environment (Fuge and Johnson, 2015).

Volatilization of I occurs also from terrestrial environments, particularly those rich in water such as peat bogs, rice paddies, and coastal salt marshes sites. Around 33 Gg yr^{-1} of CH_3I may be released by mid-latitude terrestrial organisms (Sive et al., 2007). Similar to marine organisms, terrestrial organisms such as plants (Zhao et al., 2010), soil bacteria (Amachi et al., 2003) and fungi produce CH_3I. Enzymes (halide methyltransferase) catalyze the transfer of methyl group from organic compound (S-adenosyl-L-methionine (SAM)) to halide ions forming methyl iodide CH_3I, methyl chloride CH_3Cl or methyl bromide CH_3Br. Among halide ions, iodide has the highest affinity to halide methyltransferases and the highest methylation rate (Zhao et al., 2010).

As for Se, sedimentary rocks contain generally more I than igneous rocks (**Table chap.1 – 10**). Except for shales rich in organic matter and iodine (16.7 mg kg^{-1}), the level of I in rocks is relatively low compared to soil, indicating that rock weathering is a rather minor source of I in soil reserves. Soils rich in organic matter, such as peats and peaty soils, have high iodine concentration, reaching 98 mg·kg^{-1} in peat (**Table chap.1 – 10**).

Iodine in environment – summary

- Ocean has the greatest inventories of I in Earth's surface
- Main volatile compounds emitted from soil are organic: CH_3I, CH_2I_2, CH_2ClI and inorganic: I_2, HOI
- Volatile compounds are mainly of biotic origin, but an abiotic (photochemical) origin has also been reported
- Wet and dry depositions are an important source of iodine in soils
- Soils near the coast have a higher I content
- Sedimentary rocks are generally richer in I than igneous rocks

5.3 Iodine in soil

Generally, the predominant iodine pool in soil is organic iodine (org-I), whereas I^- and IO_3^- occur in variable ratios (Fuge and Johnson, 2015). The coexistence of different chemical forms of iodine is important considering iodine mobility, bioavailability and possible volatilization. While great part of I is bonded with OM, other considerable sorbent phases are Fe, Al and Mn (hydro)-oxides and their minerals (Couture and Seitz, 1983). The mobility and availability of iodine is higher in anoxic conditions (Hansen et al., 2011). The products of I^- oxidation and IO_3^- reduction are reactive reagents such as molecular iodine I_2, hypoiodous acid HOI, and triiodide I_3^-, which are able to react with OM causing its iodination with subsequent adsorption on the mineral phase of soil or volatilization as small volatile iodinated compounds (Yeager et al., 2017). Sources of organic iodine in soil include atmospheric deposition and vegetation (Yamaguchi et al., 2010), but org-I may also be formed by microorganisms and abiotically by mineral oxides catalysis (Keppler et al., 2003).

5.3.1 Iodine and organic matter

OM-bound I fraction represents generally 30-90% of total I pool (**Table chap.1 – 11**).

Table chap.1 – 11 Proportion of organic I fraction (org-I) in soils.

org-I %	Soil type	Location	Ref.
Up to 90%	-	US	Hu et al., 2007
63%[2] (87%)[3]	-	Chiba, Japan	Shimamoto et al., 2011
51-79%	-	Norway	Qiao et al., 2012
30%	-	Denmark	Hansen et al., 2011
49%	-	Brjansk, Russia	

The type of interactions and molecular formulas of iodinated organic compounds and organic fractions resulting from OM iodination are still poorly known (Xu et al., 2013). Iodine was shown to be mainly covalently bound to OM. As summarized by Hansen et al. (2011), humic substances can be iodinated in several ways: 1) electrophilic substitution of hydrogen in phenolic ring by an iodine atom, 2) iodination of amines, 3) biotic methylation of inorganic iodine, 4) iodination of thiol fragments in proteins. Xu et al. (2012) examined humic and fulvic acid fractions from wetland soil, using NMR technique, and showed that iodine was bound to various functional groups such as aromatic regions with esterified formic and phenolic acids and other carboxylic acids, amide functionalities, hemicellulose-lignin- like complexes with

[2] determined by ICP-MS after sequential extraction
[3] determined by K-edge XANES

phenyl-glycosidic links, quinone-like structures activated by electron-donor groups like -NH_2 (**Figure chap.1 – 12**).

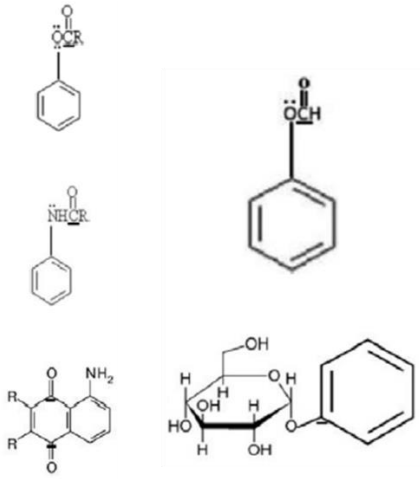

Figure chap.1 – 12 Proposed active aromatic rings in HA able to react with iodine (preferentially ortho/para positions) (adapted from Xu et al., 2012).

It has been shown that organic matter abiotically reduces iodate and then sequesters it in its structure, mainly in lignin and tannin-like compounds (Hao et al., 2018; Steinberg et al., 2008). In contrast, in presence of iodide, the formation of org-I was found negligible (≤ 1%) at pH values ≥ 5. Abiotic iodination of OM is prevalent under very acidic pH conditions, while microbially induced iodination prevails under less acidic conditions (Xu et al., 2011). The presence of oxidizing agent is necessary for org-I formation from iodide. An example of oxidizing agent is hydrogen peroxide H_2O_2, which may be formed abiotically by UV and biotically as a metabolite of microorganisms.

The formation of org-I was observed after spiking HA solution (HA extracted from conifer plantation soil and purified by dialysis against 1%v/v HCl and HF then deionised water) with $^{129}IO_3^-$, $^{129}I^-$ and mixture of $^{129}I^-$ and $^{129}IO_3^-$. Native iodine in HA extraction solution occurred as org-I and iodide (Bowley et al., 2016). After spiking, the reaction with $^{129}I^-$ was the slowest, while $^{129}IO_3^-$ was more rapidly reduced probably due to the proposed coupling reaction with native $^{127}I^-$:

$$IO_3^- + 5I^- + 6H^+_{aq} \rightarrow 3I_2 + 3H_2O$$

However, in soil, iodide reacted faster than iodate to form org-I. In real soil solution, the oxidation of iodide to iodine can be catalyzed by the presence of mineral oxides and enzymatic reactions, which is not possible in purified HA solution (Bowley et al., 2016).

5.3.2 Microbial influence

The role of microorganisms in the fate of iodine in soil has been demonstrated in many experiments, where biological activity was reduced by heating, air drying, incubation in anaerobic conditions or treatments such as chloroform fumigation, irradiation of gamma rays and addition of prokaryotic antibiotics or reducing agents. Results of these studies showed a significant reduction of soil capacity to bind iodine, suggesting that microorganisms facilitate iodine sorption in soil (Yeager et al., 2017). Sterilized soil restored its capacity to bind iodine after addition of fresh soil or microorganisms (Muramatsu et al., 2004).

Figure chap.1 – 13 presents a simplified scheme of I cycle in soil influenced by microbial activity. Microbial activity increases iodine binding to OM in soil by: 1) direct bioaccumulation and 2) extracellular oxidation. Microorganisms affect soil via direct secretion of extracellular enzymes or indirectly via production of oxidizing agents and by-products of main reactions. Reactive intermediates such as molecular iodine I_2 resulting from I^- oxidation and IO_3^- reduction can react with OM and produce org-I associated to mobile colloids.

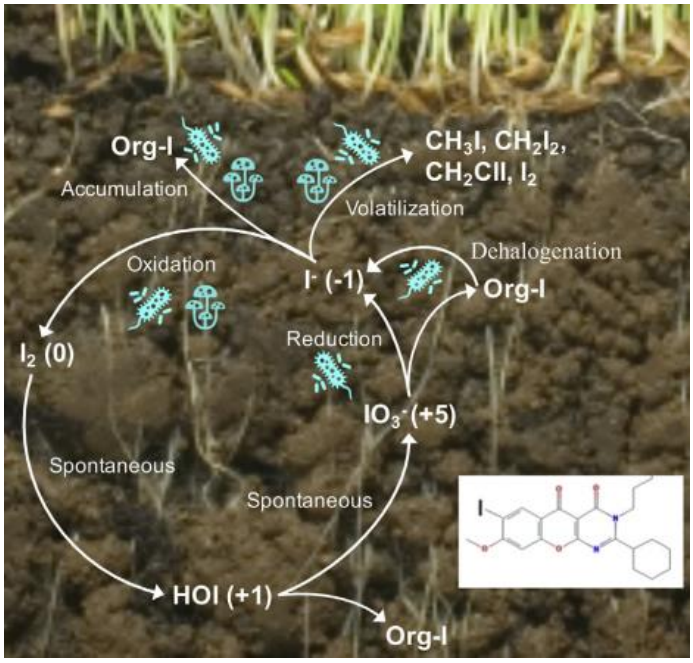

Figure chap.1 – 13 Scheme of microbial influence on I in soil organic matter (Yeager et al., 2017).

Oxidases, perhydrolases and peroxidases of microbial origin were found to be involved in OM halogenation. These purified enzymes were shown to catalyze I^- oxidation. However, their real impact is hard to assess because these enzymes are present in small concentration in the environment. Iodate-reducing strains have not been isolated, however anaerobic bacteria have

been shown to reduce IO_3^- to I^- (Amachi et al., 2003). The growth of certain strain in anaerobia was proportional to added content of IO_3^-, which played the role of electron acceptor in the reaction with acetate as proposed by Horiuchi et al. (unpublished, cited in Yeager et al., 2017):

$$3C_2H_3O_2^- + 4IO_3^- + 3H_{aq}^+ \rightarrow 4I^- + 6CO_2 + 6H_2O$$

It has also been shown that the deiodination of organoiodine compounds is of microbial origin. For example spiked 2,4,6-triiodophenol was reductively deiodinated to 4-iodophenol by bacteria present in terrestrial sediments (Oba et al., 2014).

5.3.3 Iodine and soil mineral phase

Interactions of iodine with soil mineral phases can lead to ligand exchange, formation of insoluble metallic iodides and redox reactions. The pH has a direct impact on protonation of mineral hydroxyl groups M-OH, where M = Si, Al, Fe, Mg, etc. In the range of pH 2-4, hydroxyl groups are in the protonated form $M\text{-}OH_2^+$, which maximizes the sorption of iodine anions on the mineral surface. Deprotonation with increasing pH results in iodine desorption. The mineral hydroxyl groups retaining the most iodine are those containing Al and Fe oxides, which preserve their acidic character up to pH 8, while deprotonation of Si-OH groups occurs at pH 3-4 (Kaplan, 2003). Additionally, iodate was stronger sorbed compared to iodide, which was not or only weakly adsorbed even on Fe and Al rich minerals (Söderlund et al., 2017). However, some minerals (rather sparse in soil) are able to form insoluble metallic iodides. Iodide substitution with OH^- on the surface of chalcocite (Cu_2S) or cinnabar (HgS) is easier than on Fe minerals, because I^- as a weak Lewis base reacts preferably with weak acids such as Cu^+, Hg^{2+}, Ag^+ (Park et al., 2019).

Moreover, iron and manganese oxides can change iodine speciation by oxidation (Gallard et al., 2009). MnO_2 was confirmed to oxidize iodide in the pH range below 6.5-7, with iodate being a final product in the presence of an excess of manganese oxides (Allard et al., 2009; Fox et al., 2009). Molecular iodine I_2 in acidic conditions and hypoiodous acid (HOI) in mid alkaline conditions have halogenating properties that led to the production of iodinated compounds such as methyl iodide and iodine incorporation into OM macromolecules (Allard and Gallard, 2013; Bichsel and von Gunten, 2000; Gallard et al., 2009).

Iodine in soil – summary

- Iodine concentrations range in soils is broad, 0.08-135 mg kg^{-1}, of which 30-90% of I is associated with soil organic matter.
- Iodination of OM can occur by biotic (microorganisms) and abiotic (oxides) mechanisms involving intermediate products, I_2 and HOI, able to react with OM.
- Iodine is mainly covalently bound with OM. Some structures have been proposed but the nature of iodinated compounds is still limitedly known.
- Microbial activity increases I retention in soil by oxidation and direct bioaccumulation. However some strains are responsible of organo-I reduction (deiodination).
- Iodine retention on soil mineral phase depends on the pH of soil solution; minerals with Fe/Al oxides show the highest retention capacity.
- IO_3^- is stronger adsorbed on soil mineral phase than I^-.

5.4 Iodine in plants

In most studies, iodine has been presented as a non-essential and even toxic element for higher plants (Medrano-Macías et al., 2016). Supplementation with I^- was more harmful for plant (spinach) than IO_3^- (Zhu et al., 2003). Some other studies showed that both forms can have beneficial effects such as improved growth, increased tolerance to stress and production of antioxidant compounds (Medrano-Macías et al., 2016).

Some studies suggested that I^- was preferentially taken up by plants (Fuge and Johnson, 2015; Humphrey et al., 2019), however opposite situation was also observed (Dai et al., 2006). The ability of rice roots to reduce IO_3^- to I^- was confirmed in a pot experiment, where the authors suggested that iodine reductase was secreted as physiological response of roots in the presence of iodine in aqueous solution (**Figure chap.1 – 14**; Kato et al., 2013).

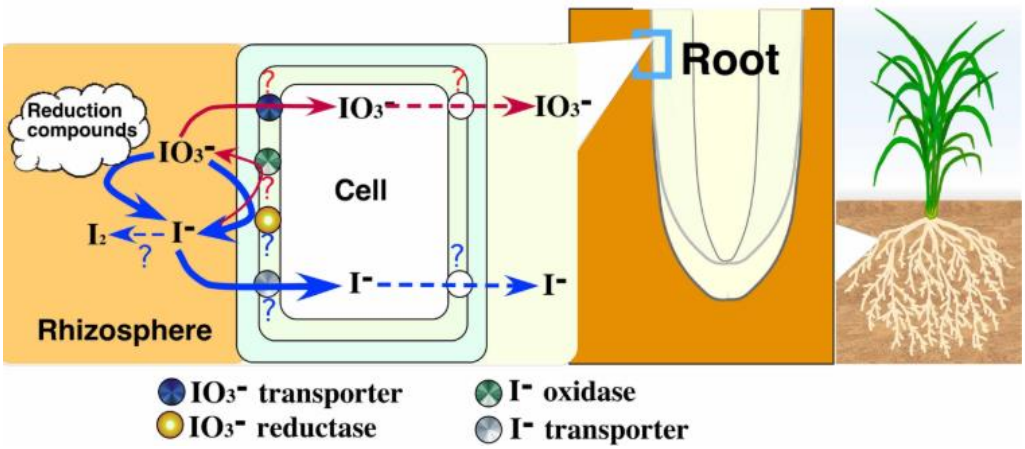

Figure chap.1 – 14 Schematic representation of hypothetical iodine uptake via roots by higher plants (Kato et al., 2013).

Another controversial aspect concerns the transport of iodine from the roots to the upper parts of the plant. Iodine accumulated in the roots was transported in small quantities in shoot tissues. A concentration of 53 mg kg^{-1} of iodine was measured in rice roots, while it decreased throughout the aboveground part of plant to 16 mg kg^{-1} and only 0.034 mg kg^{-1} in polished rice. Moreover, a lower concentration of iodine in the grains compared to the concentration in the leaves indicated a low iodine mobility in phloem (Tsukada et al., 2008).

It was suggested that atmospheric uptake by the aerial parts of the plant is a more quantitative process than roots uptake from soil. Shaw (2007) and Tschiersch et al. (2009), using radioisotopes (respectively $^{125}I^-$ and $^{131}I_2$) demonstrated that iodine was absorbed by the leaves. Not only a special attention is paid to the absorption efficiency, but also as already mentioned, to the poor translocation of iodine from the roots to another part of the plant. Cakmak et al. (2017) summed up that iodine absorbed by wheat roots is transported to shoots by xylem and is not easily accessible for re-translocation by phloem during the period of the reproductive growth stage. By contrast, translocation of iodine to younger wheat leaves and grains was observed after spraying the older leaves. Greater available iodine pool in leaf tissue is loaded and transported in the phloem to seeds during the late growth stage when intensive assimilative translocation occurs (Cakmak et al., 2017).

Nowadays, these two pathways of iodine absorption are being intensively explored to find the most prevalent method of fertilizing cultures in areas where iodine deficiency is endemic. There is no agreement on the best method to apply on a large scale, as the results strongly depend on the plant species (the most commonly studied are different kinds of maize and lettuce) and on the experimental approach (time of leaf washing, mode of iodine dispersion on the edible parts

of the plant, addition of surfactant (to facilitate its absorption) to the iodine solution) (Cakmak et al., 2017; Lawson et al., 2015).

Much of the iodine is volatilized from the soil into the atmosphere in organic forms (Subsection 5.2), so in case of contaminated soil most of re-emitted radioactive iodine should be in the form of CH_3I. Volatile CH_3I was questioned to be possibly absorbed by plants (Muramatsu et al., 1996). Collins et al. (2004) demonstrated that radioactive labelled CH_3I was absorbed by crops leaves (carrot, bean) and translocated to other parts of the plant such as pods. The atmospheric deposition of iodine on plant surface (leaves, fruits) can be a source of radioiodine for animals and humans. Barescut et al. (2009) highlighted the dry deposition of ^{131}I after Chernobyl accident as a source of milk radiocontamination.

Iodine in plants – summary

- Iodine is not an essential element for plant, most of studies report its toxic character; however beneficial effect after supplementation has been also observed.
- The mechanisms of I absorption by the roots as well as its further translocation to upper plant parts are still questioned.
- Roots are able to reduce IO_3^- to I^-, but the preferred species most likely to be absorbed by the roots is still unknown.
- Atmospheric uptake is more efficient than uptake by the roots.
- CH_3I has been shown to be absorbed by the leaves and translocated to other parts of the plant (leaves, seeds).

5.5 Iodine in forest ecosystem

The interactions between rainfall and tree canopies resulted in 2.2 fold I enrichment in throughfall, mostly due to dry deposits, and transformation of inorganic I^- and IO_3^- into unidentified iodinated organic species (Roulier et al., 2021b). Zhao et al. (2019) observed fluctuation of I concentrations (< 6 - 100 µg kg^{-1}, **Table chap.1 – 12**) in annual spruce wood discs derived rather from varying I content in the atmosphere over the years. Monitoring of annual I^{129}/I^{127} ratios in wood discs from Qinghai-Tibet region allowed to track radiocontamination from the global nuclear weapons tests (1961−1962; China: 1964−1980), from the Chernobyl accident and the continuous air releases (before 1997) and from the re-emission of marine discharges from the European nuclear fuel reprocessing plants. Mosses and

lichens with high I concentrating capacity (0.74-6.68 mg kg^{-1}) may be used as convenient bioindicators of atmospheric (radio)-contamination (Korobova, 2010; Roulier et al., 2018).

Table chap.1 – 12 Total iodine concentrations in forests.

Plant type	Forest type	Total I (mg kg^{-1})	Reference
Lichens	various	1.09	Korobova, 2010
	beech	6.68	Roulier et al., 2018
Moss	various	0.74	Korobova, 2010
	beech	4.71	Roulier et al., 2018
Forest floor			
Litterfall bulk	various	0.25 – 2.56	Roulier et al., 2019
Litterfall (leaves)	beech	0.58	Roulier et al., 2018
Litterfall (branches)	beech	0.42	Roulier et al., 2018
Humus	beech	1.81	Roulier et al., 2018
	pine	6-14	Bostock, 2004
	coniferous	11	Takeda et al., 2015
	various	1.02 – 12.65	Roulier et al., 2019
Tree parts			
Foliage	beech	0.241	Roulier et al., 2018
	pine	7-12.5	Bostock, 2004
	pine	0.13	Korobova, 2010
	birch	0.15	Korobova, 2010
	willow	0.16	Korobova, 2010
	beech	0.09	Korobova, 2010
Branches	Beech	0.016-0.047	Roulier et al., 2018
	Pine	18	Bostock, 2004
	pine	0.19	Korobova, 2010
	birch	0.12	Korobova, 2010
	willow	0.09	Korobova, 2010
	beech	0.07	Korobova, 2010
Bark	Beech	0.33	Roulier et al., 2018
	Pine	12.5	Bostock, 2004
	pine	0.11	Korobova, 2010
	birch	0.10	Korobova, 2010
	willow	0.13	Korobova, 2010
	beech	0.14	Korobova, 2010
Wood	beech	<0.006	Roulier et al., 2018
	pine	5	Bostock, 2004
	spruce	<0.006-0.1	Zhao et al., 2019
Roots (< 2mm)	beech	0.75	Roulier et al., 2018
Roots (> 2mm)		0.40	

Iodine content in roots, determined in fine and large beech roots (0.4-0.7 mg kg^{-1}), was around 6 times higher than in beech aerial tree compartment (Roulier et al., 2018). This may be evidence of low root uptake and limited transport in the upper parts of the tree. Iodine absorption

depends on I concentration in the soil solution (Humphrey et al., 2019). Iodine contents were similar in branches, leaves and bark and lower than 0.35 mg kg^{-1} with the exception of the study of Bostock (2004) who measured elevated I concentrations (5-18 mg kg^{-1}) in pine trees in Great Britain.

Litterfall stored more I (0.25 – 2.56 mg kg^{-1}) compared to young foliage probably due to absorption of atmospheric deposition and tree detoxification mechanism, which consists of I translocation from the young tree parts into the senescing organs. Roulier et al. (2018) concluded that forest vegetation returned to the forest floor has a minor impact on iodine budget compared to water below canopy fluxes. Humus enrichment in I compared to fresh plant material resulted in positive accumulation rates of 0.02 to 15.8 g ha^{-1} yr^{-1} (Roulier et al., 2019). The degradation of organic material resulted in I levels of 0.25-14 mg kg^{-1} (**Table chap.1 – 12**).

Wide range of iodine concentrations were reported in forest soils, from 0.39 to 40 mg kg^{-1} (**Table chap.1 – 13**). Xu et al. (2016) reported concentrations of I in the soil surface (< 4 cm) under different land uses as follows: coniferous forest (10.4 mg kg^{-1}) > deciduous forest (4.89 mg kg^{-1}) > urban (2.06 mg kg^{-1}) > paddy (1.74 mg kg^{-1}).

Some authors observed a decrease of I concentration with increasing soil depth and decreasing OM content (Bostock, 2004; Shetaya, 2012), whereas others reported opposite profile (Epp et al., 2020; Roulier et al., 2018; Xu et al., 2016). Roulier et al. (2018) measured the maximum of I concentration in the range -20 - -40 cm, while Xu et al. (2016) showed an increasing tendency until -15 cm in coniferous forest. Both authors hypothesized that the weathering of parent material can be the source of enrichment of subsoil. Volatilisation of organic iodine species such as CH_3I is another process that can lead to lower I concentration in topsoil (Roulier et al., 2018). Epp et al. (2020) reported I enrichment down to a depth of 60 cm, which they explained by iodination of OM and sorption of I onto pedogenic oxides.

The iodine residence time in humus and soil was estimated as 419-1756 years (Roulier et al., 2019). The negative input-output budget in beech forest implies iodine percolation from soil reserves (Roulier et al., 2018).

Table chap.1 – 13 Total iodine concentrations in forest soils.

Region	Forest type	Depth	[I] (mg kg^{-1})	Reference
Japan	coniferous	0 – 10 cm 30 – 70 cm	17 9	Takeda et al., 2015
Slovakia	nd	5–15 cm	2.98 – 8.43	Duborská et al., 2020
France	nd	0 – 5 cm 50 – 55 cm	2 10	Epp et al., 2020
UK	coniferous	Horizons A and B	4	Bostock, 2004
Japan	coniferous coniferous	0 – 10 cm 0 – 10 cm	3.2 – 36 5.7 – 32	Muramatsu et al., 2004
Japan	coniferous	0 -3 cm 3 -6 cm 6 – 9 cm 9 – 12 cm 12 – 15 cm	10.4 10.5 11.2 12.9 25.6	Xu et al., 2016
	deciduous	0 – 4 cm 4 – 8 cm 8 -12 cm 12 – 16 cm 16 – 20 cm 20 – 22 cm	4.89 4.61 8.94 6.46 4.88 8.42	
UK	deciduous	0 – 10 cm 40 – 50 cm	4.41 1.98	Almahayni et al., 2017
UK	deciduous	0 -10 cm 10 – 20 cm 20 – 110 cm	2.8 2.2 1.4	Shetaya, 2011
	deciduous	0 – 10 cm 10 – 20 cm 20 – 70 cm	1.5 1.6 1.6	
France	deciduous	0 -5 cm 5 – 15 cm 15 – 30 cm 30 – 45 cm 45 – 60 cm	5.7 8.1 9.6 11.3 10.7	Roulier et al., 2018
France	coniferous deciduous	0 – 40 cm	0.39 – 35.65 0.72 – 28.29	Roulier et al., 2019
Japon	-	0 – 40 cm 40 – 120 cm 120 – 240 cm	40.1 19.9 11.8	Yuita and Kihou, 2005

Iodine in forest

- The content of iodine in above-ground tree biomass is low compared to humus and soil, suggesting atmospheric deposition to be the main source of iodine in soil.
- Negative overall I budget reflects its percolation from forest soil.
- Contrasting iodine profiles in soil column have been observed.

6. Summary – part A

Selenium and iodine are essential for the growth and proper functioning of human organisms. Both excess and deficiency in Se are toxic, while only iodine deficiency is most often considered harmful for humans. Radionuclides ^{79}Se and ^{129}I were presented in the context of their sources and maleficent effect on human health while integrating the natural cycle of Se and I. The periods occurring after the contamination have been detailed, as well as the strategies used for radioisotopes modelling. Kd coefficient can be used as indicator of element mobility in soils. Many Kd values published in the literature have been determined during sorption experiment rather than desorption experiments.

The ocean covering around 71% of total Earth surface has been shown as an important sink of Se and I, but also a place of intensive volatilization of organic derivatives (mainly DMSe, DMSeS and DMDSe for Se and CH_3I for I) and inorganic species. Wet and dry depositions are the main source of I and Se in the soil, followed by inputs from vegetation recycling and rock weathering. Higher concentrations of these elements have been reported in soils close to the sea and a significant correlation was found between I content and coastal distance.

Generally, Se and I contents are lower in igneous rocks than in sedimentary rocks. Element contents in rocks reflect those in soil only in Se-rich and Se-poor soil regions, while in other cases the rock type is not a correct indicator of Se and I in soil reserves.

The retention of elements in soil is a result of complex interaction with OM, mineral phases and microbial activity. Among inorganic forms, selenite is more strongly sorbed than selenate and iodate more than iodide. For Se, the mechanisms of interaction with soil organic matter are poorly understood. The formation of the organo-Se fraction in soil seems to be mainly biotic, while both microbial activity and mineral oxides can induce the production of organic iodine compounds. Hydrogen peroxide H_2O_2 can contribute to this reaction in the case of iodine, which can have biotic and abiotic sources, making it hard to distinguish between microbial and abiotic sources of organic compounds formation.

A part of Se associated to OM fraction was proved to be inorganic Se(IV). However the type of interaction is still unknown. Some Se-aminoacids have also been determined in water soluble soil fraction, but the identification of organo-Se species is limited by analytical techniques. While for Se direct or indirect sorption is assumed, covalent bonds with specific HA functional groups have been proposed for iodine.

Water-soluble elements pool in soil is more available for plants. However, the forms and the mechanisms involved in absorption by roots and translocation to upper parts of plants require

further study. Both elements have been shown to be taken up by the aerial parts of the plants and this method of biofortification was considered more efficient as it avoids the limited translocation from roots to shoots. Trees have a broad surface for element absorption. However reported Se and I contents are relatively low in aerial biomass compared to reserves in soil. Tree canopy interacts with atmospheric deposits changing the composition and Se and I speciation in throughfall. Selenium prevalence and cycle in forest ecosystem are still not well established. Circulation of iodine in coniferous forest is still poorly documented.

Part B. Methods for Se and I analysis - The state of the art

This chapter provides an overview of analytical techniques used for the investigation of total content and speciation of Se and I in environmental samples.

7. Sample pre-treatment

7.1. Sequential extraction

In the literature, two approaches, sequential extractions or parallel single extractions targeting specific element fractions, have been performed on soil and humus samples in order to investigate the distribution and the mobility of Se and I. The principle of sequential extraction is that elements are associated with some particular soil components with different strength, allowing them to be separated using solvents with increasing extraction strength. Sequential extractions are usually carried out at room temperature (Moreda-Piñeiro et al., 2011b) by stirring/shaking steps (generally 1h-24h). The batch method is the most commonly applied besides following disadvantages such as: long procedure, probability of cross contamination and re-adsorption (Hou et al., 2009). Re-adsorption occurs when elements released to the solution are readsorbed on remaining solid phase before liquid/solid phase separation, which leads to overestimation of element pool in residue. The centrifugation step (generally for 10 - 20 min at 3000-15000 rpm) is indispensable to separate extractant from the residue, especially when both phases are subjected to further analyses. Moreover, efficient separation prevents underestimation of soluble element pool and cross-contamination between two solvents, which could modify the strength of the second solvent. In order to face these problems, some strategies were applied as multiple successive extractions with the same extractant in order to recover the full extractable corresponding fraction (Redon et al., 2013; Roulier et al., 2018) or, washing of the residue before adding the new extractant (Hansen et al., 2011; Qiao et al., 2012).

Generally, Se and I extractions are based on the protocol proposed by Tessier et al. (1979) for the fractionation of trace metals in sediments with some modifications proposed to minimize iodine loss (Hou et al., 2009). In this method, pools of element are defined as hydrosoluble, exchangeable, associated with carbonate, associated with Fe/Al oxides, organically bound and residual. The extractants used for fractionation are presented in **Table chap.1 – 14**.

Table chap.1 – 14 Extractants applied for Se and I fractionation from soil.

Fraction	Selenium		Iodine	
	Extractant	**Ref.**	**Extractant**	**Ref.**
water-soluble	ultrapure water	1, 2	ultrapure water	9, 10, 11, 12 15
	0.25 mol L^{-1} KCl	3, 4, 5		
	5 10^{-4} mol L^{-1} $CaCl_2$	6		
exchangeable	0.1 mol L^{-1} K_2HPO_4/KH_2PO_4 pH 5- 7.8	1, 2, 4, 5, 6, 7,	$CaCl_2$ or $MgCl_2$ pH 7–8	13
			1 mol L^{-1} NH_4OAc at pH 7 or 8.2	9, 11, 12, 14,15
Organic	0.1 mol L^{-1} NaOH	1	30% H_2O_2–HNO_3 (pH 2.0)	9
	NaOCl	5	5% TMAH	10, 11, 15
	0.1 mol L^{-1} $K_2S_2O_8$	2, 7	0.3 mol L^{-1} NaOH	13
	5% $K_2S_2O_8$, HNO_3	4	3 mol L^{-1} NaOH (step 1), 5% NaOCl to residue (step 2)	*12*
	5% TMAH	8	1 mol L^{-1} $NH_2OH{\cdot}HCl/(NH_4)_2CO_3$ (pH 8-9)	14
associated with carbonates	pH 5, 1.0 mol L^{-1} $NH_4CH_3CO_2$	2	1 mol L^{-1} acetate/acetic acid buffer (pH 5.0)	9
	1 mol L^{-1} NaOAc followed by 0.1 mol L^{-1} K_2HPO_4	5	1 mol L^{-1} NH_4OAc pH 5	11, 12, 14, 15
oxides	2.5 mol L^{-1} HCl	4	0.04 mol L^{-1} NH_2OH HCl in 25 % (v/v) HAc (pH 2-3)	11, 12, 14, 15
(amorphous)	0.2 mol L^{-1} $C_2H_8N_2O_4$ and $H_2C_2O_4$	2		
(crystalline)	0.04 mol L^{-1} NH_2OH HCl in 25% (v/v) HAOc	2		
	4 mol L^{-1} HCl	5		
elemental Se	1 mol L^{-1} Na_2SO_3 pH 7.0	8, 5	-	
	0.25 mol L^{-1} Na_2SO_3 pH 6.7	6		
Sulfide/selenide Se	0.5 mol L^{-1} $CrCl_2$, 6 mol L^{-1} HCl	7	-	
Residual	HNO_3, $HClO_4$	4	5% TMAH	11, 15
	HNO_3	2	(combustion)	12

1)°Tolu et al., 2014; 2) Favorito et al., 2017; 3) Bienvenu et al., 2007; 4) Wang et al., 2012; 5) Zhang and Moore, 1996; 6) Coppin et al., 2006; 7) Dean A. Martens and Suarez, 1997; 8) Ponce de León et al., 2003; 9)°Claret et al., 2010; 10) Roulier et al., 2018; 11) Hansen et al., 2011; 12) Qiao et al., 2012; 13) Hou et al., 2009; 14) Schmitz and Aumann, 1995 ; 15) Duborská et al., 2020

Hydrosoluble fraction can be mobilized from the soil by single or multiple deionized water extraction. Hydrosoluble fraction is considered as the most available fraction for plants and microorganisms. Deionized water does not correspond to natural conditions as it does not have the composition of the soil water solution (but generally has a similar slightly acidic pH). To address this problem, water soluble Se fraction was also extracted with KCl or $CaCl_2$ solutions, whose concentrations can be adjusted to values representative of ionic strength of natural soil solution. **Exchangeable fraction** is considered as the element pool sorbed on the mineral surface via anion exchange mechanism and is also available for organisms. It was extracted with phosphate buffer for Se, while $CaCl_2$, $MgCl_2$ or CH_3COONH_4 extractants at pH 7-8 were used for I. Hydrosoluble and exchangeable fractions include generally < 20% of total pool, with some exceptions (**Table chap.1 – 15**).

Table chap.1 – 15 Fractions of Se and I in soil.

Sample type	Fractions							
	Water soluble	Exchangeable	Carbonate	Oxides	Organic HA	Organic FA	residue	Ref
Selenium fractions (%)								
soil	~1.5	~16-20	-	~18-41	~38-42		~13-18	1
soil[a]	0-4.8	0-3.3	0-10.2	0-11.7	0-19.4		61.4-100	2
soil[a]	24-37	11-12	-	-	29-37		8-10	3
soil[b]	2.5-8	6.2-48.1	-	-	20-108		-	4
soil[b]	1.4-14	15-20	-	-	19-58		-	5
Iodine fractions (%)								
clay rocks[a]	6.7-93	0	43-94	-	0-46		-	6
soil[a]	2-6	-	-	-	59 - 75		-	7
sediment[a]	~2-8	~2-15	~1-5	~10-20	~21-40	~9-17	~5-43	8
sediment[a]	~0-5	~0-3	~0-5	~9-19	~55-75		~15-18	9
soil[a]	1.9–7.8	0.1–4.4	1.1–6.6	23.7–75.9	4.2–38.7	3.4–15.5	2.2–26.4	10

1) Wang et al., 2012; 2) Favorito et al., 2017; 3) Ponce de León et al., 2003; 4) Tolu et al., 2014; 5) Tolu et al., 2011; 6)°Claret et al., 2010; 7) Roulier et al., 2018; 8) Hansen et al., 2011; 9) Qiao et al., 2012; 10) Duborská et al., 2020

[a] sequential extraction; [b] parallel extraction

Carbonate fraction in soil accounts for 0-10% of Se pool and 0-7% of iodine pool. Carbonate fraction is separated by a common extractant for I and Se: CH_3COONH_4 at pH 5 (Favorito et al., 2017; Hansen et al., 2011; Qiao et al., 2012), or acetate/acetic acid buffer at pH 5 (Claret et al., 2010).

Metal oxides fraction accounts for 0-41 % of Se and 9-76 % of I pool. The extractants were the same for the two elements studied. For Se, Favorito et al. (2017) divided metal oxides fraction into crystalline (0.04 M Hydroxylamine HCl in 25% (v/v) CH_3COOH) and amorphous

(0.2 M $C_2H_8N_2O_4$ and $H_2C_2O_4$) metal oxides. Iodine associated to reducible oxyhydroxides was obtained by extraction with NH_2OH HCl-CH3COOHat pH 2 (Hansen et al., 2011; Qiao et al., 2012; Schmitz and Aumann, 1995).

Velinsky and Cutter (1990) developed a method to extract **elemental selenium** from sediments with 1 mol L^{-1} sodium sulfite. However, sulfite was shown to extract any form of selenium not mobilized during previous sequential extraction (Ponce de León et al., 2003). Hence, elemental selenium extraction is not frequently included in sequential extraction protocols.

Organic fraction accounts generally for 0-58 % of Se and 0-75 % of I. Alkaline extractants like NaOH and TMAH cause oxidation of OM and decomposition of organic structures. Ponce de León et al. (2003), when comparing 5% TMAH and 0.1 M NaOH, reported higher efficiency of Se extraction from sediments with TMAH (respectively 37% for TMAH and 23% for NaOH). Any noticeable transformation of Se speciation was observed for a 100 µg L^{-1} solution containing Se-methionine, selenite and selenate after extraction in 2.5 to 5 %TMAH. Subsequently, elements associated to OM can be separated as bound to FA or to HA by acidification of the alkaline extract solution. Soluble FA fraction at acidic pH (pH 2) remains in solution, whereas insoluble HA fraction precipitates. The organic fraction of I has been obtained by extraction with TMAH, NaOH or NH_2OH HCl-carbonate at pH 8-9, H_2O_2-HNO_3 at pH 2. Iodine tends to be oxidized to I_2, and re-adsorbed by OM under acidic conditions (Hou et al., 2009).

Residue fraction represents the pool of elements remaining in soil after all extraction steps. Assuming that no contamination occurred, this residual fraction may result from an inefficient extraction of the previous steps, failure in considering an important fraction in the protocol or from highly occluded elements in recalcitrant mineral phases. The extraction of the residual pool corresponds thus to extraction for total analysis and cannot be carried out together for Se and I (discussion in Subsection 7.2).

There is no agreement between authors regarding uniform protocol for element fractionation, including number and types of fractions or solvents. The absence of certain fractionation steps may lead to the overestimation of the next fraction and incorrect conclusions. Beside diverse fractions, different solutions were used to separate the same fraction, which makes questionable their correspondence and the adequacy of the comparison between the fractions separated with different protocols. Moreover, achieved separation is neither selective of one soil component nor chemically specific (for element species). Therefore, the pool of element in the extracts is representative of the solvent used, rather than being a chemically homogeneous form.

Chromatographic separation (SEC or LC) is generally used in order to characterize these species. Due to the low concentrations of Se and I and the limited number of commercially available standards, speciation analysis is very demanding. Another challenging problem is the preservation of element species, which limits the use of strong reagents and require extreme caution.

7.2 Extraction for total element analysis

Environmental and biota samples have very complex matrices that make total element extraction a challenging analytical step. The release of metalloids such as Se from organo-mineral matrix as soil is problematic and may result in incomplete recovery. Acid hydrolysis is required in order to decompose organic Se structures such as proteins containing Se-aminoacids (Shand et al., 2010). Oxydizing agents such as HNO_3, hydrogen peroxide H_2O_2 or aqua-regia (HCl/HNO_3 3/1 v/v) are usually used (Ponce de León et al., 2003). Some procedures are presented in **Table chap.1 – 16**. Microwave digestion is routinely used for assisting in total sample decomposition, when quantifying trace elements like Se. Heat produced by microwave radiation is more effective than conventional (conductive) heating plates or hot-block devices and higher temperatures and pressure are reached in shorter time. Moreover, closed-vessels microwave system allows the use of toxic solvents such as HF, which is necessary to digest silica-rich soil samples.

Alkaline extraction is the most prevalent method for total I extraction. Among commonly used alkaline extractants (TMAH, NaOH, NH_4OH), TMAH is the most frequently used for soil, sediment and vegetal sample digestion (Watts and Mitchell, 2009). TMAH acts as a base generating negative charges, which mobilize HA and organic iodine and lead to their partial hydrolysis (Shetaya et al., 2012). In addition, in the presence of TMAH, iodate is released through the generation of negative charges on the surface of hydrated Fe/Al oxides and through competition with hydroxide ions on the specific sorption sites of these oxides (Yamada et al., 1996). Furthermore, unlike inorganic alkaline extractants such as KOH and NaOH, TMAH as an organic extractant allows high pH values to be achieved without increasing the salt concentration in solution, which minimizes the risk of precipitation in the nebulizer, torch and other parts of ICP-MS analyzer (Shetaya et al., 2012).

Table chap.1 – 16 Methods for Se and I total extractions.

	Sample	Equipment	Procedure and heating program	Ref
			Selenium	
aqua-regia + HCl	Sediments	Heating block	1) 70°C for 30 min (addition of water); 2) 70°C for 30 min (addition of HCl); 3) 70°C for 2.5 h	Ponce de León et al., 2003
HF, HNO_3	Soil	Microwave	20 min at 200°C, 1000 W, temp/pr ramp until 200°C/40 bar	Tolu et al., 2011
HCl, HNO_3	Soil	Heating block	1) 60°C for 2-3 h ; 2) 105°C for 1h; 3) 140°C until the samples were dry. 4) (addition of HCl) 80°C for 20 min	Stroud et al., 2012
			Iodine	
5% TMAH	Soil	drying oven	1) 70°C for 3 h with bottles shaken at 1.5 h. Dilution and centrifugation at 2500 rpm for 20 min.	Watts and Mitchell, 2009 Watts et al., 2015
5% TMAH	Soil, humus, vegetal material	Heating block	90°C for 3 h, dilution to 0.1% and centrifugation at 4000 rpm.	Roulier et al., 2018
10% ammonia	Soils, sediments	Stainless steel bomb, electric oven	185°C for 18 h	Bing et al., 2004
HNO_3 10% v/v ammonia solution	Rocks	closed PFA (perfluoroalkoxy) vessels	90°C for 18 h 185°C for 18 h	Claret et al., 2010
HNO_3	Food products	high-pressure autoclave	130 bar at 230°C	Haldimann et al., 2005

Compared to alkaline conditions, iodine signal in acidic solution is less stable during ICP-MS analysis. Iodate and iodide were shown to form molecular iodine gas in the acid digest according to the reaction (Moreda-Piñeiro et al., 2011b):

$$IO_3^- + 5I^- + 6H_{aq}^+ \rightarrow \ 3I_2 + 3H_2O$$

Formation of I_2 gas causes loss of analyte, decrease of the sensitivity and causes a memory effect. To minimize these effects, sample neutralization can be performed after acidic digestion and before quantification (Shah et al., 2005). Acidic digestion with nitric acid, mixture of nitric acid and hydrogen peroxide, hydrofluoric acid have been reported (Haldimann et al., 2005; Hou et al., 2009).

8. Determination of total element content by ICP-MS

The inductively coupled plasma mass spectrometer (ICP-MS) has been successfully used for analysis of Se and I at trace levels in environmental and geochemical samples. ICP-MS provides low limits of detection (LOD) in the range of 3-29 ng L^{-1} for selenium (Tolu et al., 2011) and 0.04-0.23 μg L^{-1} for iodine (Roulier et al., 2018).

Selenium and iodine are not the most sensitive elements to be measured by ICP-MS. They have relatively high potential of ionization (Se: 9.75 eV; I: 10.45 eV), which makes the ionization efficiency low (~30% for selenium (Layton-Matthews et al., 2006), ~34% for iodine (Zheng et al., 2012)). Other problems are the presence of memory effect, isobaric and polyatomic interferences (**Table chap.1 – 17**) and impurities in plasma gas and sample matrix.

The volatility of I compounds does not allow the use of acids for sample preparation, as it is conventionally used in wet digestion for metal determination (Mello et al., 2013). The LOD in acidic medium can be increased by the memory effects. Iodine adsorbed on plastic tubing surfaces and on the glass spray-chamber walls is volatilized as HI and I_2 (Al-Ammar et al., 2001). For this reason, as highlighted before, alkaline extraction and digestion are recommended as pre-treatment of solid samples for ICP-MS analysis (Moreda-Piñeiro et al., 2011b). Additionally, when analyzing Se and I simultaneously, the sample introduction system cannot be rinsed with acid medium, but rather with ultrapure water, which extends the time of analysis.

All selenium isotopes (m/z 74 to 82) show mass interference in the plasma source mainly from argon (plasma gas) or charged dimers and omnipresent chlorine and bromine. Elimination of spectral interferences can be carried out in collision/reaction cell (C/RC) as a result of chemical

reactions, dissociation after collision or charge transfer with introduced gas. Depending on the mechanism, a different type of gas is supplied into C/RC cell. Hydrogen, NH_3 and CH_4 are commonly used as reaction gases, while He is the most popular collision gas. The addition of methanol (a carbon source) to sample improves the detectability of Se as it increases the signal intensity, thus minimising the random error (Sloth and Larsen, 2000). Stable iodine isotope ^{127}I has no significant plasma interferences (**Table chap.1 – 17**) and can be measured without C/RC cell.

Table chap.1 – 17 Main interferences of Se and I in MS detector (May and Wiedmeyer, 1998).

Isotope	Interferences
	Selenium
^{74}Se	$^{37}Cl_2^+$,$^{36}Ar^{38}Ar^+$, $^{38}Ar^{36}S^+$, $^{40}Ar^{34}S^+$
^{76}Se	$^{36}Ar^{40}Ar^+$, $^{38}Ar_2^+$, $^{40}Ar^{36}S^+$, $^{31}P^{14}N^+$
^{77}Se	$^{40}Ar^{37}Cl^+$, $^{38}Ar_2{}^1H^+$, $^{40}Ar^{36}Ar^1H^+$
^{78}Se	$^{38}Ar^{40}Ar^+$,$^{38}Ar^{40}Ca^+$, $^{31}P_2{}^{16}O^+$
^{80}Se	$^{40}Ar_2^+$, $^{32}S^{16}O_3^+$, $^{79}Br^1H^+$
^{82}Se	$^{12}C^{35}Cl_2^+$, $^{34}S^{16}O_3^+$, $^{82}Kr^+$, $^{40}Ar_2{}^1H_2^+$, $^1H^{81}Br^+$
	Iodine
^{127}I	–
^{129}I	$^{129}Xe^+$, $^{127}I^1H_2^+$, $^{89}Y^{40}Ar^+$, $^{115}In^{14}N^+$, $^{113}Cd^{16}O^+$

9. Species analysis by liquid chromatography hyphenated with ICP-MS

HPLC is the predominant technique for separating selenium and iodine species and ICP-MS has been used as the most sensitive detector (Moreda-Piñeiro et al., 2011b). Limits of detection of HPLC-ICP-MS coupling techniques in liquid matrices such as soil solutions and groundwaters vary between 0.003 and 0.86 $\mu g \cdot L^{-1}$ for Se species (SeMet, $SeCys_2$, MeSeOOH, Se(IV), Se(VI)) (Söderlund et al., 2016; Tolu et al., 2011) and from 0.30 to 1.51 $\mu g \cdot L^{-1}$ for I species (Söderlund et al., 2017). **Table chap.1 – 18** presents column types, mobile phases and species detected in plant material, pore soil water and, humus and soil extracts.

Ion chromatography has been widely used to separate inorganic iodide and iodate and, inorganic and organic Se species. Generally, pH values of mobile phase can be lower for Se (pH = 4.7-12.2) than for iodine (pH = 8-12.2). Inorganic Se and I species were separated with the use of the same anion exchange stationary phase (AS11 Dionex anion exchange column (4×250mm)) and mobile phase (15 mM NaOH). In different studies, the Hamilton PRP-X100 anion exchange column (25 cm×4.1 mm) was used for Se and I separation with different mobile phases

(Ruszczyńska et al., 2017; Shetaya et al., 2012; Tolu et al., 2011). Mixed mode stationary phase allowed to separate inorganic species (selenate and selenite) in standard solutions and soil extracts (Tolu et al., 2011). The separation of inorganic forms (iodide and iodate) and organic species was achieved using a reversed mode stationary phase (Han et al., 2012). However, best separation of inorganic species is generally obtained with anion exchange columns (Shimamoto et al., 2011; Söderlund et al., 2017).

To date, no significant progress has been made in identifying organo-Se and organo-I compounds. Chromatographic signals found in environmental samples not attributed to inorganic anions (SeO_4^{2-},SeO_3^{2-} and I^-, IO_3^-) are described in the literature as "unidentified organic species". The problematic issue in the identification of Se and I species in soil extracts is the lack of commercially available standards. Moreover, the identification and quantification of organo-Se species in natural water solutions and soil extracts is challenging because they typically occur at very low concentrations. Tolu et al. (2011) reported the presence of methane selenic acid (MeSeOOH) and D,L-seleno-methionine (SeMet) in water extracts of some natural soils. The proposed way to detect organo-Se at low concentration is pre-concentration (Tolu et al., 2011).

Table chap.1 – 18 Comparison of protocols for Se and I speciation analyses by HPLC-ICP-MS.

Sample	Sample pretreatment	Chromatography mechanism	Column details	Mobile phase	Detected species	Ref.
Iodine						
humus, soil	iodate or iodide batch sorption test	anion exchange	AS11 Dionex column 4×250mm	15 mmol L^{-1} NaOH	I^-; IO_3^-; two unidentified species	1
soil	$^{129}I^-$ and $^{129}IO_3^-$ sorption test	anion exchange	Hamilton PRP-X100 (25 cm×4.1 mm)	60 mmol L^{-1} NH_4NO_3, 1×10^{-5} mmol $L^{-1}Na_2$-EDTA, 2% methanol with pH 9.5	$^{129}I^-$;$^{129}IO_3^-$; two unidentified ^{129}I species	2
pore soil water	diluted with 1.25 wt % TMAH	anion exchange	TSKgel super IC-AP, Tosoh	1.25 wt % of TMAH with 0.3 wt % methanol	I^- (no IO_3^-)	3
		SEC	TSKgel G3000 PWXL; Tosoh	20 mM Tris-HCl with 0.3 wt % ethanol pH 8	I^- and org-I	
rain, snow		anion exchange	Dionex AS16	35 mmol L^{-1} NaOH	I^-; IO_3^-; unidentified species	4
seaweed, seawater	Extraction: 5% TMAH,	reversed phase	Diamonsil C18 4.6× 150 mm	2.0 mM TEAH, 10 mM L-phenylalanine, 1% v/v methanol pH 8.9	iodinated amino acids: MIT, DIT I^-; IO_3^-	5
Selenium						
humus, soil	selenite and selenate batch sorption test	anion exchange	AS11 Dionex column (4×250mm)	15 mmol L^{-1} NaOH	SeO_3^{2-}; SeO_4^{2-} No organic species	6
soil	Single extraction with: MQ water, 5×10^{-4} M $CaCl_2$, 0.1 M KH_2PO_4/K_2HPO_4 pH 7 or 8, 1M nitric acid,0.1 M NaOH	anion exchange	Hamilton PRP-X100 column (25 cm×4.1 mm)	5 mmol L^{-1} ammonium citrate, 2% methanol with pH 5.2 and 7.7		7
		mixed mode (RP and AE)	Thermo Hypercarb column	240 mmol L^{-1} formic acid, 1% methanol pH 2.4	In water extracts: MeSeOOH SeO_3^{2-} ; SeO_4^{2-}	

soil	Extraction with 0.016 M KH_2PO_4	anion exchange	AS14 Dionex Ion Pack (4 × 250 mm)	6 mmol L^{-1} Na_2CO_3 (pH 9.5)	SeO_3^{2-}; after H_2O_2 addition: SeO_4^{2-}, MeSeOOH, unknown species	8
garlic, sun flower and radish sprouts	extraction with water solution of enzymes: lipase and protease	anion exchange	Hamilton PRP-X100 (250 × 4.6 mm)	5 and 150 mmol L^{-1} ammonium acetate pH 4.7	SeO_3^{2-}; SeO_4^{2-}, SeMet, Se-methyl-SeCys, γ-glutamyl-Se-methyl-SeCys and more with ESI-Orbitrap identification	9
			Porous Graphitic Carbon (PGC) Hypercarb column (150×4.6 mm) coupled to ESI-Orbitrap	2% aqueous formic acid and acetonitrile with 0.1% formic acid		
sediment, soil	sequential extraction: water; phosphate buffer pH 7; acidic (HNO_3 or HCl) or basic solutions (ammonium acetate, NaOH or TMAH)	anion exchange	Dionex CarboPac	6 mmol L^{-1} salicylic acid-sodium salicylate	Water: SeO_3^{2-}, SeO_4^{2-} Phosphate: selenate, suspected SeMet Acidic: SeO_3^{2-}, SeO_4^{2-}, unidentified species Basic: SeO_3^{2-}, unidentified species	10
		ion-pair	C8 Luna	0.1% HFBA and 10% methanol		
		size exclusion	Superdex 75 HR 10/30	50 mmol L^{-1} Tris-HCl buffer		
Selenium and iodine						
Rainfall throughfall			Agilent G3154-65001	20 mmol L^{-1} NH_4NO_3, 2.5% MeOH, pH 8.5	SeO_3^{2-}, SeO_4^{2-} I^- ;IO_3^-; unidentified I species	11
Rainfall		mixed mode	HyperCarb, Fisher (100 × 4.6 mm, 5 μm Thermo)	240 mmol L^{-1} formic acid	SeO_3^{2-}, SeO_4^{2-} I^-; IO_3^-	12

1) Söderlund et al. (2017) 2) Shetaya et al. (2012); 3) Shimamoto et al. (2011); 4) Gilfedder et al. (2008); 5) Han et al. (2012), 6) Söderlund et al. (2016); 7) Tolu et al. (2011); 8) Stroud et al. (2012); 9) Ruszczyńska et al. (2017); 10) Ponce de León et al. (2003); 11) Roulier et al. (2021); 12) Suess et al. (2019)

Size Exclusion chromatography was applied to analyze Se and I pools associated with LMW and HMW organic fractions in complex matrix samples (**Table chap.1 – 19**) (Shimamoto et al., 2011). HA and FA fractions contain compounds with a broad range of masses (an example is given **Figure chap.1 – 15**). The separation was performed for HA soil fraction for Se (Peel et al., 2017; Ponce de León et al., 2003) and I (Bowley et al., 2016); HA and FA soil fractions for I (Yamada et al., 2002) and, soil solution for I. Selenium and iodine were analysed using the same mobile phase: 20-50 mmol L^{-1} Tris-HCl buffer with similar pH (pH = 7 for Se and pH = 8 for I). For both elements ≤ 300k MW SEC column has been used (**Table chap.1 – 19**).

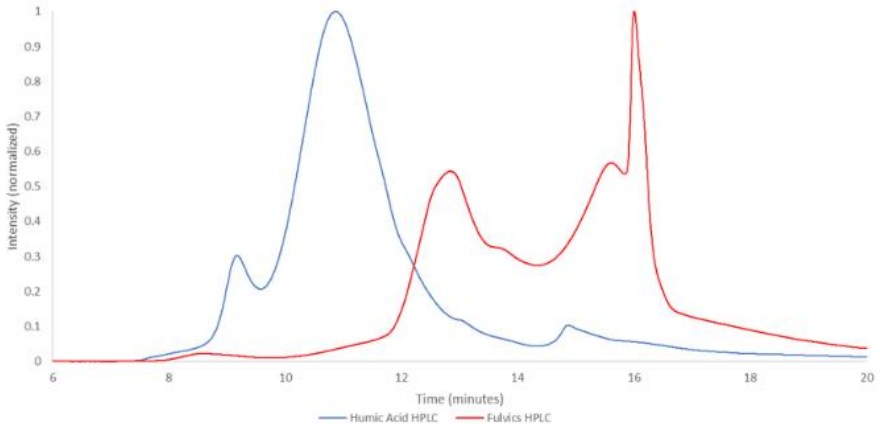

Figure chap.1 – 15 Normalized SEC-UV absorption chromatogram of purified humic acid (blue) and fulvic acid (red) fractions from the Eagle River Flats soil (Peel et al., 2017).

10. Summary – part B

Total extraction of Se and I is performed in different conditions due to their different chemical behaviors. Thus, Se is extracted in acidic media, while alkaline extractants are recommended for I. Selenium is problematic to be determined by ICP-MS, because of abundant plasma interferences, which can be eliminated in collision/reaction cell. Sequential extractions (or parallel single extractions) were performed to study Se and I mobility in soil targeting water soluble, exchangeable, carbonate, elemental (only Se), metal oxides, organic and residual element fractions. The hyphenated techniques HPLC-ICP-MS enable speciation analysis of Se and I at trace levels. Unidentified Se and I signals on chromatograms are presumed to be organic derivatives. The lack of commercially available standards and complex nature of organic matter are the limiting factors for organic Se and I compounds identification.

Table chap.1 – 19 Application of SEC to separate organic Se and I fractions.

Sample	Extractant	Column	Mobile phase	Retention times	Species	R.
Selenium						
HA [a]	0.1 mol L^{-1} NaOH	Shodex OH pak SB803 HQ 300×8mm	10 mmol L^{-1} sodium acetate, 1% methanol, pH 7.0	**Org fraction** 254 nm: 8-16 min and more) **Standards**: polystyrenesulfonate standards: 30, 20, 10, 6.5, 4.4 kDa (9-10 min)	Se coelute with the HA fraction, but no proof of ternary complex with Fe and OM	1
HA	0.001 mol L^{-1} pyrophosphate at pH 9	Superdex 75 HR 10/30	50 mmol L^{-1} Tris-HCl buffer	Pyrophosphate extract with UV detection at 254 nm: 10-20 min Pyrophosphate extracted Se: 20 min	Se not associated with HA	2
Iodine						
pore soil water	diluted with 1.25 wt % TMAH	SEC TSKgel G3000 PWXL (Tosoh)	20 mmol L^{-1} Tris-HCl with 0.3 wt % ethanol pH 8	**Org fraction 260nm**: 12 min -25min **Standards**: blue dextran: 200 k(MW); alcohol dehydrogenase (15min): 150 k; albumin: 66k; carbonic anhydrase: 29k; I^- :127 (25 min)	I^- (23-25 min) and org-I (~19min)	3
HA [a]	0.1 mol L^{-1} NaOH	SEC Superose 12 10/300 column (GE Healthcare)	0.1 mol L^{-1} Tris (Tris(hydroxymethyl) aminomethane) pH 8.8 adjusted with HNO_3	**I-Org fraction:** 5.5-13 min	I^- and Org-I	4
HA [a]	5% TMAH	SEC packing material: HW-5O TSKgel Toyopearl HW-50 in a stainless steel column (7.6 X 250 mm)	0.1 % TMAH	**Org fraction 230nm :** 3.5- 7 min	Org-I I^- (10-12 min)	5
FA			8 mmol L^{-1} $(TMA)_2S0_4$	**Org fraction 230nm :** 3.5-13min	Org-I I^- (13-16 min)	

1) Peel et al. (2017); 2) Ponce de León et al. (2003) ; 3) Shimamoto et al. (2011) ; 4) Bowley et al. (2016) ; 5) Yamada et al. (2002)

[a] The separation of HA soil fraction was obtained by acidification of NaOH or TMAH extracts (pellet-HA, supernatant-HA) and dissolution of the precipitate in NaOH or TMAH

Part C. Context of the study and objectives

The main environmental issues related to selenium and iodine concern radioactive risk from nuclear power plant activity and waste management, areas of selenium-rich soils and biofortification of plants in selenium and iodine deficient soils. Long-living radioisotopes ^{79}Se and ^{129}I occurring in HLW are actual hazard for organisms and require instant understanding of their transfer in the environment after radiocontamination. The literature review of Se and I distribution and speciation in hydro-, atmo-, bio- and litho- spheres allowed to specify their sources and the actual knowledge of their cycle in the environment. Although higher Se and I contents have been found in areas close to the coast, conflicting data underline the need for further investigation. Climate and environmental conditions affect the dynamics of elements transformation by controlling vegetation turnover, microorganisms activity in soil and degradation of organic material. In this context, especially the data about Se cycling in forest ecosystem are scarce. Additionally, most studies concern beech stands, while coniferous forests are not documented.

The persistence of radioisotopes in soil depends on their speciation and interactions with OM, mineral phase and microbial activity. Despite the lack of a unified methodology for determination, Kd coefficient remains an important indicator in the empirical approach of modelling the mobility of elements in soil solution. The literature review allowed to establish a common procedure for fractionating elements into labile and organically associated pools in soil. The challenge is the determination of organic and inorganic species of Se and I. The hyphenated techniques HPLC-ICP-MS are accurate for species determination due to multi-elemental capability and high sensitivity required for environmental samples. However, the parallel total analysis of Se and I by ICP-MS is not possible, because of the different chemical character of extractants.

Regarding all above, the main objectives of this doctoral research are to evaluate:

I. How do climate, environmental and physicochemical properties affect the distribution of selenium in forest ecosystems?
II. Do tree species influence Se and I partitioning within tree biomass and in underlying humus and soil column?
III. What are the differences in Se and I budgets in monospecific deciduous and coniferous tree stands?

IV. How do the mineral phase and organic matter of soil regulate the mobility or sorption of elements in the soil column?

In order to reach the listed objectives, this research work was conducted in two complementary parts. The first part of the study (**Chapter 2**) presents the distribution of selenium in deciduous and coniferous forests characterized by a variety of geochemical, climate and environmental conditions at the level of France. The second part (**Chapter 3**) focusses on Se and I distribution and cycle in five monospecific forest plantations located under identical climatic and edaphic conditions. Selenium and iodine contents and fluxes were compared between the five monospecific stands thanks to complete sample collection of tree compartments and, forest soil horizons. Then, a more thorough study was conducted with two of the tree species, beech and Douglas, in order to 1) quantify element inputs by atmospheric deposition, outputs from the canopies and by drainage and 2) examine the fractionation and speciation of selenium and iodine and their relation with soil organic matter constituents in the forest soil profiles. The final part of the manuscript **(Chapter 4)** summarizes the conclusions elaborated during these studies and presents perspectives proposed for further development.

Chapter 2. Influence of environmental conditions on Se distribution in forest

1. Introduction

Chapter 2 presents the broad study of Se concentrations in sample collection from 51 forest sites from France territory. The sampling sites are managed by ONF that provided the detailed characteristic database. The same sample collection was analyzed by Roulier et al. (2019) and Redon et al. (2011) for the quantification of iodine and chlorine, respectively.

The principal goals of **Chapter 2** were to discriminate how:

- climate (climate type, distance from the coast, Se concentration in rainfall),
- environmental conditions (dominant tree species, humus type),
- geochemical conditions (bedrock type, soil type, soil composition i.e. sand, clay fractions, Al/Fe minerals, OM content)

affect Se distribution in litterfall, humus and forest soil.

Analytical procedure was carefully optimized for sample preparation and quantification of Se in environmental samples by ICP-MS, and validated by Se determination in soil and plant Certified Reference Materials. In addition, a statistical study was performed on the experimental data set in order to discriminate the decisive variables controlling Se content in the forest ecosystem compartments.

This chapter was published in the article "**Selenium distribution in French forests: influence of environmental conditions**" in the journal "*Science of the Total Environment*".

2. Article 1: "Selenium distribution in French forests: influence of environmental conditions"

Paulina Pisarek[1,2], Maïté Bueno[1], Yves Thiry[2], Manuel Nicolas[3], Hervé Gallard[4], Isabelle Le Hécho[1]

[1] CNRS/Univ. Pau & Pays de l'Adour/E2S UPPA, Institut des Sciences Analytiques et de Physico-Chimie pour l'Environnement et les Matériaux (IPREM), UMR 5254, 64053 Pau, France (*pisarek.paulina@univ-pau.fr) (maite.bueno@univ-pau.fr; isabelle.lehecho@univ-pau.fr)

[2] Andra, Research and Development Division, Parc de la Croix Blanche, 92298 Châtenay-Malabry Cedex, France (yves.thiry@andra.fr)

[3] Office National des Forêts (ONF), Direction Forts et Risques Naturels, Département Recherche, Développement, Innovation, Boulevard de Constance, 77300, Fontainebleau, France (manuel.nicolas@onf.fr)

[4] IC2MP UMR 7285, Université de Poitiers, 86073 Poitiers Cedex 9, France (herve.gallard@univ-poitiers.fr)

Highlights

• Statistical study of factors influencing Se distribution in 51 French forests

• Selenium concentration in litterfall increases with proximity to the ocean.

• Low degradation rate of organic matter contributes to high Se stock in mor humus.

• Aluminium, iron, and organic matter content promote Se retention in soil.

Keywords

^{79}Se, humification, soil, litterfall, climate, statistical study

Graphical abstract

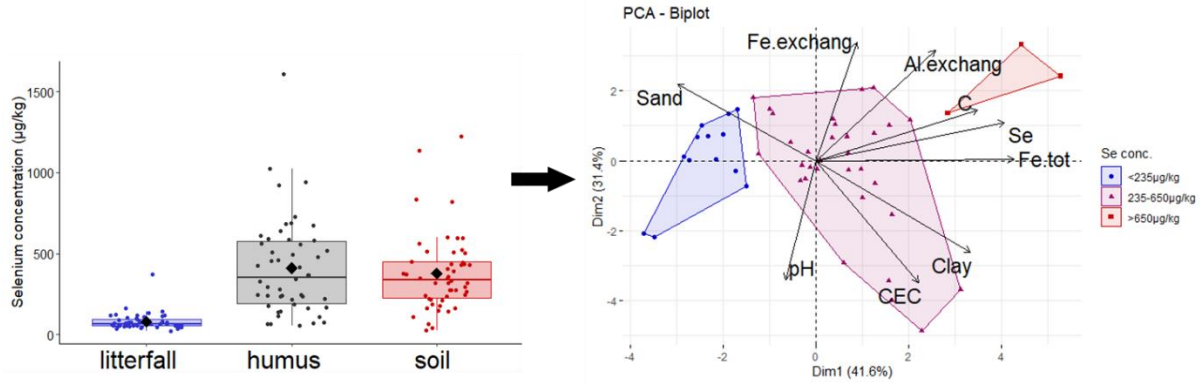

Abstract

Selenium is a trace element and an essential nutrient. Its long-lived radioisotope, selenium 79 is of potential radio-ecological concern in surface environment of deep geological repository for high-level radioactive waste. In this study, the influence of environmental, climatic and geochemical conditions on stable Se (as a surrogate of ^{79}Se) accumulation was statistically assessed (PCA analysis, Kruskall-Wallis and Spearman tests) based on the analysis of its concentration in litterfall, humus, and soil samples collected at 51 forest sites located in France. Selenium concentrations were in the ranges: 22–369, 57–1608 and 25–1222 µg kg^{-1} respectively in litterfall, humus, and soil. The proximity of the ocean and oceanic climate promoted Se enrichment of litterfall, likely due to a significant reaction of wet deposits with forest canopy. Se content was enhanced by humification (up to 6 times) suggesting that Se concentrations in humus were affected by atmospheric inputs. Selenium stock in humus decreased in the order of decreasing humus biomass and increasing turnover of organic matter: mor > moder > mull. Positive correlations between Se content and geochemical parameters such as organic carbon content, total Al and total Fe confirmed the important role of organic matter (OM) and mineral Fe/Al oxides in Se retention in soils.

1. Introduction

The radionuclide ^{79}Se is of potential radioecological concern at high-level nuclear waste storage sites (Hjerpe and Broed, 2010) due to its long half-life (3.27×10^5 years) and its capacity to be easily incorporated into natural biogeochemical cycle. Selenium is an essential element in animal nutrition and metabolism with a major physiological role associated with its presence in amino acids as selenocysteine (SeCys) and selenomethionine (SeMet) (Rayman, 2000). Selenium is not essential for higher plants, although it is absorbed by plants to various extent with some positive effects observed, especially for hyperaccumulators (El Mehdawi and Pilon-Smits, 2012).

The global average Se content in the Earth's crust is estimated to be 50 μg kg^{-1} (Taylor and McLennan, 1995), while average Se concentration in soil is 400 μg kg^{-1} (Shahid et al., 2018). Selenium accumulation in surface soils depends on different Se inputs with variable contributions. Geogenic sources appear to be the most important for Se-rich soils only, but it does not explain the large-scale distribution of Se (Blazina et al., 2014). The ocean is an important reservoir of Se, from where it can be volatilized and transported as sea spray (Blazina et al., 2014; Sun et al., 2016; Mason et al., 2018). Therefore, atmospheric deposition to nearby coast lines influences the Se content of vegetation and soil (Låg and Steinnes, 1978), but there is little evidence of oceanic transfer to more remote terrestrial regions (Blazina et al., 2014). Thus, another contribution to soil reserves appears to originate from intermediate zones due to remobilization through volatilization, and subsequent wet and dry deposition (Ross, 1985; Suess et al., 2019). In addition to natural sources, significant anthropogenic Se contamination may come from dust, coal or petroleum combustion, as well as agricultural sludges and fertilizers (Belon et al., 2012; Shahid et al., 2018).

The mobility of Se in soil is affected by various biological and geochemical factors such as redox potential, pH, salinity, microbial activity, soil organic matter, and minerals such Fe and Al oxides and clay (Dinh et al., 2017; Li et al., 2017). Among soil components, Fe/Al minerals and organic matter (OM) play a pivotal role in Se persistence, but there is still no agreement on the most important constituent (Coppin et al., 2009; Söderlund et al., 2016). It is also due to complex, and yet unclear, Se-OM interaction mechanisms that have been hypothesized to be mediated by mineral surfaces (Coppin et al., 2006) or by metal cations within ternary complexes (Li et al., 2017; Martin et al., 2017; Tolu et al., 2014). In soil, Se occurs in inorganic forms: Se(IV), Se(VI), Se(0), Se(-II) and in organic forms as complexes with OM or organo-mineral colloids (Winkel et al., 2015). The Se content associated with the organic

fraction of soils ranges from 14 to 82% (Supriatin et al., 2015; Tolu et al., 2011; Wang et al., 2012). In forest soils around 67 ± 19% of total Se is found in the organic fraction, while it is 35 ± 12% in cultivated soils and 55 ± 22% in grasslands (Tolu et al., 2014).

Limited data are available on Se content in forest compartments (Almahayni et al., 2017; Di Tullo, 2015; Tolu, 2012; Tyler, 2005), especially in contrasted geogenic ecosystems. In this study, particular attention was paid to forest ecosystems where Se inventories are expected to characterize the long-term influence of natural inputs and element recycling processes. Here, a comprehensive statistical study was proposed to determine the significance of eco-climatic and geochemical conditions in Se accumulation and distribution at various forest sites. The concentrations of selenium were determined in litterfall, humus, and soil samples from 51 different forest sites located in France. Fluxes and stocks of Se in forest compartments were estimated, as well as time-scale involved in Se retention in humus and soil. Monitored sites showed a wide variety in types of trees, climates, soils, and distance to coast. The sample collection presented also the considerable benefit of complete characterization and regular monitoring of forest sites provided by the ONF-RENECOFOR network (National Network for the long term Monitoring of Forest Ecosystems).

2. Material and methods

2.1. Study sites

Samples of soil, humus, and litterfall were obtained from the RENECOFOR network handled by ONF (French National Forest Office), which is part of the Pan-European ICP Forests intensive (Level II) monitoring network. In order to benefit from available samples and data, the same samples from 51 sites used by Redon et al. (2011) and Roulier et al. (2019) were analyzed (**Figure art.1.SI – 1**). These sites represent various forest types (dominance of 8 tree species), climates (continental, transition, oceanic and mountainous), humus forms (mor, moder, mull) and pedological properties (**Table art.1.SI – 1**). The extensive data collection and sites description was carried out as part of the RENECOFOR network (Brêthes and Urlich, 1997; Probst et al., 2003; Redon et al., 2011; Roulier et al., 2019) (**Table art.1.SI – 2**). Moreover Se concentrations and fluxes in rainfall were measured by Roulier et al. (2020) in a subset of 27 sites. The maps with the location of the sampling sites was adapted in R Studio (R Core Team, 2013; version 3.4.3). The coastal distance was estimated taking into account the closest coast and the direction of the prevailing wind.

2.2 Sampling procedure and sample treatment

Mineral soil layers of systematic depth (0–10, 10–20, 20–40 cm) and humus horizons (litter, fragmented, and humic layers) were sampled during the period 1993–1995 to measure their dry mass and chemical concentrations. For each site and layer, five samples were taken for chemical analyses from five 13.5 × 13.5 m^2 subplots distributed within the 0.5 ha central part of the site, then oven dried at 35 °C and stored in the dark at room temperature (details in Jonard et al., 2017). Litterfall was collected in ten traps of 0.5 m^2 placed at 1 m above forest floor in every plot. Litterfall samples were harvested three to five times a year in the period 1998–1999, dried and homogenized. Soil, humus and litterfall composites were prepared by mixing and grinding the individual samples in their respective mass proportions: soil layers (0–10, 10–20, 20–40 cm), humus fractions (litter, fragmented and humic layers), and litterfall (foliage, branches, fruits and 'rest material').

2.3 Selenium extractions and analysis

Approximately 0.25 g of soil, humus, or plant material were weighed in 50 ml DigiTUBE (polypropylene). Soil was mixed with 0.5 mL of HCl and 1.5 mL of HNO_3, while humus and litterfall were mixed with 2 mL of HNO_3, 0.5 mL of H_2O_2 and 3 mL of ultrapure water (18.2 MΩ.cm, Millipore Elix system). Samples were digested at 90 °C for 3 h in hot block digestion system (DigiPREP MS, SCP Science). Digested samples were diluted to 50 mL with ultrapure water, filtered on 0.45 µm acetate membrane and stored at 4 °C until analysis. Each sample was extracted and analyzed in triplicate except those in limited amount (detailed in **Table art.1.SI – 3**) and blanks were added in each digestion run. Selenium concentration was determined by inductively coupled plasma mass spectrometry (ICP-MS; 7500ce and 7900, Agilent Technologies, Tokyo, Japan) with collision/reaction cell gas flow of 5 mL min^{-1} H_2. Quantification was obtained by external calibrations in reconstituted matrices (blanks). Instrumental detection limits for Se ranged between 0.4 and 8 µg kg^{-1} depending on sample matrix. Typical analytical precision was lower than 10% (relative standard deviation, 15 replicates). Certified reference materials of soil DC 73030, DC 73032 (National Analysis Center for Iron & Steel, Beijing, China) and vegetal material ERM CD281 (Rye grass, Community Bureau of Reference, Brussels, Belgium) were analyzed in order to validate the accuracy of the extraction and analytical methods. Our experimental values (191 ± 15 µg kg^{-1} for DC 73030, 118 ± 9 µg kg^{-1} for DC 73032, 24 ± 3 µg kg^{-1} for ERM- CD281) agreed well

with the certified values (200 ± 30 μg kg^{-1} for DC 73030, 140 ± 20 μg kg^{-1} for DC 73032, 23 ± 4 μg kg^{-1} for ERM- CD281).

2.4. Calculations

Total soil mass (g ha^{-1}) was estimated as the sum of the masses of all soil layers (0–10, 10–20, 20–40 cm) that were calculated by multiplying the soil layer density by the layer thickness. Selenium stock in the top 40 cm of soil (g ha^{-1}) was calculated by multiplying Se concentration by soil mass. Selenium stocks in humus (g ha^{-1}) and annual litterfall (g ha^{-1} yr^{-1}) were calculated by multiplying selenium concentration by the masses of corresponding compartments. Information about soil bulk densities and masses of compartments was provided by ONF and is given in **Table art.1.SI – 2**.

Theoretical average residence time in forest soil ($t_{res}Se$) was calculated according to the Eq. (1):

$$\mathbf{t_{resSe}} = \frac{\text{stock of Se in humus+mineral soil}}{\text{Annual wet atmospheric Se input to soil}} \text{ (years)} \qquad (1)$$

This calculation was based on steady-state assumption and on the fact that Se input from weathering of the parent rock is negligible given the low average Se content of the Earth's crust (Taylor and McLennan, 1995). Therefore, atmospheric deposition was considered the only source of Se in the forest soil as proposed previously by Redon et al. (2011) and Bowley (2013) for chlorine and iodine. Values of annual wet atmospheric Se used for calculation were from Roulier et al. (2020). Net Se accumulation rate in humus allowed estimating accumulation associated to vegetal material decay (from litterfall to humus) and was calculated according to Eq. (2) (Redon et al., 2011):

$$\boldsymbol{Se\ accumulation\ rate} = \frac{([\mathbf{Se}]_{\mathbf{humus}} - [\mathbf{Se}]_{\mathbf{litter}}) \times \mathbf{DM_{humus}}}{\mathbf{t_{resDM}}} \text{ (g } ha^{-1}\ yr^{-1}) \qquad (2)$$

where [Se]humus and [Se]litter are Se concentrations in humus and litterfall, DM_{humus} and tresDM are dry mass and the average dry matter residence time in the humus, respectively. t_{resDM} was calculated according to Eq. (3) (Redon et al., 2011):

$$\mathbf{t_{resDM}} = \frac{\mathbf{DM_{humus}}}{\mathbf{LF} \times (\mathbf{1 - litter\ fraction\ mineralized})} \text{ (years)} \qquad (3)$$

where LF is the annual litterfall dry mass. 'litter fraction mineralized' is the average mass loss of litter due to mineralization before its total humification. For the calculation, litter fraction mineralized values were taken from the study of Osono and Takeda (2005) on different tree species (85% in pines, 70% in Douglas, 61% in spruce, 51% in silver fir, 65% in beech and 43% in oak forests).

2.5. Statistical analyses

Statistical analyses were used to determine correlations between selenium concentrations or stocks in soil, humus, and litterfall (response variables) with environmental, climatic, and geochemical conditions.

Shapiro-Wilk test was first used to determine if selenium concentrations and stocks in soil, humus and litterfall were normally distributed. As Se data were not normally distributed, a Spearman rank correlation test and Kruskal-Wallis test were performed respectively for numerical and categorical variables. Categorical variables comprised: forest type (coniferous, deciduous), tree species (oak, beech, Douglas, pine, spruce, fir), climate (mountain, continental, oceanic, transition), humus type (mor, mull, moder), rock type (sedimentary rocks, igneous rocks, other), soil type (cambisol, planosol, podzoluvisol, luvisol, andosol, podzol, letosol). Pairwise Wilcoxon test with Holm adjustment for p-values was applied in order to establish the differences within sub-groups of categorical variables.

The distributions of selenium concentrations, stocks, and accumulation rates were represented by boxplots for disparate categorical variables, with significant differences indicated by letters. Principal component analysis (PCA) was performed and a biplot correlation circle was drawn in order to visualize the relationships between soil numerical physico-chemical parameters and selenium concentrations in soil and the contribution of individual sites into the representation. Statistical analyses and boxplot representations were performed with R Studio (R Core Team, 2013; version 3.4.3).

3. Results and discussion

3.1 Selenium distribution in forest ecosystems

Selenium concentrations in litterfall, humus and soil samples of the forest sites are detailed in Appendix 1 (**Table art.1.SI – 3**). Selenium concentrations were in the ranges 22-369 µg kg^{-1}, 57-1608 µg kg^{-1} and 25-1222 µg kg^{-1} respectively for litterfall, humus and soil samples (**Figure art.1 –1**).

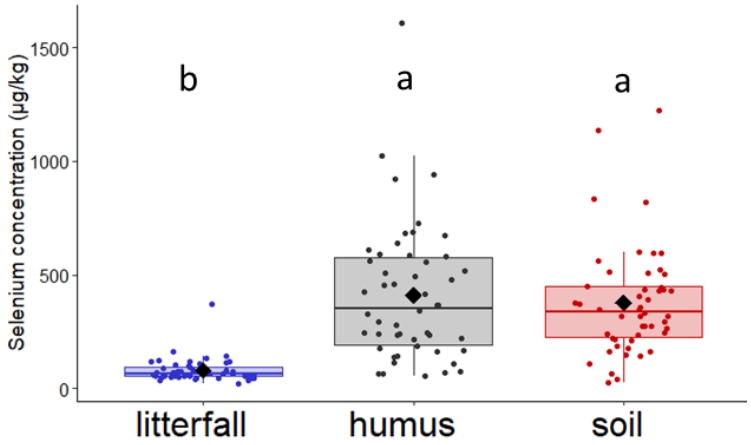

Figure art.1 – 1 Selenium concentrations in litterfall, humus and soils. Box plots show the first quartile (Q1), median and third quartile (Q3) of the data. Black diamond symbols represent average Se concentrations in groups. Lower and upper whiskers extend from the hinges by Q1 − 1.5 × IQR (IQR - interquartile range) and Q3 + 1.5 × IQR, respectively. Dots represent corresponding data. The different letters above the boxes correspond to significant differences between the groups according to pairwise Wilcoxon test, with Holm adjustment for p-value.

Selenium concentrations in humus were in the same range or higher than in soils while in litterfall they were on average 6 times lower than in humus and soils (Kruskal-Wallis rank for global test: $\chi 2=75.30$, p-value<0.001). Selenium contents in litterfall were comparable to values of 59±11 (Di Tullo, 2015) and 112 µg kg^{-1} (Tyler, 2005) previously reported for beech leaf litter. A wide range of Se concentration in humus was also observed in the literature. Di Tullo (2015) reported 151 µg kg^{-1} for beech mull type humus and Tyler (2005) the value of 650 µg kg^{-1} for mor – humus formation of soil's O-horizon. Reimann et al. (2015) also observed higher Se concentrations in the range 400–6300 µg kg^{-1} in organic O-horizon compared to 100–2700 µg kg^{-1} in mineral C-horizon (20–80 cm depth) of Norwegian forests. Selenium concentrations in soils (**Figure art.1 –2**) were coherent with average global values from 10 to 2000 µg kg^{-1} (Shahid et al., 2018) and values reported for European soils: 82 to 1119 µg kg^{-1} in France (Tolu, 2012), 100 to 4000 µg kg^{-1} in UK (Broadley et al., 2006) and 120 to 1970 µg kg^{-1} in the Netherlands (Supriatin et al., 2015). Selenium concentrations in humus were only moderately correlated with Se concentrations in litterfall (Spearman test, rs = 0.40, $p < 0.01$), whereas no correlation was found between Se concentrations in litterfall and soil (p-value >0.05). Moderate correlation between Se concentrations in humus and soil was found (Spearman test, rs = 0.43, p-value <0.01).

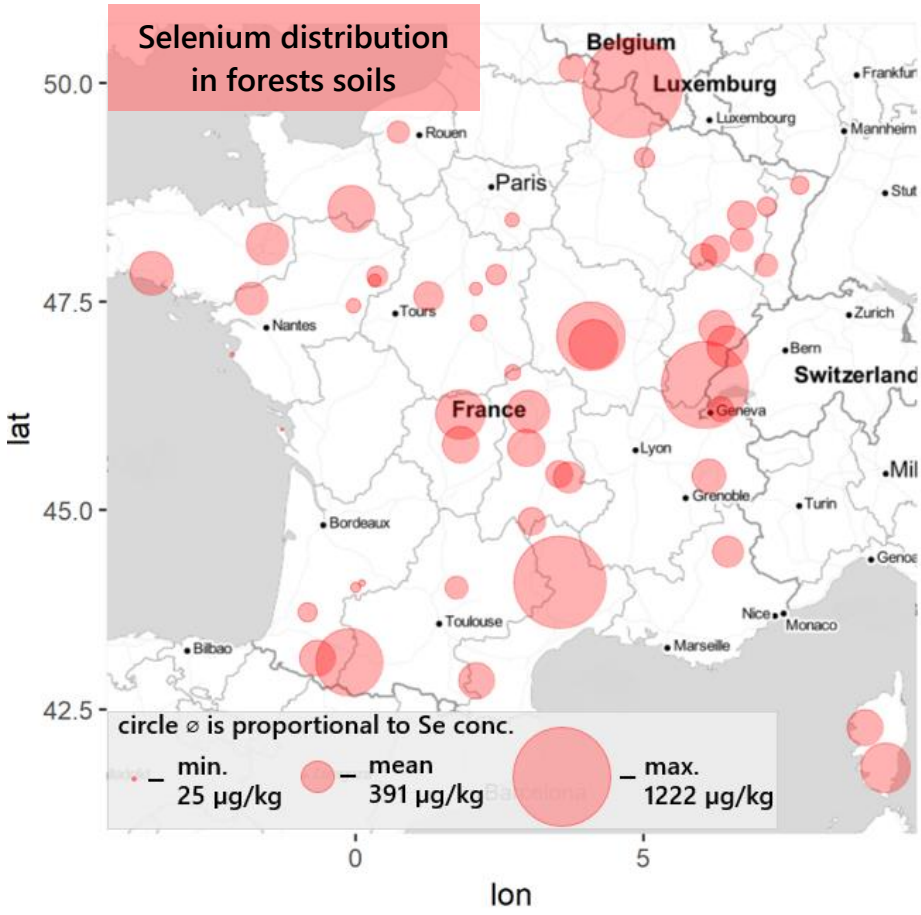

Figure art.1 – 2 Selenium concentrations in French forest soils (mean value of top 40 cm soil). Diameter of red circle is proportional to Se concentration (minimum: 25 µg kg^{-1}; maximum: 1222 µg kg^{-1}).

The Se stock in 40 cm deep soil composites varied from 142 to 3702 g ha^{-1} yr^{-1}, which is much higher than Se reserves in humus (0.3 to 121 g ha^{-1} yr^{-1}, **Table art.1.SI – 3**). The mean annual Se flux from litterfall to forest soil was 0.30 g ha^{-1} yr^{-1} with values ranging from 0.06 to 1.20 g ha^{-1} yr^{-1} (**Table art.1.SI – 3**). Roulier et al. (2020) reported annual Se fluxes in rainfall for a subset of the same surveyed sites (n=27) ranging from 0.25 to 2.01 g ha^{-1} yr^{-1} with a median value of 0.34 g ha^{-1} yr^{-1}. Combining these two fluxes would result into apparent total annual Se contribution to forest floor of 0.45–2.49 g ha^{-1} yr^{-1} (**Table art.1.SI – 3**). The sum of these two contributions might overestimate Se input to the soil given the interception (mean annual interception fraction of the precipitation can reach 31% (Ulrich et al., 2002)) and potential surface adsorption of a fraction of Se from rain by foliage before senescence. In addition to wet deposition interception, it is also possible that Se in litterfall partly originated from dry deposition or foliar or root uptake, different pathways not considered in the present budget. On the other hand, Se volatilization that is common for many plants and microorganisms (Chasteen

and Bentley, 2003) might have compensated the impact of those different processes in overall budget. In brief, the net accumulation of atmospheric Se by the foliage remains uncertain and difficult to quantify as is the case for various trace elements. Moreover, the results of correlation tests showed no direct dependence between Se concentrations in humus and soil and the sum of Se contributions from rain and litterfall ($p > 0.05$, **Table art.1 – 1**). This suggests that mobilization and immobilization processes of Se in forest soils have a greater influence on the Se concentration of soils than the contributions of rainfall and litterfall. When Se reaches the ground via litterfall, it can be released during biomass decomposition, then volatilized, or leached to deeper forest soil layers where sorption/desorption processes take place, or possibly taken up by tree roots and further recycled. Further statistical analyses were performed in order to highlight the factors affecting Se inventories in forest ecosystem.

3.2 Environmental factors affecting Se concentration in litterfall

Statistical analysis showed significant effect of distance from the coast, climate type, Se concentration, and flux in rain on Se concentration in litterfall (**Table art.1 – 1**). Furthermore, Se concentration in litterfall was statistically homogeneous through forest types and tree species (Kruskal-Wallis test, $p > 0.05$).

Table art.1 – 1 Statistical analysis for Se concentrations in soil, humus and litterfall. Spearman rank correlation coefficient rs and Kruskal-Wallis χ^2 values with p-values. Non-significant variables are in italic, significat variables are bolded

	Variables	**soil**		**humus**		**litterfall**	
Numerical variables		r_s	p	r_s	p	r_s	p
	Coastal distance	*-0.02*	*0.880*	*-0.02*	*0.885*	**-0.35**	**< 0.05**
	Se conc. in rain[1]	*-0.13*	*0.530*	*0.23*	*0.267*	**0.76**	**< 0.001**
	Se flux in rain[1]	*0.34*	*0.087*	*0.31*	*0.123*	**0.41**	**< 0.05**
	Se flux in litterfall and rain	*0.13*	*0.530*	*0.21*	*0.309*		
	Se accumulation rate in humus	0.43	< 0.01				
Categorical variable		χ^2	p	χ^2	p	χ^2	p
	Tree species (n=6)	**22.58**	**< 0.001**	**20.25**	**< 0.01**	*7.24*	*0.203*
	Forest type (n=2)	*0.17*	*0.682*	**15.53**	**< 0.001**	*0.15*	*0.697*
	Climate (n=4)	**10.74**	**< 0.05**	*3.97*	*0.265*	**11.36**	**< 0.01**
	Humus type (n=3)	**6.02**	**< 0.05**	*5.26*	*0.072*		
	Rock type (n=3)	**16.34**	**< 0.001**				
	Soil type (n=7)	*12.61*	*0.082*				

[1] test performed for 27 sites; n - number of sub-types

Slightly higher concentrations of Se in litterfall in oceanic climate compared to transition and mountain climates (**Figure art.1 –3.1**) were confirmed by weak negative correlation between Se concentration in litterfall and distance from the coast (Spearman test, $r_s = -0.35$, $p < 0.05$). The ocean is an important source of atmospheric Se (Amouroux et al., 2001; Mason et al., 2018; Wen and Carignan, 2007), reaching the ground or plant surface as dry and wet depositions.

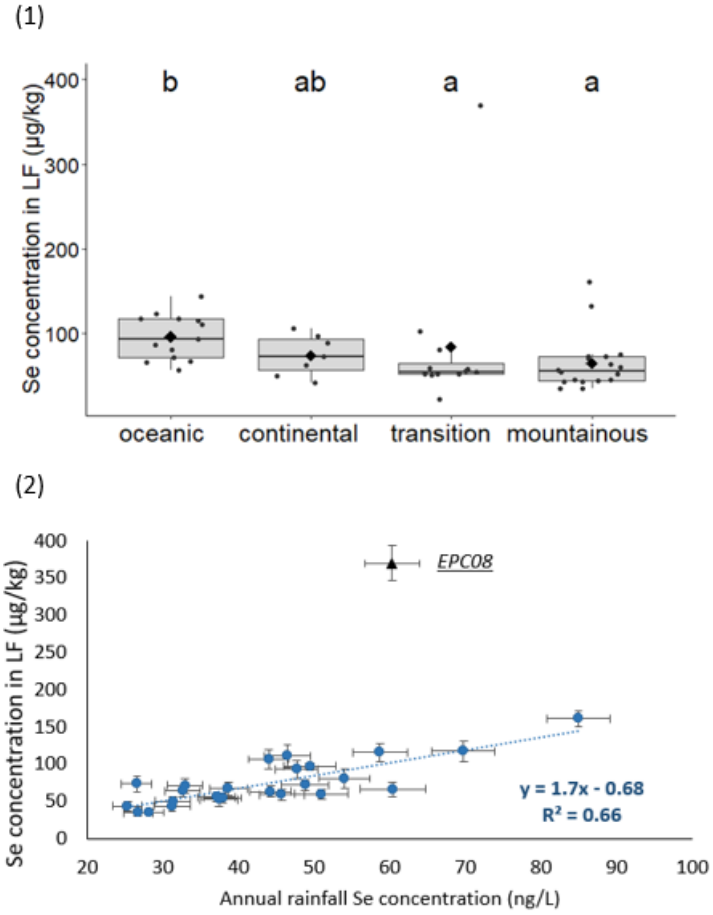

Figure art.1 – 3 Se concentration in litterfall according to 1) climate; 2) annual volume-weighted mean Se concentration in rainfall. In panel 3.1 box plots show the first quartile (Q1), median and third quartile (Q3) of the data. Black diamond symbols represent average Se concentrations in groups. Lower and upper whiskers extend from the hinges by Q1 − 1.5 × IQR (IQR - interquartile range) and Q3 + 1.5 × IQR, respectively. Dots represent corresponding data. The different letters above the boxes correspond to significant differences between the groups according to pairwise Wilcoxon test, with Holm adjustment for p-value.

Strong positive correlation was obtained between Se concentration in litterfall and in rainfall when EPC08 sitewas excluded (Spearman test, r_s=0.73, p<0.001, r2=0.66, **Figure art.1 –3.2**). This site showed a very high Se concentration in litterfall (369 µg kg^{-1}) compared to concentrations of the other sites (between 22 and 161 µg kg^{-1}), suggesting local contamination. The high concentrations of Se in soil (1222 µg kg^{-1}) and humus (1608 µg kg^{-1}) at this site

would be coherent with recurrent atmospheric emissions. The EPC08 site is located in the Ardennes montains, very close to the industrial regions of Western Europe (Cumbers et al., 2006) whose economy had been based for years on metallurgical industry requiring charcoal combustion. Nowadays, there are developed railway, car and battery recycling industries, all of which can be a potential source of long-term local pollution. Interestingly, the same site was also reported to be contaminated by As and atmospheric deposits of Pb (Pauget et al., 2013; Probst et al., 2003). In summary, Se concentration in litterfall was dependent from environmental conditions such as climate, Se input from rainfall and proximity to the coast. Furthermore, anthropogenic sources may contribute to Se deposition for some sites.

3.3 Se accumulation in humus compartment

As already discussed in Section 3.1, Se concentration in humus showed a wide range of values from 57 to 1607 μg kg^{-1} with median value of 353 μg kg^{-1} and maximum value corresponding to EPC08 potentially contaminated site. According to differences between litterfall and humus, Se concentration was increased on average six times along the litter decay continuum. Generally, Se concentrations in humus of coniferous forests were higher than in deciduous forests (**Figure art.1 – 4.1**, **Table art.1 – 1**), despite homogenous concentrations of selenium in litterfall of both forest types. Thus, humus under spruce and Douglas had significantly higher Se content compared to oak (**Figure art.1.SI – 2**, **Table art.1 – 1**). It may result from differences in the humification process, as deciduous leaves have a different composition from conifer needles (e.g. lower lignin content), which generally leads to a higher labile mass content and greater leaching losses in the early stages of litter decomposition (Prescott et al., 2000). The calculated average residence times of humus where higher for Douglas fir, spruce and pine (37.6 ± 27.7, 54.2 ±50.4 and 144.2±113.5 years, **Table art.1.SI – 2**) compared to oak and beech (5.5 ± 5.0 and 12.4 ± 12.2 years; **Table art.1.SI – 2**), which reflects slower decomposition rates of organic matter under conifers. Only humus from silver fir differed from the other coniferous species by low masses (20.3 ± 15.5 t ha^{-1}) and low average residence times (10.8 ± 6.8 years). In the RENECOFOR network, forests of silver fir were usually associated to mull humus formation on cambisol characterized by rapid litter decomposition.

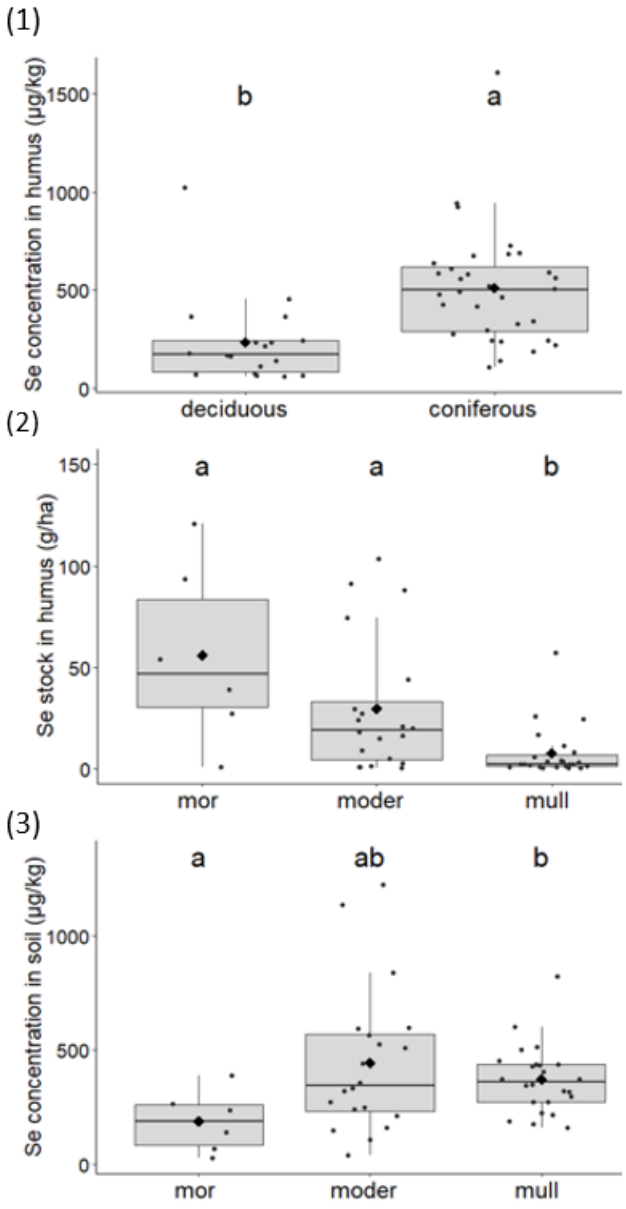

Figure art.1 – 4 Boxplot representations of: 1) Se concentrations in humus according to forest type; 2) Se stocks in humus according to humus type; 3) Se concentrations in soils according to humus type. Box plots show the first quartile (Q1), median and third quartile (Q3) of the data. Black diamond symbols represent average Se concentrations in groups. Lower and upper whiskers extend from the hinges by Q1 − 1.5 × IQR (IQR - interquartile range) and Q3 + 1.5 × IQR, respectively. Dots represent corresponding data. The different letters above the boxes correspond to significant differences between the groups according to pairwise Wilcoxon test, with Holm adjustment for p-value.

As a consequence of different litter decay rates, Se concentration in humus was strongly correlated with humus mass (Spearman rank test, rs=0.68, p-value <0.001). This resulted in lower humus Se stocks in oak, beech and silver fir forests (4 ± 6, 8 ± 15, 10 ± 9 g ha^{-1}) compared to Douglas fir, spruce and pine (16 ± 11, 47 ± 38, 41 ± 38 g ha^{-1}). It was reflected likewise in

the dependence of the Se humus stock on the type of humus. Mean Se stock in humus decreased in the order: mor > moder > mull according to decreasing humus biomass and increasing organic matter degradation rate (**Figure art.1 –4.2**, **Table art.1. – 1**). Selenium concentrations in soils followed opposite order with significantly lower concentrations in soils under mor compared to mull-humus formations (**Figure art.1 –4.3**) highlighting the importance of Se input from humus decomposition to the underlying soil layers. Selenium can be mobilized in the form of soluble (hydr)-oxyanions and/or organo-Se compounds (seleno-methionine (SeMet) and methane seleninic acid (MeSeOOH) (Tolu et al., 2014)) and colloidal OM of plant or microbial origin (Weng et al., 2011). Beside lower biomass and faster degradation, mull-humus formation is also characterized by higher microbial activity, which can lead to the release of volatile compounds such as H2Se, DMSe (dimethyl selenide) and DMDSe (dimethyl diselenide) into the atmosphere (Wessjohann et al., 2007).

The median Se accumulation rate in humus was 0.30 g ha^{-1} yr^{-1} with no clear distinction between coniferous and deciduous tree species (**Table art.1.SI – 3**). The highest accumulation rate, 1.57 g ha^{-1} yr^{-1}, was for the EPC08 site. For this site, a long lasting dry deposition from anthropogenic contamination may affect accumulation rate value. Generally, Se accumulation rates were positive, except for one beech forest site (HET55: -0.02 ± 0.01 g ha^{-1} yr^{-1}) for which Se concentrations in humus and litterfall were similar (57 ± 6 and 73 ± 8, respectively, **Table art.1.SI – 3**). Negative accumulation rates were reported for chlorine in beech and oak forests, while they were positive for chlorine in Douglas, fir, spruce, and pine forests (Redon et al., 2011), and for iodine in all tree species (Roulier et al., 2019). Negative accumulation rates were interpreted as a result of high humus decomposition rate and leaching, whereas positive accumulation rates reflect Se enrichment during the process of litterfall transformation into humus. The average rate of Se accumulation in humus (0.39 g ha^{-1} yr^{-1}) was similar to the average Se flux from litterfall (0.30 g ha^{-1} yr^{-1}), and the average rainfall Se flux (0.44 g ha^{-1} yr^{-1}). This suggests a partial humus enrichment by the capture of soluble Se from rain through sorptive accumulation. Beside the retention, Se of atmospheric origin is subject to losses by drainage and volatilization, but the contribution of each pathway remains unclear and needs further investigation.

To conclude, Se inventories in humus were mostly controlled by the litter decay process and the rate of organic matter decomposition and not directly by the input of Se to the forest floor.

3.4 Environmental variables influencing Se content in soil

The soil compartment was shown to be the main reservoir of Se. Tree species, climate and rock type were the most discriminating categorical variables (**Section 3.3**) to explain the variation in Se content in French forest soils. Although the ocean is an important reservoir of Se on a global scale, no direct correlation was found between Se concentration in soil and distance from the coast. Decreasing Se content was observed with the distance from the ocean in forest soil in Norway (Låg and Steinnes, 1978). Blazina et al. (2014) showed that over the last 6.8 million years the monsoonal climate had likely dominant role on atmospheric Se deposition and soil concentration in Chinese Loess Plateau. Winkel et al. (2015) highlighted the need for further research to determine the extent to which wet deposition influences soil Se levels on a large scale, although Se generally measured in wet deposition is not location-dependent. In our study higher Se concentrations in soil were only observed for the mountain climate compared to continental climate (**Figure art.1 – 5.1**, **Table art.1 – 2**). It may be due to reduced microbial activity and lower degradation rate of OM in colder climate or specific soil composition in the mountain climate. The former would have minor impact, as no dependence was observed between Se concentrations in humus and climate. The latter would be more important as mountainous soils had elevated total Fe, total Al and organic C contents (**Figure art.1.SI – 5-7**). Another co-correlation was found between climate and tree species, as Se-poor transition forest soils were dominated by pines and oaks, while Se-rich mountainous forest soils by Douglas. Summing up, the co-correlations between Fe, Al, C contents in soil, climate and tree species do not permit to determine which of these factors plays a dominant role in Se immobilization in soil.

No dependence was observed between Se concentrations in soil and soil type ($p > 0.05$, **Table art.1 – 2**), which may be due to large variability in soil composition within a soil type. Concerning the effect of bedrock material, soils derived from sedimentary rocks were in general poorer in Se than those from igneous rocks (**Figure art.1 – 5.2**, **Table art.1 – 1**), which is contrary to some statements in the literature (Sharma et al., 2015). Average Se level in igneous rocks was reported as 0.35 mg kg^{-1}, while the content in sedimentary rocks varies significantly within classification groups: 0.05 mg kg^{-1} in sandstone, 0.08 mg kg^{-1} in limestone and the highest values for rocks with high organic carbon content: 0.6 mg kg^{-1} for shale and 300 mg kg^{-1} for coal (Shahid et al., 2018). Thus, Se concentrations measured in 0–40 cm soil depth may not reflect the character of rock, especially for low-Se parent materials.

Additionally, as analyzed soils were from shallow soil layer (≤40 cm), Se input from litterfall and atmospheric depositions masks the influence of soil parent material weathering.

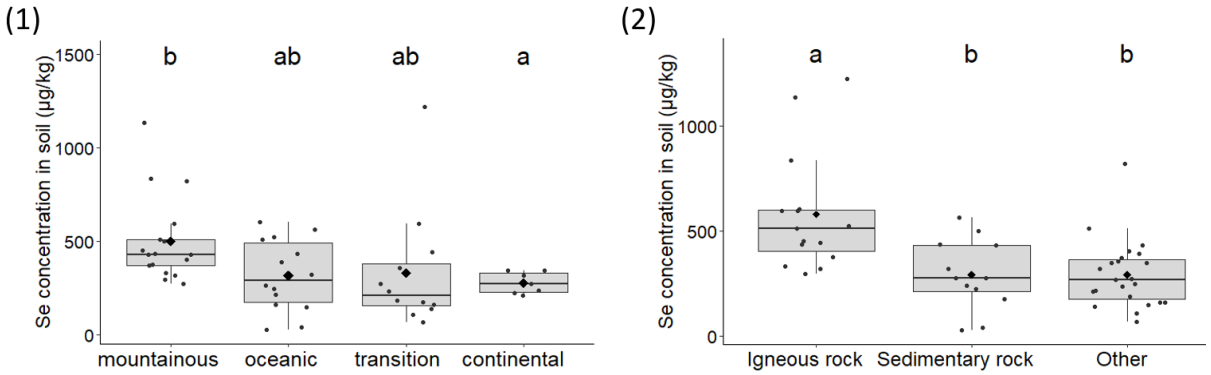

Figure art.1 – 5 Distribution of Se concentrations in soils according to 1) climate, and 2) rock type. Box plots show the first quartile (Q1), median and third quartile (Q3) of the data. Black diamond symbols represent average Se concentrations in groups. Lower and upper whiskers extend from the hinges by Q1 − 1.5 × IQR (IQR - interquartile range) and Q3 + 1.5 × IQR, respectively. Dots represent corresponding data. The different letters above the boxes correspond to significant differences between the groups according to pairwise Wilcoxon test, with Holm adjustment for p-value.

3.5 Effect of soil composition on Se content

A correlation matrix was first constructed with all numerical variables describing soil composition (**Table art.1.SI – 4**). The variables that were well correlated (Spearman rank test $r_s > 0.6$) with soil Se concentrations were total Al, total Fe, total N, organic C, and clay fraction. Moreover, there were also moderate correlations with soil exchangeable Al concentration, sand and silt fractions, and cation exchange capacity (CEC). PCA analysis was then used to depict the effect of soil composition on Se concentrations of individual soils. Sites EPC63 and EPC08 were excluded in PCA analysis because they showed peculiar characteristics, as highlighted by their position with respect to linear correlations between Se concentration and total Fe/Al and Corg (**Figure art.1.SI – 6**, $r^2 = 0.75$ and $r^2 = 0.62$, respectively). As previously discussed (Section 3.2), EPC08 was identified as a potentially contaminated site. The soil at EPC63 site was the only representative of Andosol, which is rare for French geographical location (about 1% in France) (Quantin, 2004).

The contribution of each variable to the first three principal components of PCA is presented in **Table art.1 – 2**. Further, the number of variables was reduced by removing co-correlated parameters. Therefore, organic C was selected as the sole representative of soil OM (elimination of total N) and total Fe as the sole representative of Fe/Al minerals (elimination

of total Al). Mn exchangeable was excluded as it contributed little to Dim 1 and Dim 2 components (**Table art.1 – 2**) and any significant effect (p-value >0.05) of soil exchangeable Mn on Se concentration was observed. It was not surprising as selenite is more readily released to liquid phase by anion-exchange mechanism from Mn oxides compared to goethite (Fe oxides) (Saeki and Matsumoto, 1994).

Table art.1 – 2 Contributions on the first three PC axes of i) all variables and ii) reduced number of variables.

Variables	i) contributions of all variables			ii) contribution of reduced number of variables		
	Dim.1	Dim.2	Dim.3	Dim.1	Dim.2	Dim.3
Fe tot	15.806	5.64E-05	0.067	21.585	5.498	0.610
Se	14.990	1.683	0.003	23.708	1.522	1.481
N	13.898	0.744	6.801	-	-	-
Al tot	12.761	3.301	3.463	-	-	-
C	12.262	5.510	5.761	19.620	0.378	17.124
Clay	8.555	11.535	0.071	-	-	-
Sand	6.962	12.615	9.032	3.853	17.197	50.116
Al exchang.	5.627	10.315	10.237	18.698	5.902	3.600
Slit	3.946	9.073	17.462	-	-	-
CEC	3.637	14.145	8.354	0.282	34.693	0.471
Mn exchang.	0.859	5.798	10.039	-	-	-
pH	0.364	9.701	26.421	5.268	20.562	23.163
Fe exchang.	0.333	15.580	2.288	6.987	14.248	3.435

exchang. – exchangeable

The first two principal components explained 73.0% of the variation (Dim1 41.6% and Dim2 31.4%). Selenium, Corg and Fe concentrations in soil were characterized by strongly positive coordinates on the Dim 1 axis (**Figure art.1 –6**). Moreover, PCA eigenvalues showed positive loads in the Dim1 for clay, Al exchangeable, CEC and Fe exchangeable variables. The second component was well described by pH and Fe exchangeable variables that were logically anti-correlated. Similar anti-correlation was observed between sand and clay fractions.

Soil samples were discriminated in three clusters of different Se concentrations: <235 μg kg^{-1}, 235–650 μg kg^{-1}, >650 μg kg^{-1}. Located on negative Dim 1, the first cluster with the lowest Se concentrations <235 μg kg^{-1}including 13 sites was characterized by soils with high contribution of sand and low Corg and Fe/Al content. This cluster includes mainly arenosols, podzols, and planosols in oceanic and transition climates with maritime pine and oak as the main tree species. In this cluster, sites PM17 and PM85 are two arenosols close to the ocean (≤ 2 km) with the lowest Se concentrations (25 μg kg^{-1} and 39 μg kg^{-1}, respectively). Their

position in the biplot is explained by their very high content of sand (99% and 96% respectively), high pH values (8.7 and 8.5 respectively), and low OM content (3.85 and 5.55 g kg^{-1} respectively). These results confirmed the importance of OM and Al/Fe content in Se retention and the fact that sand fraction is a weak Se carrier (Chi et al., 2019; Coppin et al., 2006; Saeki and Matsumoto, 1994).

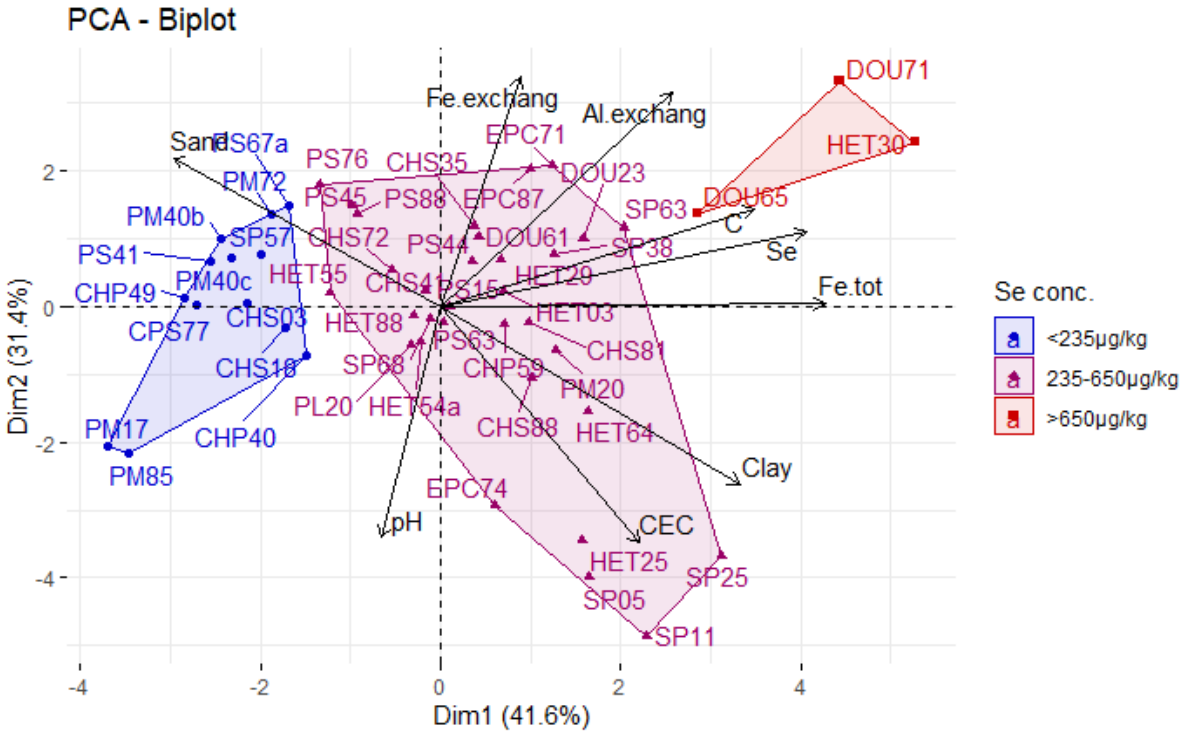

Figure art.1 – 6 PCA biplot representation of soil composition data on the first two PC axis. Individual soils (48 samples) are colored according to their Se concentration range: <235 µg kg^{-1} - blue, 235–650 µg kg^{-1} - violet, >650 µg kg^{-1} - red. Arrows represent contribution of soil geochemical numerical variables on principal component axes. (For interpretation of the references to color in this figure legend, the reader is referred to the web version of this article.)

At the opposite on the biplot graph, the three soils with the highest Se concentrations (>650 µg kg^{-1}; HET30, DOU71 and DOU65 sites) had positive coordinates on both dimensions axes associated with Se, Corg, total Fe and Al exchangeable variables. These soils are acidic podzols (HET30 and DOU 71) or cambisol (DOU65) in mountain climate with very high Corg (67–85 g kg^{-1}), Fe (8.7–14.3 g kg^{-1}) and Al (7.1–12.0 g kg^{-1}) contents. In our study the concentrations of organic C (and total N) were strongly correlated with those of total Fe and Al (**Table art.1.SI – 6**). Strong correlation between Se content and organic C concentration in soil is related to the ability of OM to interact with Se. Aluminium and Fe oxides remain protonated in a broad pH range and have relatively large surface area with densely arrayed functional groups. These

functional groups can also promote the formation of inner and outer sphere complexes with Se (Peak, 2006; Söderlund et al., 2016). Like in our study, hot spots of Se in soils were identified as co-located with Fe and Al contents suggesting possible indirect sorption on metals associated within OM surface or matrix (Coppin et al., 2009). Soils with medium Se concentrations (235–650 μg kg^{-1}) were gathered in the third cluster (32 sites for a total of 49). This cluster contains all types of soils (except the two arenosols discussed previously), tree species and climates. Within this cluster, a sub-group of 4 sites (SP25, SP11, SP05 and HET25) for three soil types (luvisol, cambisol and leptosol) was characterized by a strong contribution of clay fraction (35–50%) and neutral pH (5.76–7.21). With moderate Corg (23–31 g kg^{-1}) and Al/Fe content (from 1.9 to 5.1 g Al kg^{-1} and 4.2 to 9.7 g Fe kg^{-1}), they also exhibited moderately high Se concentrations (371–500 μg kg^{-1}).

Summarizing all of the above, our results confirm the strong relationships between Se and organic matter and Al/Fe constituents. However, it was not possible to clarify whether Fe/Al oxides or OM have a greater influence on Se sorption, as these variables were highly correlated and may act synergistically on Se retention.

The calculated selenium residence times in forest soils (t_{res}Se) were between 617 and 8406 years (median value 2735 years for n = 27 sites), which is higher than retention times of iodine (419–1756 years) and chlorine (3–67 years) for the same sites (Redon et al., 2011; Roulier et al., 2019). That pattern is in agreement with other results showing higher desorption distribution coefficients K_D in woodland for Se (41–1198 L kg^{-1} (Almahayni et al., 2017; Tolu et al., 2014)) compared to I (4–281 L kg^{-1}) as well as higher sorption coefficient K_D values for Se (4–2100 L kg^{-1}) than for I (0.01–580 L kg^{-1}) and Cl (0.04–1.2 L kg^{-1}) in all types of soils (IAEA, 2010). Summing up, radionuclide ^{79}Se has a highest potential to persist in soil compartment compared to the other radionuclides ^{129}I and ^{36}Cl. The broad range of t_{res}Se is a result of combinations of local environmental factors including input to soil, organic matter turnover, and soil properties.

4. Conclusions

In this study, the influence of environmental and geochemical conditions on Se accumulation in forest soil was analyzed. Selenium concentration in litterfall was linearly dependent on its concentration in rainfall with higher values near the coast, i.e. for oceanic climate. Deviation from correlation was observed for one site with very high concentration in litterfall (369 μg kg^{-1}) and was attributed to anthropogenic activities. The annual amount of selenium cycling

through litterfall was minor compared to Se stock in forest soils and, no direct correlation was found between the two. The higher Se concentrations of recalcitrant mor humus compared to easily degradable mull humus highlighted that organic matter degradation rate likely controls Se content in humus and more generally in soils. In forest soils, the content of organic matter and Fe/Al oxides had pivotal role among all soil constituents in long-term Se retention. Thus, acidic soils rich in organic matter and Fe/Al oxides under Douglas fir and beech forests in mountain climate are the soil properties and environmental conditions that promote the persistence of Se in forest soils.

CRediT authorship contribution statement

Paulina Pisarek: Conceptualization, Investigation, Validation, Formal analysis, Writing – original draft, Writing – review & editing. Maïté Bueno: Conceptualization, Investigation, Validation, Funding acquisition, Writing – review & editing, Supervision. Yves Thiry: Conceptualization, Validation, Funding acquisition, Writing – review & editing, Supervision. Manuel Nicolas: Resources, Writing – review & editing. Hervé Gallard: Conceptualization, Investigation, Validation, Writing – review & editing, Funding acquisition, Supervision. Isabelle Le Hécho: Conceptualization, Writing – review & editing, Funding acquisition, Supervision.

Acknowledgements

The authors would like to thank all technical support from the RENECOFOR-ONF network, which provided the collection of samples and sites data. We wish to acknowledge M. Roulier for her guidance with statistical program.
This research was financially supported by the French National Agency for Radioactive Waste Management (Andra).

References

Almahayni, T., Bailey, E., Crout, N.M.J., Shaw, G., 2017. Effects of incubation time and filtration method on Kd of indigenous selenium and iodine in temperate soils. J. Environ. Radioact. 177, 84–90. https://doi.org/10.1016/j.jenvrad.2017.06.004

Amouroux, D., Liss, P.S., Tessier, E., Hamren-Larsson, M., Donard, O.F.X., 2001. Role of oceans as biogenic sources of selenium. Earth Planet. Sci. Lett. 189, 277–283. https://doi.org/10.1016/S0012-821X(01)00370-3

Belon, E., Boisson, M., Deportes, I.Z., Eglin, T.K., Feix, I., Bispo, A.O., Galsomies, L., Leblond, S., Guellier, C.R., 2012. An inventory of trace elements inputs to French agricultural soils. Sci. Total Environ. 439, 87–95. https://doi.org/10.1016/j.scitotenv.2012.09.011

Blazina, T., Sun, Y., Voegelin, A., Lenz, M., Berg, M., Winkel, L.H.E., 2014. Terrestrial selenium distribution in China is potentially linked to monsoonal climate. Nat. Commun. 5, 1–7. https://doi.org/10.1038/ncomms5717

Brêthes A., Urlich E., 1997. Caractéristiques pédologiques des 102 peuplements du réseau. - Office national de forêts, Dépt des recherches Techniques.

Broadley, M.R., White, P.J., Bryson, R.J., Meacham, M.C., Bowen, H.C., Johnson, S.E., Hawkesford, M.J., McGrath, S.P., Zhao, F.-J., Breward, N., Harriman, M., Tucker, M., 2006. Biofortification of UK food crops with selenium. Proc. Nutr. Soc. 65, 169–181. https://doi.org/10.1079/pns2006490

Chasteen, T.G., Bentley, R., 2003. Biomethylation of selenium and tellurium: microorganisms and plants. Chem. Rev. 103, 1–25. https://doi.org/10.1021/cr010210+

Chi, F.Q., Kuang, E.J., Zhang, J.M., Su, Q.R., Chen, X.L., Zhang, Y.W., Liu, Y.D., Kuang, E.J., Zhang, J.M., Su, Q.R., Chen, X.L., Zhang, Y.W., Liu, Y.D., 2019. Fractionation and distribution of soil selenium and effects of soil properties in Heilongjiang. Selenium Research for Environment and Human Health: Perspectives, Technologies and Advancements. https://doi.org/10.1201/9780429423482-9

Coppin, F., Chabroullet, C., Martin-Garin, A., 2009. Selenite interactions with some particulate organic and mineral fractions isolated from a natural grassland soil. EJSS 60, 369–376. https://doi.org/10.1111/j.1365-2389.2009.01127.x

Coppin, F., Chabroullet, C., Martin-Garin, A., Balesdent, J., Gaudet, J.P., 2006. Methodological approach to assess the effect of soil ageing on selenium behaviour: first results concerning mobility and solid fractionation of selenium. Biol. Fertil. Soils 42, 379–386. https://doi.org/10.1007/s00374-006-0080-y

Cumbers, A., Birch, K., MacKinnon, D., 2006. Revisiting the Old Industrial Region: Adaptation and Adjustment in an Integrating Europe. CPPR Working Paper 1. University of Glasgow.

Di Tullo, P., 2015. Dynamique du cycle biogéochimique du sélénium en écosystèmes terrestres : rétention et réactivité dans le sol, rôle de la végétation (thesis). Pau.

Dinh, Q.T., Li, Z., Tran, T.A.T., Wang, D., Liang, D., 2017. Role of organic acids on the bioavailability of selenium in soil: A review. Chemosphere 184, 618–635. https://doi.org/10.1016/j.chemosphere.2017.06.034.

El Mehdawi, A.F., Pilon-Smits, E. a. H., 2012. Ecological aspects of plant selenium hyperaccumulation. Plant Biol. (Stuttg) 14, 1–10. https://doi.org/10.1111/j.1438-8677.2011.00535.x

Hjerpe, T., Broed, R., 2010. Radionuclide transport and dose assessment modelling in biosphere assessment 2009 (No. POSIVA-WR--10-79). Posiva Oy.

IAEA, 2010. Handbook of Parameter Values for the Prediction of Radionuclide Transfer in Terrestrial and Freshwater Environment.

Jonard, M., Nicolas, M., Coomes, D.A., Caignet, I., Saenger, A., Ponette, Q., 2017. Forest soils in France are sequestering substantial amounts of carbon. Sci. Total Environ. 574, 616–628. https://doi.org/10.1016/j.scitotenv.2016.09.028

Låg, J., Steinnes, E., 1978. Regional distribution of selenium and arsenic in humus layers of Norwegian forest soils. Geoderma 20, 3–14. https://doi.org/10.1016/0016-7061(78)90045-9

Li, Z., Liang, D., Peng, Q., Cui, Z., Huang, J., Lin, Z., 2017. Interaction between selenium and soil organic matter and its impact on soil selenium bioavailability: A review. Geoderma 295, 69–79. https://doi.org/10.1016/j.geoderma.2017.02.019

Martin, D.P., Seiter, J.M., Lafferty, B.J., Bednar, A.J., 2017. Exploring the ability of cations to facilitate binding between inorganic oxyanions and humic acid. Chemosphere 166, 192–196. https://doi.org/10.1016/j.chemosphere.2016.09.084

Osono, T., Takeda, H., 2005. Limit values for decomposition and convergence process of lignocellulose fraction in decomposing leaf litter of 14 tree species in a cool temperate forest. Ecol. Res. 20, 51–58. https://doi.org/10.1007/s11284-004-0011-z

Pauget, B., Gimbert, F., Coeurdassier, M., Crini, N., Pérès, G., Faure, O., Douay, F., Hitmi, A., Beguiristain, T., Alaphilippe, A., Guernion, M., Houot, S., Legras, M., Vian, J.F., Hedde, M., Bispo, A., Grand, C., de Vaufleury, A., 2013. Ranking field site management priorities according to their metal transfer to snails. Ecol. Indic. 29, 445–454. https://doi.org/10.1016/j.ecolind.2013.01.012

Peak, D., 2006. Adsorption mechanisms of selenium oxyanions at the aluminum oxide/water interface. J. Colloid Interface Sci. 303, 337–345. https://doi.org/10.1016/j.jcis.2006.08.014

Prescott, C.E., Zabek, L.M., Staley, C.L., Kabzems, R., 2000. Decomposition of broadleaf and needle litter in forests of British Columbia: influences of litter type, forest type, and litter mixtures. Can. J. For. Res. 30, 1742–1750. https://doi.org/10.1139/x00-097

Probst A., Hernandez L., Fevrier-Vauleon C., Prudent P., Probst J., Party J., 2003. Eléments traces métalliques dans les sols des écosystèmes forestiers français : distribution et facteurs de contrôle utilisation du réseau RENECOFOR. Office National des Forêts, Direction Technique.

Quantin, P., 2004. Volcanic soils of France. CATENA, Volcanic Soil Resources: Occurrence, Development and Properties 56, 95–109. https://doi.org/10.1016/j.catena.2003.10.019

Rayman, M.P., 2000. The importance of selenium to human health. Lancet 356, 233–241. https://doi.org/10.1016/S0140-6736(00)02490-9

Redon, P.O., Abdelouas, A., Bastviken, D., Cecchini, S., Nicolas, M., Thiry, Y., 2011. Chloride and organic chlorine in forest soils: storage, residence times, and influence of ecological conditions. Environ. Sci. Technol. 45, 7202–7208. https://doi.org/10.1021/es2011918

Reimann, C., Englmaier, P., Fabian, K., Gough, L., Lamothe, P., Smith, D., 2015. Biogeochemical plant–soil interaction: Variable element composition in leaves of four plant species collected along a south–north transect at the southern tip of Norway. Sci. Total Environ. 506–507, 480–495. https://doi.org/10.1016/j.scitotenv.2014.10.079

Ross, H.B., 1985. An atmospheric selenium budget for the region 30° N to 90° N. Tellus B: Chem. Phys. Meteorol. 37, 78–90. https://doi.org/10.3402/tellusb.v37i2.14999

Roulier, M., 2018. Cycle biogéochimique de l'iode en écosystèmes forestiers (thesis). http://www.theses.fr. Pau.

Roulier, M., Bueno, M., Coppin, F., Nicolas, M., Thiry, Y., Rigal, F., Le Hécho, I., Pannier, F., 2020. Atmospheric iodine, selenium and caesium depositions in France: I. Spatial and seasonal variations. Chemosphere 128971. https://doi.org/10.1016/j.chemosphere.2020.128971

Roulier, M., Coppin, F., Bueno, M., Nicolas, M., Thiry, Y., Della Vedova, C., Février, L., Pannier, F., Le Hécho, I., 2019. Iodine budget in forest soils: Influence of environmental conditions and soil physicochemical properties. Chemosphere 224, 20–28. https://doi.org/10.1016/j.chemosphere.2019.02.060

Saeki, K., Matsumoto, S., 1994. Selenite adsorption by a variety of oxides. Soil. Sci. Plant Anal. 25, 2147–2158. https://doi.org/10.1080/00103629409369178

Sharma, V.K., McDonald, T.J., Sohn, M., Anquandah, G.A.K., Pettine, M., Zboril, R., 2015. Biogeochemistry of selenium. A review. Environ. Chem. Lett. 13, 49–58. https://doi.org/10.1007/s10311-014-0487-x

Shahid, N., Shahid, M., Niazi, N.K., Khalid, S., Murtaza, B., Bibi, I., Rashid, M.I., 2018. A critical review of selenium biogeochemical behavior in soil-plant system with an inference to human health. Environ. Pollut. 234, 915–934. https://doi.org/10.1016/j.envpol.2017.12.019

Söderlund, M., Virkanen, J., Holgersson, S., Lehto, J., 2016. Sorption and speciation of selenium in boreal forest soil. J. Environ. Radioact. 164, 220–231. https://doi.org/10.1016/j.jenvrad.2016.08.006

Suess, E., Aemisegger, F., Sonke, J.E., Sprenger, M., Wernli, H., Winkel, L.H.E., 2019. Marine versus Continental Sources of Iodine and Selenium in Rainfall at Two European High-Altitude Locations. Environ. Sci. Technol. 53, 1905–1917. https://doi.org/10.1021/acs.est.8b05533

Sun, G.X., Meharg, A.A., Li, G., Chen, Z., Yang, L., Chen, S.C., Zhu, Y.G., 2016. Distribution of soil selenium in China is potentially controlled by deposition and volatilization? Scient. Rep. 6. https://doi.org/10.1038/srep20953

Supriatin, S., Weng, L., Comans, R.N.J., 2015. Selenium speciation and extractability in Dutch agricultural soils. Sci. Total Environ. 532, 368–382. https://doi.org/10.1016/j.scitotenv.2015.06.005

Taylor, S.R., McLennan, S.M., 1995. The geochemical evolution of the continental crust. Rev. Geophys. 33, 241–265. https://doi.org/10.1029/95RG00262

Tolu, J., 2012. Spéciation et mobilité du sélénium présent dans les sols à l'état de traces : contribution aux prévisions à long terme (thesis). Pau.

Tolu, J., Le Hécho, I., Bueno, M., Thiry, Y., Potin-Gautier, M., 2011. Selenium speciation analysis at trace level in soils. Anal. Chim. Acta 684, 126–133. https://doi.org/10.1016/j.aca.2010.10.044

Tolu, J., Thiry, Y., Bueno, M., Jolivet, C., Potin-Gautier, M., Le Hécho, I., 2014. Distribution and speciation of ambient selenium in contrasted soils, from mineral to organic rich. Sci. Total Environ. 479–480, 93–101. https://doi.org/10.1016/j.scitotenv.2014.01.079

Tyler, G., 2005. Changes in the concentrations of major, minor and rare-earth elements during leaf senescence and decomposition in a Fagus sylvatica forest. For. Ecol. Manag. 206, 167–177. https://doi.org/10.1016/j.foreco.2004.10.065

Ulrich, E., Coddeville, P., Lanier, M., 2002. Retombées atmosphériques humides en France entre 1993 et 1998. ADEME, Paris.

Wang, S., Liang, D., Wang, D., Wei, W., Fu, D., Lin, Z., 2012. Selenium fractionation and speciation in agriculture soils and accumulation in corn (Zea mays L.) under field conditions in Shaanxi Province, China. Sci. Total Environ. 427–428, 159–164. https://doi.org/10.1016/j.scitotenv.2012.03.091

Weng, L., Vega, F.A., Supriatin, S., Bussink, W., Riemsdijk, W.H.V., 2011. Speciation of Se and DOC in Soil Solution and Their Relation to Se Bioavailability. Environ. Sci. Technol. 45, 262–267. https://doi.org/10.1021/es1016119

Wessjohann, L.A., Schneider, A., Abbas, M., Brandt, W., 2007. Selenium in chemistry and biochemistry in comparison to sulfur. Biol. Chem. 388, 997–1006. https://doi.org/10.1515/BC.2007.138

Winkel, L.H.E., Vriens, B., Jones, G.D., Schneider, L.S., Pilon-Smits, E., Bañuelos, G.S., 2015. Selenium Cycling Across Soil-Plant-Atmosphere Interfaces: A Critical Review. Nutrients 7, 4199–4239. https://doi.org/10.3390/nu7064199

.

Supplementary information

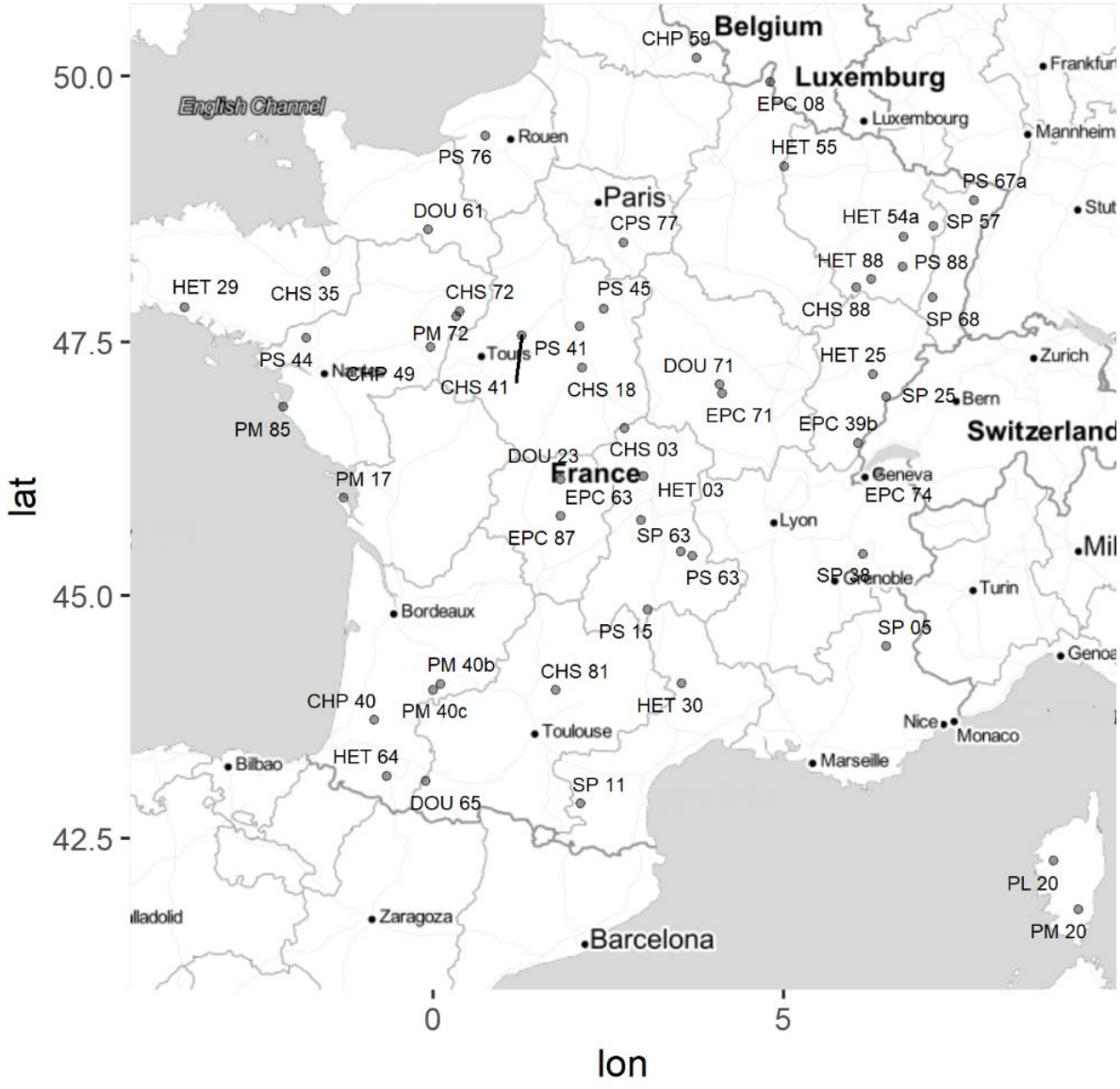

Figure art.1.SI – 1 Map of studied forest sites of the French RENECOFOR network. CHP=Pedunculate Oak; CHS=Sessile Oak; CPS=Sessile/Ped. Oak; DOU=Douglas fir; EPC=Spruce; HET=Beech; PL=Black Pine; PM=Maritime Pine; PS=Scots Pine; SP=Silver fir. The numbers correspond to number of French administrative departments

Table art.1.SI – 1 Environmental and geogenic characteristics of sites.

Forest site[1]	Dominant tree species[1]	Climate[1,2]	Coast distance (km)[3]	Humus form[1,4]	Soil type[1,5]	Geological type
CHP40	Pedunculate Oak	Oceanic	47	Eumull	Cambisol	Other
CHP49	Pedunculate Oak	Oceanic	323	Oligomull	Planosol	Other
CHP59	Pedunculate Oak	Oceanic	131	Mesomull	Podzoluvisol	Other
CHS03	Sessile Oak	Transition	655	Mesomull	Cambisol	Sedimentary rock
CHS18	Sessile Oak	Transition	377	Oligomull	Luvisol	Other
CHS35	Sessile Oak	Oceanic	232	Dysmoder	Luvisol	Igneous rock
CHS41	Sessile Oak	Transition	271	Moder	Luvisol	Other
CHS72	Sessile Oak	Oceanic	212	Moder	Planosol	Other
CHS81	Sessile Oak	Transition	243	Oligomull	Luvisol	Sedimentary rock
CHS88	Sessile Oak	Continental	633	Eumull	Cambisol	Sedimentary rock
CPS77	Sessile/Ped. Oak	Transition	381	Moder	Podzol	Other
DOU23	Douglas fir	Transition	235	Hemimoder	Cambisol	Igneous rock
DOU61	Douglas fir	Oceanic	99	Moder	Luvisol	Sedimentary rock
DOU65	Douglas fir	Mountain	126	Dysmull	Cambisol	Other
DOU71	Douglas fir	Mountain	478	Dysmoder	Podzol	Igneous rock
EPC08	Spruce	Transition	214	Moder	Podzol	Igneous rock
EPC39b	Spruce	Mountain	379	Dysmull	Leptosol	Sedimentary rock
EPC63	Spruce	Mountain	278	Dysmull	Andosol	Igneous rock
EPC71	Spruce	Mountain	385	Moder	Podzol	Igneous rock
EPC74	Spruce	Mountain	343	Mesomull	Luvisol	Igneous rock
EPC87	Spruce	Transition	231	Hemimoder	Cambisol	Igneous rock
HET03	Beech	Mountain	365	Oligomull	Cambisol	Other
HET25	Beech	Mountainous	631	Eumull	Cambisol	Sedimentary rock
HET29	Beech	Oceanic	8	Dysmoder	Luvisol	Igneous rock
HET30	Beech	Mountain	77	Dysmoder	Podzol	Igneous rock
HET54a	Beech	Continental	721	Mesomull	Planosol	Other
HET55	Beech	Continental	601	Hemimoder	Podzol	Sedimentary rock
HET64	Beech	Mountain	85	Oligomull	Cambisol	Sedimentary rock
HET88	Beech	Continental	619	Mésomull	Cambisol	Other
PL20	Black Pine	Mountain/Med.	13	Mésomull	Cambisol	Igneous rock
PM17	Maritime Pine	Oceanic	1	Mor	Arenosol	Sedimentary rock
PM20	Maritime Pine	Mediterranean	17	Amphimull	Cambisol	Igneous rock
PM40b	Maritime Pine	Transition	115	Mor	Podzol	Other
PM40c	Maritime Pine	Transition	106	Moder	Podzol	Other
PM72	Maritime Pine	Oceanic	205	Dysmoder	Planosol	Other
PM85	Maritime Pine	Oceanic	1	Moder	Arenosol	Sedimentary rock
PS15	Scots Pine	Mountain	177	Moder	Cambisol	Igneous rock
PS41	Scots Pine	Transition	302	Mor	Podzol	Other
PS44	Scots Pine	Oceanic	34	Mor	Luvisol	Other
PS45	Scots Pine	Transition	330	Mor	Planosol	Other
PS63	Scots Pine	Mountain	206	Dysmull	Cambisol	Igneous rock
PS67a	Scots Pine	Continental	817	Moder	Podzol	Other
PS76	Scots Pine	Oceanic	36	Mor	Podzol	Other
PS88	Scots Pine	Mountain	532	Dysmoder	Podzol	Sedimentary rock
SP05	Silver fir	Mountain	182	Oligomull	Cambisol	Other
SP11	Silver fir	Mountain	77	Mesomull	Luvisol	Other
SP25	Silver fir	Mountain	411	Mesomull	Leptosol	Sedimentary rock
SP38	Silver fir	Mountain	260	Amphimull	Cambisol	Other
SP57	Silver fir	Continental	775	Oligomull	Cambisol	Sedimentary rock
SP63	Silver fir	Mountain	238	Moder	Cambisol	Igneous rock
SP68	Silver fir	Continental	476	Mesomull	Cambisol	Other

[1]From Redon et al.(2011); [2] METEO FRANCE, (http://www.meteofrance.fr/climat-passe-et-futur/climat-en-france/le-climat-en-metropole (accessed 4.22.20).) [3]Estimated from www.google.fr/maps; [4]Classification according to the Référence Pédologique (AFES, 2009); [5]Classification according to WRB/FAO;

Table art.1.SI – 2 Physical and chemical properties and masses of soil, humus and litterfall (LF); residence time of humus biomass (t_{resDM}). Data was provided by ONF – RENECOFOR.

Forest site	Soil													Humus			LF
	Density g cm^{-3}	pH	CEC cmol kg^{-1}	C_{org} g kg^{-1}	N g kg^{-1}	Clay fc %	Silt fc %	Sand fc %	Al[1] g kg^{-1}	Al exchang. (cmol kg^{-1}) [1]	Fe (g kg^{-1}) [1]	Fe exchang. cmol kg^{-1} [1]	Mn exchan. cmol kg^{-1} [1]	C_{org} g kg^{-1}	Mass t ha^{-1}	t_{resDM} year	Mass t ha^{-1}yr^{-1}
CHP40	1.28	5.07	2.65	10.69	0.90	13	43	44	0.76	0.60	2.24	0.02	0.03	339	2.42	1.1	3.98
CHP49	1.57	4.77	1.17	5.30	0.43	3	8	89	0.34	0.59	0.86	0.01	0.09	434	25.43	9.2	4.87
CHP59	1.16	4.74	6.23	15.65	1.25	18	77	5	2.02	3.20	5.30	0.05	0.08	381	6.93	2.1	5.86
CHS03	1.17	4.49	1.37	12.13	0.58	10	17	73	1.03	0.95	0.92	0.01	0.11	331	9.98	3.6	4.81
CHS18	1.42	4.53	1.35	9.46	0.51	14	38	48	0.83	1.00	1.08	0.01	0.03	423	21.89	9.2	4.19
CHS35	1.09	4.44	2.50	15.65	0.93	16	53	31	1.43	2.72	3.48	0.12	0.03	409	45.67	16.8	4.77
CHS41	1.31	4.44	3.75	13.83	0.81	15	54	31	1.36	2.99	3.11	0.04	0.07	509	6.15	2.0	5.51
CHS72	1.30	4.60	2.50	11.76	0.52	12	66	22	1.10	2.54	2.78	0.09	0.09	427	6.81	2.9	4.18
CHS81	1.17	4.71	5.63	20.90	1.34	25	64	11	2.90	4.58	4.95	0.02	0.05	434	6.09	2.6	4.10
CHS88	1.06	4.86	4.36	17.36	1.09	41	52	7	2.69	3.49	3.55	0.01	0.06	390	3.94	1.3	5.26
CPS77	1.35	4.83	0.67	8.67	0.52	5	13	82	0.64	0.45	0.58	0.01	0.14	317	26.21	10.0	4.62
DOU23	0.57	4.51	3.57	60.40	4.63	19	23	58	8.26	3.22	5.40	0.03	0.02	326	24.00	23.7	3.38
DOU61	1.07	4.36	3.16	21.08	1.08	10	45	45	3.08	3.12	4.69	0.06	0.07	332	29.00	53.2	1.82
DOU65	0.49	4.44	4.54	68.02	5.00	16	28	56	11.24	3.77	8.69	0.02	0.06	491	4.96	6.2	2.65
DOU71	0.27	4.29	5.99	85.45	4.10	18	24	58	12.04	6.33	10.53	0.15	0.06	381	40.10	67.4	1.98
EPC08	0.76	4.30	4.00	28.22	2.10	29	62	9	4.81	3.49	6.43	0.13	0.04	461	64.39	50.9	3.24
EPC39b	-	-	-	-	-	-	-	-	-	-	-	-	-	460	60.52	138.1	1.12
EPC63	0.41	5.22	3.91	85.84	6.61	30	48	22	40.17	2.32	19.83	0.07	0.09	356	44.34	23.7	4.80
EPC71	0.59	4.52	3.78	40.14	1.72	14	23	63	5.89	4.27	5.00	0.12	0.02	356	122.67	87.3	3.60
EPC74	0.99	6.18	16.54	31.05	2.37	34	29	37	1.44	0.32	3.68	0.01	0.04	404	8.77	3.5	6.38
EPC87	0.69	4.57	4.06	40.22	2.59	18	14	68	5.38	5.06	4.22	0.11	0.00	400	32.29	21.5	3.84
HET03	0.85	4.32	3.67	14.69	1.04	24	30	46	3.46	3.48	5.41	0.01	0.25	446	16.15	12.6	3.61
HET25	1.00	6.19	17.52	26.96	2.37	35	64	1	5.10	0.15	5.52	0.00	0.04	412	4.73	3.1	4.32
HET29	0.92	4.51	3.65	26.76	1.34	18	45	37	3.03	2.58	4.15	0.07	0.01	464	24.39	16.8	4.10
HET30	0.45	4.58	5.73	67.49	3.17	25	27	48	7.09	4.88	14.27	0.13	0.05	347	42.99	40.8	2.98
HET54a	0.88	4.60	3.72	16.80	1.07	17	59	24	2.00	1.95	3.35	0.00	0.33	342	9.98	6.0	4.67
HET55	1.33	4.56	3.02	12.38	0.67	10	41	49	0.77	2.45	1.64	0.02	0.07	452	8.37	6.4	3.68
HET64	1.11	4.84	6.04	14.60	1.34	41	49	10	3.27	1.99	7.85	0.01	0.27	479	8.51	6.9	3.48
HET88	1.04	4.67	3.81	14.40	0.85	22	30	48	2.67	3.13	2.59	0.01	0.15	392	10.29	6.6	4.42

Forest site	Soil													Humus			LF
	Density g cm^{-3}	pH	CEC cmol kg^{-1}	C_{org} g kg^{-1}	N g kg^{-1}	Clay fc %	Silt fc %	Sand fc %	Al^{1} g kg^{-1}	Al exchang. (cmol kg^{-1}) [1]	Fe (g kg^{-1}) [1]	Fe exchang. cmol kg^{-1} [1]	Mn exchan. cmol kg^{-1} [1]	C_{org} g kg^{-1}	Mass t ha^{-1}	t_{resDM} year	Mass t ha^{-1}
PL20	1.04	5.44	3.64	25.33	0.87	17	23	60	5.50	1.05	4.30	0.01	0.08	421	13.91	22.1	4.21
PM17	1.41	8.70	4.22	3.85	0.18	1	0	99	0.00	0.00	0.38	0.00	0.00	251	92.50	183.0	3.37
PM20	0.62	5.62	5.65	53.16	2.38	20	35	45	10.02	1.01	6.01	0.01	0.07	398	30.51	53.7	3.79
PM40b	1.30	4.13	3.31	31.13	0.85	1	2	97	0.15	0.87	0.19	0.05	0.00	484	9.96	13.3	4.97
PM40c	1.36	4.53	2.77	23.45	0.86	5	2	93	1.12	1.72	0.09	0.03	0.00	480	8.33	11.5	4.81
PM72	1.09	4.35	2.50	25.67	0.84	4	11	85	0.79	1.49	0.99	0.09	0.00	372	49.90	120.3	2.77
PM85	1.35	8.55	5.77	5.55	0.26	2	2	96	0.01	0.00	0.39	0.00	0.00	101	130.22	305.0	2.85
PS15	0.80	4.89	3.47	26.33	1.60	20	25	55	5.73	2.48	5.25	0.02	0.10	398	20.42	38.4	3.54
PS41	1.35	4.61	1.40	6.39	0.37	4	9	87	0.80	1.13	1.11	0.05	0.01	421	83.65	130.9	4.26
PS44	0.97	4.28	5.01	32.82	1.35	18	55	27	1.97	3.78	0.82	0.05	0.00	444	92.93	160.5	3.86
PS45	1.18	4.34	5.84	14.87	0.64	10	20	70	1.06	2.78	1.52	0.14	0.00	259	184.64	328.8	3.74
PS63	0.54	5.00	3.92	22.49	1.06	23	31	46	2.77	2.35	3.51	0.03	0.10	401	27.60	61.7	2.98
PS67a	1.24	4.27	2.48	19.42	0.92	7	3	90	1.89	2.08	1.30	0.09	0.01	381	143.02	199.7	4.77
PS76	0.90	4.20	1.87	11.94	0.39	7	24	69	1.10	1.51	2.09	0.16	0.02	348	166.60	333.3	3.33
PS88	1.02	4.43	2.28	13.60	0.52	12	12	76	3.44	2.28	3.67	0.11	0.00	382	95.69	200.3	3.18
SP05	0.88	6.18	20.31	29.58	2.51	46	47	7	1.87	0.03	4.19	0.00	0.06	337	28.08	13.2	4.37
SP11	1.27	7.24	25.22	22.69	1.94	45	53	2	2.90	0.07	7.06	0.01	0.08	474	5.04	5.0	2.08
SP25	0.93	5.76	19.76	31.09	2.50	50	48	2	4.16	0.52	9.69	0.00	0.21	347	10.42	4.8	4.44
SP38	0.58	4.37	5.87	29.49	1.68	18	35	47	3.35	3.69	7.97	0.06	0.12	290	47.38	23.4	4.16
SP57	1.11	4.50	2.15	12.72	0.61	6	9	85	1.29	1.67	1.26	0.04	0.16	401	13.20	12.4	2.19
SP63	0.66	4.23	6.03	39.91	2.12	36	27	37	4.01	5.25	5.75	0.11	0.08	398	30.77	12.5	5.06
SP68	0.70	4.80	4.09	27.92	1.68	15	49	36	3.87	2.15	4.22	0.02	0.06	419	7.39	4.6	3.29

Table art.1.SI – 3 Selenium concentrations and stocks in soil, humus and litterfall (LF), Se flux from litterfall, Se accumulation rates in humus, and Se retention time in forest soil.

Forest site	Se concentration µg kg^{-1}			Se stock g ha^{-1}		Se flux g ha^{-1} yr^{-1}	Se acc. rate g ha^{-1} yr^{-1}	t_{resSe} years
	Soil	Humus	LF	Soil	Humus	LF		
CHP 40	216 ± 22	-	93 ± 12	1106 ± 113	-	0.37 ± 0.05	-	2124
CHP 49	160 ± 21	167 ± 10	87 ± 9	1008 ± 135	4.2 ± 0.2	0.42 ± 0.05	0.22 ± 0.04	
CHP 59	320 ± 23	364 ± 18	116 ± 12	1481 ± 106	2.5 ± 0.1	0.68 ± 0.07	0.83 ± 0.07	4415
CHS 03	176 ± 22	73 ± 9	22 ± 3	823 ± 102	0.7 ± 0.1	0.11 ± 0.01	0.14 ± 0.03	
CHS 18	186 ± 20	177 ± 12	57 ± 6	1051 ± 112	3.9 ± 0.3	0.24 ± 0.03	0.29 ± 0.03	
CHS 35	509 ± 40	454 ± 44	67 ± 9	2222 ± 175	20.7 ± 2.0	0.32 ± 0.04	1.05 ± 0.12	8406
CHS 41	357 ± 26	160 ± 12	59 ± 7	1873 ± 138	1.0 ± 0.1	0.33 ± 0.04	0.32 ± 0.04	6747
CHS 72	246 ± 25	235 ± 13	57 ± 6	1284 ± 132	1.6 ± 0.1	0.24 ± 0.03	0.43 ± 0.03	
CHS 81	273 ± 25	141 ± 12	52 ± 7	1279 ± 116	0.9 ± 0.1	0.21 ± 0.03	0.21 ± 0.03	
CHS 88	317 ± 23	215 ± 23	89 ± 9	1340 ± 97	0.8 ± 0.1	0.47 ± 0.05	0.38 ± 0.07	
CPS 77	160 ± 14	111 ± 27	56 ± 5	865 ± 74	2.9 ± 0.7	0.26 ± 0.02	0.15 ± 0.07	3479
oak	***265 ± 104***	***210 ± 112***	***68 ± 26***	***1303 ±424***	***3.9 ± 5.8***	***0.33 ± 0.15***	***0.40 ±0.29***	
DOU 23	597 ± 37	674 ± 70	102 ± 10	1361 ± 84	16.2 ± 1.7	0.35 ± 0.03	0.58 ± 0.07	
DOU 61	563 ± 36	687 ± 60	144 ± 14	2412 ± 155	19.9 ± 1.7	0.26 ± 0.02	0.30 ± 0.03	
DOU 65	820 ± 51	478 ± 40	133 ± 11	1597 ± 100	2.4 ± 0.2	0.35 ± 0.03	0.27 ± 0.03	
DOU 71	836 ± 62	684 ± 55	64 ± 7	917 ± 68	27.4 ± 2.2	0.13 ± 0.01	0.37 ± 0.03	2436
Douglas	***704 ± 134***	***631 ± 105***	***111 ± 33***	***1572 ± 554***	***16.5 ±9.2***	***0.27 ±0.09***	***0.38 ±0.12***	
EPC 08	1222 ± 149	1608 ± 127	369 ± 23	3702 ± 451	103.5 ± 8.2	1.20 ± 0.08	1.57 ± 0,16	7153
EPC 39b	-	943 ± 77	53 ± 5	-	57.1 ± 4.7	0.06 ± 0.01	0.39 ± 0,03	
EPC 63	451 ± 50	586 ± 47	35 ± 4	731 ± 81	26.0 ± 2.1	0.17 ± 0.02	1.03 ± 0,09	2706
EPC 71	594 ± 62	608 ± 49	73[a] ± 7	1405 ± 146	74.6 ± 6.0	0.26 ± 0.02	0.75 ± 0,07	
EPC 74	295 ± 19	238 ± 21	73 ± 11	1169 ± 76	2.1 ± 0.2	0.47 ± 0.07	0.41 ± 0,06	4132
EPC 87	442 ± 31	562 ± 42	54 ± 7	1227 ± 87	18.1 ± 1.3	0.21 ± 0.03	0.76 ± 0,06	2694
spruce	***601 ± 334***	***758 ±437***	***110 ± 117***	***1647 ±1074***	***46.9 ± 35.3***	***0.39 ± 0.38***	***0.82 ±0.41***	
HET 03	511 ± 49[a]	68 ± 7	45 ± 4	1741 ± 167	1.1 ± 0.1	0.16 ± 0.02	0.03 ± 0,01	
HET 25	435 ± 41	63[a] ± 7	46 ± 5	1733 ± 164	0.30 ± 0.05	0.20 ± 0.02	0.03 ± 0,01	
HET 29	524 ± 47	365 ± 27	117 ± 11	1937 ± 173	8.9 ± 0.7	0.48 ± 0.04	0.36 ± 0,04	
HET 30	1135 ± 136	1022 ± 73	161 ± 10	2020 ± 242	43.9 ± 3.2	0.48 ± 0.03	0.91 ± 0,08	1024
HET 54a	346 ± 49	234 ± 23	63 ± 8	1220 ± 174	2.3 ± 0.2	0.29 ± 0.04	0.28 ± 0,04	3594
HET 55	238 ± 20	57 ± 6	73 ± 8	1264 ± 105	0.48 ± 0.05	0.27 ± 0.03	-0.02 ± 0,01	

HET 64	429 ± 46	64[a] ± 5	60 ± 7	1902 ± 205	0.54 ± 0.04	0.21 ± 0.02	0.005 ± 0,01	2735
HET 88	345 ± 31	243 ± 16	42 ± 5	1429 ± 128	2.5 ± 0.2	0.18 ± 0.02	0.32 ± 0,03	
beech	***495 ± 264***	***264 ± 307***	***76 ± 40***	***1656 ± 340***	***7.5 ±14.1***	***0.28 ±0.12***	***0.24 ±0.29***	
PL 20	434 ± 43	240 ± 14	117 ± 14	1810 ± 179	3.3 ± 0.2	0.49 ± 0.06	0.08 ± 0,01	2294
PM 17	25 ± 6	424 ± 29	111 ± 16	142 ± 36	39.2 ± 2.7	0.37 ± 0.05	0.16 ± 0,02	617
PM 20	602 ± 59	557 ± 27	123 ± 13	1491 ± 147	17.0 ± 0.8	0.47 ± 0.05	0.25 ± 0,02	
PM 40b	65 ± 7	108 ± 10	51 ± 6	339 ± 38	1.1 ± 0.1	0.25 ± 0.03	0.04 ± 0,01	
PM 40c	107 ± 11	139 ± 15	53 ± 9	585 ± 58	1.2 ± 0.1	0.25 ± 0.04	0.06 ± 0,01	2029
PM 72	148 ± 18	591 ± 53	72 ± 7	644 ± 77	29.5 ± 2.6	0.20 ± 0.02	0.22 ± 0,02	2222
PM 85	39 ± 4	186 ± 17	66 ± 10	211 ± 24	24.2 ± 4.2	0.19 ± 0.03	0.05 ± 0,01	658
PS 15	331 ± 28	243 ± 17	55 ± 7	1053 ± 89	5.0 ± 0.4	0.19 ± 0.03	0.10 ± 0,01	
PS 41	140 ± 12	327 ± 34[a]	81 ± 10	754 ± 67	27.3 ± 2.8	0.34 ± 0.04	0.16 ± 0,02	
PS 44	390 ± 41	582 ± 39	-	1504 ± 157	54.1 ± 3.6	-		
PS 45	235 ± 21	507 ± 28[a]	52 ± 7	1108 ± 99	93.6 ± 5.2	0.20 ± 0.03	0.26 ± 0,02	
PS 63	374 ± 41	415 ± 36	43 ± 6	801 ± 88	11.4 ± 1.0	0.13 ± 0.02	0.17 ± 0,02	
PS 67a	210 ± 23	638 ± 37	97 ± 5[a]	1043 ± 116	91.2 ± 5.3	0.19 ± 0.03	0.39 ± 0,03	3705
PS 76	266 ± 23	725 ± 35	81 ± 13	959 ± 82	120.7 ± 5.8	0.27 ± 0.04	0.32 ± 0,02	3135
PS 88	273 ± 30	992 ± 76	75 ± 9	1116 ± 123	83.4 ± 13.0	0.24 ± 0.03	0.40 ± 0,04	
pine	***243 ± 160***	***440 ± 230***	***77 ± 33***	***904 ± 476***	***40.5 ± 38.5***	***0.29 ± 0.14***	***0.19 ±0.12***	
SP 05	371 ± 28	295 ± 29	44 ± 7	1298 ± 100	8.3 ± 0.6	0.19 ± 0.03	0.54 ± 0,05	5000
SP 11	431 ± 37	277 ± 27	71 ± 9	2181 ± 189	1.4 ± 0.1	0.15 ± 0.02	0.21 ± 0,03	7024
SP 25	500 ± 46	342 ± 36	35 ± 5	1861 ± 173	3.6 ± 0.4	0.15 ± 0.02	0.66 ± 0,08	5197
SP 38	403 ± 38	518 ± 35	44 ± 7	931 ± 88	24.5 ± 1.7	0.18 ± 0.03	0.96 ± 0,07	2352
SP 57	222 ± 20	461 ± 54	106 ± 13	984 ± 89	6.1 ± 0.7	0.23 ± 0.03	0.38 ± 0,06	2188
SP 63	318 ± 29	491 ± 36	57 ± 6	843 ± 78	15.1 ± 1.1	0.29 ± 0.03	1.07 ± 0,09	
SP 68	272 ± 26	220 ± 23	50 ± 6	757 ± 74	1.6 ± 0.2	0.17 ± 0.02	0.27 ± 0,04	2604
fir	***360 ± 95***	***372 ± 114***	***58 ± 24***	***1265 ± 525***	***8.7 ±7.9***	***0.19 ± 0.05***	***0.58 ±0.31***	
Min	*25*	*57*	*22*	*142*	*0.3*	*0.06*	*-0.02*	*617*
Max	*1222*	*1608*	*369*	*3702*	*121*	*1.20*	*1.57*	*8406*
Mean	*391*	*419*	*79*	*1290*	*23*	*0.30*	*0.39*	*3527*
Median	*345*	*370*	*65*	*1223*	*7*	*0.25*	*0.30*	*2735*

- : not measured; [a] single replicate; LF: Litterfall; Se acc. rate = Se accumulation rate in humus

Boxplot distributions are presented on the **Figures art.1.SI 2 – 5**. Box plots show the first quartile (Q_1), median and third quartile (Q_3) of the data. Black diamond symbols represent average Se concentrations in groups. Lower and upper whiskers extend from the hinges by Q_1 - 1.5 × IQR (IQR - interquartile range) and Q_3 + 1.5 × IQR, respectively. Dots represent corresponding data. The different letters above the boxes correspond to significant differences between the groups according to pairwise Wilcoxon test, with Holm adjustment for p-value.

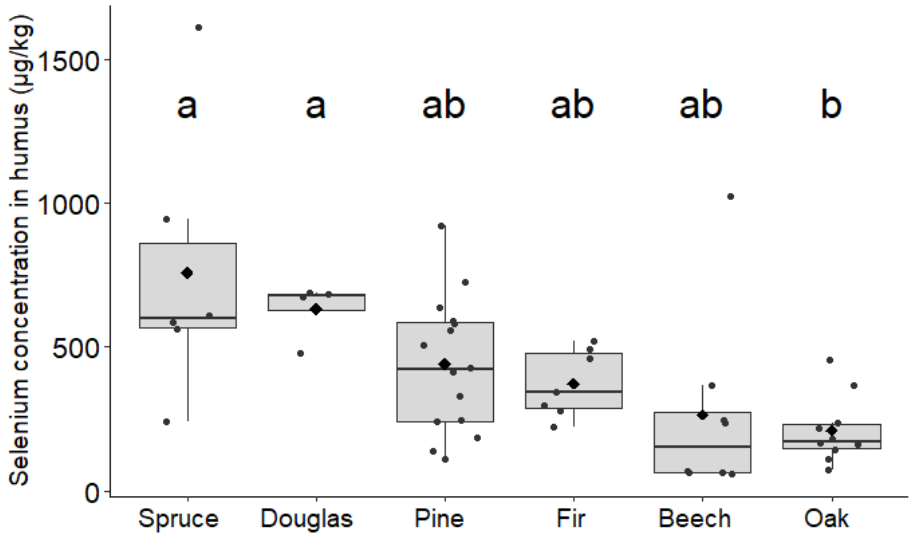

Figure art.1.SI – 2 Selenium concentration in humus according to tree species (Kruskal-Wallis rank for global test: $\chi 2 = 20.25$ p-value < 0.01).

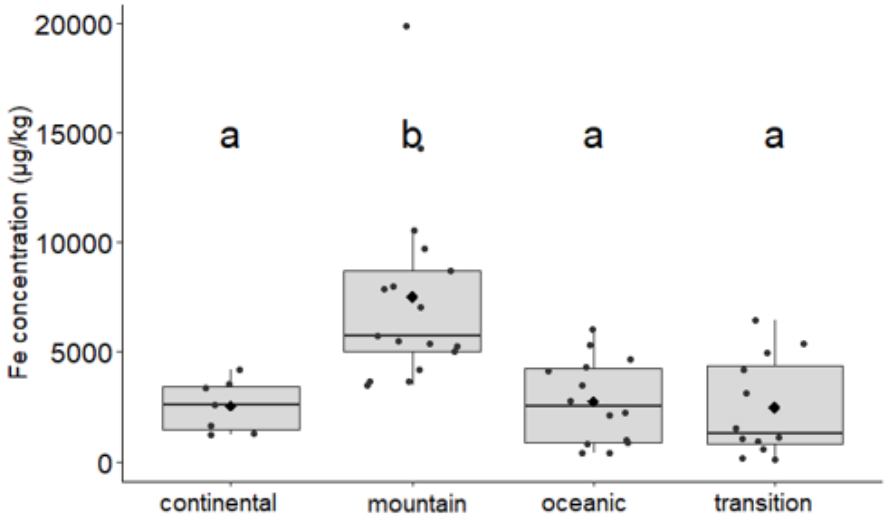

Figure art.1.SI – 3 Iron concentration in soil according to climate (Kruskal-Wallis rank for global test: $\chi 2 = 21.60$, p-value <0.001).

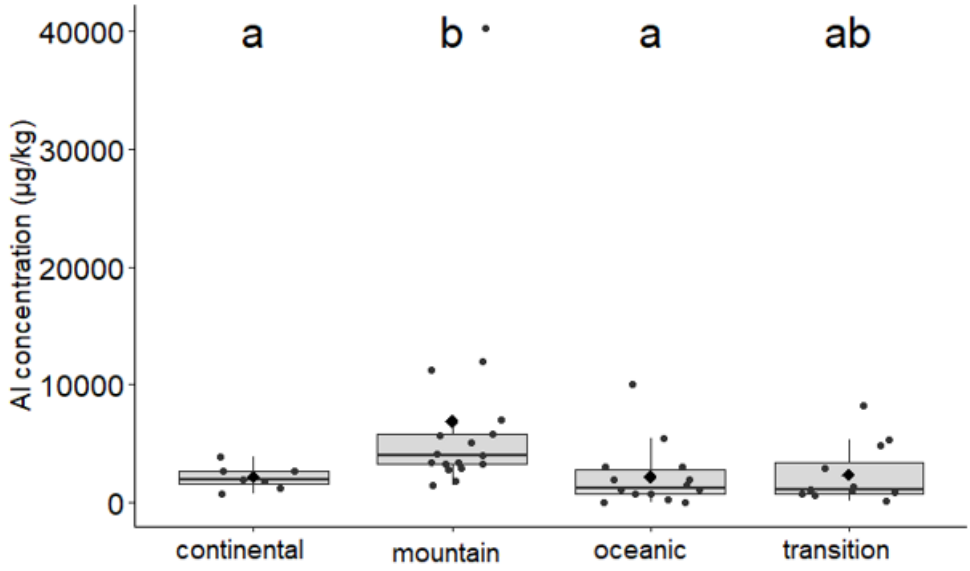

Figure art.1.SI – 4 Aluminium concentration in soil according to climate (Kruskal-Wallis chi-squared = 15.14, p-value < 0.05).

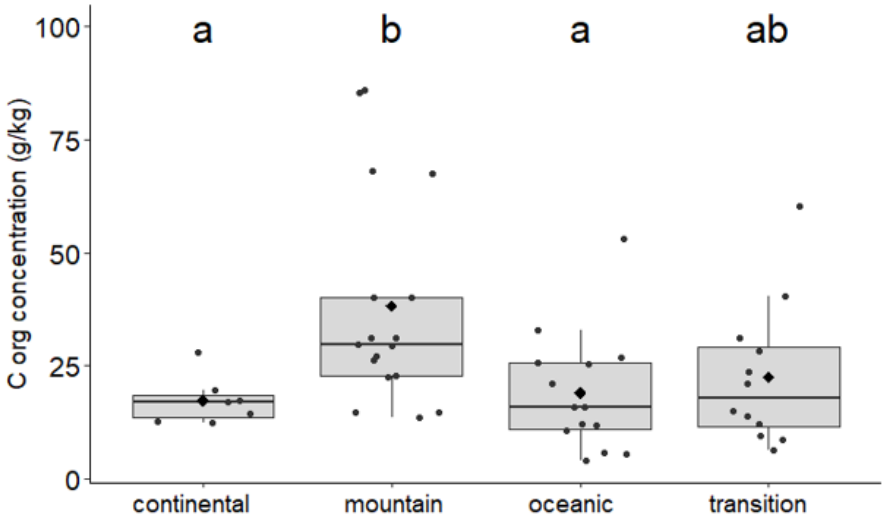

Figure art.1.SI – 5 Carbon concentration in soil according to climate (Kruskal-Wallis rank for global test: $\chi 2 = 10.945$, p-value < 0.05).

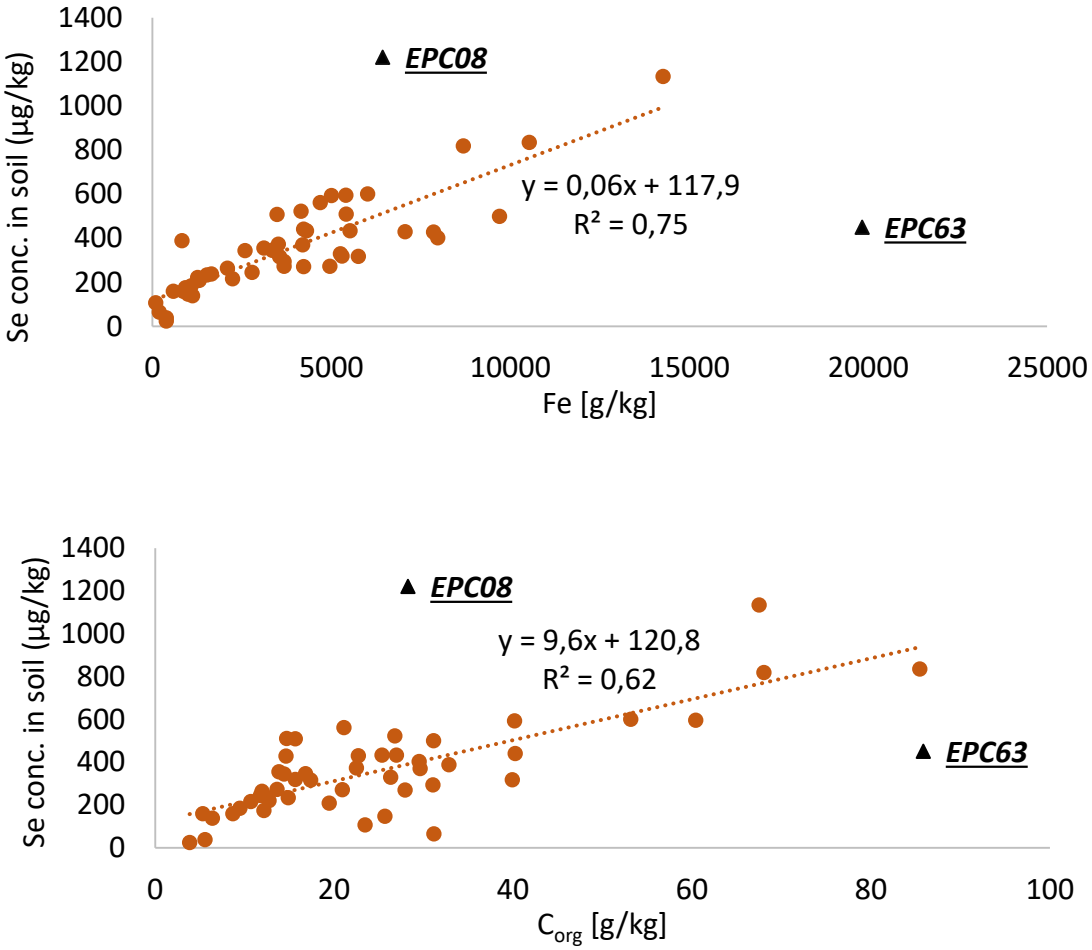

Figure art.1.SI – 6 Selenium concentration in soil as a function of a) total Fe and b) organic C. Sites EPC08 and EPC63 were not included in correlations.

Table art.1.SI – 4 Spearman correlation matrix of Se concentration in soil and soil characteristics. Strongly (r < 0.6) and very strongly (r < 0.8) correlated variables are marked on color.

	Se	pH	C	N	CEC	Clay	Slit	Sand	Al exchang	Al	Fe.exchang	Fe	Mn.exchang	Mass
Se	1.00	-												
pH	-0.07	1.00												
C	0.68	-0.13	1.00											
N	0.78	0.10	**0.90**	1.00										
CEC	0.44	0.34	0.52	0.65	1.00									
Clay	0.67	0.29	0.54	0.76	0.69	1.00								
Silt	0.47	0.17	0.16	0.40	0.41	0.63	1.00							
Sand	-0.52	-0.28	-0.28	-0.54	-0.56	**-0.80**	**-0.95**	1.00						
Al exchang.	0.53	-0.55	0.43	0.41	0.15	0.27	0.24	-0.17	1.00					
Al	**0.85**	0.00	0.77	0.82	0.44	0.66	0.29	-0.39	0.54	1.00				
Fe exchang.	0.17	-0.73	0.22	0.03	-0.24	-0.22	-0.13	0.22	0.64	0.15	1.00			
Fe	**0.83**	0.11	0.65	0.82	0.60	**0.77**	0.47	-0.59	0.43	**0.88**	0.07	1.00		
Mn exchang	0.25	0.25	-0.06	0.16	0.09	0.41	0.36	-0.40	0.01	0.25	-0.38	0.39	1.00	
Mass	-0.77	0.14	-0.79	-0.78	-0.41	-0.58	-0.20	0.29	-0.53	**-0.84**	-0.27	**-0.74**	-0.19	1.00

3. Conclusions – Chapter 2

The challenge of this study was in the numerous variables to be considered, as well as their co-correlation, preventing the exact determination of the decisive factors controlling Se persistence in the forests.

Although the type of canopy (leaves/needles) was presumed to differentiate Se absorption from atmosphere, no difference was found in litterfall Se contents of different tree species, probably due to the predominance of other factors such as climate (i.e. proximity to coast) or forest characteristics (i.e. tree density, age). Regarding Se content in soil, co-correlations between variables showed that climate and geogenic conditions predispose other environmental conditions crucial for Se persistence in humus and soil (i.e. **Figure art.1.SI – 3**: higher Se content for beech and conifer forests in mountain climate associated to acidic soil with high Fe content). It is not surprising as tree species have specific requirements/survival adaptation mechanisms (e.g. generally maritime pine growths in oceanic climate in sandy soil; **Table art.1.SI – 1-2**). Moreover, anthropogenic activities can contaminate forest compartments and artificially modify Se distribution. While anthropogenic activity is hard to access at a large scale, results showed that contaminated sites can be discriminated using statistical analysis. This was the case of forest site EPC08 located in transition climate (Ardennes, north France).

The same difficulties were faced by Roulier et al. (2019) when analyzing total iodine content in the ONF sample collection. Iodine content in soils increased with the content of OM and Al/Fe oxides, and as for Se, mountain soils under Douglas forests were the richest in I. Similarly to Se, litterfall iodine concentrations were linearly correlated with iodine concentrations in rainfall and decreased with increasing distance from the coast.

Summarizing, the environmental and geochemical factors influencing Se and I accumulation in diverse French forests may co-correlate preventing to determine those of most importance factors and the relative influence of tree species.

Chapter 3. Selenium and iodine persistence in forest ecosystem

1. Introduction

To address the problem of co-correlations between climate, edaphic and environmental variables, the additional studies presented in **Chapter 3** were performed in monospecific plantations (deciduous: oak, beech; coniferous: Douglas, pine, spruce) located on a single site and characterized by the same climate and bedrock material (Breuil-Chenue forest, France). The hypothesis is that type of vegetation would significantly alter absorption of selenium and iodine by interception of atmospheric depositions (type and shape of tree canopy, leaves, tree high) and influence mobilization/immobilization in soils (type of vegetal material, degradation of organic matter, accompanying soil microbiota). Tree and soil samples from 2001 – 2006 were completed by a sampling campaign conducted in 2019. Additionally, the infrastructure of Breuil site allowed us to monitor monthly fluxes of Se and I in water samples from January 2019 to December 2019 and to calculate the Se and I fluxes in the different compartments of the ecosystem.

Figure chap.2 – 1 presents a simplified schema of Se and I transfers in forest environment. Atmospheric depositions (wet and dry) interact with the surface of tree canopy resulting in the enrichment of throughfall and stemflow or leaves/bark surface. It leads to negative (absorption) or positive (leaching) overall canopy fluxes. While element content in atmospheric deposition can be directly measured in rainfall sample (bulk or wet-only deposition), specific measurement of dry deposition input is problematic. In our study, it was assessed with Na as inert tracer.

The annual cycle of elements within tree biomass was quantitatively described using three different fluxes (Di Tullo, 2015; Roulier et al., 2018; Thiry et al., 2005, **Figure chap.2 – 1**):

- Requirement (the total element intake into annual aboveground biomass growth),
- Uptake (element absorbed by the roots calculated as the amount accumulated in tree compartments and returns of the element to soil with litterfall and crown leaching),
- Translocation (internal movement of element from senescing to younger organs).

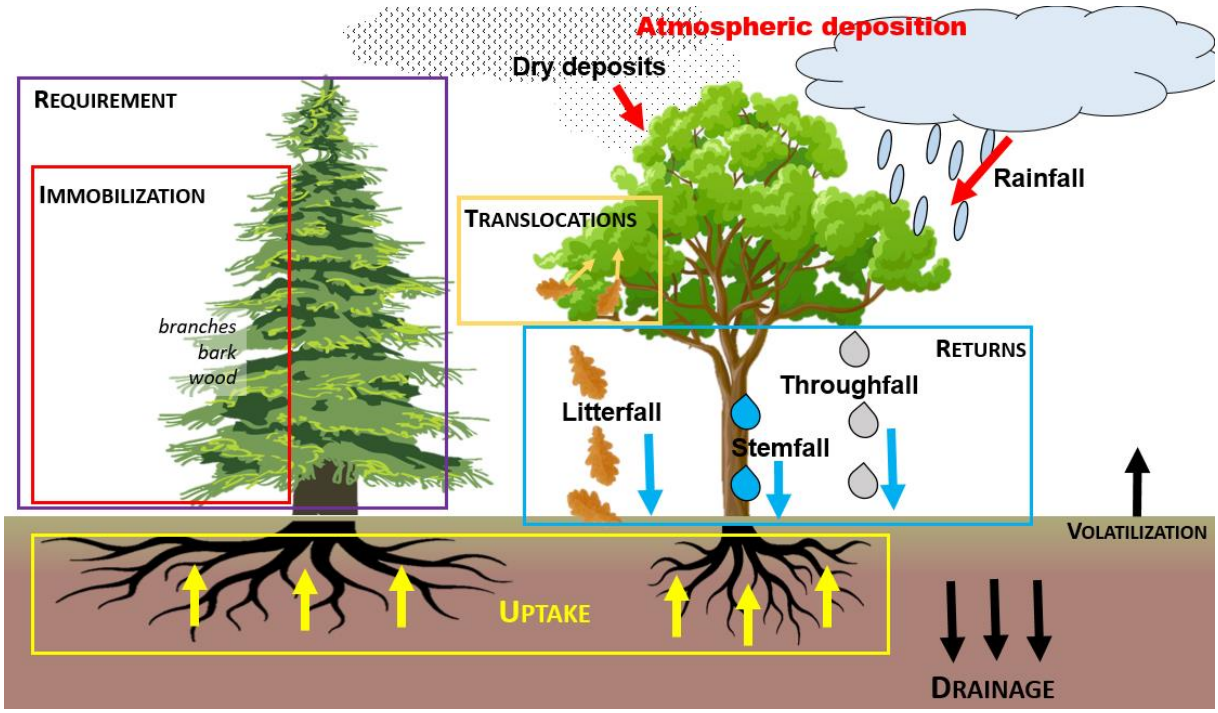

Figure chap.3 – 1 Schema of element fluxes in forest ecosystem.

For Se and I, the principal objectives of **Chapter 3** were to compare for coniferous and deciduous tree species located under identical climatic and edaphic conditions:

- Canopy exchange fluxes of elements quantifying absorption/leaching of atmospheric inputs,
- Total concentrations, stocks and Requirement, Uptake and Translocation fluxes in aboveground tree parts,
- Total concentrations, stocks and fluxes in forest soil profiles,
- Fractionation and speciation controlling elements mobility in soils and their relation with soil organic matter characteristics,
- Overall input-output element budgets

The results presented in this chapter have been organized in two manuscripts:

- "**Influence of tree species on selenium and iodine partitioning in an experimental forest ecosystem**" published in the journal "*Science of the Total Environment*" and,
- "**Selenium and iodine cycles in beech and Douglas forests**" in preparation for submission in the journal "*Chemosphere*".

2. Article 2: Influence of tree species on selenium and iodine partitioning in an experimental forest ecosystem

Paulina Pisarek[1,2], Maïté Bueno[1], Yves Thiry[2], Arnaud Legout[3], Hervé Gallard[4], Isabelle Le Hécho[1]

[1] CNRS/Univ. Pau & Pays de l'Adour, Institut des Sciences Analytiques et de Physico-Chimie pour l'Environnement et les Matériaux (IPREM), UMR 5254, 64053 Pau, France (*pisarek.paulina@univ-pau.fr) (maite.bueno@univ-pau.fr;isabelle.lehecho@univ-pau.fr)

[2] Andra, Research and Development Division, Parc de la Croix Blanche, 92298 Châtenay-Malabry Cedex, France (yves.thiry@andra.fr)

[3] INRAE, BEF, F-54000 Nancy, France (arnaud.legout@inrae.fr)

[4] IC2MP UMR 7285, Université de Poitiers, 86073 Poitiers Cedex 9, France (herve.gallard@univ-poitiers.fr)

Keywords

1. Soil depth profile, 2. Humus horizons, 3.Stocks, 4. Uptake, 5. Coniferous, 6. Deciduous

Highlights

- Se and I contents in tree and humus depend on tree species.
- The lowest Se and I contents were in tree wood.
- Quality of organic material controls residence time of Se and I in humus.
- Se and I accumulation increases with humus decomposition stage.
- "Enrichment-depletion" profile of I was observed in soil column.

Graphical abstract

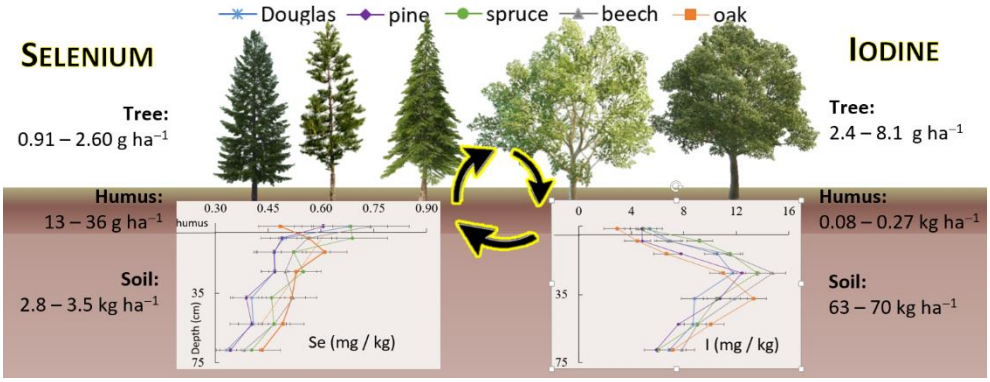

Abstract

Storage of selenium and iodine can greatly vary between forest ecosystems, but the influence of tree species on partitioning and recycling of those elements remains elusive. In this study, contents of Se and I were measured in tree compartments, litterfall, humus and soil horizons in monospecific stands of Douglas, pine, spruce, beech and oak under identical climatic and edaphic conditions. The cycle of each element was characterized in terms of stocks and fluxes. The lowest concentrations were reported for wood (Se: 8-13 µg kg^{-1}; I: < 16.5 µg kg^{-1}). Senescing organs had higher Se and I content, than the living parts of trees due to direct exposure to atmospheric deposits, with some variations between coniferous and deciduous trees. For all stands, the biological cycle involved a very weak amount of Se and I in relation to a low root uptake. In humus, the enrichment of elements greatly increased with the stage of organic matter (OM) degradation with average factors of 10 and 20 for Se and I. Tree species influenced both OM degradation and elements persistence in humus. Deciduous trees with low biomass and short residence time of OM stored less Se and I in humus compared to Douglas and spruce with high humus biomass. Interestingly, tree species did not remarkably affect soil reserves of Se and I. Concentration ranges were 331-690 µg Se kg^{-1} and 4.3-14.5 mg I kg^{-1}. However, the divergent vertical profiles of the elements in the soil column highlighted their distinctive downward transport. Selenium concentrations regularly decreased with depth in correlation with OM and Fe oxides content. For iodine, we hypothesised that the "enrichment-depletion profile" is mainly caused by a parallel precipitation/sorption behaviour of aluminium and dissolved organic iodine in topsoil.

1. Introduction

Selenium and iodine are omnipresent in the environment and essential elements for mammals. Forests which cover ~33% of land in Europe (Alberdi et al., 2015) can absorb, recycle, and accumulate these elements. Tree canopies interact with dry and wet deposition (De Schrijver et al., 2007) and in throughfall concentrations and speciation relative to that deposited may be changed (Roulier et al., 2020a). Selenium and iodine can remain on the leaf surface and/or be integrated into the biomass through foliar absorption (Cakmak et al., 2017; Kikkert and Berkelaar, 2013; Roulier et al., 2020b). After interaction with foliar surfaces, these elements are deposited to topsoil via precipitation and litterfall, and subsequently recycled through root uptake (Kato et al., 2013; Li et al., 2008). Decomposers of decaying material (earthworm, fungi and bacteria communities) influence the biological, physical, and chemical properties of soils, thus affecting cycling of elements, e.g. C, N, K, Ca, Mg, and Na, in forest (Aponte et al., 2013; Berger and Berger, 2012; Mareschal et al., 2010; Prescott and Grayston, 2013). It has been demonstrated that both elements strongly interact with the organic and mineral soil phases (Coppin et al., 2009; Pisarek et al., 2021; Roulier et al., 2019; Tolu et al., 2014; Xu et al., 2016). Previous studies assessed the influence of different forest types on the distribution of Se and I and showed similar contents in litterfall, while differences were observed for humus and soil (Pisarek et al., 2021; Roulier et al., 2019). However, in these studies the different tree species, climate, and geochemical conditions made it difficult to determine the dominant variables influencing observations (Pisarek et al., 2021; Roulier et al., 2019). In this study we postulated that the quantitative description of Se and I cycle in monospecific forest stands developing under identical climatic and edaphic conditions may help in characterizing the influence of tree vegetation. For that purpose, the concentrations of Se and I were quantified in the aboveground tree compartments (wood, bark, branches, leaves), litterfall (leaves, branches), forest floor/ humus and soil horizons for five tree species: Douglas fir, pine, spruce, beech and oak. The objectives were, for the five tree species, (i) to identify the differences in Se and I distribution and recycling, (ii) to establish Se and I retention times and accumulation rates in humus, (iii) to investigate differences in Se and I soil profiles.

2. Methods

2.1 Study site

The study site is situated in the forest of Breuil-Chenue in Bourgogne, France (lat 47°18′10″ N; long 4°4′44″ E). The climate is temperate with a warm summer without a dry season (Cornelis et al., 2010). The experimental site, managed by INRAE-BEF, is part of the ANAEE France Platform (n.d.) (www.anaee-france.fr - breuil). In 1975 the original coppice forest was removed. Monospecific plots (each 1000 m^2) were then planted in 1976 with five tree species: i) coniferous: Douglas fir (*Pseudotsuga menziesii*), Corsican pine (*P. nigra* var. *corsicana*), Norway spruce (*Picea abies*); ii) deciduous: European beech (*Fagus sylvatica*), sessile oak (*Quercus sessiliflora*) (**Figure art.2.SI – 1**). The soil is an acid brown soil, classified as Alumnic Cambisol (IUSS Working Group WRB, 2006), derived from granite and very poor in major cations (0.5% magnesium oxide, 0.6% calcium oxide and 4.4% potassium oxide) (Montelius et al., 2015). All the introduced tree species decreased soil base saturation and increased acidification. Douglas fir, Corsican pine and secondarily oak strongly amplified the acidification process. In these two stands the major soil process shifted from weak acidification and crypto podzolisation to strong soil acidification (Legout et al., 2016). Soil characteristics under each tree stands are presented in **Table art.2.SI – 1**.

2.2 Sampling

One composite sample of wood, bark, and branches from 10 trees of each stand collected in 2001 was used. Annual composite samples of green leaves, litterfall-leaves and litterfall-branches were obtained from 2002 to 2006. Humus samples included 8 replicates of bulk humus (sampled in 2005) for each stand and single samples of four humus horizons (collected in 2006): *oln* (organic, litter, new), *olv* (organic, litter, old), *of* (organic, fragmented) and *oh* (organic, humified). For each stand, the mineral soil profiles were sampled in 2006 at three sampling points at the following depths (cm): 0–7.5; 7.5–15; 15–30; 30–45; 45–60 and 60–75. Only the soil profile of the oak stand was collected at one sampling point and different depths: 0–5; 5–10; 10–15; 15–25; 25–40; 40–55; 55–70 cm. For comparison, concentrations in oak soil were thus calculated for horizons similar to those used for the other soils. Soils were sieved to <2 mm and dried. The 2–5 mm soil fraction of the deepest layer (60–75 cm, Douglas fir) was considered to be representative of the soil parent material. All samples of plant material, litterfall, humus, and soils were dried and grounded.

2.4 Total element extraction and determination

Acidic extraction was used to extract total Se. Briefly, soil samples (~0.25 g) were mixed with 0.5 mL of 38% HCl and 1.5 mL of 68% HNO_3, while humus and litterfall (~0.25 g) were mixed with 2 mL of 68% HNO3, 0.5 mL of 30% H_2O_2 and 3 mL of ultrapure water (Milli-Q System, 18.2 MΩ cm; Elix, Millipore). Samples were heated at 90 °C for 3 h in hot block digestion system (DigiPREP MS, SCP Science). Digested samples were diluted to 50 mL with ultrapure water, filtered on 0.45 µm acetate membrane and stored at 4 °C until analysis. Blanks were added in each digestion run.

Total iodine was extracted with a previously established protocol (Roulier et al., 2018; Watts et al., 2015; Watts and Mitchell, 2009). Approximately 0.2 g of soil or humus, or 0.4 g of plant material was mixed with 5 mL of 5% tetramethylammonium hydroxide (TMAH). Digestion was performed in hot block digestion system at 85 °C for 3 h. Digested samples were diluted to 10 mL with Milli-Q water, centrifuged at 4000 rpm for 10 min, filtered on 0.45 µm acetate membrane and stored at 4 °C until analysis. Before analysis, digested soils and humus were diluted 50-fold and plant materials 25-fold. Blanks were added in each digestion run.

Selenium and iodine concentrations were determined by inductively coupled plasma mass spectrometry (ICP-MS; 7500ce, Tokyo, Japan). For Se analysis, collision/reaction cell gas flow was 5 mL min^{-1} H_2. When sample replicates were available (i.e. for bulk humus (n=8/stand), soil (n=3/depth/stand), annual samples of litterfall and leaves (n=5/stand)), each replicate was digested and analyzed once and result is given as the mean value with the combined uncertainties of the analysis and sampling (weighted by the biomass produced during the year for foliage and litterfall). When only one sample was available (i.e. for wood, bark, branch and humus horizons), it was digested and analyzed in triplicate and result is given as the mean value with the analytical uncertainty of the mean. Total selenium quantification of Certified Reference Materials (118 ± 9 µg $kg^{-1}$for DC 73032, 191 ± 15 µg kg^{-1} for DC 73030, 24 ± 3 µg kg^{-1} for ERM-CD281, 23 ± 2 µg kg^{-1} for BCR-129) agreed well with the certified values (140 ± 20 µg kg^{-1} for DC 73032, 200 ± 30 µg kg^{-1} for DC 73030, 23 ± 4 µg kg^{-1} for ERM-CD281, 25 µg kg^{-1} (information value) for BCR-129). Furthermore, experimental results of iodine concentrations on certified materials (9.2 ± 0.3 mg kg^{-1} for DC 73022, 6.3 ± 0.1 mg kg^{-1} for DC 73030 and 137 ± 11 µg kg^{-1} for BCR-129) confirmed the accuracy of the methods (certified values: 9.4 ± 1.2 mg kg^{-1} for DC 73022, 6.4 ± 0.5 mg kg^{-1} for DC 73030, 167 ± 24 µg $kg^{-1}$for BCR-129). The instrumental limit of detection (LOD) depended from daily sensitivity and

varied between 0.01-0.03 µg L^{-1} for selenium and between 0.02-0.08 µg L^{-1} for iodine, leading to detection limit in solid samples of 1.6 µg kg^{-1} for Se and 8.5-16.5 µg kg^{-1} for I.

2.4 Calculations

The biomass values of standing tree compartments (needles, branches, bole-bark, bole-wood) were taken from Montelius et al. (2015). The biomass of broadleaves was estimated at 121.6% of litterfall mass to account for the average loss of mass of living foliage during senescence (Vergutz et al., 2012). The total masses of humus (kg ha^{-1}) were estimated from the weighing of a reference surface of 0.5 m^2 (Mareschal et al., 2010). Annual litterfall (kg ha^{-1} yr^{-1}) was estimated using 5 collectors covering a total of 2.5 m^2 (collected every 3 months, from 2002 to 2006). The annual biomass production was calculated as the average of annual increments of standing biomass over the period 2001–2006. Biomass pools and annual productivities are presented in **Tables art.2.SI – 2** and **SI – 3**.

The stocks of elements in each soil layer (g ha^{-1}) were calculated by multiplying the element concentrations by the bulk density and the thickness of the soil layer. Element stocks in tree compartments and humus (g ha^{-1}) were estimated by multiplying element concentrations by the corresponding biomass pool. Annual fluxes through litterfall (g ha^{-1} yr^{-1}) and production of biomass from tree compartments (g ha^{-1} yr^{-1}) were estimated by multiplying the element concentrations by average annual productivities. As iodine was not detected in wood compartment (<16.5 µg kg^{-1}), a value of half the detection limit with an uncertainty of 100% was used for the calculation of iodine stock and annual immobilization in wood.

The cycle of elements in tree biomass was estimated with three main annual fluxes: requirement (R); uptake (U) and translocation (T) according to equations presented in **Tables art.2 – 1**. This model, with some modifications, has already been used for Se, I and many other elements (Di Tullo, 2015; Goor and Thiry, 2004; Ranger and Colin-Belgrand, 1996; Roulier et al., 2018). Requirement includes the total element pool implemented during annual aboveground biomass production. Uptake corresponds to the amount of element absorbed from the soil by the roots calculated as the amount accumulated in tree compartments and returns of the element to soil through litterfall and crown leaching. Crown leaching was shown to have negligible influence on Se and I budgets (Di Tullo, 2015; Roulier et al., 2018), thus it was neglected in this model. Translocation reflects the internal element transfer from senescing foliage to the rest of the tree, calculated as the difference between the element content in living foliage and litterfall.

Table art.2 – 1 Equations to calculate main annual fluxes of Se and I in forest ecosystem.

Annual flux	Equation	Variables
Requirement (R)	$R = \sum_i (\text{annual biomass production})_i \times [X]_i$	i = leaves, branches, bark, wood
Uptake (U)	$U = (U_1) + (U_2)$	
(U_1) Immobilization	$U_1 = \sum_i (\text{annual biomass production})_i \times [X]_i$	i = branches, wood, bark
(U_2) Returns	$U_2 = \sum_i (\text{annual biomass production})_i \times [X]_i$	i = litterfall leaves , branches
Translocations (T)	$T = (\text{annual biomass production})_i \times ([X]_j - [X]_i)$	i = litterfall leaves; j = leaves

Where: [X] is Se or I concentration

Selenium and iodine accumulation rates, X acc.rate, in humus were calculated according to Eq. (1) from Redon et al., 2011:

$$\boldsymbol{X}\ \mathbf{acc.rate} = \frac{([\mathbf{X}]_{\mathbf{humus}} - [\mathbf{X}]_{\mathbf{litter}}) \times \mathbf{DM}_{\mathbf{humus}}}{\mathbf{t}_{\mathbf{resDM}}} \quad (\text{g ha}^{-1}\ \text{yr}^{-1}) \qquad (1)$$

where $[X]_{humus}$ and $[X]_{litter}$ are Se or I concentrations in humus and litterfall. DM_{humus} is the humus dry mass, t_{resDM} is the average dry matter residence time in humus. t_{resDM} was estimated according to Eq. 2:

$$\mathbf{t}_{\mathbf{resDM}} = \frac{\mathbf{DM}_{\mathbf{humus}}}{\mathbf{LF} \times (\mathbf{1} - \mathbf{litter\ fraction\ mineralized})} \ (\text{years}) \qquad (2)$$

where LF is the annual litterfall dry mass and 'litter fraction mineralized' is the average decrease in the mass of the litter through the transformation of OM (43% in oak, 65% in beech, 70% in Douglas, 61% in spruce, 85% in pine forests; from Osono and Takeda, 2005).

2.5 Statistical analysis

The distribution of data was examined using the Shapiro-Wilk test. Pearson correlations and ANOVA test were performed for normally distributed data, while the Spearman correlation and the Kruskal-Wallis rank test were used for data that did not follow normal distribution. The t-test was performed in order to indicate if the difference in element concentration between soil layers and forest compartments of monospecific stands are significant. Tukey test and pairwise Wilcoxon test were used to identify the contrast (indicated by letters) within sub-groups of categorical variables, respectively for normally and not normally distributed data. The apportionment of element concentrations within categorical sub-groups was represented with boxplots. Stocks and fluxes were compared between tree species based on t-tests. Statistical study was performed in R Studio (R Core Team, 2013; version 3.4.3).

3. Results: Se and I contents in the compartments of the five soil tree systems

3.1 Tree compartments and litterfall

Selenium and iodine concentrations in forest stands of Douglas fir, pine, spruce, beech and oak are presented in **Tables art.2 – 2**. The lowest concentrations of iodine (<16.5 μg kg^{-1}, i.e. under LOD) and selenium (8–13 μg kg^{-1}) were found in wood stem of all trees. Similarly, Zhao et al. (2019) found low I concentrations (<6 μg kg^{-1}–100 μg kg^{-1}) in spruce tree rings, the fluctuation of which was due to the variation of I content in the atmosphere over the years. The ranges of selenium concentrations in bole-bark (16–47 μg kg^{-1}) and branches (18–37 μg kg^{-1}) compartments were comparable. Selenium concentrations in beech foliage (43 ± 5 μg kg^{-1}) and bole-bark (47 ± 5 μg kg^{-1}) were slightly higher than those reported by Di Tullo (2015) in 54 years-old beech forest (30 ± 1 and 28 ± 6 μg kg^{-1}, respectively). Iodine contents in leaves (86–223 μg kg^{-1}), branches (41–165 μg kg^{-1}) and bole-barks (59–226 μg kg^{-1}) corresponded well to the concentrations reported in the literature (92–241, 16–186, 180–329 μg kg^{-1}, respectively; from Korobova, 2010 and Roulier et al., 2018). In woody compartments, differences were noticeable (t-test, $p < 0.05$):

- For Se, in branches: [Douglas fir, spruce] > [oak, beech, pine] and, in bole-bark: [beech] > [Douglas fir] > [spruce] > [pine, oak],
- For I, in branches: [spruce] > [Douglas fir] > [pine] > [oak] > [beech] and, in bole-bark: [beech] > [Douglas fir] > [spruce, pine] > [oak].

In average, considering functional tree types, the five-year survey showed that leaves from deciduous trees were richer in Se and I (Se mean: 39 μg kg^{-1}; I mean: 212 μg kg^{-1}) than conifer needles (Se mean: 23 μg kg^{-1}, I mean: 116 μg kg^{-1}). The lowest concentrations were found in spruce and pine needles, while concentrations found in Douglas fir needles were not statistically different from those in oak leaves (**Tables art.2 – 2; Figure art.2 – 1.1-1.2**; Se, I: Kruskal-Wallis, p-value < 0.001). In litterfall-leaves, Se concentrations (range of 60–90 μg kg^{-1}) were higher under pine compared to spruce and oak (**Figure art.2 – 1.3**; ANOVA, p-value < 0.001). Pine, spruce and oak had lower I concentration compared to Douglas fir (**Figure art.2 – 1.4**; ANOVA p-value < 0.001). Unlike leaves, litterfall-branches of deciduous trees contained lower concentrations of elements (Se mean: 51 μg kg^{-1}, I mean: 367 μg kg^{-1}) than that of coniferous trees (Se mean: 245 μg kg^{-1}, I mean: 2346 μg kg^{-1}). Tree species effect was only noticeable for selenium with lower concentrations found in litterfall-branches under pine compared with spruce (**Figure art.2 – 1.5-1.6**, Kruskal-Wallis, Se: p-value < 0.01, I: p-value < 0.001).

Table art.2 – 2 Selenium and iodine concentrations in Breuil forest stands (mean value ± standard deviation). Concentrations with various letters are significantly different among tree species at the 95% level (2tailed t-test).

	Douglas	Pine	Spruce	Beech	Oak
Selenium concentrations					
Tree parts (µg kg^{-1})					
Bole-wood	9 ± 3	13 ± 4	11 ± 3	11 ± 4	8 ± 2
Branches	32 ± 4^{a}	23 ± 4^{b}	36 ± 5^{a}	18 ± 3^{b}	19 ± 3^{b}
Bole-bark	33 ± 5^{b}	20 ± 4^{d}	24 ± 3^{c}	47 ± 5^{a}	16 ± 2^{d}
Foliage	31 ± 4^{b}	20 ± 3^{c}	19 ± 3^{c}	43 ± 4^{a}	35 ± 4^{b}
Forest floor (µg kg^{-1})					
LF leaves	89 ± 8^{ab}	90 ± 7^{a}	62 ± 6^{c}	74 ± 6^{bc}	60 ± 6^{c}
LF branches	222 ± 26^{ab}	187 ± 14^{b}	291 ± 24^{a}	40 ± 11^{c}	65 ± 8^{c}
LF total	108 ± 26	92 ± 53	85 ± 33	66 ± 27	62 ± 18
Humus bulk	682 ± 137 ^{a}	500 ± 98^{b}	684 ± 134^{a}	742 ± 174^{a}	484 ± 61^{b}
oln	129 ± 14	37 ± 6	40 ± 7	60 ± 10	103 ± 12
olv	197 ± 18	98 ± 14	94 ± 14	194 ± 17	122 ± 13
of	449 ± 35	347 ± 48	425 ± 34	516 ± 30	414 ± 33
oh	902 ± 70	624 ± 83	774 ± 59	830 ± 61	626 ± 47
Soil (µg kg^{-1})					
0-7.5 cm	494 ± 37^{b}	488 ± 59^{b}	690 ± 99^{a}	564 ± 82^{ab}	566 ± 64^{ab}
7.5-15 cm	466 ± 59^{b}	468 ± 52^{b}	522 ± 103^{ab}	522 ± 36^{ab}	610 ± 63^{a}
15-30 cm	467 ± 58	469 ± 39	550 ± 50	499 ± 47	530 ± 58
30-45 cm	408 ± 54	388 ± 74	459 ± 38	520 ± 36	517 ± 72
45-60 cm	404 ± 42	403 ± 62	467 ± 45	468 ± 34	491 ± 62
60-75(70) cm	331 ± 59	343 ± 38	405 ± 54	382 ± 43	433 ± 51
0-70 cm	*417 ± 47*	*415 ± 55*	*493 ± 55*	*482 ± 42*	*510 ± 64*
Bedrock material	46 ± 5				
Iodine concentrations					
Tree parts (µg kg^{-1})					
Bole-wood	<16.5	<16.5	<16.5	<16.5	<16.5
Branches	118 ± 5^{b}	104 ± 5^{c}	158 ± 5^{a}	39 ± 2^{e}	57 ± 2^{d}
Bole-Bark	144 ± 6^{b}	89 ± 6^{c}	100 ± 5^{c}	226 ± 20^{a}	49 ± 5 ^{d}
Foliage	163 ± 14^{a}	89 ± 8^{b}	82 ± 9^{b}	208 ± 21^{a}	182 ± 32^{a}
Forest floor (mg kg^{-1})					
LF leaves	0.63 ± 0.04^{a}	0.40 ± 0.02^{b}	0.28 ± 0.04^{b}	0.44 ± 0.04^{ab}	0.36 ± 0.02^{b}
LF branches	2.1 ± 0.3^{a}	1.9 ± 0.1^{a}	2.5 ± 0.2^{a}	0.34 ± 0.05^{b}	0.40 ± 0.06^{b}
LF total	0.83 ± 0.20	0.40 ± 0.20	0.51 ± 0.20	0.41 ± 0.16	0.37 ± 0.11
Humus bulk	5.4 ± 0.8 ^{b}	4.8 ± 0.7 ^{b}	4.9 ± 1.2 ^{b}	4.5 ± 0.8 ^{b}	2.9 ± 0.5 ^{a}
oln	0.24 ± 0.02	0.12 ± 0.01	0.09 ± 0.01	0.39 ± 0.03	0.51 ± 0.03
olv	1.4 ± 0.1	0.58 ± 0.03	0.64 ± 0.05	1.1 ± 0.1	0.68 ± 0.05
of	3.4 ± 0.2	2.8 ± 0.1	3.5 ± 0.2	3.1 ± 0.2	2.6 ± 0.1
oh	7.1 ± 0.3	5.0 ± 0.2	6.0 ± 0.3	5.4 ± 0.3	4.0 ± 0.2
Soil (mg kg^{-1})					
0-7.5 cm	6.7 ± 0.5 ^{a}	4.8 ± 0.4 ^{b}	9.0 ± 1.7 ^{a}	6.6 ± 1.9 ^{ab}	4.5 ± 0.3 ^{b}
7.5-15 cm	10.3 ± 1.9^{ab}	7.7 ± 2.1^{ab}	11.3 ± 2.5^{a}	11.1 ± 2.8^{ab}	6.7 ± 0.2^{b}
15-30 cm	11.4 ± 4.3	12.2 ± 0.8	13.3 ± 1.4	14.5 ± 1.4	11.0 ± 0.4
30-45 cm	8.6 ± 1.3	10.5 ± 2.5	10.3 ± 1.6	11.6 ± 1.2	13.3 ± 0.5
45-60 cm	8.5 ± 0.7	7.4 ± 1.6	8.8 ± 1.2	8.9 ± 0.6	10.1 ± 0.4
60-75(70) cm	6.8 ± 2.4	5.8 ± 1.2	5.9 ± 1.1	7.7 ± 1.3	7.2 ± 0.2
0-70 cm	*8.8 ± 1.9*	*8.7 ± 1.5*	*9.8 ± 1.5*	*10.5 ± 1.3*	*9.9 ± 0.4*
Bedrock material	0.30 ± 0.03				

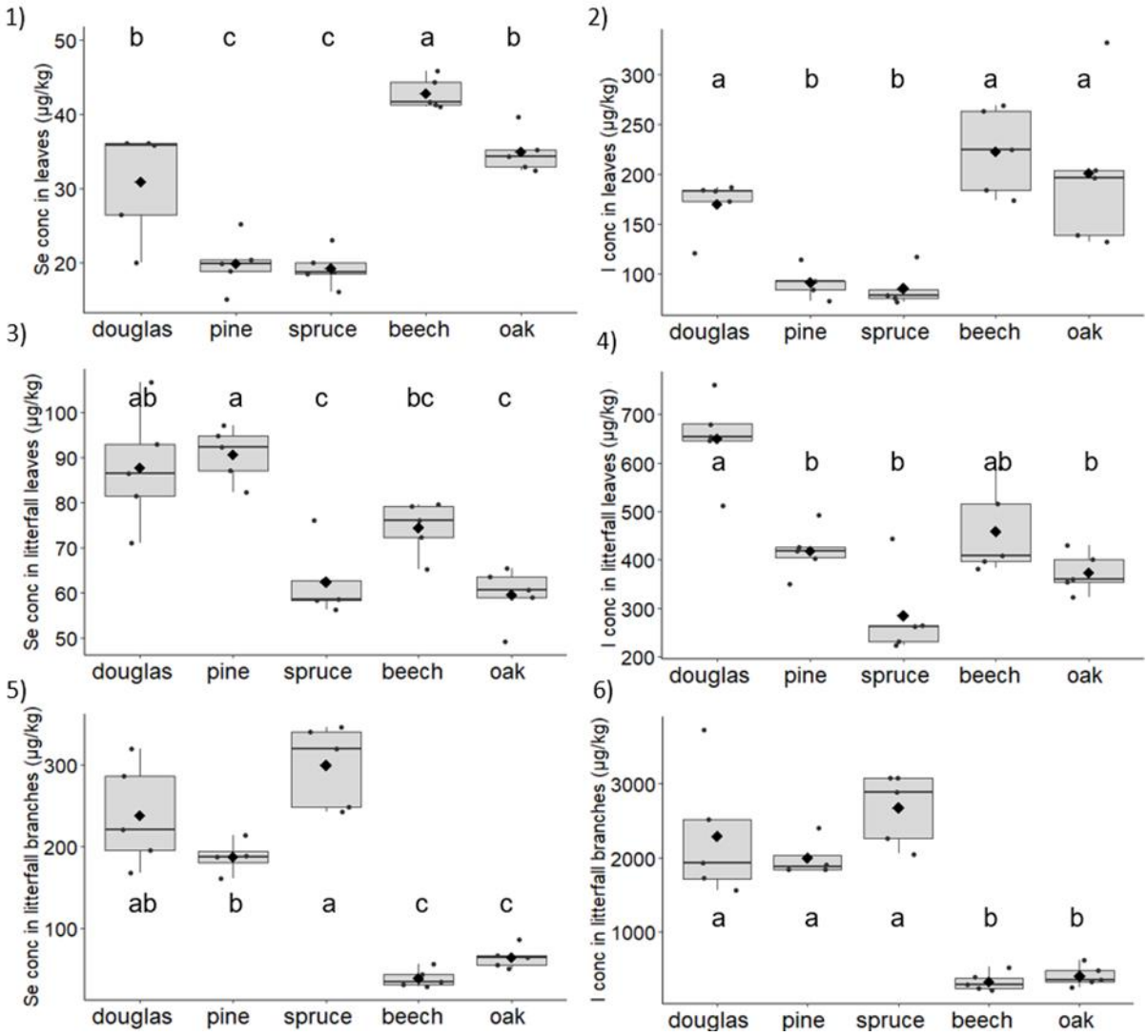

Figure art.2 – 1 Selenium and iodine concentrations (dots) in (1), (2) leaves; (3), (4) litterfall-leaves and (5), (6) litterfall-branches in forest stands (n = 5/stand). Box plots show the first quartile (Q_1), third quartile (Q_3) and median of the data. Black diamond symbols indicate average element concentrations in groups. Upper and lower whiskers extend from the hinges by Q1 − 1.5 × IQR (IQR - interquartile range) and Q_3 + 1.5 × IQR, respectively. Letters above the boxes correspond to significant differences between the groups according to Wilcoxon or Tukey tests.

3.2 Humus

Both element concentrations increased considerably from oln to oh horizon in the forest floor of each stand (**Figure art.2 – 2.1-2.2** and **Table art.2 – 2**). On average, Se content increased from 74 to 751 µg kg−1 and I content from 0.27 to 5.5 mg kg^{-1} resulting in average enrichment factors from upper to deeper humus layers of 10 and 20 for Se and I, respectively. Resulting selenium concentrations in bulk humus varied from 484 µg kg^{-1} to 742 µg kg^{-1} (**Table art.2 – 1**), which is within the ranges of values of 57 to 1022 µg kg^{-1} reported for deciduous forests and 108 to 1608 µg kg^{-1} for conifers (Di Tullo, 2015; Pisarek et al., 2021; Tyler, 2005). The

range of iodine concentrations varied from 3.1 to 5.5 mg kg^{-1} that was also in agreement with ranges of 1.0–5.5 mg kg^{-1} for deciduous forests and 1.2–14 mg kg^{-1} for coniferous forests reported by Roulier et al. (2019), Takeda et al. (2015), and Bostock (2004). Oak and pine bulk humus showed the lowest Se concentrations (484 ± 61 µg kg–1 for oak and 500 ± 98 µg kg^{-1} for pine), while Douglas fir, spruce and beech humus were characterized by similar Se levels (682 ± 137 µg kg^{-1}, 684 ± 134, 742 ±174 µg kg^{-1}) (Fig. 2.3, Kruskal-Wallis, p-value < 0.001). Oak bulk humus had the lowest I concentration varying from 2.2 to 3.9 mg kg^{-1} (**Figure art.2 – 2.4**, ANOVA, p-value < 0.001).

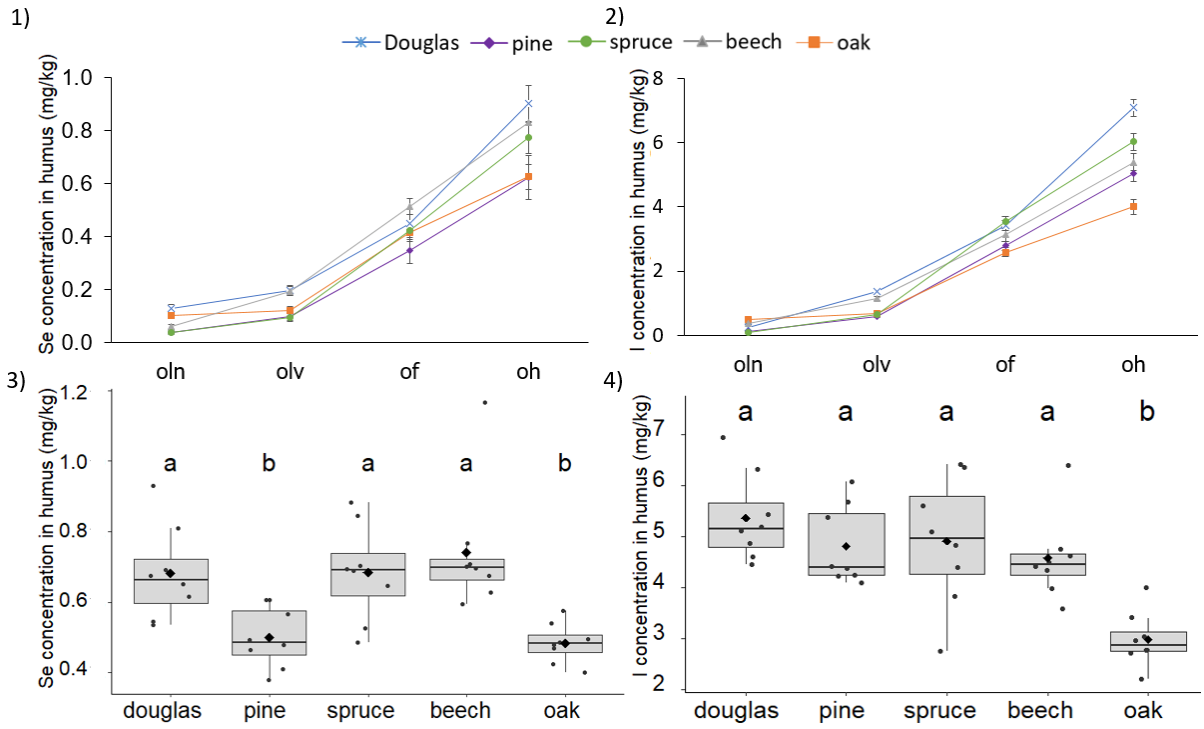

Figure art.2 – 2 Selenium and iodine concentrations in (1), (2) humus horizons: oln (organic, litter, new), olv (organic, litter, old), of (organic, fragmented), oh (organic, humified) and (3), (4) bulk humus (n = 8/stand) of Douglas, pine, spruce, beech and oak monospecific stands. Box plots show the first quartile (Q_1), third quartile (Q_3) and median of the data. Black diamond symbols indicate average element concentrations in groups. Upper and lower whiskers extend from the hinges by $Q_1 - 1.5 \times IQR$ (IQR - interquartile range) and $Q_3 + 1.5 \times IQR$, respectively. Letters above the boxes correspond to significant differences between the groups according to Wilcoxon or Tukey tests.

3.3 Soil

Selenium and iodine soil profiles under the five tree stands are presented in **Figure art.2 – 3.1-3.2**. Selenium concentrations in all profiles ranged from 331 to 690 µg kg^{-1} (**Table art.2 – 2**) with mean of weighted concentrations for the entire profile of 461 µg kg^{-1}, which is similar to the global average of 400 µg kg^{-1} (Shahid et al., 2018) and in agreement with the range of

concentrations (25–1222 µg kg^{-1}) for French forest soils (Tolu et al., 2014). Typical low Se concentration of 46 ± 5 µg·kg^{-1} was found in 2–5 mm soil fraction (depth 60–75 cm) derived from granite bedrock material that corresponds well to average levels of 25–50 µg (Se) kg^{-1} reported for granites (Shahid et al., 2018; Sharma et al., 2015).

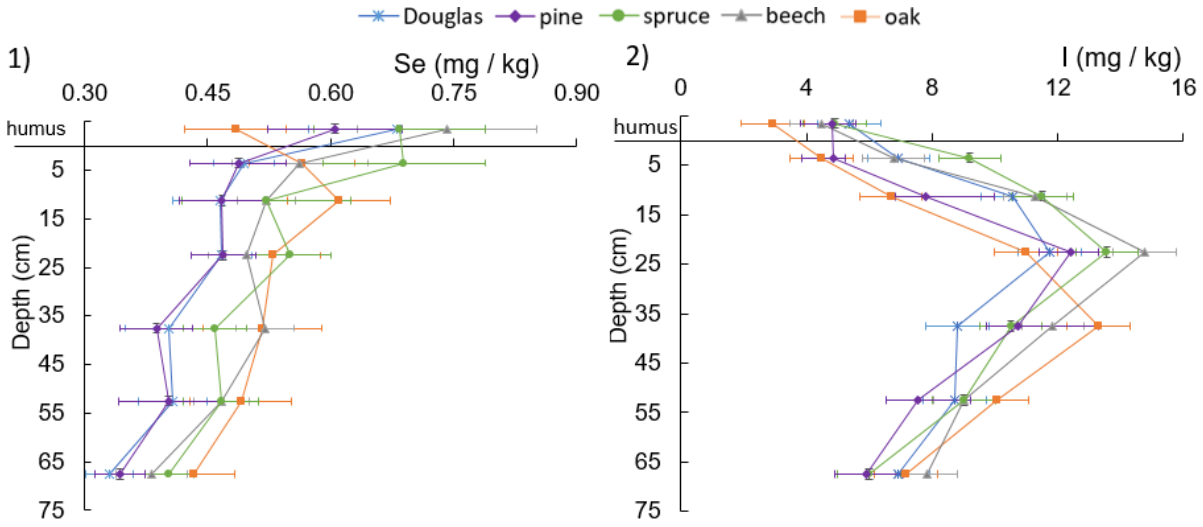

Figure art.2 – 3 Soil profiles of selenium (1) and iodine (2) in forest stands (mean value ± standard deviation).

Iodine concentration in soils varied with depth from 4.5 to 14.5 mg kg^{-1}. The average iodine concentration was 9.5 mg kg^{-1} that is slightly higher than the European mean of 5.6 mg kg^{-1} (Fuge and Johnson, 2015). These results were within the same range as iodine levels of 2–10 mg kg^{-1} reported in Germany (Epp et al., 2020), 0.39–35.65 mg kg^{-1} in French forests (Roulier et al., 2019) and 2.89–32.0 mg kg^{-1} in Ireland (Bowley et al., 2019). Iodine concentrations showed maximum values at a depth of 15 to 30 cm, and then decreased to 70 to 75 cm depth to values similar to those measured at the soil surface (**Figure art.2 – 3.2**). Low iodine concentration of 0.30 ± 0.03 mg kg^{-1} found in soil fraction > 2 mm confirmed that the granite material is generally poor in iodine (mean of 0.25 mg kg^{-1}, Fuge and Johnson, 2015).

Selenium concentrations showed strong positive correlation (Pearson test, rp > 0.6) with Corg and exchangeable Al and Fe (**Table art.2.SI – 4**). Moreover, moderate positive correlations (Pearson test, rp > 0.4) were observed with oxalate extractable Fe and the cationic exchange capacity (CEC). Iodine concentrations were positively correlated with oxalate extractable Al and negatively correlated with Corg, CEC, and exchangeable Fe (Pearson test, |rp| > 0.4). Significant statistical differences between tree species were visible for Se and I concentrations only in topsoil layers (**Table art.2 – 2**; t-test, $p < 0.05$; 0 to 7.5 cm: Se: [Douglas fir, pine] < [spruce]; I: [pine, oak] < [spruce, Douglas fir]; 7.5 to 15 cm: Se: [Douglas fir, pine] < [oak]; I:

[oak] < [spruce]). For the whole soil column (0 to 70 cm), differences between mean concentrations were observed for Se: [Douglas fir, pine] < [spruce, beech, oak], and for I: [pine] < [beech]. Differences with oak stand should be viewed with caution as soil profile was obtained from single sampling point.

3.4 Stocks in forest ecosystem

Selenium and iodine stocks are presented in **Table art.2 – 3**. The average total pools of elements in monospecific stands were 3.2 ± 0.5 kg Se ha^{-1} and 67 ± 11 kg I ha^{-1}, lowest values being observed in the pine forest. The average total element partitioning between the forest compartments decreased as follow: soil (≥98.8%), humus (≤1.2%), tree compartments (≤0.09%). The higher stocks of elements for conifers compared to deciduous trees (**Table art.2 – 3**) can be explained by the higher biomass of conifers (**Table art.2.SI – 2**). Selenium stock in bole-wood represented generally the largest reservoir (34–60%) among the aboveground tree compartments. The very low iodine concentrations (<LoD) was compensated by a large biomass (≈70% of the tree biomass), leading to iodine stocks in bole-wood of 8–17%. Except beech, bole-bark and foliage compartments stored less Se than branches. Iodine stocks were homogeneously distributed between bole-bark, branches and foliage in oak and Douglas fir, while main reservoirs were branches for spruce and pine, and bole-bark for beech. For both elements, their total stock in aboveground tree parts increased in the order: oak < beech, pine ≤ spruce, Douglas fir (t-test, $p < 0.05$). This is in agreement with the increase in biomass pools from oak to Douglas fir stands, while beech, pine and spruce have similar intermediary biomass pools.

Table art.2 – 3 Selenium and iodine stocks in monospecific forest stands (mean value ± standard deviation). Tree and humus stocks with various letters are significantly different among tree species at the 95% level (t-test).

	Douglas	**Pine**	**Spruce**	**Beech**	**Oak**
Selenium stocks (g ha^{-1})					
Tree	**2.60 ± 0.34** [a]	**2.00 ± 0.38** [a,b]	**2.57 ± 0.30** [a]	**1.82 ± 0.33** [b]	**0.91 ± 0.12** [c]
	(0.09%)	*(0.07%)*	*(0.07%)*	*(0.06%)*	*(0.03%)*
Bole-wood	0.96 ± 0.29	1.21 ± 0.37	0.86 ± 0.25	0.92 ± 0.32	0.38 ± 0.10
Branches	0.65 ± 0.08	0.36 ± 0.07	0.93 ± 0.13	0.38 ± 0.07	0.25 ± 0.04
Bole-bark	0.53 ± 0.08	0.28 ± 0.05	0.22 ± 0.03	0.38 ± 0.04	0.14 ± 0.02
Foliage	0.45 ± 0.13	0.15 ± 0.04	0.56 ± 0.10	0.14 ± 0.05	0.14 ± 0.04
Forest soil	**2988 ± 335**	**2824 ± 370**	**3535 ± 389**	**3071 ± 264**	**3553 ± 441**
Humus	34.5 ± 7.3 [a]	19.3 ± 4.6 [b]	35.6 ± 8.0 [a]	16.4 ± 6.9 [b,c]	13.3 ± 1.7 [c]
	(1.2%)	*(0.7%)*	*(1%)*	*(0.5%)*	*(0.4%)*
Soil (0-70 cm)	2954 ± 335	2805 ± 370	3499 ± 389	3054 ± 264	3540 ± 441
	(98.8%)	*(99.2%)*	*(98.9%)*	*(99.4%)*	*(99.6%)*
Total stock	***2991 ± 335***	***2826 ± 370***	***3538 ± 389***	***3073 ± 264***	***3554 ± 441***
Iodine stocks (g ha^{-1})					
Tree	**8.09 ± 0.99** [a]	**4.49 ± 0.81** [b]	**7.99 ± 0.77** [a]	**4.07 ± 0.74** [b]	**2.40 ± 0.45** [c]
	(0.013%)	*(0.008%)*	*(0.011%)*	*(0.006%)*	*(0.003%)*
Bole-wood	0.86 ± 0.86	0.78 ± 0.78	0.66 ± 0.66	0.70 ± 0.70	0.39 ± 0.39
Branches	2.47 ± 0.09	1.76 ± 0.08	3.99 ± 0.14	0.84 ± 0.03	0.76 ± 0.03
Bole-bark	2.39 ± 0.17	1.28 ± 0.13	0.97 ± 0.12	1.85 ± 0.16	0.50 ± 0.12
Foliage	2.37 ± 0.44	0.67 ± 0.13	2.37 ± 0.34	0.68 ± 0.18	0.75 ± 0.18
Iodine stocks (kg ha^{-1})					
Forest soil	**63 ± 14**	**59 ± 10**	**70 ± 10**	**67 ± 8**	**68 ± 3**
Humus	0.27 ± 0.05 [a]	0.19 ± 0.04 [b]	0.26 ± 0.07 [a]	0.10 ± 0.04 [c]	0.08 ± 0.01 [c]
	(0.4%)	*(0.3%)*	*(0.4%)*	*(0.15%)*	*(0.12%)*
Soil (0-70 cm)	63 ± 14	59 ± 10	70 ± 10	66 ± 8	68 ± 3
	(99.6%)	*(99.7%)*	*(99.6%)*	*(99.8%)*	*(99.9%)*
Total stock	***63 ± 14***	***59 ± 10***	***70 ± 10***	***67 ± 8***	***68 ± 3***

4. Discussion

4.1 Biological distribution and cycling in tree compartments

Calculated requirement fluxes of Se and I were significantly lower for pine (**Table art.2 – 4**, $p < 0.05$), as expected due to its lower aboveground biomass productivity compared to the other stands. For both elements, foliage compartment accounted for the pool for deciduous stands (57–85%) and a minor part for conifer plots (8–26%), in agreement with the low foliage productivity of conifers (**Table art.2.SI – 3**). Mean annual uptake fluxes (Se: 0.29–0.58 g ha^{-1} y^{-1}; I: 1.52–3.52 g ha^{-1} y^{-1}) increased as follows: beech ≤ oak, spruce, pine < Douglas fir. The proportion of element uptake annually restituted through litterfall was lower for Se (65–86%) compared to I (84–92%). Immobilization in ligneous organs was thus a minor part of the uptake, accounting for about 25% for Se and 14% for I. Uptake exceeded requirement flux, indicating that the amount of absorbed elements surpassed that involved in new biomass production. These gaps were higher for conifers, especially pine, compared to deciduous stands (uptake/requirement ratios; **Table art.2 – 4**). A large fraction of the absorbed elements was accumulated in the senescing foliage, as shown by negative annual fluxes of internal translocation for all tree species. Translocated fractions were similar for both elements with the highest values for pine (63% of uptake fluxes) compared to other trees (20–39%). The returns by litterfall contributed 0.19–0.38 g ha^{-1} yr^{-1} of Se and 1.40–2.94 g ha^{-1} yr^{-1} of I to the forest floor. For comparison, average atmospheric inputs by wet deposition in continental climate were reported to be 0.35 g ha^{-1} yr^{-1} of Se and 8.8 g ha^{-1} yr^{-1} of I (Roulier et al., 2020a).

Table art.2 – 4 Selenium and iodine annual fluxes in monospecific forest stands (mean value ± standard deviation). Fluxes with various letters are significantly different among tree species at the 95% level (t-test).

	Se annual flux (g ha^{-1} y^{-1})				
Annual flux	**Douglas**	**Pine**	**Spruce**	**Beech**	**Oak**
Requirement (R)	***0.24 ± 0.04*** [a]	***0.06 ± 0.02*** [c]	***0.17 ± 0.05*** [a]	***0.21 ± 0.02*** [a]	***0.25 ± 0.07*** [a]
Wood	0.079 ± 0.032	0.032 ± 0.014	0.055 ± 0.034	0.033 ± 0.012	0.044 ± 0.036
Branches	0.078 ± 0.024	0.017 ± 0.006	0.069 ± 0.038	0.025 ± 0.005	0.050 ± 0.041
Bark	0.046 ± 0.014	0.007 ± 0.002	0.012 ± 0.007	0.009 ± 0.003	0.014 ± 0.011
Leaves	0.04 ± 0.01	0.005 ± 0.002	0.03 ± 0.02	0.14 ± 0.01	0.14 ± 0.05
Uptake (U)	***0.58 ± 0. 08*** [a]	***0.39 ± 0.13*** [b]	***0.47 ± 0.10*** [b]	***0.29 ± 0.07*** [c]	***0.41 ± 0.09*** [b]
(U_1) Immobilization	**0.20 ± 0.04**	**0.06 ± 0.02**	**0.14 ± 0.05**	**0.07 ± 0.01**	**0.11 ± 0.06**
Wood	0.079 ± 0.032	0.032 ± 0.014	0.055 ± 0.034	0.033 ± 0.012	0.044 ± 0.036
Branches	0.078 ± 0.024	0.017 ± 0.006	0.069 ± 0.038	0.025 ± 0.005	0.050 ± 0.041
Bark	0.046 ± 0.014	0.007 ± 0.002	0.012 ± 0.007	0.009 ± 0.003	0.014 ± 0.011
(U_2) Returns	**0.38 ± 0.07**	**0.34 ± 0.13**	**0.34 ± 0.08**	**0.22 ± 0.07**	**0.31 ± 0.07**
Litterfall leaves	0.27 ± 0.05	0.32 ± 0.13	0.22 ± 0.08	0.19 ± 0.07	0.19 ± 0.06
Litterfall branches	0.11 ± 0.04	0.017 ± 0.004	0.12 ± 0.03	0.03 ± 0.01	0.11 ± 0.02
Translocation (T)	**-0.17 ± 0.04**	**-0.25 ± 0.11**	**-0.15 ± 0.06**	**-0.08 ± 0.03**	**-0.08 ± 0.03**
	Se Uptake/Se Requirement				
Ratio	2.4 ± 0.6	6.4 ± 2.7	2.8 ± 1.1	1.4 ± 0.4	1.6 ± 0.6
	I annual flux (g ha^{-1} y^{-1})				
Annual flux	**Douglas**	**Pine**	**Spruce**	**Beech**	**Oak**
Requirement (R)	***0.78 ± 0.14*** [a]	***0.16 ± 0.03*** [b]	***0.53 ± 0.19*** [a]	***0.81 ± 0.07*** [a]	***1.00 ± 0.30*** [a]
Wood	0.07 ± 0.07	0.02 ± 0.02	0.04 ± 0.05	0.03 ± 0.03	0.05 ± 0.06
Branches	0.29 ± 0.08	0.08 ± 0.02	0.30 ± 0.16	0.056 ± 0.004	0.16 ± 0.12
Bark	0.21 ± 0.06	0.03 ± 0.01	0.05 ± 0.03	0.04 ± 0.01	0.05 ± 0.04
Leaves	0.20 ± 0.06	0.02 ± 0.01	0.14 ± 0.08	0.68 ± 0.07	0.75 ± 0.26
Uptake (U)	***3.52 ± 0.57*** [a]	***1.72 ± 0.59*** [b,c]	***2.39 ± 0.47*** [b]	***1.52 ± 0.41*** [c]	***2.11 ± 0.41*** [b,c]
(U_1) Immobilization	**0.57 ± 0.13**	**0.14 ± 0.03**	**0.39 ± 0.17**	**0.12 ± 0.03**	**0.25 ± 0.14**
Wood	0.07 ± 0.07	0.02 ± 0.02	0.04 ± 0.05	0.03 ± 0.03	0.05 ± 0.06
Branches	0.29 ± 0.08	0.08 ± 0.02	0.30 ± 0.16	0.056 ± 0.004	0.16 ± 0.12
Bark	0.21 ± 0.06	0.03 ± 0.01	0.05 ± 0.03	0.04 ± 0.01	0.05 ± 0.04
(U_2) Returns	**2.94 ± 0.55**	**1.58 ± 0.59**	**2.00 ± 0.43**	**1.40 ± 0.40**	**1.86 ± 0.38**
Litterfall leaves	1.90 ± 0.35	1.41 ± 0.59	0.98 ± 0.35	1.13 ± 0.39	1.16 ± 0.36
Litterfall branches	1.04 ± 0.43	0.17 ± 0.04	1.02 ± 0.25	0.27 ± 0.10	0.70 ± 0.15
Translocation (T)	**-1.41 ± 0.27**	**-1.10 ± 0.46**	**-0.69 ± 0.27**	**-0.59 ± 0.23**	**-0.57 ± 0.21**
	I Uptake/I Requirement				
Ratio	4.5 ± 1.1	10.8 ± 4.4	4.5 ± 1.8	1.9 ± 0.5	2.1 ± 0.7

Elements occurring in tree compartments can originate from both the soil solution and the atmosphere. The very low quantities of Se and I in bole-wood (**Table art.2 – 2**) in addition to relatively low apparent root uptake is indicative of a low biological recycling of these elements from the soil. Elements originating from atmospheric deposition can accumulate on tree surface or/and be absorbed by the leaves (Roulier et al., 2020b). Selenium and iodine have been shown to be taken up by aerial parts of plants (Cakmak et al., 2017; Hurtevent et al., 2013; Kikkert and Berkelaar, 2013). Only 13% of total I content was washable from beech leaf surface, which would indicate that most of iodine was absorbed into leaf (Roulier et al., 2018). Deciduous trees showed higher concentrations of elements in leaves compared to conifers, which, combined with higher annual foliage production (**Table art.2.SI – 3**), resulted in an apparent higher requirement flux for foliage production (**Table art.2 – 4**).

Leaves and needles in litterfall showed an average increase in Se and I concentrations by a factor of 2.5 to 4 compared to living foliage, which can be explained by the translocation of elements to senescing leaves, longer exposure to atmospheric deposition, and loss of litterfall mass. The former process is a detoxification mechanism, in which excessive or redundant elements (e.g. Se, I, Ca, Mn, Zn, Fe, U) are translocated to the older organs to be eliminated by defoliation (Di Tullo, 2015; Roulier et al., 2018; Thiry et al., 2005; Ukonmaanaho et al., 2008), but its contribution to the net litterfall enrichment remains uncertain. Moreover, much higher concentrations of Se and I were measured in litterfall-branches compared to branches, especially for conifers (**Figure art.2 – 1**). The increase was even higher than previously discussed for leaves and, almost twice for iodine compared to selenium for all tree species. The observed differences between tree species may be caused by longer living period of conifer branches compared to deciduous trees (as reflected in higher ratios of biomass branches productivity to litterfall-branches for conifers), and thus longer exposure to atmospheric deposits. These results indicated that sorption of elements from atmospheric deposits might lead to overestimation of the apparent uptake fluxes and biological recycling capacities of forest.

4.2 The influence of tree species on Se and I contents in humus and soil

The gradual enrichment in Se and I of humus horizons was observed for all tree species (**Figure art.2 – 2.1-2.2**). A part of element enrichment in humus layers is merely associated to the loss of biomass during the ageing of organic matter and the mineralization/stabilization processes (Laganière et al., 2010; Prescott et al., 2000). Another part may originate from atmospheric

deposition via throughfall, and further sorptive retention by decaying organic matter as demonstrated for other elements (van der Heijden et al., 2013). Faster decomposition under deciduous trees was reflected by lower calculated average residence times for humus from oak and beech (10 and 19 years) than for Douglas fir, spruce and pine (48, 34 and 71 years, **Table art.2 – 5**).

Table art.2 – 5 Humus residence time and Se and I average accumulation rates in humus of different tree species.

Tree	Humus $\mathbf{t_{resDM}}$ (years)	Accumulation rate (g $ha^{-1}yr^{-1}$)	
		Selenium	Iodine
oak	10 ± 2	1.2 ± 0.3	7.2 ± 2.1
beech	19 ± 8	0.8 ± 0.5	4.8 ± 2.8
Douglas	48 ± 8	0.6 ± 0.2	4.8 ± 1.3
spruce	34 ± 11	0.9 ± 0.4	6.8 ± 3.0
pine	71 ± 30	0.2 ± 0.1	2.4 ± 1.2

Even so, the net accumulation rates for all stands, which varied between 0.2 and 1.2 g ha^{-1} $yr^{-1}$for Se, and between 2.4 and 7.2 g ha^{-1} yr^{-1} for I (**Table art.2 – 5**). In general, annual accumulation rates were higher than litterfall fluxes, corroborating the atmospheric origin of a significant fraction of both elements retained in humus. Element accumulation rates were within the ranges reported for French forests (Se: −0.02–1.6 g ha^{-1} yr^{-1}; I: 0.02–15.8 g ha^{-1} yr^{-1}; Pisarek et al., 2021; Roulier et al., 2019). Despite similar element restitution to the forest soil (**Table art.2 – 4**), rapid organic matter degradation in humus of oak and beech plots led to low humus biomass pools and the lowest storage of Se (next to pine) and I. Additionally, oak had the lowest concentration of Se (next to pine) and I in humus bulk. The homogenous element concentrations observed among other tree species might be due to the relatively long residence times of humus compared to the age of the stands (29 years at the time of sampling). Considering the mean concentration in soil column (0 to 70 cm), pine and Douglas fir had generally lower concentration of Se and I, probably due to lower input from humus caused by its long residence time (71 and 48 years; **Table art.2 – 5**). Although the effect of tree species on composition of the soil solution (e.g. anions content) was noticeable (Legout et al., 2016), Se and I contents in soil layers were statistically different only in topsoil, and these differences disappeared below 15 cm depth. It is supposed, that recently introduced tree species did not yet affect the content and distribution of Se and I in deeper soil layers and that their storage depends rather on longer term influence of atmospheric deposition and soil functional parameters.

4.3 Selenium and iodine distributions in soil profiles

The Se- and I-poor status of bedrock material (46 µg Se kg^{-1} and 0.30 mg I kg^{-1}; **Table art.2. – 2**) combined with the observed enrichment of both elements in bulk humus indicated that rock weathering was a minor source of Se and I in soil reserves compared to atmospheric deposition. Contrasting vertical profiles of concentrations suggest that external inputs of each element at the surface were redistributed by different processes during downward transports.

In general, Se concentrations slightly decreased with soil depth, by 30% on average from topsoil layer to the deepest mineral layer. Reimann et al. (2015) similarly observed a decrease from 400 to 6300 µg Se kg^{-1} in O-horizon to 100–2700 µg Se kg^{-1} in the deeper mineral C-horizon in Norwegian forest soils. High correlation between Se and C concentrations ($r_p = 0.64$, $p < 0.01$, **Table art.2.SI – 4**) underlined the pivotal role of OM in Se redistribution and possible retention in soil (Sharma et al., 2015). Selenium concentrations were positively correlated with the mineral soil constituents: Al exchangeable, Fe exchangeable, and Fe oxalate. However, co-correlations with C_{tot} and Fe concentrations prevented the discrimination of a dominant carrier phase for Se.

In contrast to selenium, iodine concentration increased from the forest floor to a maximum at a soil depth of 15 to 35 cm, and then decreased until 70 to 75 cm to values similar to those measured at the soil surface (**Figure art.2 – 3.1**). Different soil iodine profiles have been reported in the literature. Bostock (2004) and Shetaya et al. (2012) reported a gradual decrease of I content with soil depth (until 110 cm) and decreasing OM content. Like in our study, increase of I with soil depth and anti-correlation with OM content were observed in some studies (Epp et al., 2020; Roulier et al., 2018; Xu et al., 2016). Roulier et al. (2018) measured a modest increase in I concentration at 15 to 45 cm depth in beech forest. Xu et al. (2016) reported also an increase of I concentration until a 15 cm depth in a coniferous forest but no depth-related variation in a deciduous forest.

In surface forest soil, iodine is rapidly transformed into organic forms (Takeda et al., 2015), that determines its mobility in the soil profile. The behavior of dissolved organo-iodine (DOI) in forest soil is strongly affected by dynamic of dissolved organic carbon DOC (Takeda et al., 2019). At our forest site, it is postulated that iodine that is derived from the surface horizon as DOI may accumulate on Al oxides (Takeda et al., 2018; Cortizas et al., 2016; Whitehead, 1978). That hypothesis is supported by the co-existence of a maximum of oxalate extracted Al and total I at the depth of 15 to 35 cm (**Figure art.2.SI – 2**, $r^2 = 0.63$). An enrichment-depletion profile is common for Al in acid soils, where conditions in the topsoil promote the dissolution

of Al and the formation of secondary Al precipitates in deeper profile (Brantley et al., 2007). The sorption capacity of Al oxides for DOC (Kalbitz et al., 2000), and thus including DOI, is well documented (Söderlund et al., 2017). Similarly, an iodine retention front was noticed by Unno et al. (2017) at 20 to 30 cm in a forest soil, in close agreement with the partitioning of OC between solid and liquid soil phases. That means that leaching and further immobilization of both Al and OC may have a strong influence on iodine migration in acid forest soils.

The possible influence of volatilization and root uptake on iodine depletion in surface horizon is less clear. Our estimation of iodine absorption by roots, based on calculated uptake flux, would represent no more than 0.02% of iodine stored in the 0 to 15 cm soil. Given this meager annual output, root uptake would not radically influence the distribution of I in soil. Even though volatilization from terrestrial environment contributes to the global atmospheric budget (Feinberg et al., 2020; Kadowaki et al., 2020), iodine loss by volatilization is probably a minor process to explain iodine depletion in the upper layer of these soil profiles. In experiments with spiked forest soils, the loss of ^{125}I through volatilization accounted for 0.011–0.07% of total iodine for reaction times ≤66 days (Bostock et al., 2003; Sheppard et al., 1994). According to the poor knowledge on the magnitude of I volatilization and its environmental controls in different site conditions, further studies are needed to investigate the balance between retention and volatilization depending on the physicochemical properties of the soil.

5. Conclusions

Monitoring of monospecific stands located under identical climatic and geogenic conditions enabled specifying the impact of tree species on inventories of Se and I. For both elements, stocks in aboveground tree parts were marginal compared to forest soil (≤0.09% for Se, ≤0.013% for I). Tree species affected element stocks in aboveground tree parts (oak < beech, pine ≤ spruce, Douglas fir) and uptake fluxes (beech ≤ oak, pine, spruce < Douglas fir). Returns to forest floor through litterfall were lower at beech stand for Se and higher at Douglas fir stand for I. Vegetation type influenced the organic material and element turnover in humus. The stands with high humus biomass (i.e. Douglas fir and spruce) stored more Se and I, while low biomass and short residence time of OM resulted in reduced pools of elements in deciduous humus. Under our edaphic conditions and stand ages, tree species did not influence soil Se and I reserves. In the soil profile, selenium concentrations slightly decreased with soil depth while iodine showed an “enrichment-depletion profile” that could be explained by downward leaching of DOI and enrichment with depth by sorption onto Al oxides.

Supplementary information

Additional information as noted in the text.

CRediT statements

Paulina Pisarek: Conceptualization, Investigation, Validation, Formal analysis, Writing-original draft, Writing - review & editing. **Maïté Bueno**: Conceptualization, Investigation, Validation, Funding acquisition, Writing-original draft, Writing -review & editing, Supervision. **Yves Thiry**: Conceptualization, Funding acquisition, Writing-original draft, Writing - review & editing, Supervision. **Arnaud Legout**: Resources, Writing-original draft, Writing - review & editing. **Hervé Gallard**: Conceptualization, Validation, Writing-original draft, Writing - review & editing, Funding acquisition, Supervision. **Isabelle Le Hécho**: Conceptualization, Writing-original draft, Writing - review & editing, Funding acquisition, Supervision.

Declaration of interests

The authors declare that they have no known competing financial interests or personal relationships that could have appeared to influence the work reported in this paper.

Acknowledgements

We would like to acknowledge all technical staff from the Breuil site network for providing samples and data collection. This research was financially supported by the French National Radioactive Waste Management Agency (Andra).

References

Alberdi, I., BaychevaMerger, T., Alain, B., Bozzano, M., Caudullo, G., Cienciala, E., Corona, P., Domínguez, G., Houston-Durrant, T., Edwards, D., Estreguil, C., Ferreti, M., Fischer, U., Freudenschuss, A., Gasparini, P., Godinho-Ferreira, P., Hansen, K., Hiederer, R., Inhaizer, H., Zingg, A., 2015. State of Europe's Forests 2015 - Summary for Policy Makers.

AnaEE France - Breuil. [WWW Document], URL https://www.anaee-france.fr/en/infrastructure-services/in-natura-experimentation/forest-ecosystems/temperate-and-continental-forests/breuil (accessed 5.2.21).

Aponte, C., García, L.V., Marañón, T., 2013. Tree species effects on nutrient cycling and soil biota: a feedback mechanism favouring species coexistence. For. Ecol. Manag. 309, 36–46. https://doi.org/10.1016/j.foreco.2013.05.035.

Berger, T.W., Berger, P., 2012. Greater accumulation of litter in spruce (Picea abies) compared to beech (Fagus sylvatica) stands is not a consequence of the inherent recalci-trance of needles. Plant Soil 358, 349–369. https://doi.org/10.1007/s11104-012-1165-z.

Bostock, A.C., 2004. Chemical speciation, volatilisation and cycling of 36Cl, 129I and 99Tc in coniferous forest systems. PhD Thesis. University of London.

Bostock, A.C., Shaw, G., Bell, J.N.B., 2003. The volatilisation and sorption of 129I in conifer-ous forest, grassland and frozen soils. J. Environ. Radioact. 70, 29–42. https://doi.org/10.1016/S0265-931X(03)00120-6 International workshop on the mobility of iodine, technetium, selenium and uranium in the biosphere.

Bowley, H.E., Young, S.D., Ander, E.L., Crout, N.M.J., Watts, M.J., Bailey, E.H., 2019. Iodine bioavailability in acidic soils of Northern Ireland. Geoderma 348, 97–106. https://doi.org/10.1016/j.geoderma.2019.04.020.

Brantley, S.L., Goldhaber, M.B., Ragnarsdottir, K.V., 2007. Crossing disciplines and scales to understand the critical zone. Elements 3, 307–314. https://doi.org/10.2113/gselements.3.5.307.

Cakmak, I., Promuthai, C., Guilherme, L.R.G., Rashid, A., Hora, K.H., Yazici, A., Savasli, E., Kalayci, M., Tutus, Y., Phuphong, P., Rizwan, M., Martins, F.A.D., Dinali, G.S., Ozturk, L., 2017. Iodine biofortification of wheat, rice and maize through fertilizer strategy. Plant Soil 418, 319–335. https://doi.org/10.1007/s11104-017-3295-9.

Coppin, F., Chabroullet, C., Martin-Garin, A., 2009. Selenite interactions with some particulate organic and mineral fractions isolated from a natural grassland soil. Eur. J. Soil Sci. 60, 369–376. https://doi.org/10.1111/j.1365-2389.2009.01127.x.

Cornelis, J.T., Ranger, J., Iserentant, A., Delvaux, B., 2010. Tree species impact the terrestrial cycle of silicon through various uptakes. Biogeochemistry 97, 231–245. https://doi.org/10.1007/s10533-009-9369-x.

Cortizas, A.M., Vázquez, C.F., Kaal, J., Biester, H., Casais, M.C., Rodríguez, T.T., Lado, L.R., 2016. Bromine accumulation in acidic black colluvial soils. Geochim. Cosmochim. Acta 174, 143–155. https://doi.org/10.1016/j.gca.2015.11.013.

De Schrijver, A., Geudens, G., Augusto, L., Staelens, J., Mertens, J., Wuyts, K., Gielis, L., Verheyen, K., 2007. The effect of forest type on throughfall deposition and seepage flux: a review. Oecologia 153, 663–674. https://doi.org/10.1007/s00442-007-0776-1.

Di Tullo, P., 2015. Dynamique du cycle biogéochimique du sélénium en écosystèmes terrestres: rétention et réactivité dans le sol, rôle de la végétation (thesis). Pau.

Epp, T., Neidhardt, H., Pagano, N., Marks, M.A.W., Markl, G., Oelmann, Y., 2020. Vegetation canopy effects on total and dissolved cl, br, F and I concentrations in soil and their fate along the hydrological flow path. Sci. Total Environ. 712, 135473. https://doi.org/10.1016/j.scitotenv.2019.135473.

Feinberg, A., Stenke, A., Peter, T., Winkel, L., 2020. Constraining atmospheric selenium emissions using observations, global modeling, and bayesian inferencef. Environ. Sci. Technol. 54, 7146–7155.

Fuge, R., Johnson, C.C., 2015. Iodine and human health, the role of environmental geochemistry and diet, a review. Appl. Geochem. 63, 282–302. https://doi.org/10.1016/j.apgeochem.2015.09.013.

Goor, F., Thiry, Y., 2004. Processes, dynamics and modelling of radiocaesium cycling in a chronosequence of Chernobyl-contaminated scots pine (Pinus sylvestris L.) plantations. Sci. Total Environ. 325, 163–180. https://doi.org/10.1016/j.scitotenv.2003.10. 037.

Hurtevent, P., Thiry, Y., Levchuk, S., Yoschenko, V., Henner, P., Madoz-Escande, C., Leclerc, E., Colle, C., Kashparov, V., 2013. Translocation of 125I, 75Se and 36Cl to wheat edible parts following wet foliar contamination under field conditions. J. Environ. Radioact. 121, 43–54. https://doi.org/10.1016/j.jenvrad.2012.04.013.

IUSS Working Group WRB, 2006. World Reference Base for Soil Resources 2006. World Soil Resources Reports No. 103. FAO, Rome.

Kadowaki, M., Terada, H., Nagai, H., 2020. Global budget of atmospheric 129I during 2007–2010 estimated by a chemical transport model: GEARN–FDM. Atmos. Environ. X 8, 100098. https://doi.org/10.1016/j.aeaoa.2020.100098.

Kalbitz, K., Solinger, S., Park, J.H., Michalzik, B., Matzner, E., 2000. Controls on the dynamics of dissolved organic matter in soils: a review. Soil Sci. 165, 277–304.

Kato, S., Wachi, T., Yoshihira, K., Nakagawa, T., Ishikawa, A., Takagi, D., Tezuka, A., Yoshida, H., Yoshida, S., Sekimoto, H., Takahashi, M., 2013. Rice (Oryza sativa L.) roots

have iodate reduction activity in response to iodine. Front. Plant Sci. 4, 227. https://doi.org/10.3389/fpls.2013.00227.
Kikkert, J., Berkelaar, E., 2013. Plant uptake and translocation of inorganic and organic forms of selenium. Arch. Environ. Contam. Toxicol. 65, 458–465. https://doi.org/10. 1007/s00244-013-9926-0.
Korobova, E., 2010. Soil and landscape geochemical factors which contribute to iodine spatial distribution in the main environmental components and food chain in the central russian plain. J. Geochem. Explor. 107, 180–192. https://doi.org/10.1016/j. gexplo.2010.03.003.
Laganière, J.L., Paré, D.P., Bradley, R.L.B.L., 2010. How does a tree species influence litter decomposition? Separating the relative contribution of litter quality, litter mixing, and forest floor conditions. Can. J. For. Res. https://doi.org/10.1139/X09-208.
Legout, A., van der Heijden, G., Jaffrain, J., Boudot, J.P., Ranger, J., 2016. Tree species effects on solution chemistry and major element fluxes: a case study in the morvan (Breuil, France). For. Ecol. Manag. 378, 244–258. https://doi.org/10.1016/j.foreco.2016.07. 003.
Li, H.F., McGrath, S.P., Zhao, F.J., 2008. Selenium uptake, translocation and speciation in wheat supplied with selenate or selenite. New Phytol. 178, 92–102. https://doi.org/10.1111/j.1469-8137.2007.02343.x.
Mareschal, L., Bonnaud, P., Turpault, M.P., Ranger, J., 2010. Impact of common european tree species on the chemical and physicochemical properties of fine earth: an unusual pattern. Eur. J. Soil Sci. 61, 14–23. https://doi.org/10.1111/j.1365-2389.2009.01206.x.
Montelius, M., Thiry, Y., Marang, L., Ranger, J., Cornelis, J.T., Svensson, T., Bastviken, D., 2015. Experimental evidence of large changes in terrestrial chlorine cycling following altered tree species composition. Environ. Sci. Technol. 49, 4921–4928. https://doi.org/10.1021/acs.est.5b00137.
Osono, T., Takeda, H., 2005. Limit values for decomposition and convergence process of lignocellulose fraction in decomposing leaf litter of 14 tree species in a cool temperate forest. Ecol. Res. 20, 51–58. https://doi.org/10.1007/s11284-004-0011-z.
Pisarek, P., Bueno, M., Thiry, Y., Nicolas, M., Gallard, H., Hécho, I.L., 2021. Selenium distribution in french forests: influence of environmental conditions. Sci. Total Environ. 144962. https://doi.org/10.1016/j.scitotenv.2021.144962.
Prescott, C.E., Grayston, S.J., 2013. Tree species influence on microbial communities in litter and soil: current knowledge and research needs. For. Ecol. Manag. 309, 19–27. https://doi.org/10.1016/j.foreco.2013.02.034 Influence of tree species on forest soils: New evidence from field studies.
Prescott, C.E., Zabek, L.M., Staley, C.L., Kabzems, R., 2000. Decomposition of broadleaf and needle litter in forests of British Columbia: influences of litter type, forest type, and litter mixtures. Can. J. For. Res. 30, 1742–1750. https://doi.org/10. 1139/x00-097.
R Core Team, 2013. R: A Language and Environment for Statistical Computing. R Foundation for Statistical Computing, Vienna, Austria.
Ranger, J., Colin-Belgrand, M., 1996. Nutrient dynamics of chestnut tree (Castanea sativa mill.) coppice stands. For. Ecol. Manag. 86, 259–277. https://doi.org/10.1016/S0378-1127(96)03733-4.
Redon, P.O., Abdelouas, A., Bastviken, D., Cecchini, S., Nicolas, M., Thiry, Y., 2011. Chloride and organic chlorine in forest soils: storage, residence times, and influence of ecological conditions. Environ. Sci. Technol. 45, 7202–7208. https://doi.org/10.1021/ es2011918.
Reimann, C., Englmaier, P., Fabian, K., Gough, L., Lamothe, P., Smith, D., 2015. Biogeochemical plant–soil interaction: variable element composition in leaves of four plant species collected along a south–north transect at the southern tip of Norway. Sci. Total Environ. 506–507, 480–495. https://doi.org/10.1016/j. scitotenv.2014.10.079.

Roulier, M., Bueno, M., Thiry, Y., Coppin, F., Redon, P.O., Le Hécho, I., Pannier, F., 2018. Iodine distribution and cycling in a beech (Fagus sylvatica) temperate forest. Sci. Total Environ. 645, 431–440. https://doi.org/10.1016/j.scitotenv.2018. 07.039.

Roulier, M., Coppin, F., Bueno, M., Nicolas, M., Thiry, Y., Della Vedova, C., Février, L., Pannier, F., Le Hécho, I., 2019. Iodine budget in forest soils: influence of environmental conditions and soil physicochemical properties. Chemosphere 224, 20–28. https://doi.org/10.1016/j.chemosphere.2019.02.060.

Roulier, M., Bueno, M., Coppin, F., Nicolas, M., Thiry, Y., Rigal, F., Le Hécho, I., Pannier, F., 2020a. Atmospheric iodine, selenium and caesium depositions in France: I. Spatial and seasonal variations. Chemosphere, 128971 https://doi.org/10.1016/j.chemosphere.2020.128971.

Roulier, M., Bueno, M., Coppin, F., Nicolas, M., Thiry, Y., Rigal, F., Pannier, F., Le Hécho, I., 2020b. Atmospheric iodine, selenium and caesium depositions in France: II. Influence of forest canopies. Chemosphere, 128952 https://doi.org/10.1016/j.chemosphere. 2020.128952.

Shahid, N., Shahid, M., Niazi, N.K., Khalid, S., Murtaza, B., Bibi, I., Rashid, M.I., 2018. A critical review of selenium biogeochemical behavior in soil-plant system with an inference to human health. Environ. Pollut. 234, 915–934. https://doi.org/10.1016/j.envpol.2017.12.019.

Sharma, V.K., McDonald, T.J., Sohn, M., Anquandah, G.A.K., Pettine, M., Zboril, R., 2015. Biogeochemistry of selenium. A review. Environ. Chem. Lett. 13, 49–58. https://doi.org/10.1007/s10311-014-0487-x.

Sheppard, M.I., Thibault, D.H., Smith, P.A., Hawkins, J.L., 1994. Volatilization: a soil degassing coefficient for iodine. J. Environ. Radioact. 25, 189–203. https://doi.org/10.1016/0265-931X(94)90072-8.

Shetaya, W.H., Young, S.D., Watts, M.J., Ander, E.L., Bailey, E.H., 2012. Iodine dynamics in soils. Geochim. Cosmochim. Acta 77, 457–473. https://doi.org/10.1016/j.gca.2011. 10.034.

Söderlund, M., Virkanen, J., Aromaa, H., Gracheva, N., Lehto, J., 2017. Sorption and speciation of iodine in boreal forest soil. J. Radioanal. Nucl. Chem. 311, 549–564. https://doi.org/10.1007/s10967-016-5022-z.

Takeda, A., Tsukada, H., Takahashi, M., Takaku, Y., Hisamatsu, S., 2015. Changes in the chemical form of exogenous iodine in forest soils and their extracts. Radiat. Prot. Dosim. 167, 181–186. https://doi.org/10.1093/rpd/ncv240.

Takeda, A., Nakao, A., Yamasaki, S., Tsuchiya, N., 2018. Distribution and speciation of bromine and iodine in volcanic ash soil profiles. Soil Sci. Soc. Am. J. 82, 815–825. https://doi.org/10.2136/sssaj2018.01.0019.

Takeda, A., Unno, Y., Tsukada, H., Takaku, Y., Hisamatsu, S., 2019. Speciation of iodine in soil solution in forest and grassland soils in Rokkasho, Japan. Radiat. Prot. Dosim. 184, 368–371. https://doi.org/10.1093/rpd/ncz103.

Thiry, Y., Schmidt, P., Van Hees, M., Wannijn, J., Van Bree, P., Rufyikiri, G., Vandenhove, H., 2005. Uranium distribution and cycling in scots pine (Pinus sylvestris L.) growing on a revegetated Umining heap. J. Environ. Radioact. 81, 201–219. https://doi.org/10.1016/j.jenvrad.2004.01.036.

Tolu, J., Thiry, Y., Bueno, M., Jolivet, C., Potin-Gautier, M., Le Hécho, I., 2014. Distribution and speciation of ambient selenium in contrasted soils, from mineral to organic rich. Sci. Total Environ. 479–480, 93–101. https://doi.org/10.1016/j.scitotenv.2014. 01.079.

Tyler, G., 2005. Changes in the concentrations of major, minor and rare-earth elements during leaf senescence and decomposition in a Fagus sylvatica forest. For. Ecol. Manag. 206, 167–177. https://doi.org/10.1016/j.foreco.2004.10.065.

Ukonmaanaho, L., Merilä, P., Nöjd, P., Nieminen, T., 2008. Litterfall production and nutrient return to the forest floor in scots pine and Norway spruce stands in Finland. Boreal Environ. Res. 13, 67–91.

Unno, Y., Tsukada, H., Takeda, A., Takaku, Y., Hisamatsu, S., 2017. Soil-soil solution distribution coefficient of soil organic matter is a key factor for that of radioiodide in surface and subsurface soils. J. Environ. Radioact. 169–170, 131–136. https://doi.org/10.1016/j.jenvrad.2017.01.016.

van der Heijden, G., Legout, A., Midwood, A.J., Craig, C.-A., Pollier, B., Ranger, J., Dambrine, E., 2013. Mg and Ca root uptake and vertical transfer in soils assessed by an in situ ecosystem-scale multi-isotopic (26Mg & 44Ca) tracing experiment in a beech stand (Breuil-Chenue, France). Plant Soil 369, 33–45.

Vergutz, L., Manzoni, S., Porporato, A., Novais, R.F., Jackson, R.B., 2012. Global resorption efficiencies and concentrations of carbon and nutrients in leaves of terrestrial plants. Ecol. Monogr. 82, 205–220. https://doi.org/10.1890/11-0416.1.

Watts, M.J., Mitchell, C.J., 2009. A pilot study on iodine in soils of Greater Kabul and Nangarhar provinces of Afghanistan. Environ. Geochem. Health 31, 503–509. https://doi.org/10.1007/s10653-008-9202-9.

Watts, M.J., Joy, E.J.M., Young, S.D., Broadley, M.R., Chilimba, A.D.C., Gibson, R.S., Siyame, E.W.P., Kalimbira, A.A., Chilima, B., Ander, E.L., 2015. Iodine source apportionment in the Malawian diet. Sci. Rep. 5, 15251. https://doi.org/10.1038/srep15251.

Whitehead, D.C., 1978. Iodine in soil profiles in relation to iron and aluminium oxides and organic matter. J. Soil Sci. 29, 88–94. https://doi.org/10.1111/j.1365-2389.1978.tb02035.x.

Xu, C., Zhang, S., Sugiyama, Y., Ohte, N., Ho, Y.F., Fujitake, N., Kaplan, D.I., Yeager, C.M., Schwehr, K., Santschi, P.H., 2016. Role of natural organic matter on iodine and 239,240Pu distribution and mobility in environmental samples from the northwestern Fukushima Prefecture, Japan. J. Environ. Radioact. 153, 156–166. https://doi.org/10.1016/j.jenvrad.2015.12.022.

Zhao, X., Hou, X., Zhou, W., 2019. Atmospheric iodine (127I and 129I) record in spruce tree rings in the Northeast Qinghai-Tibet Plateau. Environ. Sci. Technol. 53, 8706–8714. https://doi.org/10.1021/acs.est.9b01160.

Supplementary information

Influence of tree species on selenium and iodine partitioning in an experimental forest ecosystem

Paulina Pisarek[1,2], Maïté Bueno[1], Yves Thiry[2], Arnaud Legout[3], Hervé Gallard[4], Isabelle Le Hécho[1]

[1] CNRS/Univ. Pau & Pays de l'Adour, Institut des Sciences Analytiques et de Physico-Chimie pour l'Environnement et les Matériaux (IPREM), UMR 5254, 64053 Pau, France (*pisarek.paulina@univ-pau.fr) (maite.bueno@univ-pau.fr;isabelle.lehecho@univ-pau.fr)

[2] Andra, Research and Development Division, Parc de la Croix Blanche, 92298 Châtenay-Malabry Cedex, France (yves.thiry@andra.fr)

[3] INRAE, BEF, F-54000 Nancy, France (arnaud.legout@inrae.fr)

[4] IC2MP UMR 7285, Université de Poitiers, 86073 Poitiers Cedex 9, France (herve.gallard@univ-poitiers.fr)

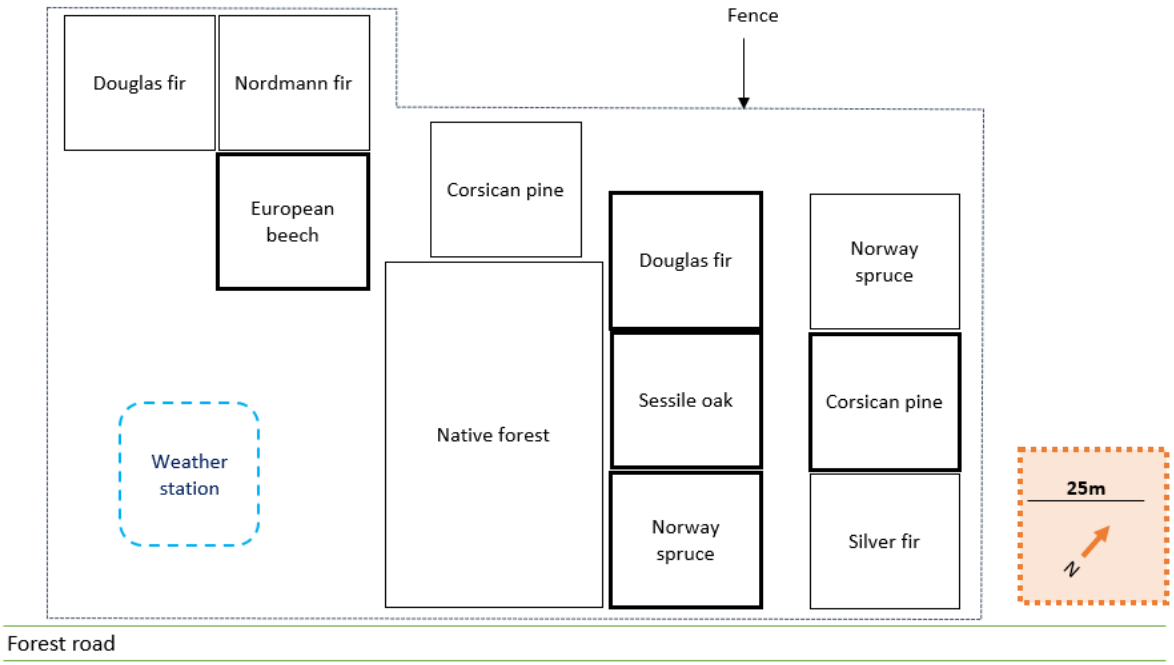

Figure art.2.SI – 1 Map of the Breuil-Chenue experimental site (modified from van der Heijden et al., 2013).

Table art.2.SI – 1 Physical and chemical properties of soil **(Levrel and Ranger, 2006; Mareschal et al., 2010)**. The data correspond to samples collected in 2001 (for more details see **Mareschal et al., 2010)**

Tree species	Soil depth (cm)	Density* g cm^{-3}	C organic g/kg	N g/kg	Clay g/kg	Silt g/kg	pH	Fe exchang. cmol kg^{-1}	Mn exchang. cmol kg^{-1}	Al exchang. cmol kg^{-1}	Fe oxalate g/kg	Al oxalate g/kg
Douglas	0-7.5	0.76	50.7	2.70	189	225	4.07	0.16	0.16	6.22	3.20	2.59
Douglas	7.5-15	0.74	32.9	1.79	184	223	4.32	0.07	0.07	5.35	3.50	2.82
Douglas	15-30	0.97	19.6	1.12	190	243	4.51	0.01	0.06	3.73	3.25	3.58
Douglas	30-45	1.03	10.3	0.61	200	260	4.50	0.01	0.06	3.18	2.67	3.35
Douglas	45-60	1.16	0.0	0.00	200	253	4.50	0.01	0.06	3.04	2.32	2.81
Douglas	60-75	1.21	0.0	0.00	193	250	4.50	0.01	0.05	3.05	2.15	2.53
pine	0-7.5	0.61	57.1	3.14	166	-	4.07	0.24	0.13	6.12	3.23	2.41
pine	7.5-15	0.73	37.4	2.04	156	-	4.43	0.08	0.06	5.23	3.53	2.93
pine	15-30	0.99	22.1	1.27	145	-	4.68	0.02	0.05	3.43	3.22	3.72
pine	30-45	1.01	10.3	0.66	143	-	4.65	0.01	0.05	2.63	2.78	4.64
pine	45-60	1.09	0.0	0.00	144	-	4.63	0.01	0.05	2.63	2.60	3.82
pine	60-75	1.12	0.0	0.00	139	-	4.63	0.01	0.06	2.91	2.35	3.60
spruce	0-7.5	0.68	51.8	2.77	166	211	4.30	0.21	0.08	6.25	3.10	2.95
spruce	7.5-15	0.75	32.3	1.75	156	214	4.60	0.06	0.06	5.07	3.10	3.92
spruce	15-30	1.02	18.1	2.76	164	228	4.76	0.02	0.06	3.51	2.71	3.80
spruce	30-45	1.05	8.3	3.93	157	228	4.75	0.03	0.06	2.98	2.46	3.21
spruce	45-60	1.13	0.0	0.00	151	233	4.70	0.05	0.06	3.10	2.13	2.73
spruce	60-75	1.23	0.0	0.00	153	232	4.69	0.03	0.07	3.16	1.95	2.53
beech	0-7.5	0.55	63.7	3.54	199	217	4.13	0.25	0.19	6.21	2.64	2.48
beech	7.5-15	0.66	38.2	2.12	184	229	4.45	0.08	0.09	5.25	2.98	3.40
beech	15-30	0.89	20.2	1.14	164	243	4.69	0.01	0.06	3.43	2.47	4.37
beech	30-45	0.96	9.3	0.54	178	254	4.68	0.03	0.06	2.69	2.11	3.57
beech	45-60	1.07	0.0	0.00	182	256	4.67	0.07	0.06	2.68	1.84	3.05
beech	60-75	1.05	0.0	0.00	175	253	4.67	0.01	0.06	2.80	1.68	2.75
oak	0-7.5	0.63	65.7	3.60	184	211	3.95	0.20	0.19	6.50	3.27	2.36
oak	7.5-15	0.73	39.2	2.06	178	201	4.30	0.09	0.06	6.06	3.94	3.15
oak	15-30	1.00	22.1	1.19	161	204	4.63	0.03	0.04	4.06	3.25	4.48
oak	30-45	1.05	9.8	0.57	169	211	4.63	0.02	0.04	3.24	2.93	4.13
oak	45-60	1.12	0.0	0.00	164	252	4.58	0.02	0.04	3.26	2.93	3.98
oak	60-75	1.15	0.0	0.00	161.5	242	4.55	0.01	0.05	3.44	2.80	3.70

- Density of fine earth fraction

Soil extraction methods for aluminium and iron

Aluminium and iron content in soil were determined in exchangeable (Al exchang.; Fe exchang.; extracted with 1 mol L^{-1} KCl; Espiau and Peyronel, 1976; Mareschal et al., 2010) and oxalate extracted (Al Oxalate; Fe oxalate; Tamm, 1922) fractions of soil. Extraction with oxalate according to Tamm (1922) method leads to mobilization of amorphous, poorly crystalline oxides and allophonic minerals of Fe and Al (Chao and Zhou, 1983; Rennert, 2019).

Table art.2.SI – 2 Masses (kg ha^{-1}) of Douglas, pine, spruce, beech and oak forest stands compartments (Mareschal et al., 2010; Montelius et al., 2015).

Compartment	Mass (kg ha^{-1})				
	Douglas	**Pine**	**Spruce**	**Beech**	**Oak**
Bole-Wood	104705	94543	80115	84721	47165
Branches	20863	16861	25249	21360	13422
Bole-Bark	16016	13583	9001	8168	8583
Foliage; 2002	10944	7076	23487	3849	4732
Foliage; 2003	12302	7036	25947	1701	2305
Foliage; 2004	13111	7311	28425	2841	3544
Foliage; 2005	14636	7628	28684	2605	3193
Foliage; 2006	15575	7773	30089	1847	2449
LF leaves; 2002	3548	5476	4286	3849	4732
LF leaves; 2003	3620	3770	3364	1701	2305
LF leaves; 2004	2743	2292	5179	2841	3544
LF leaves; 2005	2472	4256	2442	2605	3193
LF leaves; 2006	2722	1888	2457	1847	2449
LF branches; 2002	251	83	264	1032	1897
LF branches; 2003	373	76	511	933	1453
LF branches; 2004	635	96	453	573	1466
LF branches; 2005	694	125	388	484	1847
LF branches; 2006	591	72	383	976	1965
Humus bulk	50600	38600	52100	22100	27500
Soil					
0-7.5 cm	570000	457500	510000	412500	472500
7.5-15 cm	555000	547500	562500	495000	547500
15-30 cm	1455000	1485000	1530000	1335000	1500000
30-45 cm	1545000	1515000	1575000	1440000	1575000
45-60 cm	1740000	1635000	1695000	1605000	1680000
60-70 cm	1815000	1120000	1230000	1575000	1150000

Table art.2.SI – 3 Annual biomass production (kg ha^{-1} yr^{-1}) in Douglas, pine, spruce, beech and oak forest stands. LF=Litterfall.

Compartment	Annual biomass production (kg ha^{-1} yr^{-1})				
	Douglas	Pine	Spruce	Beech	Oak
Bole-Wood	8590 ± 2358	2536 ± 751	5075 ± 2755	3038 ± 463	5502 ± 4337
Branches	2488 ± 703	789 ± 229	1881 ± 1012	1416 ± 74	2743 ± 2173
Bole-Bark	1403 ± 386	356 ± 105	481 ± 263	184 ± 54	862 ± 679
Foliage	1243 ± 349	252 ± 75	1718 ± 926	3277 ± 1102	4139 ± 1247
LF leaves	3021 ± 526	3536 ± 1466	3546 ± 1189	2569 ± 864	3245 ± 977
LF branches	509 ± 188	90 ± 21	400 ± 92	800 ± 252	1726 ± 247

Table art.2.SI – 4 Pearson's correlation coefficients of Se and I concentrations in soil column and soil parameters (n= 5). Significant correlations are bolded.

Soil parameter	Selenium concentration		Iodine concentration	
	r_p	p-value	r_p	p-value
CEC	**0.50**	**< 0.05**	**-0.48**	**< 0.05**
C	**0.64**	**< 0.01**	**-0.50**	**< 0.05**
Al exchang.	**0.68**	**< 0.001**	**-0.37**	**< 0.05**
Al Oxalate	**0.37**	**< 0.05**	**0.80**	**< 0.001**
Fe exchang.	**0.61**	**< 0.001**	**-0.49**	**< 0.05**
Fe oxalate	**0.56**	**< 0.05**	-0.03	0.88
Mn exchang.	0.20	0.29	-0.41	**< 0.05**

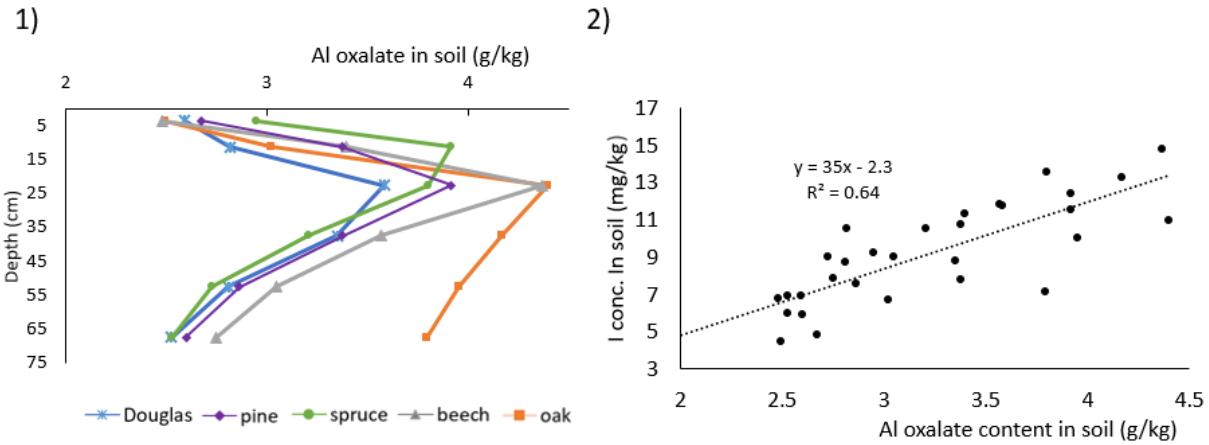

Figure art.2.SI – 2 Soil profile of Al oxalate (g/kg) and 2) iodine concentration in soil (mg/kg) as a function of Al oxalate.

References

Chao, T.T., Zhou, L., 1983. Extraction Techniques for Selective Dissolution of Amorphous Iron Oxides from Soils and Sediments. Soil Science Society of America Journal 47, 225–232. https://doi.org/10.2136/sssaj1983.03615995004700020010x

Espiau, P., Peyronel, A., 1976. L'acidité d'échange des sols, le taux d'acidité d'échange et sa signification pédologique sous climat tempéré. Annales Agronomiques 31, 363–383.

Legout, A., van der Heijden, G., Jaffrain, J., Boudot, J.P., Ranger, J., 2016. Tree species effects on solution chemistry and major element fluxes: A case study in the Morvan (Breuil, France). Forest Ecology and Management 378, 244–258. https://doi.org/10.1016/j.foreco.2016.07.003

Levrel, G., Ranger, J., 2006. Effet des substitutions d'essences forestières et des amendements sur les propriétés physiques d'un Alocrisol. Etude et Gestion des Sols 13, 71–88.

Mareschal, L., Bonnaud, P., Turpault, M.P., Ranger, J., 2010. Impact of common European tree species on the chemical and physicochemical properties of fine earth: an unusual pattern. European Journal of Soil Science 61, 14–23. https://doi.org/10.1111/j.1365-2389.2009.01206.x

Montelius, M., Thiry, Y., Marang, L., Ranger, J., Cornelis, J.T., Svensson, T., Bastviken, D., 2015. Experimental evidence of large changes in terrestrial chlorine cycling following altered tree species composition. Environ. Sci. Technol. 49, 4921–4928. https://doi.org/10.1021/acs.est.5b00137

Rennert, T., 2019. Wet-chemical extractions to characterise pedogenic Al and Fe species – a critical review. Soil Res. 57, 1–16. https://doi.org/10.1071/SR18299

Tamm, O., 1922. Um best ämning ow de oorganiska komponenterna i markens gelcomplex. Medd. Statens Skogsförsökanst 19, 385–404.

van der Heijden, G., Legout, A., Midwood, A.J., Craig, C.A., Pollier, B., Ranger, J., Dambrine, E., 2013. Mg and Ca root uptake and vertical transfer in soils assessed by an in situ ecosystem-scale multiisotopic (^{26}Mg & ^{44}Ca) tracing experiment in a beech stand (Breuil-Chenue, France). Plant and Soil 369, 33–45.

3. Article 3: Selenium and iodine cycles in beech and Douglas fir forests

Paulina Pisarek[1,2], Maïté Bueno[1], Yves Thiry[2], Arnaud Legout[3], Laurent Grasset[4], Hervé Gallard[4], Isabelle Le Hécho[1]

[1] Universite de Pau et des Pays de l'Adour, E2S UPPA, CNRS, Institut des Sciences Analytiques et de Physicochimie pour l'Environnement et les Matériaux-IPREM, UMR5254, 64000 Pau, France (*pisarek.paulina@univ-pau.fr; maite.bueno@univ-pau.fr; isabelle.lehecho@univ-pau.fr)

[2] Andra, Research and Development Division, Parc de la Croix Blanche, 92298 Châtenay-Malabry Cedex, France (yves.thiry@andra.fr)

[3] Institut National de la Recherche en Agriculture, Alimentation et Environnement (INRAE), BEF, 54000 Nancy, France

[4] IC2MP UMR 7285, Université de Poitiers, 86073 Poitiers Cedex 9, France (herve.gallard@univ-poitiers.fr)

(in preparation)

1. Introduction

Selenium and iodine are two elements of ecological importance. However, knowledge about their cycling and input-output budgets in forest ecosystems are sparse in the literature. These elements originate mainly from atmospheric deposition (wet and dry) and as a consequence, the content of Se and I in litterfall increased with the element concentration in rainfall (Pisarek et al., 2021; Roulier et al., 2019). The structure of coniferous canopy (twigs and needles) promotes accumulation of the airborne deposits compared to deciduous trees due to higher deposition velocity (by impaction and diffusion) and aerodynamic resistance (Le Mellec et al., 2010). Uptake of the elements by leaf surface resulted mainly in negative annual canopy exchange fluxes for both Se and I (Roulier et al., 2021). Although not statistically different, dry deposition and canopy exchange (in absolute terms) fluxes tended to be higher for coniferous trees compared to deciduous (Roulier et al., 2021). The absence of statistically significant differences could be due to the variability of climatic conditions in the studied forests, as well as the age and height of the trees.

Forest soil was shown to act as a sink for Se (positive input-output budget; Di Tullo, 2015) and a source of I for ground water (negative input-output budget; Roulier et al., 2018). However, these data were obtained in deciduous forests (with beech as the dominant species) and, to our knowledge, there is no similar information in coniferous forests. Our previous study showed that tree species can influence the distribution of elements in the aboveground tree parts, litterfall and humus, while soil was only affected in the upper layer (Pisarek et al., 2021). The mechanisms of Se and I associations with mineral and organic phases in soil are complex and remain unclear. These include electrostatic interactions with metal oxides, indirect organo-mineral complexes (as Se-OM-metal ternary complexes) and direct covalent bond with high molecular weight humic substances (Li et al., 2017; Xu et al., 2011). In soil solution, elements are present as soluble (hydr)-(oxy)-anions (Se(IV), Se(VI), I(–I), I(V)) and colloidal organic Se and I (Bowley et al., 2016; Li et al., 2017; Tolu et al., 2011; Weng et al., 2011; Xu et al., 2011). The speciation of Se and I strongly affects their immobilization in soil (Söderlund et al., 2017, 2016), as well as their bioavailability to plants (Kato et al., 2013; Kikkert and Berkelaar, 2013) and their potential recycling from soil to aboveground tree biomass.

In this study, we investigated the fate of selenium and iodine in monospecific Douglas fir and beech forests (as representatives of coniferous and deciduous trees), under identical geogenic and climatic conditions. Annual monitoring of rainfall, throughfall, stemflow and soil solutions was conducted to study element inputs by atmospheric deposition and outputs by drainage. The

determination of total Se and I was also performed in tree parts (leaves, roots), humus and soil depth profile. Speciation analysis of Se and I was carried out on soil fractions (water soluble and associated to soil organic matter) to better understand their immobilization, potential availability to trees and the nature of their association with organic matter. For this purpose, the characterization of OM included analysis of lignin monomers and carbohydrates. The objectives of this study were to: i) quantify the element annual fluxes (atmospheric inputs and outputs from the canopy including dry deposition and canopy exchange) to examine the differences between coniferous and deciduous canopies; ii) estimate overall input-output budgets; iii) determine Se and I fractionation and speciation in forest soils under both stands and their relation with soil organic matter constituents.

2. Methods

2.1 Site description

The site was located in the Breuil-Chenue forest (latitude 47°18'10"N and longitude 4°4'44"E) in Bourgogne, France. The experimental site is included in the ANAEE France Platform (www.anaee-france.fr) and managed by INRAE-BEF. The mean annual air temperature is 9°C and mean annual precipitation is 1180 mm yr^{-1}. The native coppiced forest was felled in 1975 and monospecific plantations (each about 1000 m^2) were planted in 1976. Douglas fir (*Pseudotsuga menziesii*) and European beech (*Fagus sylvatica*) were chosen for this study as representatives of the coniferous and deciduous classes. The area occupied by Douglas fir has doubled in the last 25 years and represents 9% of the forest area in France and beech is one of the most ubiquitous deciduous species in European forests (Jung et al., 2005; IGD 2015). Soil, classified as Alumnic Cambisol (IUSS Working Group WRB 2006), developed on granite bedrock. Soil and humus characteristics under Douglas fir and beech stands are presented in **Table art.3.SI – 1**.

2.2 Sampling

Monthly (28-day periods) sampling of soil solutions, throughfall, stemflow and rainfall was carried out from January 2019 to December 2019. Rainfall was collected in a funnel attached to the top of the weather station mast. Throughfall was collected using four gutters (2 m long), while stem flow was collected using collars attached horizontally to the tree trunks. Forest floor solutions were collected below the organic layer (noted as 0 cm – forest floor) with zero-tension lysimeters (2 replicates, each composed of 9 polypropylene lysimeters: 40 × 2.5 cm). Soil solutions from three different depths (-15, -30 and -60 cm, 5 repetitions per depth) were

collected using tension controlled lysimeters with an applied pressure of 0.6 bars. Water samples were filtered through a 0.45 µm polyethersulfone (PES) membrane and stored at 4°C.

Fresh needles, leaves and roots were sampled from four trees in August and September 2020. Roots were collected from a depth of 0-10 cm and separated into fractions > 2 mm and < 2 mm. Roots were washed with tap water to remove soil particles and rinsed 10 times with ultrapure water, dried at 40°C and grinded. Humus and soil were sampled in February 2019. At each stand, four soil cores were sampled and divided into 6 layers (0 – 7.5 cm, 7.5 – 15 cm, 15 – 30 cm, 30 – 45 cm, 45 – 60 cm, 60 – 75 cm) and, the respective layers of the four cores were pooled together and sieved to 2 mm. One part of the soil samples was freeze-dried and stored in glass containers at 4° C; the second part was dried at 40°C and ground; the third part was stored at 4° C. For each tree species, two humus layers, classified as *ol* (organic, litter) and *oh* (pool of organic, fragmented/humified layers *of/oh*) were collected from four 15 × 15 cm square plots. Humus layers from the four square plots were pooled, freeze-dried and grinded.

2.3 Organic matter analysis and characterization

Total carbon (TC) and total inorganic carbon (TIC) were determined using a Shimadzu TOC-L analyzer equipped with a SSM-5000A solid sample module. Total organic carbon (TOC) was calculated as the difference between TC and TIC. Lignin monomers and carbohydrates were analysed in lyophilized humus and soil samples. The analysis of lignin was performed after alkaline oxidation with CuO (Otto and Simpson, 2006). The sum of cinnamyl C, syringyl S and vanillyl V compounds, VSC sum, was considered as a quantitative representation of soil lignin content (Younes et al., 2017). Differences in the C/V, S/V, H/V, Ferulic acid/Coumaric acid ratio and, acids to aldehydes of lignin vanillyl phenols ((Ac/Ad)v) ratio (defined in SI) reflected changes in the composition of vegetal material and/or microbial activity. The sugar composition was determined after reduction to alditols (Rumpel and Dignac 2006). Gas chromatography analysis was performed with a Shimadzu GC-2010 Plus equipped with flame ionization detection (FID; 300 °C). Separation was achieved with a fused silica column (Supelco Equity 5%, 30 m × 0.25 mm i.d., 0.25 µm film thickness) and He as carrier gas. The oven temperature was programmed from 60 to 300 °C at 5 °C min^{-1} and held for 15 min. Ethylvanillin was added as internal standard (IS) for assessing the recovery of lignin products (50 µL of 20 mg L^{-1} solution). D-deoxy-2-glucose (1 mL of 2 g L^{-1} solution) was added as IS in the sugar analysis procedure.

GC–MS was performed, for assignment of different compounds, with a Trace GC instrument (Thermo Finnigan) coupled to a mass spectrometer (Thermo Finnigan Automass). The injector (Thermo Finnigan (PTV) was at 250 °C) and a fused silica column (Supelco Equity 5%, 30 m × 0.25 mm i.d., 0.25 μm film thickness) was used with He as carrier gas (1 mL min^{-1}). The oven temperature was programmed from 60 to 300 °C (held 15 min) at 5 °C min^{-1}. The MS instrument was operated in the electron ionization mode at 70 eV and ion separation was carried out with a quadripole mass filter. For each analysis, full scan mode was used (*m/z* 50–650, 2 scans/s). The various products were assigned on the basis of GC retention times, mass spectra (comparison with standards) and literature data.

2.4 Selenium and iodine extractions

2.4.1 Fractionation of selenium and iodine pools from humus and soil

Sequential extractions were used to fractionate selenium and iodine pools into water-soluble fraction (Se_{water}, I_{water}) and fraction associated to organic matter (Se_{NaOH}, I_{NaOH}). The water-soluble fraction was collected after three successive extractions with ultrapure water (Milli-Q System, 18.2 MΩ cm; Elix, Millipore) at room temperature. Then, two successive extractions with 0.1 mol L^{-1} NaOH were performed to collect the fraction associated to OM. Fractionation was performed using field-moist samples of humus and soil (~20% humidity) in order to preserve the distribution of elements. Each extraction was performed with 1.4 g of humus or soil and 11 mL of extractant in 15 mL polypropylene centrifuge tube. Tubes were rotated for 3 h at 20 rpm (Rotator Drive STR4, Stuart) and centrifuged at 4000 rpm for 20 min. For each sequential extraction, successive extracts were filtered on 0.45 μm PES membrane and stored at 4 °C before analysis. Procedure was done in duplicate and a blank consisting of the extraction solution was added to each run.

2.4.2 External and internal I and Se concentrations in leaves and needles

To estimate the internal and external contents of Se and I, leaves and needles were either i) washed with mixture of tetrahydrofuran/toluene (1 vol./1 vol.), ii) washed with ultrapure water or iii) not washed. Washing was performed by vigorous shaking for 2 min, followed by rinsing in ultrapure water for 1 min (Gandois, 2009). Leaves and needles were then dried at 60°C and grinded. Washing with water was supposed to rinse out the dry deposit adsorbed to the cuticle, while organic solvent washing released element absorbed in the cuticle at the upper surface of leaf/needle (Roulier et al., 2018). The concentrations measured in the unwashed needles and

leaves reflect the total element contents while the inner cells content of elements in leaves/needles correspond to concentrations measured after organic washing (Gandois, 2009).

2.4.3 Total element extraction

Acidic extractions with HCl and HNO_3 for soil and, HNO_3 and H_2O_2 for humus and tree materials were carried out to extract total Se from solid samples as previously described (Pisarek et al., 2021). Total I was extracted with a 5% tetra methyl ammonium hydroxide (TMAH) solution (Roulier et al., 2019; Shetaya et al., 2012; Watts and Mitchell, 2008).

2.5 Selenium and iodine analysis

The determination of total selenium and iodine concentrations were performed on an Agilent 7500ce ICPMS (Agilent Technologies , Japan) equipped with reaction cell (gas flow for Se analysis: 5 ml min^{-1} H_2). The quantification was performed with an external calibration prepared in reconstituted corresponding matrices. The detection limits of Se were in the range of 0.003-2.1 μg kg^{-1} and in the range of 0.02-21.3 μg kg^{-1} for I, depending on daily instrument sensibility and sample matrix. The HPLC system coupled to ICP-MS was an Agilent 1100 HPLC (Agilent Technologies, Japan). Chromatographic separation was performed on Agilent G3154-65001 analytical column and G3154-65002 guard column (Agilent Technologies, Japan). The sample injection volume was 200 μL. The mobile phase was a 20 mmol L^{-1} ammonium nitrate (99.5%, Sigma-Aldrich) solution with 2.5% v/v of methanol (99.9%, Sigma-Aldrich) adjusted to pH 8.5 with ammonia (25% NH_4OH solution, Fluka). The flow rate of the mobile phase was 1 mL min^{-1}. The quantification was carried out by the method of standard addition using daily diluted certified aqueous standards: 1 g L^{-1} iodide (Sigma-Aldrich), 1 g L^{-1} iodate, 1 g L^{-1} Se as selenite and 0.1 g L^{-1} Se as selenate (Spectracer), 1 g L^{-1} Se as D,L-seleno-methionine (Sigma-Aldrich, dissolved in ultrapure water). The detection limits varied between 0.009 and 0.036 μg L^{-1} for Se species and between 0.014 and 0.060 μg L^{-1} for iodine species. They corresponded to mean values of 0.092 μg kg^{-1} for Se species and 0.14 μg kg^{-1} for I species in ultrapure water extracts and 13 μg kg^{-1} for Se species and 16 μg kg^{-1} for I species in NaOH extracts.

2.6 Calculations

2.6.1 Selenium and iodine hydrological fluxes

The annual volume-weighted mean (AVWM) concentrations in water samples were calculated according to Eq. 1:

$$AVWM = \frac{\sum(C(X)_i \times V_i)}{\sum V_i} \quad (1)$$

Where $C(X)_i$ is the monthly element (X = Se or I) concentration, V is the monthly volume of sample solution and i is the analyzed period of 28 days ($1 \leq i \leq 13$). The hydrological fluxes of Se and I (g ha^{-1} yr^{-1}) in rainfall (RF), throughfall (TF) and drainage (at -60 cm; DR) were calculated as the sum of monthly concentrations of Se and I in samples multiplied by the corresponding monthly water sample flux obtained from Météo-France weather station located at the sampling site. The other water fluxes were determined based on linear correlations obtained from previous monthly measurements in the period 2002-2012 (**Figure art.3.SI – 1**) and monthly RF fluxes from January 2019 to December 2019. Monthly TF water fluxes were thus calculated as 61% and 72% of monthly RF water fluxes for Douglas fir and beech stands, respectively (**Figure art.3.SI – 1-2**). Monthly drainage water fluxes of 77% of TF fluxes were used for the beech and Douglas fir plots (**Figure art.3.SI – 3-4**). RF and TF annual fluxes of selenium and iodine were used to calculate their net throughfall fluxes (NTF in g ha^{-1} yr^{-1}) as the difference between TF and RF fluxes. The input – output budget in beech and Douglas fir stands was calculated for Se and I as the difference between their annual RF and DR fluxes.

Selenium and iodine fluxes from dry deposition were estimated by the filtering approach with Na as a tracer ion (Urlich, 1983). Sodium is considered to be an inert cation that does not interact with tree canopy, thus its net throughfall flux (NTF(Na); g ha^{-1} yr^{-1}) is assumed to come from dry deposition only. It is assumed that dry deposition of Se, I, and Na occurs on the canopy surface with the same efficiency. The dry deposition flux of Se and I (DD (X)) was estimated as follows (Eq.2):

$$\boldsymbol{DD(X)} = RF(X) \times \frac{NTF(Na)}{RF(Na)} \quad (2)$$

Where RF(Na) is annual rainfall flux of Na (g ha^{-1} yr^{-1}). Sodium concentrations were provided by INRAE.

Further, the canopy exchange flux (CE(X) in g ha^{-1} yr^{-1}) was calculated according to Eq.3:

CE(X) = NTF(X) – DD (X) (3)

When CE < 0, the tree canopy is supposed to absorb elements and when CE > 0, elements are leached from the canopy surface. When dry deposition flux is nil, the canopy exchange flux equals net throughfall flux.

2.6.1 Determination of element residence time and K_D in forest soil

Theoretical residence time of Se and I in forest soil (t_{res}) was estimated according to Redon et al. (2011) (Eq.4):

$$\boldsymbol{t_{res}} = \frac{X_{stock\ in\ humus+soil}}{total\ X\ input\ to\ soil}\ (years) \quad (4)$$

Where total element input to soil includes the sum of litterfall and throughfall annual fluxes and excludes rock weathering as a significant source of elements (Pisarek et al., 2021).

Two approaches were used to calculate the solid-liquid partition coefficient K_d (L kg^{-1}). The desorption coefficient $K_{d\ des}$ was estimated from the first step of water extraction experiments (Eq.5), while the *in situ* coefficient $K_{d\ in\ situ}$ was calculated based on the element concentrations in the forest soil layer and in the corresponding soil solution (Eq 6; Roulier et al., 2018):

$$\mathbf{K_{d\ des}} = \frac{[\text{X in forest soil layer}]_{residual}}{[\text{X in first water extract}]}\ (\text{L kg}^{-1}) \quad (5)$$

$$\mathbf{K_{d\ in\ situ}} = \frac{[\text{X in forest soil layer}]}{\text{AVWM [X in corresponding soil solution]}}\ (\text{L kg}^{-1}) \quad (6)$$

2.7 Data treatment and Statistical analysis

Missing samples in the annual monitoring of soil solutions were assigned a concentration value corresponding to the mean of monthly concentrations over the 2019 period. A value of one half the quantification limit (with 100% uncertainty) was also assigned to species (selenite, selenate, iodide, iodate) concentrations in soil extracts that did not contain quantifiable levels.

The normality of data was evaluated with Shapiro-Wilks normality test. Differences between element contents in beech and Douglas fir were examined with two-tailed t-test. Correlations between soil properties and Se and I contents were carried out with Pearson test (normally distributed data) or Spearman test (not-normally distributed data). Co-correlation of soil properties were presented in Pearson matrix (**Table art.3.SI – 3)**. Statistical study was performed with R studio (R Core Team, 2013, version 3.4.3).

3. Results and discussion

3.1 Atmospheric selenium and iodine inputs to forest ecosystem

3.1.1 Influence of beech and Douglas fir canopies on the seasonal variability of elemental concentrations in throughfall and stemflow

Monthly concentrations in rainfall ranged from 0.012 to 0.07 µg L^{-1} for Se and 0.57 to 1.64 µg L^{-1} for I (**Figure art.3.SI – 2**). Monthly concentrations of Se and I in throughfall and stemflow were higher than rainfall by a mean factor of 1.8 for beech trees (**Figure art.3.SI – 2**; $[Se]_{throughfall}$: 0.02-0.18; $[Se]_{stemflow}$: 0.01-0.14 µg L^{-1}; $[I]_{throughfall}$: 0.7-3.3; $[I]_{stemflow}$: 0.3-5.3 µg L^{-1}). For Douglas fir these factors were 5 in throughfall and 10 in stemflow ($[Se]_{throughfall}$: 0.01-0.56; $[Se]_{stemflow}$: 0.06-1.4 µg L^{-1}; $[I]_{throughfall}$: 0.35-16; $[I]_{stemflow}$: 1.8-42 µg L^{-1}). A low part of water flows down the tree stem of conifers (Seiler and Matzner, 1995), resulting in higher concentrations of elements in stemflow solutions.

The ratios between elemental concentrations in throughfall or stemflow to rainfall, for each tree type, followed the same monthly variation for both elements during the year (**Figure art.3.SI – 3**), with maximum values in September 2019. Highest enrichment in stemflow and throughfall coincided with the lowest monthly rainfall amount (**Figure art.3.SI – 4)**, probably due to concentration and leaching of dry deposits accumulated during the dry period.

The concentration increase in September was also observed for dissolved organic carbon (DOC) (**Figure art.3.SI – 5**). Le Mellec et al. (2010) hypothesized that the maximum DOC content in throughfall from deciduous and coniferous stands in late summer might be the result of leaf senescence, when the cuticle at the surface becomes more permeable and releases DOC. Similar mechanism could mobilize Se and I stored in leaves/needles, however its contribution in stemflow and throughfall is difficult to estimate.

3.1.2 Annual elemental hydrological fluxes and absorption/leaching from the tree canopies

The annual rainfall flux from January 2019 to December 2019 was 1023 mm (**Table art.3 – 1**), which was typical for the studied site (mean of 1111 ± 218 mm yr^{-1} reported in the period 2002-2012). Annual volume weighted mean (AVWM) concentrations in rainfall were 0.032 µg (Se) L^{-1} and 0.95 µg (I) L^{-1}, resulting in annual rainfall fluxes of 0.32 g (Se) ha^{-1} yr^{-1} and 9.7 g (I) ha^{-1} yr^{-1} (**Table art.3 – 1**). AVWM concentrations in beech throughfall (0.053 µg (Se)

L^{-1} and 1.35 µg (I) L^{-1}) were around half lower than for Douglas fir (0.12 µg (Se) L^{-1} and 3.5 µg (I) L^{-1}). Element TF were thus roughly double in Douglas fir stand in comparison with beech stand. Net throughfall flux was thus lower at beech stand and close to zero considering the uncertainties. Dry deposition fluxes of 0.08 ± 0.02 g (Se) ha^{-1} yr^{-1} and 2.40 ± 0.02 g (I) ha^{-1} yr^{-1} were determined for Douglas fir (**Table art.3 – 1**), whereas they were equal to zero for beech stand, theDD(Na) flux being zero. This difference can only be due to a more efficient trapping of dry deposition by conifers compared to deciduous trees (Augusto et al., 2002; De Schrijver et al., 2007; Pace and Grote, 2020), as climatic conditions were homogenous (e.g. rainfall amount, temperature). The exchange flux with the Douglas fir canopy was positive for both elements (CE(Se) = 0.4 ± 0.1 and CE(I) = 10 ± 1 g ha^{-1} yr^{-1}), indicating leaching of selenium and iodine from the canopies. The washing procedures used to differentiate internal and external element concentrations showed that selenium and iodine concentrations were generally not significantly different (t-test, p-value>0.05) between unwashed or water-washed leaves/needles, except for Se in Douglas needles (**Table art.3 – 2**). Around 22 ± 11% of total I content in beech leaves and 39 ± 7% in Douglas needles were mobilized by organic solvent (**Table art.3 – 2**). As observed by Roulier et al. (2018) for beech leaves, no difference of I concentration was observed after washing with water or organic solvent, indicating that the great majority of I was incorporated into the beech leaves. Loss of Se with organic solvent washing was much higher and accounted for 49 ± 15% for beech and 62 ± 21% for Douglas fir. The greater pool of elements on the surface of needles may be due to a thicker waxy layer on the needle cuticle compared to beech leaf (Gower and Richards, 1990). Our results suggest that this cuticular pool of elements, available for uptake or release by the leaves, is more easily solubilized during exchange processes with the Douglas canopy compared to beech.

Table art.3 – 1 Annual water fluxes (2019 year), volume weighted mean concentrations and fluxes of Se and I. DD: dry deposition flux in throughfall; NTF: net throughfall flux. Concentrations with various letters (Se: upper scale; I: lower case) are significantly different at the 95% level (2-tailed t-test).

		Selenium				**Iodine**			
	Water flux ($mm\ yr^{-1}$)	AVWM Conc. ($\mu g\ L^{-1}$)	Flux ($g\ ha^{-1}\ yr^{-1}$)	AVWM Conc. ($\mu g\ L^{-1}$)	Flux ($g\ ha^{-1}\ yr^{-1}$)	AVWM Conc. ($\mu g\ L^{-1}$)	Flux ($g\ ha^{-1}\ yr^{-1}$)	AVWM Conc. ($\mu g\ L^{-1}$)	Flux ($g\ ha^{-1}\ yr^{-1}$)
Rainfall	1023	0.032 ± 0.006	0.32 ± 0.06			0.95 ± 0.05	9.7 ± 0.5		
		Beech		**Douglas fir**		**Beech**		**Douglas fir**	
Throughfall	735^{I}	0.053 ± 0.008^{C}	0.39 ± 0.06			1.35 ± 0.07^{c}	9.9 ± 0.5		
	624^{II}			0.12 ± 0.02^{B}	0.77 ± 0.10			$3.5 \pm 0.\ 2^{b}$	22 ± 1
Stemflow		0.041 ± 0.007^{C}		0.20 ± 0.02^{A}		1.31 ± 0.06^{c}		6.2 ± 0.3^{a}	
DD			/		0.08 ± 0.02		/		2.4 ± 0.2
NTF			0.06 ± 0.08		0.44 ± 0.12		0.2 ± 0.7		12 ± 1
Canopy exchange			0.06 ± 0.08		0.36 ± 0.12		0.2 ± 0.7		10 ± 1
Forest floor solution		0.16 ± 0.02^{B}		0.18 ± 0.02^{A}		2.5 ± 0.3^{e}		3.7 ± 0.2^{d}	
-15 cm soil solution		0.09 ± 0.02^{C}		0.16 ± 0.03^{A}		5.4 ± 0.7^{ab}		6.2 ± 0.6^{a}	
-30 cm soil solution		0.03 ± 0.01^{F}		0.07 ± 0.01^{D}		1.5 ± 0.4^{f}		5.2 ± 0.4^{b}	
-60 cm soil solution	564^{I}	0.022 ± 0.006^{G}	0.12 ± 0.03			2.2 ± 0.6^{e}	12 ± 3		
	478^{II}			0.04 ± 0.01^{E}	0.17 ± 0.04			4.7 ± 0.4^{c}	18 ± 1
Input-output budget			0.21 ± 0.07		0.16± 0.07		-2 ± 3		-8.0 ± 1

^{I} beech, ^{II} Douglas

Table art.3 – 2 Concentrations of Se and I in leaves and roots of beech and Douglas fir. Concentrations with various letters (Se: upper case; I: lower case) are significantly different at the 95% level (2-tailed t-test).

Tree part	[Se] (µg kg^{-1})		[I] (µg kg^{-1})	
	Beech	**Douglas**	**Beech**	**Douglas**
Leaves				
unwashed	182 ± 54^{BC}	348 ± 54^{A}	203 ± 20^{a}	228 ± 18^{a}
washed in water	135 ± 35^{C}	242 ± 43^{B}	187 ± 32^{a}	218 ± 25^{a}
(% of total conc.)	(76 ± 9%)	(70 ± 10%)	(92 ± 12%)	(96 ± 8%)
washed in organic solvent	88 ± 17^{C}	126 ± 52^{C}	160 ± 27^{ab}	140 ± 19^{b}
(% of total conc.)	(51 ± 14%)	(38 ± 20%)	(78 ± 10%)	(61 ± 6%)
Roots				
Fine roots (<2mm)	328 ± 48^{B}	689 ± 78^{A}	671 ± 54^{b}	2353 ± 630^{a}
Large roots (>2mm)	193 ± 66^{C}	273 ± 59^{BC}	285 ± 45^{d}	514 ± 37^{c}

3.2 Selenium and iodine in humus and soil column

3.2.1 Total concentrations in humus and soil

Total selenium and iodine concentrations in humus and soil profiles and in their water and NaOH extractable fractions are presented in **Figure art.3 – 1**. Soil selenium concentrations ranged from 464 to 763 µg kg^{-1} and decreased from topsoil to subsoil under Douglas fir, while no difference was observed under beech. Iodine concentrations increased with soil depth showing a maximum of around 11 mg kg^{-1} at 15-45 cm depth for beech stand and 30-60 cm for Douglas fir stand. Humus under Douglas fir was richer in both elements compared to beech (t-test, $p < 0.05$). No statistical difference in soil profile may suggest that the 43-year period between the introduction of these tree stands and the present study was too short to influence the distribution of Se and I. The proportions of both elements in the water extractable fraction were similar (**Figure art.3 – 1.2**) and represented, on average for both stands, 4 % of their total content in humus (Se_{water}: 2.2-5.7%; I_{water}: 2.0-5.4%) and 1.1 % of their total content in the soil column (Se_{water}: 0.2-1.6%; I_{water}: 0.1-2.9%). The water soluble pool of iodine was in the range of 3.2-7.4% of total I in humus (Roulier, 2018) and 1.9-7.8% in soil (Duborská et al., 2020; Roulier et al., 2018), while water-soluble Se fraction reached up to 4.8% in forest soils (Tolu et al., 2014). The proportions of the water-soluble fractions of selenium and iodine decreased with soil depth (**Figure art.3 – 1.2**), while the NaOH-soluble fractions increased (**Figure art.3 – 1.3**).

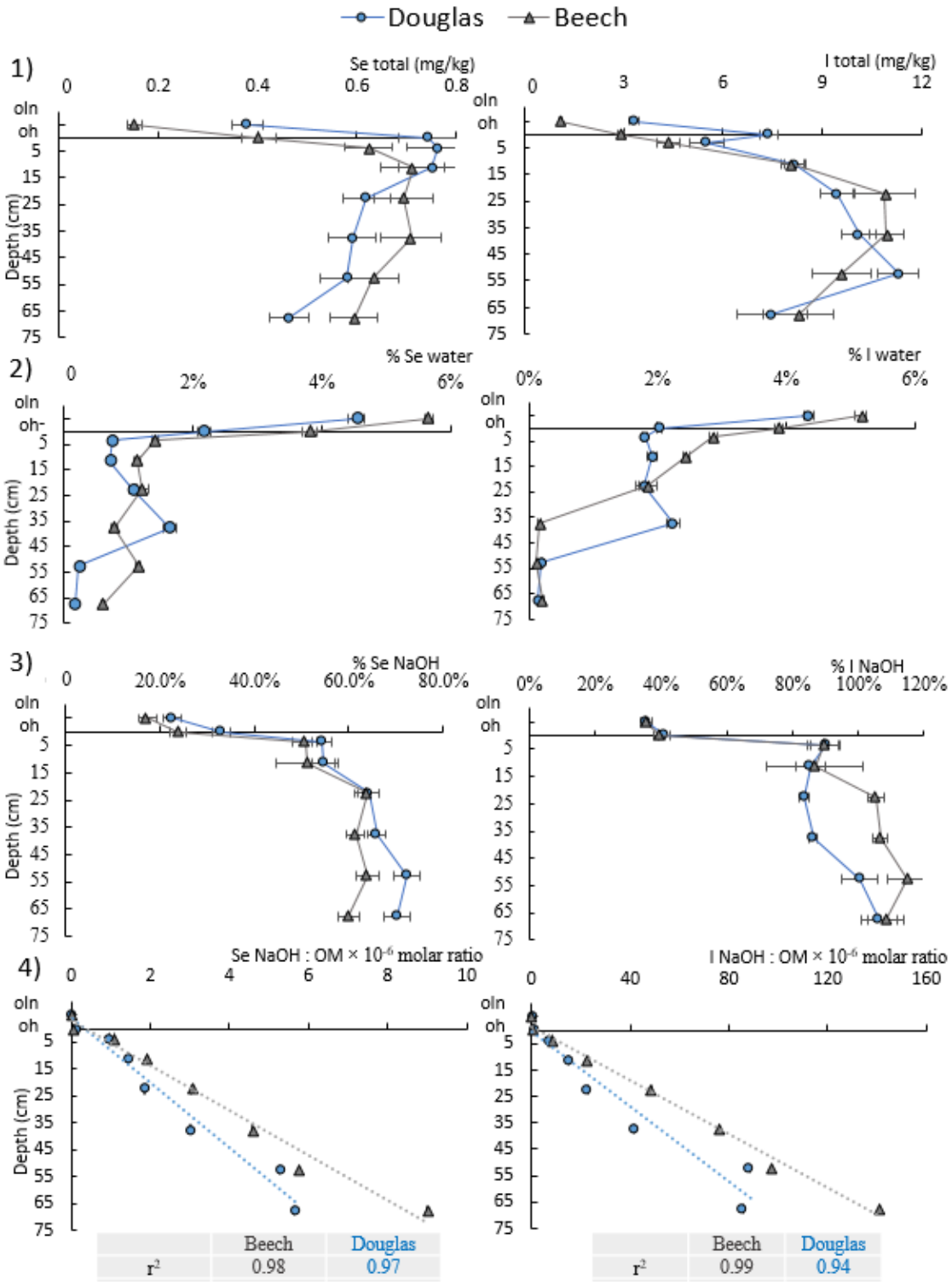

Figure art.3 – 1 Total selenium and iodine concentrations in soil layers under beech and Douglas fir stands (1) and their proportions in 2) water-soluble fraction and 3) NaOH-soluble fraction. 4) molar ratios Se_{NaOH} :OM and I_{NaOH} :OM.

The proportion of the NaOH extractable fraction of selenium increased with forest soil depth representing, on average for the two stands, 24% of its total content in humus (Se_{NaOH}: 17-32%) and 63% of its total content in the soil column (Se_{NaOH}: 51-72%; **Figure art.3 – 1.3**). The

NaOH soluble fraction was higher for iodine and represented, on average for Douglas fir and beech stands, 38% in humus (I_{NaOH}: 36-41%) and 100% in the soil column (I_{NaOH}: 84-100%). Molar ratios, Se_{NaOH}:OM and I_{NaOH}:OM, increased with increasing soil depth under both tree species as previously reported for these elements (Di Tullo, 2015; Roulier et al., 2018; Shetaya et al., 2012; Xu et al., 2016). Moreover, linear regressions (r^2 = 0.94-0.99) were obtained in our study between these molar ratios and soil depth as shown in **Figure art.3 – 1.4**. This is consistent with the immobilization of I and Se associated to highly degraded, humic acid-like organic matter. Thus, molecular characterization of OM constituents can help to understand these processes. While total Se was correlated with carbon ($r = 0.65$, $p < 0.01$) and lignin ($r = 0.62$, $p < 0.05$) contents (C_{org} and lignin were co-correlated), Se_{NaOH} was positively correlated with aluminium ($r = 0.60$, $p < 0.05$) and the ratio (Ac/Ad)v (acids to aldehydes of lignin vanillyl phenols) ($r = 0.63$, $p < 0.05$). Selenium binding to organic matter was hypothesised to be an indirect process, occurring in the presence of Fe/Al oxides by the formation of ternary complexes (Peel et al., 2017), surface or matrix association (Coppin et al., 2009) and, the presence of anoxic zones promoting microbial reduction and binding of Se (Kausch et al., 2012; Lusa et al., 2015). Microbial activity contributes to the degradation of organic material, leading to the formation of organic acids such as humic and fulvic acids, which strongly retain Se (Dinh et al., 2017). The positive correlation of Se_{NaOH} with the ratio (Ac/Ad)v, reflecting the progressive microbial oxidation of lignin, may highlight the role of microorganisms in the retention of Se in organic matter.

Negative correlations between I_{NaOH} and organic carbon ($r = - 0.85$, $p < 0.001$), the sum VSC ($r = - 0.86$, $p < 0.001$) and sugars ($r = - 0.77$, $p < 0.001$) indicate that formation of organic iodinated compounds was concomitant with the degradation of organic matter. Positive moderate correlation ($r = 0.52$, $p < 0.05$) between I_{NaOH} fraction and the ratio C/V (cinnamyl to vanillyl compounds) and strong negative correlation between total iodine (or I_{NaOH} fraction) and lignin content suggest that iodine would be rather associated with non-woody derived lignin. Moreover, positive correlation of the ratio C6/C5 sugars with I_{water} fraction ($r = 0.59$, $p < 0.05$) and the negative correlation with I_{NaOH} fraction ($r = -0.50$, $p < 0.05$) suggest, that non-cellulosic carbohydrates would not contribute to I retention in soil. Xu et al. (2012) suggested that iodine may be bonded to aromatic regions with esterified formic and phenolic acids and other carboxylic acids, amide functionalities and hemicellulose-lignin complexes with phenyl-glycosidic bonds and quinone-like structures.

3.2.2 Selenium speciation in humus and soil fractions

Table art.3 – 3 presents the speciation results for selenium and iodine in the water and NaOH extractable fractions in humus and soil layers.

Only selenate, SeO_4^{2-}, was detected in the water extracts. Selenite, SeO_3^{2-}, was the only inorganic species in the NaOH extracts. Selenite was not observed in water-soluble extracts, as previously reported for acidic French forest soils (Tolu et al., 2014). No other chromatographic peak was detected with our chromatographic separation conditions. Thus, 48-98% and 65-97% of extracted Se remained unidentified respectively in water and NaOH extracts.

Selenate content was lower in Douglas fir (0.18-0.29 µg kg^{-1}) than in beech stands (0.28 to 2.9 µg kg^{-1}). Selenate was not detected in humus water extracts, i.e. in the presence of high organic matter and high microbiological activity. Main differences between the two stands in the proportion of selenate in the Se_{water} pool were noticeable below 15 cm depth, with values ranging from 9 to 52% in beech soil water extracts while they were less than 2% in those of Douglas soil.

Selenite was below detection limit (< 13 µg kg^{-1}) in humus and upper layers of soils (0 – 15 cm) under both stands and, ranged between 74 to 162 µg kg^{-1} for deeper soil layers with no significant difference between Douglas and beech stands. Selenite accounted for 17 to 45% of Se_{NaOH} fraction, increasing with depth similarly to Se_{NaOH} extractable proportion. The absence of SeO_3^{2-} in the water-soluble extracts may be explained by its low leaching potential from soil metal oxides, especially in acidic conditions (Goldberg and Glaubig, 1988). Selenate is more weakly adsorbed by electrostatic interactions to mineral phases (Hayes et al., 1988), and thus more water soluble and available for plants than SeO_3^{2-} (Sharma et al., 2015).

Seleno-methionine (SeMet) was not detected in water and NaOH extracts of humus and soil as it is often the case in such an environment (Söderlund et al., 2016). Tolu et al. (2014) reported the presence of seleno-methionine and methane seleninic acid in the water extracts of some meadow soils. The low content of SeMet and other organic species may require pre-concentration or special treatment of the extract, such as oxidation with peroxide in order to degrade colloidal organic material (plant or microbial origin) and release org-Se compounds (Stroud et al., 2012). Another explanation for the absence of SeMet may be its rapid mineralization or volatilization, as it was shown to disappear from soil after a few days (Martens and Suarez, 1997).

Table art.3 – 3 Total and species concentrations in water-soluble and organic fractions of humus and soil (μg kg^{-1}).

	Total concentration		Water soluble fraction					NaOH soluble fraction				
	Se_{total}	**I_{total}**	**Se_{water}**	**$SeO_4^{2-}{}_{water}$**	**I_{water}**	$I^-{}_{water}$	$IO_3^-{}_{water}$	**Se_{NaOH}**	**$SeO_3^{2-}{}_{NaOH}$**	**I_{NaOH}**	$I^-{}_{NaOH}$	$IO_3^-{}_{NaOH}$
Beech stand												
Humus												
ol	152 ± 15	1113 ± 43	8.6 ± 0.7	<0.09	57 ± 1	6.4 ± 0.3	<0.14	26 ± 3	<13	396 ± 21	110 ± 5	<16
oh	402 ± 36	2925 ± 113	15.3 ± 1.1	<0.09	114 ± 2	17 ± 1	<0.14	96 ± 7	<13	1161 ± 53	200 ± 12	<16
Soil (cm)												
0-7.5	623 ± 49	4365 ± 360	8.7 ± 0.5	0.28 ± 0.06	125 ± 3	4.6 ± 0.1	<0.14	317 ± 16	<13	3903 ± 206	532 ± 35	<16
7.5-15	713 ± 65	8084 ± 348	8.1 ± 0.4	0.58 ± 0.05	197 ± 4	2.8 ± 0.1	<0.14	365 ± 47	<13	7032 ± 1184	1164 ± 60	<16
15-30	694 ± 60	10872 ± 921	8.4 ± 0.9	0.78 ± 0.06	200 ± 18	2.8 ± 0.1	<0.14	444 ± 17	89 ± 16	11454 ± 261	340 ± 21	<16
30-45	709 ± 60	10931 ± 507	5.5 ± 0.5	2.9 ± 0.2	18 ± 2	1.3 ± 0.1	0.38 ± 0.02	436 ± 13	74 ± 6	11665 ± 231	262 ± 15	<16
45-60	633 ±51	9575 ± 901	7.3 ± 0.4	2.7 ± 0.3	11.0 ± 0.3	1.1 ± 0.1	0.81 ± 0.07	405 ± 15	150 ± 24	10998 ± 557	1443 ± 159	26 ± 4
60-75	595 ± 48	8287 ± 1049	3.5 ± 0.2	1.1 ± 0.1	18 ± 1	1.03 ± 0.03	7.3 ± 0.4	357 ± 13	162 ± 15	8992 ± 453	812 ± 87	280 ± 25
Douglas stand												
Humus												
ol	380 ± 31	3317 ± 128	17 ± 1	<0.09	145 ± 2	10.5 ± 0.3	<0.14	86 ± 7	<13	1184 ± 52	256 ± 17	<16
oh	743 ± 60	7389 ± 290	16 ± 1	<0.09	150 ± 3	18 ± 1	<0.14	246 ± 14	<13	3041 ± 134	490 ± 27	<16
Soil (cm)												
0-7.5	763 ± 65	5500 ± 523	5.8 ± 0.3	0.18 ± 0.03	99 ± 3	2.8 ± 0.1	<0.14	415 ± 16	<13	4957 ± 247	553 ± 27	<16
7.5-15	750 ± 67	8175 ± 331	5.3 ± 0.3	0.29 ± 0.03	157 ± 6	2.5 ± 0.1	<0.14	411 ± 17	<13	6985 ± 368	976 ± 56	<16
15-30	619 ± 48	9451 ± 514	6.6 ± 0.6	<0.09	170 ± 7	1.8 ± 0.1	<0.14	398 ± 14	103 ± 10	7915 ± 147	334 ± 18	<16
30-45	590 ±47	10111 ± 532	10 ± 1	0.15 ± 0.01	227 ± 11	2.1 ± 0.1	<0.14	390 ± 12	111 ± 13	8737 ± 130	289 ± 18	<16
45-60	579 ± 55	11289 ± 639	1.27 ± 0.08	<0.09	22.5 ± 0.4	1.11 ± 0.03	<0.14	419 ± 16	149 ± 16	11334 ± 623	1280 ± 121	<16
60-75	464 ± 40	7482 ± 1060	0.79 ± 0.05	<0.09	10.5 ± 0.2	0.13 ± 0.02	0.34 ± 0.04	326 ± 14	139 ± 9	7959 ± 417	660 ± 34	22 ± 2

3.2.3 Iodine speciation in humus and soil fractions

The sum of inorganic iodine species (I^- and IO_3^-) accounted for 1-46% of total I in water soil soluble fraction, while the remaining 54-99% are supposed to be dissolved organic I (**Table art.3 – 3**). No unidentified signal was observed on chromatograms. Iodate IO_3^- was not detected in soil water soluble fraction until the depth of 60-75 cm in beech plot and 30-45 cm in Douglas fir plot. The highest IO_3^- concentrations were determined at 60-75 cm depth with values of 7.3 µg kg^{-1} for beech and 0.34 µg kg^{-1} for Douglas fir. In NaOH extracts, IO_3^- was detectable only below 45 cm, where it was a minor form. Similarly, IO_3^- was not detected in humus, soil and soil solution of other forest soils (Söderlund et al., 2017; Takeda et al., 2019). Iodate has higher affinity to soil mineral phase than I^- (Kodama et al., 2006). Moreover, incubation studies showed that IO_3^- was reduced to I^- or organic I in the presence of C_{org} from humic acids, soil and soil extracts (Bowley et al., 2016; Humphrey et al., 2020; Takeda et al., 2015). The presence of IO_3^- in the deeper soil may be due to desorption from mineral phase or mineralisation of OM in anaerobic conditions probably due to microbial activity (Oba et al., 2014). The direct oxidation of I^- into IO_3^- in soil conditions is kinetically unfavorable and occurs with the formation of reactive intermediate products like I_2 and IOH, which lead to the rapid formation of covalent bond between iodine and OM (Yeager et al., 2017).

Iodide, with concentrations between 0.13-22.0 µg kg^{-1}, was the main inorganic species in humus and topsoil water extracts. The higher content of I^- in humus was in agreement with its proportion in throughfall (mean value of 14% of total I) (Roulier et al., 2021). In NaOH extracts, iodide was similarly more prevailing in humus (16-28%) than in soil (2-17%), showing that iodination of organic matter occurs in the topsoil layers. Moreover, maximum value of soil total iodine (and I_{NaOH}) at the depth of 15-45 cm is in agreement with iodination of OM and adsorption of dissolved org-I on mineral phase such as Al oxides. As previously observed with Se, our results indicate also only slight differences of soil I distribution under both stands, with higher water-solubility combined with higher iodate proportion below 30 cm depth under beech compared to Douglas soils.

3.3 Element outputs from the soil

3.3.1 Element recycling from the forest soil

In addition to atmospheric inputs, Se and I in aboveground tree biomass may come from root uptake leading to element recycling from soil reserves. Element content in fine (< 2 mm) and large (> 2 mm) Douglas fir roots were 689 and 273 µg Se kg^{-1} and, 2353 and 514 µg I kg^{-1} (**Table art.3 – 2**). Concentrations in beech roots were around 2-4 times lower i.e. 328 and 193 µg Se kg^{-1} and 671 and 285 µg I kg^{-1}. In the literature, the content in tree roots was reported only for beech as 264 µg (Se) kg^{-1} (< 2 mm, Di Tullo, 2015) and, 748 (< 2 mm) – 399 (> 2 mm) µg (I) kg^{-1} (Roulier et al., 2018). Higher concentrations of Se and I in Douglas fir roots compared to beech were accompanied by slightly higher element concentrations in Douglas soil solution at the depth of -15cm (**Table art.3 – 1**), where 80% of biologically active roots are located. Little is known about the uptake of Se and I by tree roots. Although Se uptake occurs mostly via active transport and the role of simple diffusion is minor (Li et al., 2008), Se content in aboveground plant depends on its reserves in the soil (Dinh et al., 2018; Hart et al., 2011). Passive uptake is the main pathway for iodine uptake by roots and is therefore dependent on I concentration in soil solution (Humphrey et al., 2019) in agreement with our results.

3.3.2 Elements immobilization in soil and input-output budgets

Annual element losses by drainage were slightly higher for Douglas (0.17 g (Se) ha^{-1} yr^{-1} and 18 g (I) ha^{-1} yr^{-1}; **Table art.3 – 1**) compared to beech (Se: 0.12 g $ha^{-1}yr^{-1}$; I: 12 g $ha^{-1}yr^{-1}$). The input-output Se budget was positive (beech: 0.21 g ha^{-1} yr^{-1}; Douglas: 0.16 g ha^{-1} yr^{-1}) suggesting that Se is accumulated in forest soil. Conversely, the input-output balance for iodine was null at beech stand (-2 ± 3 g ha^{-1} yr^{-1}) and negative at Douglas fir plot (-8 ± 1 g ha^{-1} yr^{-1}) indicating I percolation to groundwater. K_d coefficients were lower for humus and upper soil layer than in the subsoil meaning higher (bio)availability of elements in the forest floor (**Table art.3 – 4**). The desorption solid-liquid partition coefficients $K_{d\,des}$ were in the ranges of 216-12 619 L kg^{-1} for Se and 291-18 896 L kg^{-1} for I, which is higher than data reported for European forest dry soil samples (Se: 4-2066 L kg^{-1}; I: 4-1031 L kg^{-1}; Almahayni et al., 2017; Roulier et al., 2018; Tolu et al., 2014). Unno et al. (2017) found also relatively high K_D of 120-14000 L kg^{-1} for fresh forest Japanese soil spiked with $^{125}I^-$, which was attributed to the use of moist (not dried) soil, as was the case of our work, that maintains sorption capacities related to microorganisms activity. Moreover, the values of $K_{d\,in\ situ}$ calculated from element concentrations in the forest soil layer and in the corresponding soil solution (Se: 925-29 173 L

kg^{-1} and I: 445-7061 L kg^{-1}; **Table art.3 – 4**) were up to ten times higher than $K_{d\ des}$ values estimated from the first step of water batch extraction. This illustrates the difficulties in simulating processes involved in element retention in soil.

Table art.3 – 4 The solid-liquid partition coefficients K_d (L kg^{-1}): in situ coefficient K_d ($K_{d\ in\ situ}$) and the desorption coefficient K_d ($K_{d\ des}$).

	Selenium				**Iodine**			
	Beech		**Douglas**		**Beech**		**Douglas**	
	$K_{d\ in\ situ}$	**$K_{d\ des}$**	**$K_{d\ in\ situ}$**	**$K_{d\ des}$**	**$K_{d\ in\ situ}$**	**$K_{d\ des}$**	**$K_{d\ in\ situ}$**	**$K_{d\ des}$**
oln	925±142	216±30	2143±301	314±39	445±52	291±13	907±59	399±18
oh	2451±356	418±53	4187±589	772±93	1169±137	495±22	2020±133	951±42
0-7.5		1481±178		4351±548		655±60		1737±171
7.5-15	7677±1745	1949±246	4637±836	4760±596	1200±165	836±40	1109±126	1676±205
15-30	19910±6755	1751±372	9139±1802	3121±509	7061±1715	1164±220	1828±173	1724±173
30-45		3459±571		1024±164		13443±3286		788±58
45-60	29173±8416	1975±235	13249±3084	9713±1256	4307±1270	18896±1831	2404±390	10555±642
60-75		3825±564		12619±1683		7413±1073		13162±1899

Selenium residence time was estimated as 7857 ± 1111 years for beech stand and 4219 ± 494 years for Douglas fir. Calculated t_{res}I were slightly lower: 6003 ± 368 years for beech and 2980 ± 170 years for Douglas. These values are similar to previously reported ranges for French forests (soil depth until 20 cm or 40 cm) of 617 - 8406 years for Se (Pisarek et al., 2021) and 419 – 4511 years for I (Bowley, 2013; Roulier et al., 2019).

4. Conclusions

- Enrichment factors (i.e. in throughfall and stemflow compared to rainfall) were higher for Douglas fir (5 and 10, respectively) than beech (1.8 for both), highligting the greater capacity of coniferous canopy to intercept atmospheric deposits.
- Selenium and I concentrations in humus were lower under beech than under Douglas fir, while no difference was found in the soil profile probably due to the forest age.
- The characteristics of OM suggest that activity of oxidizing microorganisms would enhance formation of Se organic fraction, while non-cellulosic carbohydrates would minimize OM storing capacities of iodine.
- Inorganic species were identified in water (SeO_4^{2-}, I^-, IO_3^-) and NaOH (SeO_3^{2-}, IO_3^-) extracts. No additional chromatographic peak containing Se or I was detected, significant

proportions of Se and I remaining unidentified in water and NaOH soluble extracts probably in dissolved or colloidal organic structures.

- With negative input-output budget, soil under Douglas was a source of I for ground water, while annual I input from the atmosphere was equal to the output by drainage from beech soil. With slightly positive input-output budgets, soils under both tree species acted as a sink for atmospheric Se.

Supplementary information

Additional information as noted in the text.

CRediT statements

Paulina Pisarek: Conceptualization, Investigation, Validation, Formal analysis, Writing-original draft, Writing - Review & Editing;
Maïté Bueno: Conceptualization, Investigation, Validation, Writing-original draft, Funding acquisition, Writing -Review & Editing, Supervision;
Yves Thiry: Conceptualization, Funding acquisition, Writing-original draft, Writing - Review & Editing, Supervision;
Laurent Grasset: Investigation, Validation, Formal analysis, Writing-original draft, Writing - Review & Editing
Arnaud Legout: Resources, Writing-original draft, Writing - Review & Editing;
Hervé Gallard: Conceptualization, Validation, Writing-original draft, Writing - Review & Editing, Funding acquisition, Supervision;
Isabelle Le Hécho: Conceptualization, Writing-original draft , Writing - Review & Editing, Funding acquisition, Supervision.

Declaration of interests

The authors declare that they have no known competing financial interests or personal relationships that could have appeared to influence the work reported in this paper

Acknowledgements

We would like to thank all technical support from the Breuil site network with special regard to Serge Didier, which provided the collection of samples and sites data.
This research was financially supported by the French National Radioactive Waste Management Agency (Andra).

References

Almahayni, T., Bailey, E., Crout, N.M.J., Shaw, G., 2017. Effects of incubation time and filtration method on Kd of indigenous selenium and iodine in temperate soils. J. Environ. Radioact. 177, 84–90. https://doi.org/10.1016/j.jenvrad.2017.06.004

AnaEE France - Breuil [WWW Document], n.d. URL https://www.anaee-france.fr/en/infrastructure-services/in-natura-experimentation/forest-ecosystems/temperate-and-continental-forests/breuil (accessed 5.2.21).

Augusto, L., Ranger, J., Binkley, D., Rothe, A., 2002. Impact of several common tree species of European temperate forests on soil fertility. Ann. For. Sci. 59, 233–253. https://doi.org/10.1051/forest:2002020

Bowley, H.E., 2013. Iodine dynamics in the terrestrial environment [WWW Document]. URL http://eprints.nottingham.ac.uk/13241/ (accessed 7.22.19).

Bowley, H.E., Young, S.D., Ander, E.L., Crout, N.M.J., Watts, M.J., Bailey, E.H., 2016. Iodine binding to humic acid. Chemosphere 157, 208–214. https://doi.org/10.1016/j.chemosphere.2016.05.028

Budke, C., Mühling, K.H., Daum, D., 2020. Iodine uptake and translocation in apple trees grown under protected cultivation. J. Plant Nutr. Soil Sci. 183, 468–481. https://doi.org/10.1002/jpln.202000099

Coppin, F., Chabroullet, C., Martin-Garin, A., 2009. Selenite interactions with some particulate organic and mineral fractions isolated from a natural grassland soil. EJSS 60, 369–376. https://doi.org/10.1111/j.1365-2389.2009.01127.x

De Schrijver, A., Geudens, G., Augusto, L., Staelens, J., Mertens, J., Wuyts, K., Gielis, L., Verheyen, K., 2007. The effect of forest type on throughfall deposition and seepage flux: a review. Oecologia 153, 663–674. https://doi.org/10.1007/s00442-007-0776-1

Di Tullo, P., 2015. Dynamique du cycle biogéochimique du sélénium en écosystèmes terrestres : rétention et réactivité dans le sol, rôle de la végétation (thesis). Pau.

Dinh, Q.T., Cui, Z., Huang, J., Tran, T.A.T., Wang, D., Yang, W., Zhou, F., Wang, M., Yu, D., Liang, D., 2018. Selenium distribution in the Chinese environment and its relationship with human health: A review. Environment International 112, 294–309. https://doi.org/10.1016/j.envint.2017.12.035

Dinh, Q.T., Li, Z., Tran, T.A.T., Wang, D., Liang, D., 2017. Role of organic acids on the bioavailability of selenium in soil: A review. Chemosphere 184, 618–635. https://doi.org/10.1016/j.chemosphere.2017.06.034.

Duborská, E., Bujdoš, M., Urík, M., Matúš, P., 2020. Iodine fractionation in agricultural and forest soils using extraction methods. CATENA 195, 104749. https://doi.org/10.1016/j.catena.2020.104749

Gandois, L., 2009. Dynamique et bilan des Elements Traces Métalliques (ETM) dans des écosystèmes forestiers français. Modélisation, spéciation et charges critiques.

Goldberg, S., Glaubig, R.A., 1988. Anion sorption on a calcareous, montmorillonitic soil: selenium. SSSAJ (USA).

Gower, S.T., Richards, J.H., 1990. Larches: Deciduous Conifers in an Evergreen World. BioScience 40, 818–826. https://doi.org/10.2307/1311484

Hart, D.J., Fairweather-Tait, S.J., Broadley, M.R., Dickinson, S.J., Foot, I., Knott, P., McGrath, S.P., Mowat, H., Norman, K., Scott, P.R., Stroud, J.L., Tucker, M., White, P.J., Zhao, F.J., Hurst, R., 2011. Selenium concentration and speciation in biofortified flour and bread: Retention of selenium during grain biofortification, processing and production of Se-enriched food. Food Chem. 126, 1771–1778. https://doi.org/10.1016/j.foodchem.2010.12.079

Hayes, K.F., Papelis, C., Leckie, J.O., 1988. Modeling ionic strength effects on anion adsorption at hydrous oxide/solution interfaces. J. Colloid Interface Sci. 125, 717–726. https://doi.org/10.1016/0021-9797(88)90039-2

Humphrey, O.S., Young, S.D., Bailey, E.H., Crout, N.M.J., Ander, E.L., Hamilton, E.M., Watts, M.J., 2019. Iodine uptake, storage and translocation mechanisms in spinach (Spinacia oleracea L.). Environ. Geochem. Health 41. https://doi.org/10.1007/s10653-019-00272-z

Humphrey, O.S., Young, S.D., Crout, N.M.J., Bailey, E.H., Ander, E.L., Watts, M.J., 2020. Short-Term Iodine Dynamics in Soil Solution. Environ. Sci. Technol. 54, 1443–1450. https://doi.org/10.1021/acs.est.9b02296

Jung, T., Hudler, G.W., Jensen-tracy, S.L., Griffiths, H.M., Fleischmann, F., Osswald, W., 2005. Involvement of Phytophthora species in the decline of European beech in Europe and the USA. Mycologist 19, 159–166. https://doi.org/10.1017/S0269-915X(05)00405-2

Kato, S., Wachi, T., Yoshihira, K., Nakagawa, T., Ishikawa, A., Takagi, D., Tezuka, A., Yoshida, H., Yoshida, S., Sekimoto, H., Takahashi, M., 2013. Rice (Oryza sativa L.) roots have iodate reduction activity in response to iodine. Front. Plant. Sci. 4, 227. https://doi.org/10.3389/fpls.2013.00227

Kausch, M., Ng, P., Ha, J., Pallud, C., 2012. Soil-Aggregate-Scale Heterogeneity in Microbial Selenium Reduction. VZJ 11, vzj2011.0101. https://doi.org/10.2136/vzj2011.0101

Kikkert, J., Berkelaar, E., 2013. Plant Uptake and Translocation of Inorganic and Organic Forms of Selenium. Arch. Environ. Contam. Toxicol. 65, 458–465. https://doi.org/10.1007/s00244-013-9926-0

Kodama, S., Takahashi, Y., Okumura, K., Uruga, T., 2006. Speciation of iodine in solid environmental samples by iodine K-edge XANES: application to soils and ferromanganese oxides. Sci. Total. Environ. 363, 275–284. https://doi.org/10.1016/j.scitotenv.2006.01.004

Le Mellec, A., Meesenburg, H., Michalzik, B., 2010. The importance of canopy-derived dissolved and particulate organic matter (DOM and POM) — comparing throughfall solution from broadleaved and coniferous forests. Ann. For. Sci. 67, 411–411. https://doi.org/10.1051/forest/2009130

Li, H.-F., McGrath, S.P., Zhao, F.-J., 2008. Selenium uptake, translocation and speciation in wheat supplied with selenate or selenite. New Phytol. 178, 92–102. https://doi.org/10.1111/j.1469-8137.2007.02343.x

Li, Z., Liang, D., Peng, Q., Cui, Z., Huang, J., Lin, Z., 2017. Interaction between selenium and soil organic matter and its impact on soil selenium bioavailability: A review. Geoderma 295, 69–79. https://doi.org/10.1016/j.geoderma.2017.02.019

Lusa, M., Bomberg, M., Aromaa, H., Knuutinen, J., Lehto, J., 2015. The microbial impact on the sorption behaviour of selenite in an acidic, nutrient-poor boreal bog. J. Environ. Radioact. 147, 85–96. https://doi.org/10.1016/j.jenvrad.2015.05.014

Martens, D.A., Suarez, D.L., 1997. Mineralization of selenium-containing amino acids in two California soils. Soil Science Society of America (USA).

Oba, Y., Futagami, T., Amachi, S., 2014. Enrichment of a microbial consortium capable of reductive deiodination of 2,4,6-triiodophenol. J. Biosci. Bioeng. 117, 310–317. https://doi.org/10.1016/j.jbiosc.2013.08.011

Otto, A., Simpson, M.J., 2006. Evaluation of CuO oxidation parameters for determining the source and stage of lignin degradation in soil. Biogeochemistry 80, 121–142. https://doi.org/10.1007/s10533-006-9014-x

Pace, R., Grote, R., 2020. Deposition and Resuspension Mechanisms Into and From Tree Canopies: A Study Modeling Particle Removal of Conifers and Broadleaves in Different Cities. Front. For. Glob. Change 3. https://doi.org/10.3389/ffgc.2020.00026

Peel, H.R., Martin, D.P., Bednar, A.J., 2017. Extraction and characterization of ternary complexes between natural organic matter, cations, and oxyanions from a natural soil. Chemosphere 176, 125–130. https://doi.org/10.1016/j.chemosphere.2017.02.101

Pisarek, P., Bueno, M., Thiry, Y., Nicolas, M., Gallard, H., Hécho, I.L., 2021. Selenium distribution in French forests: influence of environmental conditions. Sci. Total Environ. 144962. https://doi.org/10.1016/j.scitotenv.2021.144962

Qin, H., Zhu, J., Su, H., 2012. Selenium fractions in organic matter from Se-rich soils and weathered stone coal in selenosis areas of China. Chemosphere 86, 626–633. https://doi.org/10.1016/j.chemosphere.2011.10.055

Redon, P.-O., Abdelouas, A., Bastviken, D., Cecchini, S., Nicolas, M., Thiry, Y., 2011. Chloride and organic chlorine in forest soils: storage, residence times, and influence of ecological conditions. Environ. Sci. Technol. 45, 7202–7208. https://doi.org/10.1021/es2011918

Roulier, M., 2018. Cycle biogéochimique de l'iode en écosystèmes forestiers (thesis). http://www.theses.fr. Pau.

Roulier, M., Bueno, M., Coppin, F., Nicolas, M., Thiry, Y., Rigal, F., Pannier, F., Le Hécho, I., 2021. Atmospheric iodine, selenium and caesium depositions in France: II. Influence of forest canopies. Chemosphere 273, 128952. https://doi.org/10.1016/j.chemosphere.2020.128952

Roulier, M., Bueno, M., Thiry, Y., Coppin, F., Redon, P.-O., Le Hécho, I., Pannier, F., 2018. Iodine distribution and cycling in a beech (Fagus sylvatica) temperate forest. Sci. Total Environ. 645, 431–440. https://doi.org/10.1016/j.scitotenv.2018.07.039

Roulier, M., Coppin, F., Bueno, M., Nicolas, M., Thiry, Y., Della Vedova, C., Février, L., Pannier, F., Le Hécho, I., 2019. Iodine budget in forest soils: Influence of environmental conditions and soil physicochemical properties. Chemosphere 224, 20–28. https://doi.org/10.1016/j.chemosphere.2019.02.060

Rumpel, C., Dignac, M.-F., 2006. Gas chromatographic analysis of monosaccharides in a forest soil profile: Analysis by gas chromatography after trifluoroacetic acid hydrolysis and reduction–acetylation. Soil Biology and Biochemistry 38, 1478–1481. https://doi.org/10.1016/j.soilbio.2005.09.017

Seiler, J., Matzner, E., 1995. Spatial variability of throughfall chemistry and selected soil properties as influenced by stem distance in a mature Norway spruce (Picea abies, Karst.) stand. Plant Soil 176, 139–147. https://doi.org/10.1007/BF00017684

Sharma, V.K., McDonald, T.J., Sohn, M., Anquandah, G.A.K., Pettine, M., Zboril, R., 2015. Biogeochemistry of selenium. A review. Environ Chem Lett 13, 49–58. https://doi.org/10.1007/s10311-014-0487-x

Sherrard, J.C., Hunter, K.A., Boyd, P.W., 2004. Selenium speciation in subantarctic and subtropical waters east of New Zealand: trends and temporal variations. Deep Sea Research Part I: Oceanogr. Res. Pap. 51, 491–506. https://doi.org/10.1016/j.dsr.2003.11.001

Shetaya, W.H., Young, S.D., Watts, M.J., Ander, E.L., Bailey, E.H., 2012. Iodine dynamics in soils. Geochim. Cosmochim. Acta 77, 457–473. https://doi.org/10.1016/j.gca.2011.10.034

Söderlund, M., Virkanen, J., Aromaa, H., Gracheva, N., Lehto, J., 2017. Sorption and speciation of iodine in boreal forest soil. J. Radioanal. Nucl. Chem. 311, 549–564. https://doi.org/10.1007/s10967-016-5022-z

Söderlund, M., Virkanen, J., Holgersson, S., Lehto, J., 2016. Sorption and speciation of selenium in boreal forest soil. J. Environ. Radioact. 164, 220–231. https://doi.org/10.1016/j.jenvrad.2016.08.006

Stroud, J.L., McGrath, S.P., Zhao, F.-J., 2012. Selenium speciation in soil extracts using LC-ICP-MS. Int. J. Environ. Anal. Chem. 92, 222–236. https://doi.org/10.1080/03067310903111661

Takeda, A., Tsukada, H., Takahashi, M., Takaku, Y., Hisamatsu, S., 2015. Changes in the chemical form of exogenous iodine in forest soils and their extracts. Radiat. Prot. Dosimetry 167, 181–186. https://doi.org/10.1093/rpd/ncv240

Takeda, A., Unno, Y., Tsukada, H., Takaku, Y., Hisamatsu, S., 2019. Speciation of iodine in soil solution in forest and grassland soils in Rokkasho, Japan. Radiat. Prot. Dosim. 184, 368–371. https://doi.org/10.1093/rpd/ncz103

Tolu, J., Le Hécho, I., Bueno, M., Thiry, Y., Potin-Gautier, M., 2011. Selenium speciation analysis at trace level in soils. Anal. Chim. Acta 684, 126–133. https://doi.org/10.1016/j.aca.2010.10.044

Tolu, J., Thiry, Y., Bueno, M., Jolivet, C., Potin-Gautier, M., Le Hécho, I., 2014. Distribution and speciation of ambient selenium in contrasted soils, from mineral to organic rich. Sci. Total Environ. 479–480, 93–101. https://doi.org/10.1016/j.scitotenv.2014.01.079

Ulrich, B., 1983. Interaction of forest canopies with atmospheric constituents SO_2, alkali and earth alkali cations and chloride," In B. Ulrich and J. Pankrath, Eds., Effect of accumulation of air pollutants in forest ecosystems, D. Reidel Publishers, Dordrecht, 330-345

Unno, Y., Tsukada, H., Takeda, A., Takaku, Y., Hisamatsu, S., 2017. Soil-soil solution distribution coefficient of soil organic matter is a key factor for that of radioiodide in surface and subsurface soils. J. Environ. Radioact. 169–170, 131–136. https://doi.org/10.1016/j.jenvrad.2017.01.016

Watts, M.J., Mitchell, C.J., 2008. A pilot study on iodine in soils of Greater Kabul and Nangarhar provinces of Afghanistan. Environ. Geochem. Health 31, 503. https://doi.org/10.1007/s10653-008-9202-9

Weng, L., Vega, F.A., Supriatin, S., Bussink, W., Riemsdijk, W.H.V., 2011. Speciation of Se and DOC in Soil Solution and Their Relation to Se Bioavailability. Environ. Sci. Technol. 45, 262–267. https://doi.org/10.1021/es1016119

Xu, C., Miller, E.J., Zhang, S., Li, H.-P., Ho, Y.-F., Schwehr, K.A., Kaplan, D.I., Otosaka, S., Roberts, K.A., Brinkmeyer, R., Yeager, C.M., Santschi, P.H., 2011. Sequestration and remobilization of radioiodine (129I) by soil organic matter and possible consequences of the remedial action at Savannah River Site. Environ. Sci. Technol. 45, 9975–9983. https://doi.org/10.1021/es201343d

Xu, C., Zhang, S., Sugiyama, Y., Ohte, N., Ho, Y.-F., Fujitake, N., Kaplan, D.I., Yeager, C.M., Schwehr, K., Santschi, P.H., 2016. Role of natural organic matter on iodine and 239,240Pu distribution and mobility in environmental samples from the northwestern Fukushima Prefecture, Japan. J. Environ. Radioact. 153, 156–166. https://doi.org/10.1016/j.jenvrad.2015.12.022

Yeager, C.M., Amachi, S., Grandbois, R., Kaplan, D.I., Xu, C., Schwehr, K.A., Santschi, P.H., 2017. Chapter Three - Microbial Transformation of Iodine: From Radioisotopes to Iodine Deficiency, in: Sariaslani, S., Gadd, G.M. (Eds.), Adv. Appl.Microbiol., pp. 83–136. https://doi.org/10.1016/bs.aambs.2017.07.002

Younes, K., Laduranty, J., Descostes, M., Grasset, L., 2017a. Molecular biomarkers study of an ombrotrophic peatland impacted by an anthropogenic clay deposit. Org. Geochem. 105, 20–32. https://doi.org/10.1016/j.orggeochem.2016.12.005

Supplementary information

Selenium and iodine cycles in beech and Douglas forests

Paulina Pisarek[1,2], Maïté Bueno[1], Yves Thiry[2], Arnaud Legout[3], Laurent Grasset[4], Hervé Gallard[4], Isabelle Le Hécho[1]

[1] Universite de Pau et des Pays de l'Adour, E2S UPPA, CNRS, Institut des Sciences Analytiques et de Physicochimie pour l'Environnement et les Matériaux-IPREM, UMR5254, 64000 Pau, France (*pisarek.paulina@univ-pau.fr) (maite.bueno@univ-pau.fr;isabelle.lehecho@univ-pau.fr)

[2] Andra, Research and Development Division, Parc de la Croix Blanche, 92298 Châtenay-Malabry Cedex, France (yves.thiry@andra.fr)

[3] Institut National de la Recherche en Agriculture, Alimentation et Environnement (INRAE), BEF, 54000 Nancy, France

[4] IC2MP UMR 7285, Université de Poitiers, 86073 Poitiers Cedex 9, France (herve.gallard@univ-poitiers.fr)

Table art.3.SI – 1 Physical and chemical properties of soil (from Legout et al., 2016; Levrel and Ranger, 2006; Mareschal et al., 2010).

Tree species	Soil depth (cm)	C mg/kg	Density g cm^{-3}	N g/kg	Clay g/kg	Sand g/kg	Silt g/kg	pH	Fe exchang. g/kg	Mn exchang. g/kg	Al exchang. g/kg	Fe oxalate g/kg	Al oxalate g/kg
Douglas	0-7.5	64.6	1.04	2.70	189	586	225	4.07	0.16	0.16	6.22	0.32	0.26
Douglas	7.5-15	42.4	1.04	1.79	184	593	223	4.32	0.07	0.07	5.35	0.35	0.28
Douglas	15-30	31.7	1.25	1.12	190	567	243	4.51	0.01	0.06	3.73	0.33	0.36
Douglas	30-45	19.2	1.28	0.61	200	540	260	4.50	0.01	0.06	3.18	0.27	0.34
Douglas	45-60	11.8	1.41	0.00	200	547	253	4.50	0.01	0.06	3.04	0.23	0.28
Douglas	60-75	8.5	1.47	0.00	193	557	250	4.50	0.01	0.05	3.05	0.22	0.25
beech	0-7.5	43.1	0.83	3.54	199	585	217	4.13	0.25	0.19	6.21	0.26	0.25
beech	7.5-15	28.4	1.04	2.12	184	587	229	4.45	0.08	0.09	5.25	0.30	0.34
beech	15-30	21.6	1.25	1.14	164	593	243	4.69	0.01	0.06	3.43	0.25	0.44
beech	30-45	14.1	1.29	0.54	178	564	254	4.68	0.03	0.06	2.69	0.21	0.36
beech	45-60	10.4	1.47	0.00	182	562	256	4.67	0.07	0.06	2.68	0.18	0.31
beech	60-75	5.9	1.50	0.00	175	573	253	4.67	0.01	0.06	2.80	0.17	0.28

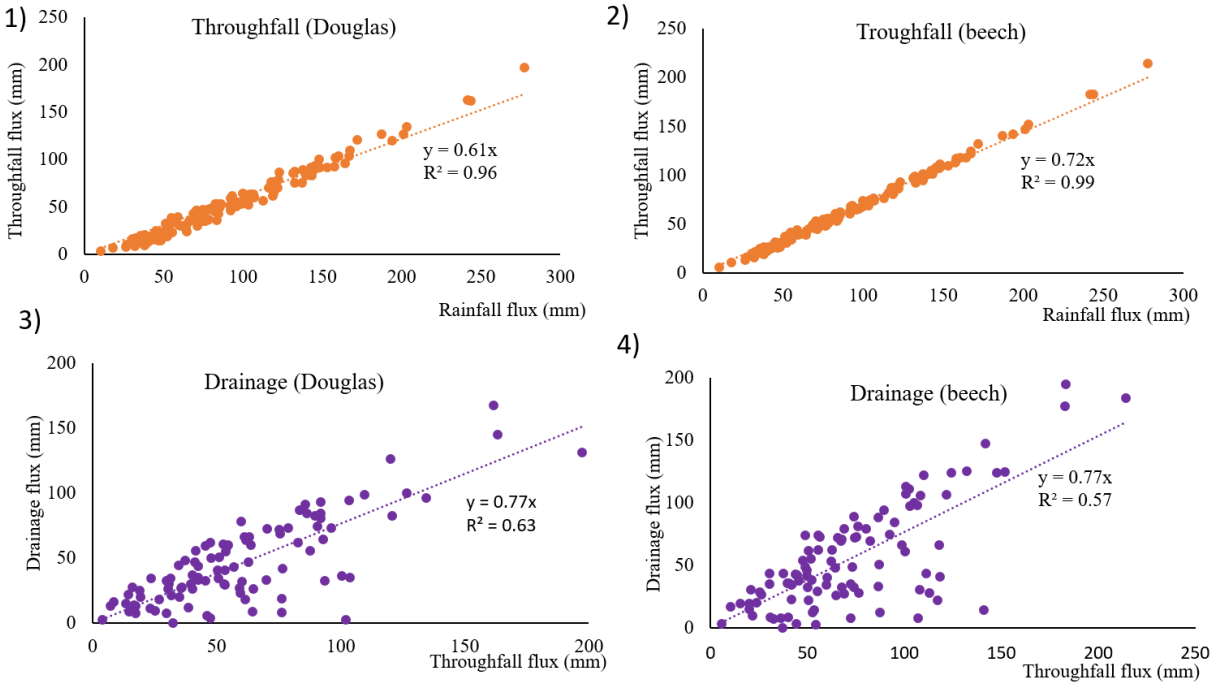

Figure art.3.SI – 1 Monthly fluxes (mm) of: 1-2) throughfall as a function of rainfall fluxes and 3-4) drainage (-60 cm) as a function of throughfall; in Douglas fir and beech forest stands during the period 2002-2012.

Organic matter characteristic

Lignin oxidation with CuO resulted in depolymerization into four groups of methoxy phenol monomers, which can be detected in their three forms: aldehyde (R_1 = H), ketone (R_1 = CH_3) and acid (R_1 = COOH):

- H group : p-hydroxyphenols (R_2 = R_3 = H);
- V group : vanillyl compounds (R_2 = H and R_3 = OCH_3; detailed also as acids to aldehydes ratios (Ac/Ad)v);
- S group : syringyl compounds (R_2 = R_3 = OCH_3);
- C group, cinnamyl compounds: p-coumaric acid (R_4 = H) and ferulic acid (R_4 = OCH_3) (Younes et al., 2017).

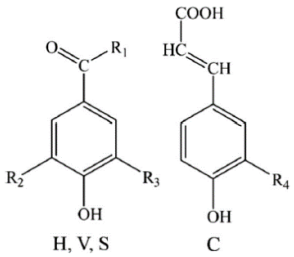

Methoxy phenols derived from CuO oxidation (Younes et al., 2017)

Table art.3.SI – 2 Characteristic of organic matter in humus and soil of beech and Douglas fir stands.

Layer	Carbon		Sugars				Lignin monomers							
	C_{org} (mg/g)	C_{inorg} (mg/g)	g/kg sol	g/ kg C	deoxy/C5	C6/C5	Sum SVC (mg/g soil)	g/kg C	Ac/Ad	C/V	S/V	H/V	Fer/Coum	(Ac/Ad)v
Beech														
oln	462 ± 13	3.4	16.24	34.92	0.06	0.81	4.12	8.87	0.20	0.14	1.39	0.49	1.23	0.36
oh	384 ± 19	3.9	42.38	109.40	0.12	0.99	4.15	10.72	0.51	0.14	0.93	0.31	1.37	0.86
0-7.5 cm	43 ± 2	0.04	11.52	267.01	0.14	0.76	0.32	7.46	0.26	0.14	0.69	0.16	7.01	0.35
7.5-15 cm	28 ± 1	<0.03	6.96	245.26	0.33	1.00	0.12	4.39	0.30	0.29	0.67	0.23	2.26	0.43
15-30 cm	22 ± 1	<0.03	0.64	29.35	n.d.	n.d.	0.03	1.39	0.44	0.39	1.09	0.24	4.61	1.14
30-45 cm	14 ± 1	<0.03	0.48	33.96	n.d.	n.d.	0.07	5.25	0.32	0.41	1.20	0.23	3.35	0.82
45-60 cm	10 ± 0.5	<0.03	0.17	16.43	n.d.	n.d.	0.03	2.79	0.51	0.20	0.72	0.17	5.18	0.73
60-75 cm	5.9 ± 0.3	<0.03	0.21	34.91	n.d.	n.d.	0.03	4.28	0.24	0.04	0.17	0.19	0.70	0.27
Douglas														
oln	436 ± 31	2.8	70.73	161.04	0.15	1.07	4.25	9.68	0.34	0.06	0.06	0.07	3.79	0.34
oh	281 ± 14	2.5	48.01	169.39	0.09	0.97	2.84	10.01	0.65	0.08	0.11	0.08	4.25	0.72
0-7.5 cm	65 ± 3	0.29	19.56	301.54	0.35	0.75	0.67	10.37	1.62	0.12	0.17	0.08	3.30	1.74
7.5-15 cm	42 ± 2	0.27	7.33	171.63	0.25	1.43	0.21	4.85	0.99	0.09	0.16	0.10	6.86	1.08
15-30 cm	32 ± 2	<0.03	8.33	262.57	0.51	0.84	0.10	3.25	1.01	0.10	0.23	0.11	4.71	1.02
30-45 cm	19 ± 1	<0.03	5.20	270.64	0.22	1.42	0.04	2.07	1.10	0.20	0.29	0.16	4.65	1.49
45-60 cm	12 ±1	<0.03	1.60	135.58	0.37	0.96	0.02	1.70	0.62	0.17	0.39	0.11	8.10	0.61
60-75 cm	8.5 ± 0.4	<0.03	1.20	139.99	0.22	0.31	0.06	6.93	0.20	0.06	0.56	0.18	6.40	0.28

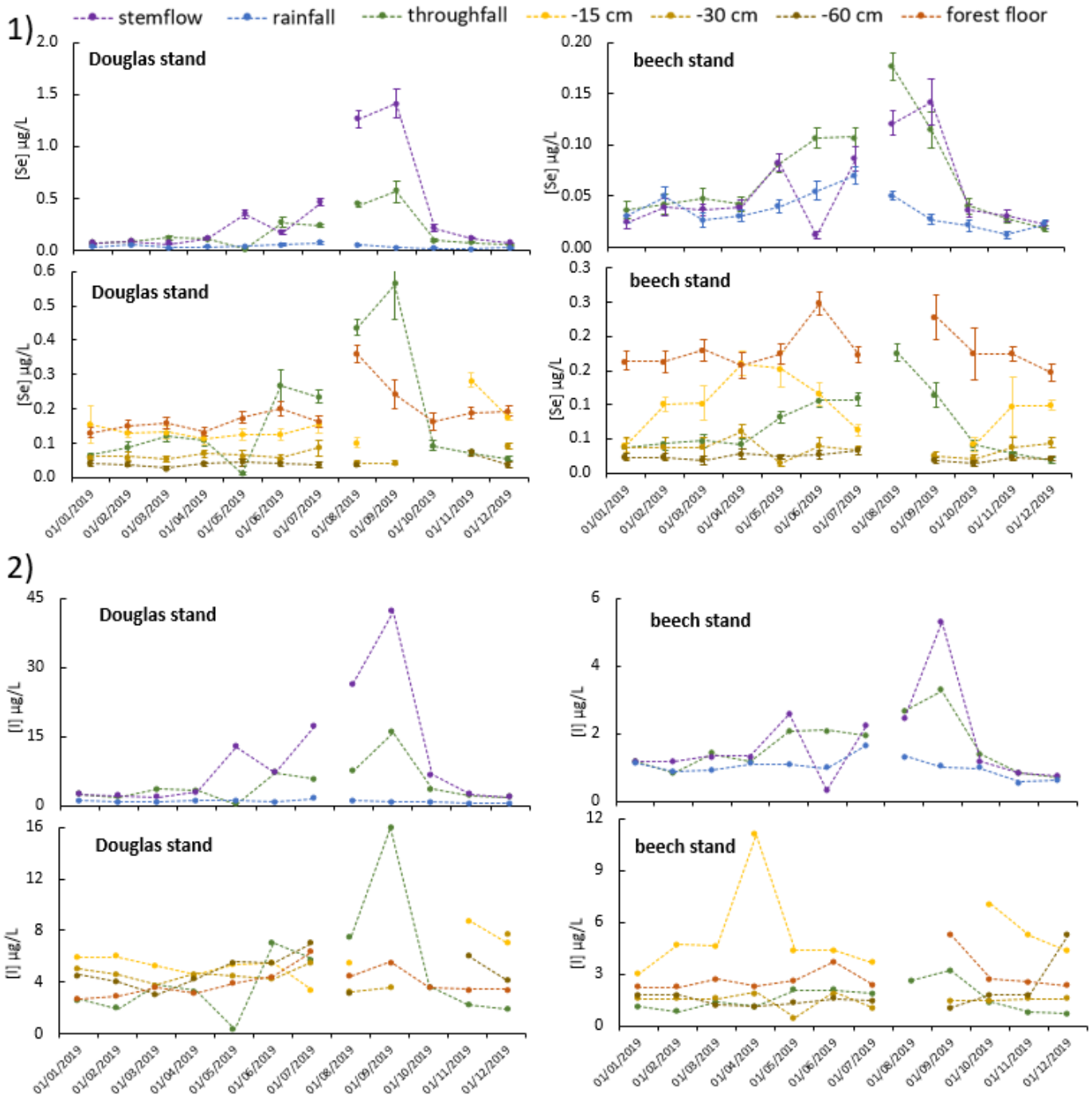

Figure art.3.SI – 2 Selenium (1) and iodine (2) concentrations in rainfall, throughfall, stemflow and soil solutions of beech and Douglas plots in Breuil site for 2019 period.

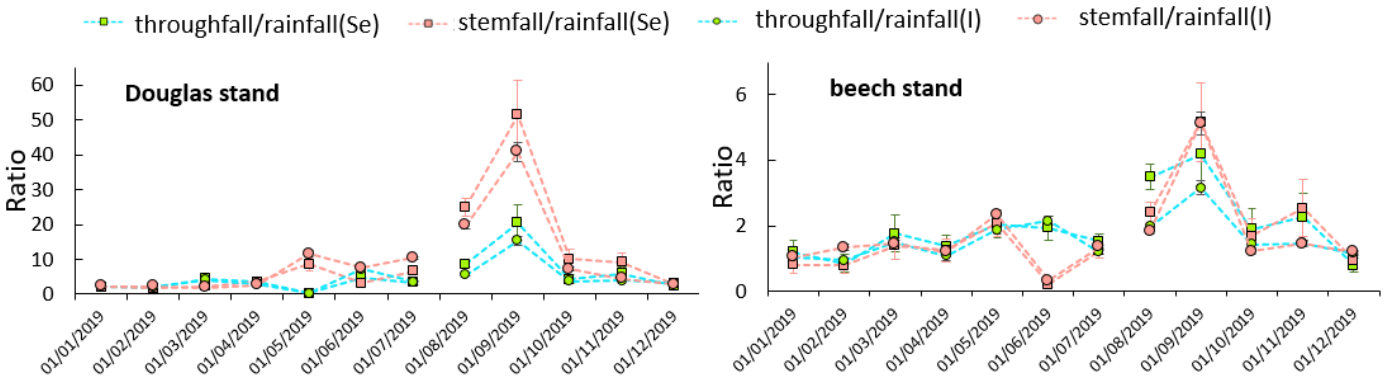

Figure art.3.SI – 3 Ratios of selenium and iodine concentration in:throughfall/rainfall and stemflow/rainfall in beech and Douglas forest.

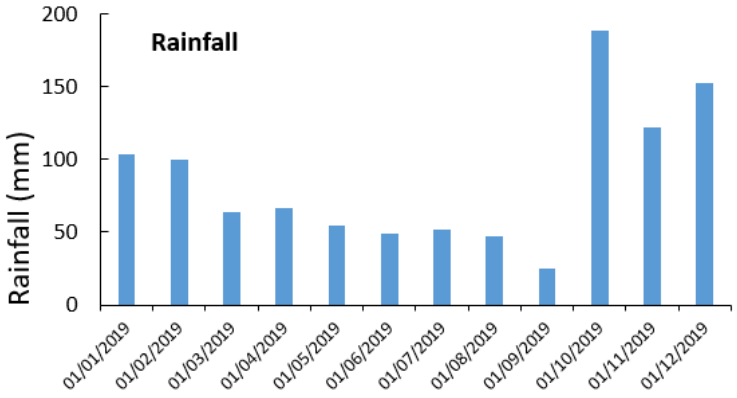

Figure art.3.SI – 4 Monthly rainfall fluxes (mm) in Breuil site.

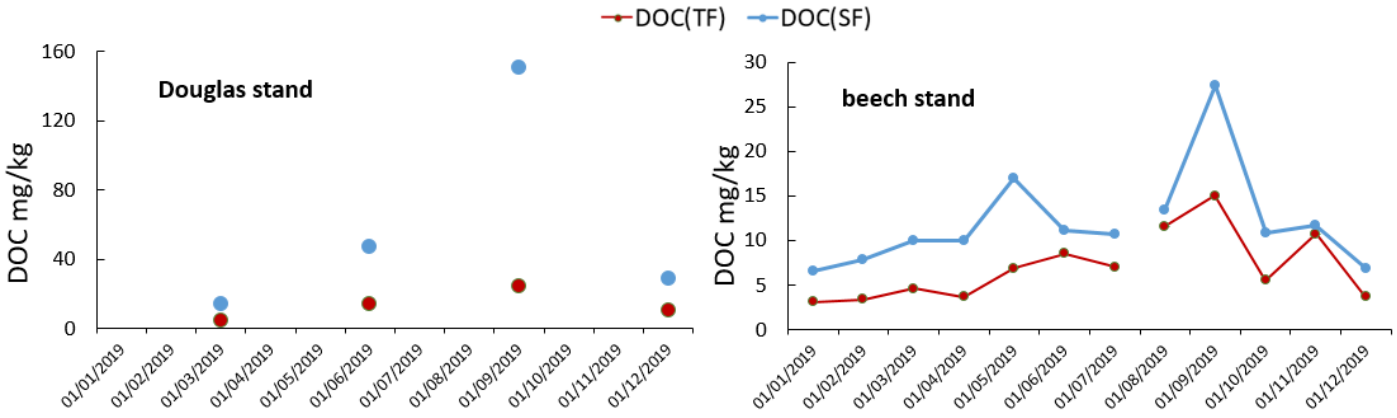

Figure art.3.SI – 5 Concentration of dissolved organic carbon (DOC) in throughfall (TF/R) and stemflow in beech and Douglas forest.

Table art.3.SI – 3 Pearson's correlation coefficients between total and fractions concentrations of Se and I in soil column and soil parameters (n= 5/stand). Non-significant correlations are grey. Significant correlations are bolded: Significance of the correlation: ***p < 0.001; ** p < 0.01; * p < 0.05.

	Se_{tot}	Se_{MQ}	Se_{NaOH}	Se_{MQ} / Se_{NaOH}	I_{tot}	I_{MQ}	I_{NaOH}	I_{MQ} / I_{NaOH}
Se_{tot}	1	-	-	-	-	-	-	-
Se_{MQ}	0.43	1	-	-	-	-	-	-
Se_{NaOH}	0.56	0.13	1	-	-	-	-	-
I_{tot}	-0.006	-0.082	**0.66***	-	1	-	-	-
I_{MQ}	0.35	**0.78****	0.11	-	-0.029	1	-	-
I_{NaOH}	-0.15	-0.24	**0.60***	-	**0.94*****	-0.21	1	-
Carbon	**0.65****	0.39	0.079	0.48	**-0.80*****	0.44	**-0.85*****	**0.67***
Sugars	0.46	0.36	-0.11	0.33	**-0.62****	0.27	**-0.77*****	**0.67***
Deoxy/C5	-0.004	-0.011	-0.049	-0.10	0.11	0.29	-0.004	0.39
C6/C5	0.14	0.32	-0.076	0.23	-0.29	**0.59***	**-0.50***	**0.65***
Sum SVC	**0.62***	0.18	-0.042	0.34	**-0.80*****	0.082	**-0.86*****	0.43
Ac/Ad	0.41	0.34	0.41	0.20	0.17	0.37	0.052	0.35
C/V	0.41	0.34	0.55	0.46	0.46	0.11	**0.52***	0.019
S/V	0.10	0.09	0.21	0.25	-0.13	-0.23	0.044	-0.18
H/V	-0.063	0.077	-0.060	0.097	-0.39	-0.19	-0.23	-0.16
Fer/Coum	-0.28	-0.17	-0.033	-0.076	0.41	0.018	0.36	0.043
(Ac/Ad)v	0.52	0.51	**0.63***	0.30	0.29	0.44	0.19	0.33
Fe exch	0.35	0.31	-0.35	0.49	**-0.82****	0.087	**-0.75****	0.53
Al exch	0.53	0.33	-0.24	0.41	**-0.79****	0.42	**-0.87*****	**0.76****
Fe oxalate	0.52	0.41	0.14	0.29	-0.29	**0.70***	**-0.57***	**0.76****
Al oxalate	0.28	0.44	**0.60***	0.30	**0.66***	0.48	0.55	0.10

Table art.3.SI – 4 Pearson correlation matrix of soil parameters. Non-significant correlations are grey. Significant correlations are bolded: Significance of the correlation: ***p < 0.001; ** p < 0.01; * p < 0.05.

	deoxy/C5	C6/C5	Sugars	Carbon	SVC	Ac/Ad	C/V	S/V	H/V	Fer/Coum	(Ac/Ad)v	Fe exch	Al exch	Fe oxalate	Al oxalate
deoxy/C5	1														
C6/C5	**0.71***	1													
Sugars	0.56	0.5	1												
Carbon	0.45	0.46	**0.95*****	1											
SVC	0.33	0.26	**0.93*****	**0.92*****	1										
Ac/Ad	0.55	0.54	**0.68***	**0.68***	**0.6***	1									
C/V	-0.38	-0.29	-0.28	-0.14	-0.23	-0.24	1								
S/V	**-0.58***	-0.57	-0.43	-0.31	-0.3	**-0.59***	**0.85*****	1							
H/V	**-0.65***	**-0.58***	**-0.58***	-0.53	-0.51	**-0.75****	**0.67***	**0.78****	1						
Fer/Coum	0.26	0.36	0	0.05	-0.04	0.05	-0.17	-0.01	-0.43	1					
(Ac/Ad)v	0.26	0.35	0.49	0.57	0.46	**0.89*****	0.16	-0.22	-0.42	-0.04	1				
Fe exch	0.04	0.17	**0.71****	**0.69***	**0.75****	0.12	-0.11	0	-0.23	0.14	0.01	1			
Al exch	0.39	0.5	**0.88*****	**0.9*****	**0.82****	0.37	-0.19	-0.25	-0.37	0.09	0.22	**0.83****	1		
Fe oxalate	**0.71****	**0.76****	**0.73****	**0.8*****	0.54	**0.65***	-0.12	-0.39	-0.52	0.19	0.54	0.31	**0.72****	1	
Al oxalate	-0.18	-0.21	-0.34	-0.2	-0.42	-0.06	**0.76****	0.53	0.53	-0.26	0.29	-0.46	-0.34	0.05	1

4. Conclusions – Chapter 3

By studying the distribution of Se and I in monospecific stands on the same forest site,variables such as climate (e.g. the distance from the coast, atmospheric input), bedrock material, soil type were eliminated for consideration from consideration.

In the first part (**Article 2**) the attention was paid on stocks and fluxes of both elements in aboveground tree compartments. The variability of concentrations, stocks and fluxes of requirement, uptake and translocation between the five tree species was determined. The second study (**Article 3**) focused on beech and Douglas fir stands by monitoring Se and I in rainfall, throughfall, stemflow and soil solutions, as well as fractionation and element speciation analysis in soil extracts. The novelty of this work was the characterization of OM to better understand the importance of its structure in the associations with Se and I.

Douglas canopy showed more efficient interception of atmospheric deposits compared to beech, resulting in higher Se and I enrichments in throughfall and stemflow. Positive canopy exchange fluxes of Se and I indicated leaching of these elements from Douglas needles while they were close to zero for beech canopy. This may be the result of the higher proportion of cuticular pool of elements in Douglas needles compared to beech leaves. Element enrichment of litterfall leaves and litterfall branches compared to living organs, especially noticeable for conifers, was attributed to longer exposure to atmospheric deposits and internal translocation.

The inputs of elements by throughfall were 0.39 and 0.77 g Se ha^{-1} y^{-1} and, 9.9 and 22 g I ha^{-1} y^{-1} for beech and Douglas, respectively. At the same time, thereturns of elements to the soil through litterfall were lower, i.e. 0.22 and 0.38 g Se ha^{-1} y^{-1} and, 1.40 and 2.94 g I ha^{-1} y^{-1} respectively for beech and Douglas. At the interface between inputs (by litterfall, throughfall and stemflow) and soil surface, humus showed both a greater water soluble proportion of elements than the underlying soil and subsequent accumulation of elements. The stocks of elements in humus were dependent on humus mass and residence time. Water-soluble element fractions decreased from humus to subsoil (even: Se_{MQ}: 5.7 → 0.2%; I_{MQ}: 5.4 → 0.1%). The proportion of elements associated with organic matter increased from humus to the soil column ((Se_{NaOH}: 17 → 72%; I_{MQ}: 36 → 100%). Moreover, total Se concentrations in the soil profiles were correlated with OM content (and Fe oxides). Inorganic species, SeO_4^{2-} in water and SeO_3^{2-} in NaOH extracts, were not preponderant and the remaining unidentified Se was supposed to be organic. Iodide was the most prevailing inorganic I species in water and NaOH extracts, IO_3^- being detected only below -30 cm. As for Se, unidentified iodine species assimilated to organic

iodine species were predominant. The “increasing-decreasing” profile of total iodine in soil was indicative of immobilization of dissolved organic iodine (54-99% of I_{MQ}) by Al minerals.

Chapter 4. General discussion and perspectives

1. General discussion

The objective of this study was to better understand the biological and geochemical aspects involved in selenium and iodine cycling in forest ecosystems. The work was carried out in two parts: i) an holistic approach involving Se analysis in different compartments of French forests covering a wide variety of climate, soil conditions and tree species (**Chapter 2**) and ii) a study focusing on the fate of Se and I in a well-characterized experimental forest site (**Chapter 3**). The general discussion presented below summarizes the most important results of the thesis.

- **The canopy and its interaction with atmospheric deposits**

Oceanic climate and proximity to the coast (taking into account prevailing wind direction) were conditions for increased exposure of litterfall to Se deposition. This was demonstrated by linear dependencies between Se concentrations in litterfall and rainfall. In contrast, varying climatic conditions did not result in differences in Se concentrations in litterfall of coniferous and deciduous trees. For the same climate, contents of elements and their annual immobilization and requirement fluxes were influenced by tree species. Longer exposure to atmospheric deposition explained the higher element content in senescing organs compared to living parts of tree, which was particularly visible for coniferous litterfall-branches. Higher enrichment of Se and I in stemflow and throughfall from conifer species indicates more efficient trapping and subsequent leaching of wet and dry atmospheric deposition.

The larger pool of mobile elements at the cuticule of needles resulted in their leaching from the Douglas canopy (CE > 0). In comparison, the exchange flux with beech canopy was equal to net throughfall (as dry deposit = 0) and close to zero considering the uncertainties. Throughfall was assessed as the major source of elements for beech and Douglas forest floors compared to returns by litterfall, contributing 66% of the total Se and 88% of the total I inputs.

- **Elements recycling from the soil**

Selenium and iodine uptakes correspond to the amount of element absorbed from the soil by the roots calculated as the amount immobilized in tree compartments and returns of the element to soil through litterfall and crown leaching. Annual root uptake was estimated to account for 0.07 % of total Se and 0.02% of total I stored in the top -15 cm of soil layer (where most biologically active tree roots are located). This implies that biorecycling through root uptake is a minor process affecting soil element reserves.

Compared with other tree compartments, concentrations of Se and I in bole-wood were the lowest which was indicative of little transport of these elements in upper tree parts. However, given its important biomass, bole-wood compartment represented the most important stock of Se in aboveground tree and a significant stock of I.

- **Humus enrichment**

Humus, as an intermediary compartment between element inputs from atmosphere and soil reserves, accumulates elements before they are gradually released into the soil. The layered structure of humus showed a continuous enrichment from fresh plant material to highly humified organic matter. With one exception, all sites were characterized by positive accumulation rates of 0.005–1.57 g Se ha^{-1} yr^{-1} and 2.4-7.2 g I ha^{-1} yr^{-1}.

Enrichment of elements in humus depends on i) loss of biomass during humification of plant material, ii) the capacity of OM to sorb elements from atmospheric deposits and iii) mobilization of elements during degradation of plant material. Fractionation study showed that the proportion of water-soluble elements decreased from fresh material to highly degraded OM (Se_{MQ}: 5.7 → 2.2%; I_{MQ}: 5.4- → 2.0%), which, together with higher element content in humified layer, is an indicator of leaching from the top and subsequent partial association with highly degraded OM. High humus residence times and biomass pools led to limited release of Se and I into soil. Decreasing Se stocks for humus types in the order: mor > moder > mull resulted in opposite order in the concentration of Se in the underlying soil.

- **Persistence in soil**

The decreasing profile of Se in the soil column and the high correlation with C_{org} highlight the pivotal role of OM in Se retention in soil. Also, Fe/Al oxides are mineral soil phases known to exhibit strong interactions with Se in soil. Direct correlation was observed between Se and Fe in soil column of the forest sites. The highest Se content was in Douglas mountain climate (Fe-rich soil) and the lowest in oceanic pine forest (sandy soil). Thus, properties of soil appeared to prevail over environmental conditions in controlling Se reserves in soil.

The "enrichment-depletion' profile of I in soil column was explained by iodine leaching as dissolved organic iodine in the upper soil layer and its subsequent association on Al minerals. Volatilization and root uptake would constitute minor processes to explain iodine fate in topsoil. It was estimated that root uptake would represent no more than 0.02% of iodine stored in the 0-15 cm soil. In contrast to Se, negative correlation was found between I and total content of OM.

Soil fractionation with water and NaOH, followed by speciation analysis of extracts, contributed to the understanding of element mobility and bioavailability. The water soluble fraction of elements was in average only 1.1% of their total soil content, while the NaOH extracts contained 51-72% of total Se and 84-100% of total iodine. Species identified in water extracts were: SeO_4^{2-}, I^-, IO_3^- and in NaOH extracts: SeO_3^{2-}, IO_3^-. Unidentified part of elements in water extracts (48-98% of Se and 54-99% of I) was supposed to be dissolved organic Se and I. In in NaOH extracts, unidentified proportion was even higher (65-97% of Se and 83-98% of I) and presumably included organo-mineral forms. Characterization of OM showed that Se organic fraction was strongly correlated to indicator of microbial activity, while non-cellulosic sugars minimized OM storing capacities of I.

- **Monitoring of radionuclides in forest ecosystem**

Soil accumulated the largest pool of Se (99.2% of total Se stocks) and I (99.7% of total I stocks) of any forest compartments. Therefore, its monitoring appears very important in the long-term in case of radiocontamination by long-living radio-isotopes. Solid-liquid partition coefficients K_D are generally used to compare element mobility in soils. The values obtained with two determination methods ranged from 216 to 29173 L kg^{-1} for Se and from 291 to 18896 L kg^{-1} for I. The mean mobile fraction of elements in soil represented only 1.1 % of their total contents. Calculated residence times in forest soil ranged between 617 and 8406 years for Se (calculated for 28 sampling sites) and 2980 – 6003 years for I (calculated for 1 sampling site), which confirmed long-term persistence of elements in soil. From estimated input-output budgets, forest soils acted as a sink for selenium (positive budgets) and a potential source of iodine (negative budget under Douglas stand) for ground water and deeper Earth crust. However, it should be noted that the calculations were based on one year monitoring of the experimental site and longer observation should be made to confirm these conclusions.

2. General conclusions

This doctoral research has achieved the main objectives and answered questions remaining after literature review:

I. How do climate, environmental and physicochemical properties affect the distribution of selenium in forest ecosystem?

- Selenium content in litterfall is higher in oceanic climate and increases with proximity to the coast and Se content in rainfall.
- Slow degradation of organic matter promotes Se accumulation in humus and soil.
- As strong carrier phases of Se, OM and Fe oxides would control Se content in soils, from the lowest levels in alkaline sandy soils in coastal Maritime pine forest to the highest contents in OM-rich, acidic soils in Douglas-fir and beech forests in mountain climate.

II. Do tree species influence Se and I partitioning within tree biomass and in underlying humus and soil column?

- Coniferous trees absorb Se and I from the atmosphere with higher efficiency than deciduous trees.
- While Se and I inputs from litterfall are similar for all tree species, differences in Se and I contents of humus and topsoil among tree species confirm that the rate of OM degradation is critical in controlling element reserves.

III. What are the differences in Se and I budgets in monospecific deciduous and coniferous tree stands?

- The enrichment factors of Se and I in throughfall and stemflow are greater for conifer species
- Forest ecosystem is a sink of selenium and a potential source of iodine, which is reflected as positive and negative input-output budgets, respectively.

IV. How do the mineral phase and organic matter of soil regulate the mobility or sorption of elements in the soil column?

- Selenium content in forest soil depended on the content of OM, including lignin, and Fe oxides (but not Al oxides).
- "Enrichment-depletion' profile of iodine derived from association on Al oxides.

3. Perspectives

Many research perspectives remain to expand our knowledge of Se and I dynamics in forest ecosystem. The proposed perspectives have been organized into several categories, taking into account a more holistic approach to the fields of environmental and analytical chemistry.

- **Speciation study**

Speciation analysis of Se and I in forest soil extracts is still challenging to elucidate their associations with soil organic matter. Considering the absence of unidentified signals in soil extracts on chromatograms obtained in this study, chemical treatments could be applied in order to degrade colloidal or HMW organic structures into smaller organic derivatives that would be easier to detect and identify by mass spectrometry. Regarding the lack of commercially available extracts, non-targeted analysis could be performed using liquid chromatography coupled with ESI-HRMS to propose chemical structures with selenium or iodine. Such studies have not been performed on humus and soil samples, but are successfully used on plant samples (Ruszczyńska et al., 2017).

- **Environmental study**

We showed that tree species influenced selenium and iodine contents only in humus and upper soil layers, which could be explained by the limited age of tree stands (~46 years) compared to residence time of organic matter in such ecosystem. It would be interesting to investigate older monospecific forests under similar climatic and edaphic conditions.

Although volatilization of iodine from forest soil surface may not explain alone the "enrichment-depletion profile" observed in soil column, volatilization does contribute to the overall iodine budget, but its contribution in forest ecosystem is not really known, especially in comparison with drainage. Likewise, volatilization is a key process in selenium cycle, however the quantitative data about Se emission, expecially from forest floor, are scarse. The possible method to monitor volatilization from humus and soil would be i) field flux chambers combined with chemotrapping system (Vriens et al., 2014b) and ii) incubation system for sample spiked with a monoisotopic solution (^{75}Se or ^{77}Se and ^{125}I) and trapping on activated carbon (Roulier, 2018; Stork et al., 1999).

- **Statistical study**

The statistical study is a powerful tool to discriminate conditions that influence element contents in the environment. An interesting perspective is the application of statistical study on literature data obtained in wider area (e.g. focusing on the European forest). Taking into account

a larger number of data would improve the versatility of the results and the predictive potential. In addition to the Se concentration data, detailed characteristics of the studied forests will be needed. Experimental literature data set would also ideally include fractionation/speciation data, which would provide further insights about mobility and bioavailability of elements.

- **Modeling study**

Field data obtained in this project will be used for calibration of dynamic compartment models of elements (including their radioisotopes) in forest ecosystem. The dynamic compartment models take into account the characteristics of the forest (i.e. biogeochemical soil properties, tree biomass) and simulate element fluxes (both organic and inorganic fractions) between atmosphere, lithosphere and biosphere and for various tree parts (root, tree surface, internal tree). Predicted element fluxes between compartments are determined using kinetic equations from field data. It allows to estimate the input-output of elements as well as their persistence time in all compartments. Such study will be performed within the framework of Andra's modelling activity and will be applied to scenarios for assessing radiocontamination. Similar models have been already elaborated for ^{36}Cl (Tanaka and Thiry, 2020) and ^{137}Cs (Thiry et al., 2018).

References

-A-

Adeleke, R., Nwangburuka, C., Oboirien, B., 2017. Origins, roles and fate of organic acids in soils: A review. S. Afr. J. Bot. 108, 393–406. https://doi.org/10.1016/j.sajb.2016.09.002

Adriano, D.C., 2001b. Selenium, in: Adriano, D.C. (Ed.), Trace Elements in Terrestrial Environments: Biogeochemistry, Bioavailability, and Risks of Metals. Springer, New York, NY, pp. 707–758. https://doi.org/10.1007/978-0-387-21510-5_18Al-Ammar, A., Reitznerová, E., Barnes, R.M., 2001. Thorium and iodine memory effects in inductively-coupled plasma mass spectrometry. Fresenius J. Anal. Chem. 370, 479–482.

Alberdi, I., Baycheva-Merger, T., Alain, B., Bozzano, M., Caudullo, G., Cienciala, E., Corona, P., Domínguez, G., Houston-Durrant, T., Edwards, D., Estreguil, C., Ferreti, M., Fischer, U., Freudenschuss, A., Gasparini, P., Godinho-Ferreira, P., Hansen, K., Hiederer, R., Inhaizer, H., Zingg, A., 2015. State of Europe's Forests 2015 - summary for policy makers.

Aldahan, A., Alfimov, V., Possnert, G., 2007. 129I anthropogenic budget: Major sources and sinks. Appl. Geochem., Halogens and Their Isotopes in Marine and Terrestrial Systems 22, 606–618. https://doi.org/10.1016/j.apgeochem.2006.12.006

Allard, S., Gallard, H., 2013. Abiotic formation of methyl iodide on synthetic birnessite: A mechanistic study. Sci. Total Environ. 463–464, 169–175. https://doi.org/10.1016/j.scitotenv.2013.05.079

Allard, S., von Gunten, U., Sahli, E., Nicolau, R., Gallard, H., 2009. Oxidation of iodide and iodine on birnessite (δ-MnO2) in the pH range 4–8. Water Research 43, 3417–3426. https://doi.org/10.1016/j.watres.2009.05.018Almahayni, T., Bailey, E., Crout, N.M.J., Shaw, G., 2017. Effects of incubation time and filtration method on Kd of indigenous selenium and iodine in temperate soils. J. Environ. Radioact. 177, 84–90. https://doi.org/10.1016/j.jenvrad.2017.06.004

Amachi, S., Kasahara, M., Hanada, S., Kamagata, Y., Shinoyama, H., Fujii, T., Muramatsu, Y., 2003. Microbial participation in iodine volatilization from soils. Environ. Sci. Technol. 37, 3885–3890. https://doi.org/10.1021/es0210751

Amouroux, D., Liss, P.S., Tessier, E., Hamren-Larsson, M., Donard, O.F.X., 2001. Role of oceans as biogenic sources of selenium. Earth Planet. Sci. Lett. 189, 277–283. https://doi.org/10.1016/S0012-821X(01)00370-3

AnaEE France - Breuil [WWW Document], URL https://www.anaee-france.fr/en/infrastructure-services/in-natura-experimentation/forest-ecosystems/temperate-and-continental-forests/breuil (accessed 5.2.21).

Andreetta, A., Ciampalini, R., Moretti, P., Vingiani, S., Poggio, G., Matteucci, G., Tescari, F., Carnicelli, S., 2011. Forest humus forms as potential indicators of soil carbon storage in Mediterranean environments. Biol. Fertil. Soils. 47, 31–40. https://doi.org/10.1007/s00374-010-0499-z

Aponte, C., García, L.V., Marañón, T., 2013. Tree species effects on nutrient cycling and soil biota: A feedback mechanism favouring species coexistence. For. Ecol. Manag., 309, 36–46. https://doi.org/10.1016/j.foreco.2013.05.035

Augusto, L., Ranger, J., Binkley, D., Rothe, A., 2002. Impact of several common tree species of European temperate forests on soil fertility. Ann. For. Sci. 59, 233–253. https://doi.org/10.1051/forest:2002020

-B-

Balistrieri, L.S., Chao, T.T., 1987. Selenium adsorption by goethite. SSSA 51, 11451151. https://doi.org/10.2136/sssaj1987.03615995005100050009x

Barescut, J., Zvonova, I., Bratilova, A., Jesko, T., Sarycheva, S., Fomintceva, M., 2009. Ecological half-life of I-131 in milk after dry and wet radionuclide deposition due to the Chernobyl accident. Radioprotection 44, 731–734. https://doi.org/10.1051/radiopro/20095133

Belon, E., Boisson, M., Deportes, I.Z., Eglin, T.K., Feix, I., Bispo, A.O., Galsomies, L., Leblond, S., Guellier, C.R., 2012. An inventory of trace elements inputs to French agricultural soils. Sci. Total Environ. 439, 87–95. https://doi.org/10.1016/j.scitotenv.2012.09.011

Bergman, R., 1994. 4.5. The Distribution of Radioactive Caesium in Boreal Forest Ecosystems, in: Dahlgaard, H. (Ed.), Studies in Environmental Science, Nordic Radioecology. Elsevier, pp. 335–379. https://doi.org/10.1016/S0166-1116(08)71718-7

Bichsel, Y., von Gunten, U., 2000. Formation of Iodo-Trihalomethanes during Disinfection and Oxidation of Iodide-Containing Waters. Environ. Sci. Technol. 34, 2784–2791. https://doi.org/10.1021/es9914590

Bienvenu, P., Cassette, P., Andreoletti, G., Bé, M.M., Comte, J., Lépy, M.C., 2007. A new determination of 79Se half-life. Appl. Radiat. Isot. 65, 355–364. https://doi.org/10.1016/j.apradiso.2006.09.009

Bing, L., Xinrong, M., Lirong, H., Hongxia, Y., 2004. Pressurised extraction using dilute ammonia: A simple method for determination of iodine in soil, sediment and biological samples by inductively coupled plasma-mass spectrometry. Geostand. Geoanalyt. Res. 28, 317–323. https://doi.org/10.1111/j.1751-908X.2004.tb00747.x

Blazina, T., Sun, Y., Voegelin, A., Lenz, M., Berg, M., Winkel, L.H.E., 2014. Terrestrial selenium distribution in China is potentially linked to monsoonal climate. Nat. Commun. 5, 1–7. https://doi.org/10.1038/ncomms5717

Bostock, A.C., 2004. Chemical speciation, volatilisation and cycling of 36Cl, 129I and 99Tc in coniferous forest systems. University of London.

Bowley, H.E., Young, S.D., Ander, E.L., Crout, N.M.J., Watts, M.J., Bailey, E.H., 2016. Iodine binding to humic acid. Chemosphere 157, 208–214. https://doi.org/10.1016/j.chemosphere.2016.05.028

Bowley, H.E., Young, S.D., Ander, E.L., Crout, N.M.J., Watts, M.J., Bailey, E.H., 2019. Iodine bioavailability in acidic soils of Northern Ireland. Geoderma 348, 97–106. https://doi.org/10.1016/j.geoderma.2019.04.020

Bowley, H.E., 2013. Iodine dynamics in the terrestrial environment PhD Thesis. University of Nottingham.

Bowley, H.E., Young, S.D., Ander, E.L., Crout, N.M.J., Watts, M.J., Bailey, E.H., 2016. Iodine binding to humic acid. Chemosphere 157, 208–214. https://doi.org/10.1016/j.chemosphere.2016.05.028

Brantley, S.L., Goldhaber, M.B., Ragnarsdottir, K.V., 2007. Crossing Disciplines and Scales to Understand the Critical Zone. Elements 3, 307–314. https://doi.org/10.2113/gselements.3.5.307

Brêthes A., Urlich E., 1997. Caractéristiques pédologiques des 102 peuplements du réseau. - Office national de forêts, Dépt des recherches Techniques.

Brigelius-Flohé, R., 2018. Selenium in Human Health and Disease: An Overview, in: Michalke, B. (Ed.), Selenium, Molecular and Integrative Toxicology. Springer International Publishing, Cham, pp. 3–26. https://doi.org/10.1007/978-3-319-95390-8_1

Broadley, M.R., White, P.J., Bryson, R.J., Meacham, M.C., Bowen, H.C., Johnson, S.E., Hawkesford, M.J., McGrath, S.P., Zhao, F.-J., Breward, N., Harriman, M., Tucker, M.,

2006. Biofortification of UK food crops with selenium. Proc. Nutr. Soc. 65, 169–181. https://doi.org/10.1079/pns2006490

Bruggeman, C., Maes, A., Vancluysen, J., 2007. The interaction of dissolved Boom Clay and Gorleben humic substances with selenium oxyanions (selenite and selenate). Appl. Geochem. 22, 1371–1379. https://doi.org/10.1016/j.apgeochem.2007.03.027

Budke, C., Mühling, K.H., Daum, D., 2020. Iodine uptake and translocation in apple trees grown under protected cultivation. J. Plant Nutr. Soil Sci. 183, 468–481. https://doi.org/10.1002/jpln.202000099

-C-

Cakmak, I., Prom-u-thai, C., Guilherme, L.R.G., Rashid, A., Hora, K.H., Yazici, A., Savasli, E., Kalayci, M., Tutus, Y., Phuphong, P., Rizwan, M., Martins, F.A.D., Dinali, G.S., Ozturk, L., 2017. Iodine biofortification of wheat, rice and maize through fertilizer strategy. Plant Soil 418, 319–335. https://doi.org/10.1007/s11104-017-3295-9

Calmon, P., Thiry, Y., Zibold, G., Rantavaara, A., Fesenko, S., 2009. Transfer parameter values in temperate forest ecosystems: a review. J. Environ. Radioact. 100, 757–766. https://doi.org/10.1016/j.jenvrad.2008.11.005

Chao, T.T., Zhou, L., 1983. Extraction Techniques for Selective Dissolution of Amorphous Iron Oxides from Soils and Sediments. SSSAJ 47, 225–232. https://doi.org/10.2136/sssaj1983.03615995004700020010x

Charlet, L., Scheinost, A.C., Tournassat, C., Greneche, J.M., Géhin, A., Fernández-Martı´nez, A., Coudert, S., Tisserand, D., Brendle, J., 2007. Electron transfer at the mineral/water interface: Selenium reduction by ferrous iron sorbed on clay. Geochim. Cosmochim. Acta 71, 5731–5749. https://doi.org/10.1016/j.gca.2007.08.024

Chasteen, T.G., Bentley, R., 2003. Biomethylation of selenium and tellurium: microorganisms and plants. Chem. Rev. 103, 1–25. https://doi.org/10.1021/cr010210+

Charro, E., Pardo, R., Peña, V., 2013. Statistical analysis of the spatial distribution of radionuclides in soils around a coal-fired power plant in Spain. J. Environ. Radioact. 124, 84–92. https://doi.org/10.1016/j.jenvrad.2013.04.011

Chen, J., Gu, B., LeBoeuf, E.J., Pan, H., Dai, S., 2002. Spectroscopic characterization of the structural and functional properties of natural organic matter fractions. Chemosphere 48, 59–68. https://doi.org/10.1016/S0045-6535(02)00041-3

Chi, F.Q., Kuang, E.J., Zhang, J.M., Su, Q.R., Chen, X.L., Zhang, Y.W., Liu, Y.D., Kuang, E.J., Zhang, J.M., Su, Q.R., Chen, X.L., Zhang, Y.W., Liu, Y.D., 2019. Fractionation and distribution of soil selenium and effects of soil properties in Heilongjiang. Selenium Research for Environment and Human Health: Perspectives, Technologies and Advancements. https://doi.org/10.1201/9780429423482-9

Claret, F., Lerouge, C., Laurioux, T., Bizi, M., Conte, T., Ghestem, JP., Wille, G., Sato, T., Gaucher, E.C., Giffaut, E., Tournassat, C., 2010. Natural iodine in a clay formation: Implications for iodine fate in geological disposals. Geochim. Cosmochim. Acta 74, 16–29. https://doi.org/10.1016/j.gca.2009.09.030

Collins, C.D., Gravett, A.E., Bell, J.N.B., 2004. The deposition and translocation of methyl iodide by crops. Health. Phys. 87, 512–516.

Conde, J.E., Sanz Alaejos, M., 1997. Selenium Concentrations in Natural and Environmental Waters. Chem. Rev. 97, 1979–2004. https://doi.org/10.1021/cr960100g

Coppin, F., Chabroullet, C., Martin-Garin, A., Balesdent, J., Gaudet, J.P., 2006. Methodological approach to assess the effect of soil ageing on selenium behaviour: first results concerning mobility and solid fractionation of selenium. Biol. Fertil. Soils 42, 379–386. https://doi.org/10.1007/s00374-006-0080-y

Coppin, F., Chabroullet, C., Martin-Garin, A., 2009. Selenite interactions with some particulate organic and mineral fractions isolated from a natural grassland soil. EJSS 60, 369–376. https://doi.org/10.1111/j.1365-2389.2009.01127.x

Cornelis, J.-T., Ranger, J., Iserentant, A., Delvaux, B., 2010. Tree species impact the terrestrial cycle of silicon through various uptakes. Biogeochemistry 97, 231–245. https://doi.org/10.1007/s10533-009-9369-x

Couture, R.A., Seitz, M.G., 1983. Sorption of anions of iodine by iron oxides and kaolinite. Nuclear and Chemical Waste Management 4, 301–306. https://doi.org/10.1016/0191-815X(83)90055-4

Cumbers, A., Birch, K., MacKinnon, D., 2006. Revisiting the Old Industrial Region: Adaptation and Adjustment in an Integrating Europe. CPPR Working Paper 1. University of Glasgow.

-D-

Dai, J.-L., Zhang, M., Zhu, Y.-G., 2004. Adsorption and desorption of iodine by various Chinese soils: I. Iodate. Environ Int 30, 525–530. https://doi.org/10.1016/j.envint.2003.10.007

Dai, J.L., Zhu, Y.G., Huang, Y.Z., Zhang, M., Song, J.L., 2006. Availability of iodide and iodate to spinach (Spinacia oleracea L.) in relation to total iodine in soil solution. Plant Soil 289, 301–308. https://doi.org/10.1007/s11104-006-9139-7

Daniel Hillel, 2005. Encyclopedia of Soils in the Environment. Elsevier.

De Schrijver, A., Geudens, G., Augusto, L., Staelens, J., Mertens, J., Wuyts, K., Gielis, L., Verheyen, K., 2007. The effect of forest type on throughfall deposition and seepage flux: a review. Oecologia 153, 663–674. https://doi.org/10.1007/s00442-007-0776-1

Di Tullo, P., 2015. Dynamique du cycle biogéochimique du sélénium en écosystèmes terrestres : rétention et réactivité dans le sol, rôle de la végétation (thesis). Pau.

Diener, A., Hartmann, P., Urso, L., Vives I Batlle, J., Gonze, M.A., Calmon, P., Steiner, M., 2017. Approaches to modelling radioactive contaminations in forests - Overview and guidance. J Environ Radioact 178–179, 203–211. https://doi.org/10.1016/j.jenvrad.2017.09.003

Dinh, Q.T., Cui, Z., Huang, J., Tran, T.A.T., Wang, D., Yang, W., Zhou, F., Wang, M., Yu, D., Liang, D., 2018. Selenium distribution in the Chinese environment and its relationship with human health: A review. Environ. Internat. 112, 294–309. https://doi.org/10.1016/j.envint.2017.12.035

Dinh, Q.T., Li, Z., Tran, T.A.T., Wang, D., Liang, D., 2017. Role of organic acids on the bioavailability of selenium in soil: A review. Chemosphere 184, 618–635. https://doi.org/10.1016/j.chemosphere.2017.06.034.

Dowdle, P.R., Oremland, R.S., 1998. Microbial Oxidation of Elemental Selenium in Soil Slurries and Bacterial Cultures. Environ. Sci. Technol. 32, 3749–3755. https://doi.org/10.1021/es970940s

Drahoňovský, J., Száková, J., Mestek, O., Tremlová, J., Kaňa, A., Najmanová, J., Tlustoš, P., 2016. Selenium uptake, transformation and inter-element interactions by selected wildlife plant species after foliar selenate application. Environ. Exp. Bot. 125, 12–19. https://doi.org/10.1016/j.envexpbot.2016.01.006

Duborská, E., Bujdoš, M., Urík, M., Matúš, P., 2020. Iodine fractionation in agricultural and forest soils using extraction methods. CATENA 195, 104749. https://doi.org/10.1016/j.catena.2020.104749

Duchaufour, P., 1998. Handbook of Pedology, Masson Editeur, Paris.

-E-

El Mehdawi, A.F., Pilon-Smits, E. a. H., 2012. Ecological aspects of plant selenium hyperaccumulation. Plant Biol. 14, 1–10. https://doi.org/10.1111/j.1438-8677.2011.00535.x

El-Ramady, H., domokos-szabolcsy, E., Shalaby, T., Joe, P., Fári, M., 2015. Selenium in Agriculture: Water, Air, Soil, Plants, Food, Animals and Nanoselenium. https://doi.org/10.1007/978-3-319-11906-9_5

Epp, T., Neidhardt, H., Pagano, N., Marks, M.A.W., Markl, G., Oelmann, Y., 2020. Vegetation canopy effects on total and dissolved Cl, Br, F and I concentrations in soil and their fate along the hydrological flow path. Sci. Total Environ. 712, 135473. https://doi.org/10.1016/j.scitotenv.2019.135473

Espiau, P., Peyronel, A., 1976. L'acidité d'échange des sols, le taux d'acidité d'échange et sa signification pédologique sous climat tempéré. Annales Agronomiques 31, 363–383.

Eszenyi, P., Sztrik, A., Babka, B., Prokisch, J., 2011. Elemental, Nano-Sized (100-500 nm) Selenium Production by Probiotic Lactic Acid Bacteria. IJBBB 148–152. https://doi.org/10.7763/IJBBB.2011.V1.27

-F-

Fairweather-Tait, S.J., Bao, Y., Broadley, M.R., Collings, R., Ford, D., Hesketh, J.E., Hurst, R., 2011. Selenium in human health and disease. Antioxid. Redox Signal. 14, 1337–1383. https://doi.org/10.1089/ars.2010.3275

Favorito, J.E., Luxton, T.P., Eick, M.J., Grossl, P.R., 2017. Selenium speciation in phosphate mine soils and evaluation of a sequential extraction procedure using XAFS. Environ. Pollut. 229, 911–921. https://doi.org/10.1016/j.envpol.2017.07.071

Feinberg A., Stenke A., Peter T., Winkel L., 2020. Constraining Atmospheric Selenium Emissions Using Observations, Global Modeling, and Bayesian Inferencef. Environ. Sci. Technol. 54, 7146−7155.

Fernández-Martínez, A., Charlet, L., 2009. Selenium environmental cycling and bioavailability: a structural chemist point of view. Rev. Environ. Sci. Biotechnol. 8, 81–110. https://doi.org/10.1007/s11157-009-9145-3

Fox, P.M., Davis, J.A., Luther, G.W., 2009. The kinetics of iodide oxidation by the manganese oxide mineral birnessite. Geochim. Cosmochim. Acta 73, 2850–2861. https://doi.org/10.1016/j.gca.2009.02.016

Fuge, R., 2007. Iodine Deficiency: An Ancient Problem in a Modern World. Ambio 36, 70–72.

Fuge, R., Johnson, C.C., 2015. Iodine and human health, the role of environmental geochemistry and diet, a review. Appl. Geochem. 63, 282–302. https://doi.org/10.1016/j.apgeochem.2015.09.013

-G-

Gallard, H., Allard, S., Nicolau, R., von Gunten, U., Croué, J.P., 2009. Formation of Iodinated Organic Compounds by Oxidation of Iodide-Containing Waters with Manganese Dioxide. Environ. Sci. Technol. 43, 7003–7009. https://doi.org/10.1021/es9010338

Gandois, L., 2009. Dynamique et bilan des Elements Traces Métalliques (ETM) dans des écosystèmes forestiers français. Modélisation, spéciation et charges critiques.

Gilfedder, B.S., Lai, S.C., Petri, M., Biester, H., Hoffmann, T., 2008. Iodine speciation in rain, snow and aerosols. Atmos. Chem. Phys. 8, 6069–6084. https://doi.org/10.5194/acp-8-6069-2008

Goor, F., Thiry, Y., 2004. Processes, dynamics and modelling of radiocaesium cycling in a chronosequence of Chernobyl-contaminated Scots pine (Pinus sylvestris L.) plantations. Sci. Total Environ. 325, 163–180. https://doi.org/10.1016/j.scitotenv.2003.10.037

Goldberg, S.U., Glaubig, R., Anion Sorption on a Calcareous , Montmorillonitic Soil — Selenium. Soil Sci. Soc. Am. J. 52:954-958 (1988)

Gower, S.T., Richards, J.H., 1990. Larches: Deciduous Conifers in an Evergreen World. BioScience 40, 818–826. https://doi.org/10.2307/1311484

Guggenberger, G., 2005. Humification and Mineralization in Soils, in: Varma, A., Buscot, F. (Eds.), Microorganisms in Soils: Roles in Genesis and Functions, Soil Biology. Springer Berlin Heidelberg, Berlin, Heidelberg, pp. 85–106. https://doi.org/10.1007/3-540-26609-7_4

Gustafsson, J.P., Johnsson, L., 1994. The association between selenium and humic substances in forested ecosystems—laboratory evidence. Appl. Organomet. Chem. 8, 141–147. https://doi.org/10.1002/aoc.590080209

Gwynn, J.P., Nalbandyan, A., Rudolfsen, G., 2013. 210Po, 210Pb, 40K and 137Cs in edible wild berries and mushrooms and ingestion doses to man from high consumption rates of these wild foods. J. Environ. Radioact. 116, 34–41. https://doi.org/10.1016/j.jenvrad.2012.08.016

-H-

Haldimann, M., Alt, A., Blanc, A., Blondeau, K., 2005. Iodine content of food groups. J. Food Compos. Anal. 18, 461–471. https://doi.org/10.1016/j.jfca.2004.06.003

Han, X., Cao, L., Cheng, H., Liu, J., Xu, Z., 2012. Determination of iodine species in seaweed and seawater samples using ion-pair reversed phase high performance liquid chromatography coupled with inductively coupled plasma mass spectrometry. Anal. Methods 4, 3471–3477. https://doi.org/10.1039/C2AY25871D

Hansen, V., Roos, P., Aldahan, A., Hou, X., Possnert, G., 2011. Partition of iodine (129I and 127I) isotopes in soils and marine sediments. J. Environ. Radioact. 102, 1096–1104. https://doi.org/10.1016/j.jenvrad.2011.07.005

Hao, Z., Wang, J., Yin, Y., Cao, D., Liu, J., 2018. Abiotic formation of organoiodine compounds by manganese dioxide induced iodination of dissolved organic matter. Environ. Pollut. 236, 672–679. https://doi.org/10.1016/j.envpol.2018.02.001

Hart, D.J., Fairweather-Tait, S.J., Broadley, M.R., Dickinson, S.J., Foot, I., Knott, P., McGrath, S.P., Mowat, H., Norman, K., Scott, P.R., Stroud, J.L., Tucker, M., White, P.J., Zhao, F.J., Hurst, R., 2011. Selenium concentration and speciation in biofortified flour and bread: Retention of selenium during grain biofortification, processing and production of Se-enriched food. Food Chem 126, 1771–1778. https://doi.org/10.1016/j.foodchem.2010.12.079

Hjerpe, T., Broed, R., 2010. Radionuclide transport and dose assessment modelling in biosphere assessment 2009 (No. POSIVA-WR--10-79). Posiva Oy.

Hou, X., Hansen, V., Aldahan, A., Possnert, G., Lind, O.C., Lujaniene, G., 2009. A review on speciation of iodine-129 in the environmental and biological samples. Anal. Chim. Acta 632, 181–196. https://doi.org/10.1016/j.aca.2008.11.013

Howard, B.J. (Institute of T.E., Hove, K., Strand, P., Pronevich, V., 1995. Aggregated transfer coefficients: a simple approach to modelling transfer of radionuclides to food products from semi-natural eco-systems, in: Proceedings Series (IAEA), 1995, IAEA.

Hu, Q., Moran, J.E. & Blackwood, V., 2007. Geochemicalcycling of iodine species in soils. https://inis.iaea.org/search/search.aspx?orig_q=RN:40026411

Humphrey, O.S., Young, S.D., Bailey, E.H., Crout, N.M.J., Ander, E.L., Hamilton, E.M., Watts, M.J., 2019. Iodine uptake, storage and translocation mechanisms in spinach (Spinacia oleracea L.). Environ. Geochem. Health 41. https://doi.org/10.1007/s10653-019-00272-z

Humphrey, O.S., Young, S.D., Crout, N.M.J., Bailey, E.H., Ander, E.L., Watts, M.J., 2020. Short-Term Iodine Dynamics in Soil Solution. Environ. Sci. Technol. 54, 1443–1450. https://doi.org/10.1021/acs.est.9b02296

Hurtevent, P., Thiry, Y., Levchuk, S., Yoschenko, V., Henner, P., Madoz-Escande, C., Leclerc, E., Colle, C., Kashparov, V., 2013. Translocation of 125I, 75Se and 36Cl to wheat edible parts following wet foliar contamination under field conditions. J. Environ. Radioact. 121, 43–54. https://doi.org/10.1016/j.jenvrad.2012.04.013

-I-

IAEA, 2010. Handbook of Parameter Values for the Prediction of Radionuclide Transfer in Terrestrial and Freshwater Environment.

-J-

Jonard, M., Nicolas, M., Coomes, D.A., Caignet, I., Saenger, A., Ponette, Q., 2017. Forest soils in France are sequestering substantial amounts of carbon. Sci. Total Environ. 574, 616–628. https://doi.org/10.1016/j.scitotenv.2016.09.028

Jung, T., Hudler, G.W., Jensen-tracy, S.L., Griffiths, H.M., Fleischmann, F., Osswald, W., 2005. Involvement of Phytophthora species in the decline of European beech in Europe and the USA. Mycologist 19, 159–166. https://doi.org/10.1017/S0269-915X(05)00405-2

-K-

Kadowaki, M., Terada, H., Nagai, H., 2020. Global budget of atmospheric 129I during 2007–2010 estimated by a chemical transport model: GEARN–FDM. Atmos. Environ.: X 8, 100098. https://doi.org/10.1016/j.aeaoa.2020.100098

Kalbitz, K., Solinger, S., Park, J.-H., Michalzik, B., Matzner, E., 2000. Controls on the dynamics of dissolved organic matter in soils: A review. Soil Sci. 165, 277–304.

Kaplan, D.I., 2003. Influence of surface charge of an Fe-oxide and an organic matter dominated soil on iodide and pertechnetate sorption. Radiochim. Acta 91, 173–178.

Kaplan, D.I., Zhang, S., Roberts, K.A., Schwehr, K., Xu, C., Creeley, D., Ho, Y.-F., Li, H.-P., Yeager, C.M., Santschi, P.H., 2014. Radioiodine concentrated in a wetland. J Environ. Radioact. 131, 57–61. https://doi.org/10.1016/j.jenvrad.2013.09.001

Kápolna, E., Hillestrøm, P.R., Laursen, K.H., Husted, S., Larsen, E.H., 2009. Effect of foliar application of selenium on its uptake and speciation in carrot. Food Chem. 115, 1357–1363. https://doi.org/10.1016/j.foodchem.2009.01.054

Kápolna, E., Laursen, K.H., Husted, S., Larsen, E.H., 2012. Bio-fortification and isotopic labelling of Se metabolites in onions and carrots following foliar application of Se and 77Se. Food Chem. 133, 650–657. https://doi.org/10.1016/j.foodchem.2012.01.043

Kato, S., Wachi, T., Yoshihira, K., Nakagawa, T., Ishikawa, A., Takagi, D., Tezuka, A., Yoshida, H., Yoshida, S., Sekimoto, H., Takahashi, M., 2013. Rice (Oryza sativa L.) roots have iodate reduction activity in response to iodine. Front. Plant. Sci. 4, 227. https://doi.org/10.3389/fpls.2013.00227

Kausch, M., Ng, P., Ha, J., Pallud, C., 2012. Soil-Aggregate-Scale Heterogeneity in Microbial Selenium Reduction. VZJ 11, vzj2011.0101. https://doi.org/10.2136/vzj2011.0101

Kazakov, V.S., Demidchik, E.P., Astakhova, L.N., 1992. Thyroid cancer after Chernobyl. Nature 359, 21. https://doi.org/10.1038/359021a0

Kikkert, J., Berkelaar, E., 2013. Plant Uptake and Translocation of Inorganic and Organic Forms of Selenium. Arch. Environ. Contam. Toxicol. 65, 458–465. https://doi.org/10.1007/s00244-013-9926-0

Kodama, S., Takahashi, Y., Okumura, K., Uruga, T., 2006. Speciation of iodine in solid environmental samples by iodine K-edge XANES: application to soils and

ferromanganese oxides. Sci. Total. Environ. 363, 275–284. https://doi.org/10.1016/j.scitotenv.2006.01.004
Korobova, E., 2010. Soil and landscape geochemical factors which contribute to iodine spatial distribution in the main environmental components and food chain in the central Russian plain. J. Geochem. Explor. 107, 180–192. https://doi.org/10.1016/j.gexplo.2010.03.003
Kwon, J.H., Wilson, L.D., Sammynaiken, R., 2015. Sorptive uptake of selenium with magnetite and its supported materials onto activated carbon. J. Colloid Interface Sci. 457, 388–397. https://doi.org/10.1016/j.jcis.2015.07.013

-L-

Laganière, J.L., Paré, D.P., Bradley, R.L.B.L., 2010. How does a tree species influence litter decomposition? Separating the relative contribution of litter quality, litter mixing, and forest floor conditions. Can. J. For. Res.. https://doi.org/10.1139/X09-208
Låg, J., Steinnes, E., 1978. Regional distribution of selenium and arsenic in humus layers of Norwegian forest soils. Geoderma 20, 3–14. https://doi.org/10.1016/0016-7061(78)90045-9
Lal, R., 2017. Encyclopedia of Soil Science. CRC Press.
Lawson, P.G., Daum, D., Czauderna, R., Meuser, H., Härtling, J.W., 2015. Soil versus foliar iodine fertilization as a biofortification strategy for field-grown vegetables. Front. Plant Sci. 6. https://doi.org/10.3389/fpls.2015.00450
Layton-Matthews, D., Leybourne, M.I., Peter, J.M., Scott, S.D., 2006. Determination of selenium isotopic ratios by continuous-hydride-generation dynamic-reaction-cell inductively coupled plasma-mass spectrometry. J. Anal. At. Spectrom. 21, 41–49. https://doi.org/10.1039/B501704A
Legout, A., van der Heijden, G., Jaffrain, J., Boudot, J.-P., Ranger, J., 2016. Tree species effects on solution chemistry and major element fluxes: A case study in the Morvan (Breuil, France). For. Ecol. Manag. 378, 244–258. https://doi.org/10.1016/j.foreco.2016.07.003
Le Mellec, A., Meesenburg, H., Michalzik, B., 2010. The importance of canopy-derived dissolved and particulate organic matter (DOM and POM) — comparing throughfall solution from broadleaved and coniferous forests. Ann. For. Sci. 67, 411–411. https://doi.org/10.1051/forest/2009130
Levrel, G., Ranger, J., 2006. Effet des substitutions d'essences forestières et des amendements sur les propriétés physiques d'un Alocrisol. Etude et Gestion des Sols 13, 71–88.
Li, H.-F., McGrath, S.P., Zhao, F.-J., 2008. Selenium uptake, translocation and speciation in wheat supplied with selenate or selenite. New Phytol. 178, 92–102. https://doi.org/10.1111/j.1469-8137.2007.02343.x
Li, Z., Liang, D., Peng, Q., Cui, Z., Huang, J., Lin, Z., 2017. Interaction between selenium and soil organic matter and its impact on soil selenium bioavailability: A review. Geoderma 295, 69–79. https://doi.org/10.1016/j.geoderma.2017.02.019
Lin, C.C., Chao, J.H., 2009. Chapter 17 - Radiochemistry of Iodine: Relevance to Health and Disease, in: Preedy, V.R., Burrow, G.N., Watson, R. (Eds.), Comprehensive Handbook of Iodine. Academic Press, San Diego, pp. 171–182. https://doi.org/10.1016/B978-0-12-374135-6.00017-0
Lovett, G.M., Lindberg, S.E., 1984. Dry Deposition and Canopy Exchange in a Mixed Oak Forest as Determined by Analysis of Throughfall. J. Appl. Ecol. 21, 1013–1027. https://doi.org/10.2307/2405064
Lusa, M., Bomberg, M., Aromaa, H., Knuutinen, J., Lehto, J., 2015. The microbial impact on the sorption behaviour of selenite in an acidic, nutrient-poor boreal bog. J. Environ. Radioact. 147, 85–96. https://doi.org/10.1016/j.jenvrad.2015.05.014

-M-

Maes, N., Bruggeman, C., 2010. Behaviour of Selenium in Boom Clay. ref: CCHO2004/00/00 DS251eA44/2.1. External Report of the Belgian Nuclear Research Centre. SCK CEN-ER-120.
Mareschal, L., Bonnaud, P., Turpault, M.P., Ranger, J., 2010. Impact of common European tree species on the chemical and physicochemical properties of fine earth: an unusual pattern. EJSS 61, 14–23. https://doi.org/10.1111/j.1365-2389.2009.01206.x
Martens, D. A., Suarez, D.L., 1997. Mineralization of selenium-containing amino acids in two California soils. SSSA (USA).
Martens, Dean A., Suarez, D.L., 1997. Selenium Speciation of Soil/Sediment Determined with Sequential Extractions and Hydride Generation Atomic Absorption Spectrophotometry. Environ. Sci. Technol. 31, 133–139. https://doi.org/10.1021/es960214+
Martin, D.P., Seiter, J.M., Lafferty, B.J., Bednar, A.J., 2017. Exploring the ability of cations to facilitate binding between inorganic oxyanions and humic acid. Chemosphere 166, 192–196. https://doi.org/10.1016/j.chemosphere.2016.09.084
Martínez, M., Giménez, J., de Pablo, J., Rovira, M., Duro, L., 2006. Sorption of selenium(IV) and selenium(VI) onto magnetite. Appl. Surf. Sci. 252, 3767–3773. https://doi.org/10.1016/j.apsusc.2005.05.067
Mason, R.P., Soerensen, A.L., DiMento, B.P., Balcom, P.H., 2018. The global marine selenium cycle: insights from measurements and modeling. Global Biogeochem. Cycles 32, 1720–1737. https://doi.org/10.1029/2018GB006029
May Thomas W., Wiedmeyer Ray H., 1998. A table of polyatomic interferences in ICP-MS. At. Spectrosc. 19, 150–155.
Medrano-Macías, J., Leija-Martínez, P., González-Morales, S., Juárez-Maldonado, A., Benavides-Mendoza, A., 2016. Use of Iodine to Biofortify and Promote Growth and Stress Tolerance in Crops. Front. Plant. Sci. 7, 1146. https://doi.org/10.3389/fpls.2016.01146
Meija, J., Coplen, T.B., Berglund, M., Brand, W.A., De Bièvre, P., Gröning, M., Holden, N.E., Irrgeher, J., Loss, R.D., Walczyk, T., Prohaska, T., 2016. Isotopic compositions of the elements 2013 (IUPAC Technical Report). Pure Appl. Chem. https://doi.org/10.1515/pac-2015-0503
Mello, P.A., Barin, J.S., Duarte, F.A., Bizzi, C.A., Diehl, L.O., Muller, E.I., Flores, E.M.M., 2013. Analytical methods for the determination of halogens in bioanalytical sciences: a review. Anal. Bioanal. Chem. 405, 7615–7642. https://doi.org/10.1007/s00216-013-7077-9
Michel, R., Handl, J., Ernst, T., Botsch, W., Szidat, S., Schmidt, A., Jakob, D., Beltz, D., Romantschuk, L.D., Synal, H.-A., Schnabel, C., López-Gutiérrez, J.M., 2005. Iodine-129 in soils from Northern Ukraine and the retrospective dosimetry of the iodine-131 exposure after the Chernobyl accident. Sci Total Environ 340, 35–55. https://doi.org/10.1016/j.scitotenv.2004.08.006
Miyake, Y., Matsuzaki, H., Fujiwara, T., Saito, T., Yamagata, T., Honda, M., Muramatsu, Y., 2012. Isotopic ratio of radioactive iodine (129I/131I) released from Fukushima Daiichi NPP accident. Geochemical Journal 46, 327–333. https://doi.org/10.2343/geochemj.2.0210
Monte, L., Periañez, R., Kivva, S., Laptev, G., Angeli, G., Barros, H., Zheleznyak, M., 2006. Assessment of state-of-the-art models for predicting the remobilisation of radionuclides following the flooding of heavily contaminated areas: the case of Pripyat River floodplain. J. Environ. Radioact. 88, 267–288. https://doi.org/10.1016/j.jenvrad.2006.02.006
Montelius, M., Thiry, Y., Marang, L., Ranger, J., Cornelis, J.-T., Svensson, T., Bastviken, D., 2015. Experimental evidence of large changes in terrestrial chlorine cycling following

altered tree species composition. Environ. Sci. Technol. 49, 4921–4928. https://doi.org/10.1021/acs.est.5b00137
Moore, R. M., Groszko, M., 1999. Methyl iodide distribution in the ocean and fluxes to the atmosphere. J. Geophys. Res. Atmos. 50, 11163–11172.
Moreda-Piñeiro, A., Romarís-Hortas, V., Bermejo-Barrera, P., 2011a. A review on iodine speciation for environmental, biological and nutrition fields. J. Anal. At. Spectrom. 26, 2107–2152. https://doi.org/10.1039/C0JA00272K
Moreda-Piñeiro, A., Romarís-Hortas, V., Bermejo-Barrera, P., 2011b. A review on iodine speciation for environmental, biological and nutrition fields. J. Anal. At. Spectrom. 26, 2107–2152. https://doi.org/10.1039/C0JA00272K
Muramatsu, Y., Yoshida, S., Fehn, U., Amachi, S., Ohmomo, Y., 2004. Studies with natural and anthropogenic iodine isotopes: iodine distribution and cycling in the global environment. J. Environ. Radioact. 74, 221–232. https://doi.org/10.1016/j.jenvrad.2004.01.011

-N-

Nancharaiah, Y.V., Lens, P.N.L., 2015. Ecology and Biotechnology of Selenium-Respiring Bacteria. Microbiol. Mol. Biol. Rev. 79, 61–80. https://doi.org/10.1128/MMBR.00037-14

-O-

Oba, Y., Futagami, T., Amachi, S., 2014. Enrichment of a microbial consortium capable of reductive deiodination of 2,4,6-triiodophenol. J. Biosci. Bioeng. 117, 310–317. https://doi.org/10.1016/j.jbiosc.2013.08.011
Ohno, T., Muramatsu, Y., Toyama, C., Nakano, K., Kakuta, S., Matsuzaki, H., 2013. Determination of 129I in Fukushima soil samples by ICP-MS with an octopole reaction system. Anal. Sci. 29, 271–274.
Osono, T., Takeda, H., 2005. Limit values for decomposition and convergence process of lignocellulose fraction in decomposing leaf litter of 14 tree species in a cool temperate forest. Ecol. Res. 20, 51–58. https://doi.org/10.1007/s11284-004-0011-z
Otto, A., Simpson, M.J., 2006. Evaluation of CuO oxidation parameters for determining the source and stage of lignin degradation in soil. Biogeochemistry 80, 121–142. https://doi.org/10.1007/s10533-006-9014-x

-P-

Pace, R., Grote, R., 2020. Deposition and Resuspension Mechanisms Into and From Tree Canopies: A Study Modeling Particle Removal of Conifers and Broadleaves in Different Cities. Front. For. Glob. Change 3. https://doi.org/10.3389/ffgc.2020.00026
Paikaray, S., 2016. Origin, Mobilization and Distribution of Selenium in a Soil/Water/Air System: A Global Perspective With Special Reference to the Indian Scenario. CLEAN – Soil, Air, Water 44, 474–487. https://doi.org/10.1002/clen.201300454
Park, C.-K., Park, T.-J., Lee, S.-Y., Lee, J.-K., 2019. Sorption characteristics of iodide on chalcocite and mackinawite under pH variations in alkaline conditions. NET 51, 1041–1046. https://doi.org/10.1016/j.net.2019.01.014
Pathak, P., Singh, D. n., Pandit, G. g., Rakesh, R. r., 2014. Determination of distribution coefficient: a critical review. Int. J. Environ. Waste Manag. 14, 27–64. https://doi.org/10.1504/IJEWM.2014.062980
Pauget, B., Gimbert, F., Coeurdassier, M., Crini, N., Pérès, G., Faure, O., Douay, F., Hitmi, A., Beguiristain, T., Alaphilippe, A., Guernion, M., Houot, S., Legras, M., Vian, J.-F., Hedde, M., Bispo, A., Grand, C., de Vaufleury, A., 2013. Ranking field site

management priorities according to their metal transfer to snails. Ecol. Indic. 29, 445–454. https://doi.org/10.1016/j.ecolind.2013.01.012
Peak, D., 2006. Adsorption mechanisms of selenium oxyanions at the aluminum oxide/water interface. J. Colloid Interface Sci. 303, 337–345. https://doi.org/10.1016/j.jcis.2006.08.014
Peel, H.R., Martin, D.P., Bednar, A.J., 2017. Extraction and characterization of ternary complexes between natural organic matter, cations, and oxyanions from a natural soil. Chemosphere 176, 125–130. https://doi.org/10.1016/j.chemosphere.2017.02.101
Pisarek, P., Bueno, M., Thiry, Y., Nicolas, M., Gallard, H., Hécho, I.L., 2021. Selenium distribution in French forests: influence of environmental conditions. Sci. Total Environ. 144962. https://doi.org/10.1016/j.scitotenv.2021.144962
Ponce de León, C.A., DeNicola, K., Montes Bayón, M., Caruso, J.A., 2003. Sequential extractions of selenium soils from Stewart Lake: total selenium and speciation measurements with ICP-MS detection. J. Environ. Monit. 5, 435–440.
Prescott, C.E., Grayston, S.J., 2013. Tree species influence on microbial communities in litter and soil: Current knowledge and research needs. For. Ecol. Manag., Influence of tree species on forest soils: New evidence from field studies 309, 19–27. https://doi.org/10.1016/j.foreco.2013.02.034
Prescott, C.E., Zabek, L.M., Staley, C.L., Kabzems, R., 2000. Decomposition of broadleaf and needle litter in forests of British Columbia: influences of litter type, forest type, and litter mixtures. Can. J. For. Res. 30, 1742–1750. https://doi.org/10.1139/x00-097
Probst A., Hernandez L., Fevrier-Vauleon C., Prudent P., Probst J., Party J., 2003. Eléments traces métalliques dans les sols des écosystèmes forestiers français: distribution et facteurs de contrôle -utilisation du réseau RENECOFOR. Office National des Forêts, Direction Technique.

-Q-

Qiao, J., Hansen, V., Hou, X., Aldahan, A., Possnert, G., 2012. Speciation analysis of 129I, 137Cs, 232Th, 238U, 239Pu and 240Pu in environmental soil and sediment. Appl. Radiat. Isot. 70, 1698–1708. https://doi.org/10.1016/j.apradiso.2012.04.006
Qin, H., Zhu, J., Su, H., 2012. Selenium fractions in organic matter from Se-rich soils and weathered stone coal in selenosis areas of China. Chemosphere 86, 626–633. https://doi.org/10.1016/j.chemosphere.2011.10.055
Quantin, P., 2004. Volcanic soils of France. CATENA, Volcanic Soil Resources: Occurrence, Development and Properties 56, 95–109. https://doi.org/10.1016/j.catena.2003.10.019

-R-

R Core Team, 2013. R: A Language and Environment for Statistical Computing. R Foundation for Statistical Computing, Vienna, Austria
Raisbeck, G.M., Yiou, F., 1999. 129I in the oceans: origins and applications. Sci. Total Environ. 237–238, 31–41.
Ranger, J., Colin-Belgrand, M., 1996. Nutrient dynamics of chestnut tree (Castanea sativa Mill.) coppice stands. For. Ecol. Manag. 86, 259–277. https://doi.org/10.1016/S0378-1127(96)03733-4
Rawlins, B G, McGrath, S. P., Scheib, A. J., Breward, N., Cave, M., Lister, T. R., Ingham, M., Gowing, C., Carter, S., 2012. The Advanced Soil Geochemical Atlas of England and Wales. Nottingham: British Geological Survey.
Rayman, M.P., 2000. The importance of selenium to human health. Lancet 356, 233–241. https://doi.org/10.1016/S0140-6736(00)02490-9

Redon, P.-O., Jolivet, C., Saby, N.P.A., Abdelouas, A., Thiry, Y., 2013. Occurrence of natural organic chlorine in soils for different land uses. Biogeochemistry 114, 413–419. https://doi.org/10.1007/s10533-012-9771-7

Redon, P.-O., Abdelouas, A., Bastviken, D., Cecchini, S., Nicolas, M., Thiry, Y., 2011. Chloride and organic chlorine in forest soils: storage, residence times, and influence of ecological conditions. Environ. Sci. Technol. 45, 7202–7208. https://doi.org/10.1021/es2011918

Reimann, C., Englmaier, P., Fabian, K., Gough, L., Lamothe, P., Smith, D., 2015. Biogeochemical plant–soil interaction: Variable element composition in leaves of four plant species collected along a south–north transect at the southern tip of Norway. Sci. Total Environ. 506–507, 480–495. https://doi.org/10.1016/j.scitotenv.2014.10.079

Rennert, T., 2019. Wet-chemical extractions to characterise pedogenic Al and Fe species – a critical review. Soil Res. 57, 1–16. https://doi.org/10.1071/SR18299

Ross, H.B., 1985. An atmospheric selenium budget for the region 30° N to 90° N. Tellus B: Chem. Phys. Meteorol. 37, 78–90. https://doi.org/10.3402/tellusb.v37i2.14999

Roulier, M., 2018. Cycle biogéochimique de l'iode en écosystèmes forestiers (thesis). http://www.theses.fr. Pau.

Roulier, M., Bueno, M., Coppin, F., Nicolas, M., Thiry, Y., Rigal, F., Le Hécho, I., Pannier, F., 2021a. Atmospheric iodine, selenium and caesium depositions in France: I. Spatial and seasonal variations. Chemosphere 273, 128971. https://doi.org/10.1016/j.chemosphere.2020.128971

Roulier, M., Bueno, M., Coppin, F., Nicolas, M., Thiry, Y., Rigal, F., Pannier, F., Le Hécho, I., 2021b. Atmospheric iodine, selenium and caesium depositions in France: II. Influence of forest canopies. Chemosphere 273, 128952. https://doi.org/10.1016/j.chemosphere.2020.128952

Roulier, M., Bueno, M., Thiry, Y., Coppin, F., Redon, P.-O., Le Hécho, I., Pannier, F., 2018. Iodine distribution and cycling in a beech (Fagus sylvatica) temperate forest. Sci. Total Environ. 645, 431–440. https://doi.org/10.1016/j.scitotenv.2018.07.039

Roulier, M., Coppin, F., Bueno, M., Nicolas, M., Thiry, Y., Della Vedova, C., Février, L., Pannier, F., Le Hécho, I., 2019. Iodine budget in forest soils: Influence of environmental conditions and soil physicochemical properties. Chemosphere 224, 20–28. https://doi.org/10.1016/j.chemosphere.2019.02.060

Rumpel, C., Dignac, M.-F., 2006. Gas chromatographic analysis of monosaccharides in a forest soil profile: Analysis by gas chromatography after trifluoroacetic acid hydrolysis and reduction–acetylation. Soil Biology and Biochemistry 38, 1478–1481. https://doi.org/10.1016/j.soilbio.2005.09.017

Ruszczyńska, A., Konopka, A., Kurek, E., Torres Elguera, J.C., Bulska, E., 2017. Investigation of biotransformation of selenium in plants using spectrometric methods. Spectrochim. Acta: At. Spectrosc.130, 7–16. https://doi.org/10.1016/j.sab.2017.02.004

-S-

Saeki, K., Matsumoto, S., 1994. Selenite adsorption by a variety of oxides. Soil. Sci. Plant Anal. 25, 2147–2158. https://doi.org/10.1080/00103629409369178

Saikat, S.Q., Carter, J.E., Mehra, A., Smith, B., Stewart, A., 2004. Goitre and environmental iodine deficiency in the UK--Derbyshire: a review. Environ Geochem Health 26, 395–401. https://doi.org/10.1007/s10653-005-7165-7

Scheinost, A.C., Kirsch, R., Banerjee, D., Fernandez-Martinez, A., Zaenker, H., Funke, H., Charlet, L., 2008. X-ray absorption and photoelectron spectroscopy investigation of selenite reduction by FeII-bearing minerals. Journal of Contaminant Hydrology,

Radiogeochemical Aspects of Nuclear Waste Disposal 102, 228–245. https://doi.org/10.1016/j.jconhyd.2008.09.018
Schmitz, K., Aumann, D.C., 1995. A study on the association of two iodine isotopes, of natural127I and of the fission product129I, with soil components using a sequential extraction procedure. Journal of Radioanalytical and Nuclear Chemistry, Articles 198, 229–236. https://doi.org/10.1007/BF02038260
Séby, F., Potin-Gautier, M., Giffaut, E., Borge, G., Donard, O.F.X., 2001. A critical review of thermodynamic data for selenium species at 25°C. Chemical Geology 171, 173–194. https://doi.org/10.1016/S0009-2541(00)00246-1
Seiler, J., Matzner, E., 1995. Spatial variability of throughfall chemistry and selected soil properties as influenced by stem distance in a mature Norway spruce (Picea abies, Karst.) stand. Plant Soil 176, 139–147. https://doi.org/10.1007/BF00017684
Shah, M., Wuilloud, R.G., Kannamkumarath, S.S., Caruso, J.A., 2005. Iodine speciation studies in commercially available seaweed by coupling different chromatographic techniques with UV and ICP-MS detection. J. Anal. At. Spectrom. 20, 176–182. https://doi.org/10.1039/B415756G
Shahid, N., Shahid, M., Niazi, N.K., Khalid, S., Murtaza, B., Bibi, I., Rashid, M.I., 2018. A critical review of selenium biogeochemical behavior in soil-plant system with an inference to human health. Environ. Pollut. 234, 915–934. https://doi.org/10.1016/j.envpol.2017.12.019
Shand, C.A., Balsam, M., Hillier, S.J., Hudson, G., Newman, G., Arthur, J.R., Nicol, F., 2010. Aqua regia extractable selenium concentrations of some Scottish topsoils measured by ICP-MS and the relationship with mineral and organic soil components. J. Sci. Food Agric. 90, 972–980. https://doi.org/10.1002/jsfa.3905
Sharma, V.K., McDonald, T.J., Sohn, M., Anquandah, G.A.K., Pettine, M., Zboril, R., 2015. Biogeochemistry of selenium. A review. Environ Chem Lett 13, 49–58. https://doi.org/10.1007/s10311-014-0487-x
Shaw, G., 2007. Radionuclides in forest ecosystems, in: Shaw, G. (Ed.), Radioactivity in the Environment, Radioactivity in the Terrestrial Environment. Elsevier, pp. 127–155. https://doi.org/10.1016/S1569-4860(06)10006-6
Shcheglov, A.I., Tsvetnova, O.B., 2001. Biogeochemical migration of technogenic radionuclides in forest ecosystems: by the materials of a multiyear study in the areas severely contaminated due to the Chernobyl accident. Nauka.
Sheppard, S., Long, J., Sanipelli, B., Sohlenius, G., 2009. Solid/liquid partition coefficients (Kd) for selected soils and sediments at Forsmark and Laxemar-Simpevarp (No. SKB-R--09-27). Swedish Nuclear Fuel and Waste Management Co.
Sherrard, J.C., Hunter, K.A., Boyd, P.W., 2004. Selenium speciation in subantarctic and subtropical waters east of New Zealand: trends and temporal variations. Deep Sea Research Part I: Oceanogr. Res. Pap. 51, 491–506. https://doi.org/10.1016/j.dsr.2003.11.001
Sheppard, M. I., Thibault, D. H., Smith, P. A., Hawkins, J. L., 1994. Volatilization: a soil degassing coefficient for iodine. J. Environ. Radioact. 25, 189–203. https://doi.org/10.1016/0265-931X(94)90072-8
Shetaya, W.H., Young, S.D., Watts, M.J., Ander, E.L., Bailey, E.H., 2012. Iodine dynamics in soils. Geochim. Cosmochim. Acta 77, 457–473. https://doi.org/10.1016/j.gca.2011.10.034
Shimamoto, Y.S., Takahashi, Y., Terada, Y., 2011. Formation of organic iodine supplied as iodide in a soil-water system in Chiba, Japan. Environ. Sci. Technol. 45, 2086–2092. https://doi.org/10.1021/es1032162

Sive, B.C., Varner, R.K., Mao, H., Blake, D.R., Wingenter, O.W., Talbot, R., 2007. A large terrestrial source of methyl iodide. Geophysical Research Letters 34. https://doi.org/10.1029/2007GL030528

Sloth, J.J., Larsen, E.H., 2000. The application of inductively coupled plasma dynamic reaction cell mass spectrometry for measurement of selenium isotopes, isotope ratios and chromatographic detection of selenoamino acids. J. Anal. At. Spectrom. 15, 669–672. https://doi.org/10.1039/B001798L

Söderlund, M., Virkanen, J., Aromaa, H., Gracheva, N., Lehto, J., 2017. Sorption and speciation of iodine in boreal forest soil. J Radioanal Nucl Chem 311, 549–564. https://doi.org/10.1007/s10967-016-5022-z

Söderlund, M., Virkanen, J., Holgersson, S., Lehto, J., 2016. Sorption and speciation of selenium in boreal forest soil. J Environ Radioact 164, 220–231. https://doi.org/10.1016/j.jenvrad.2016.08.006

Sposito, G., 2008. The Chemistry of Soils. Oxford University Press, USA.

Stable isotopes [WWW Document], 2016. URL https://www.iaea.org/topics/nuclear-science/isotopes/stable-isotopes (accessed 9.3.19).

Steinberg, S.M., Kimble, G.M., Schmett, G.T., Emerson, D.W., Turner, M.F., Rudin, M., 2008. Abiotic reaction of iodate with sphagnum peat and other natural organic matter. J Radioanal Nucl Chem 277, 185–191. https://doi.org/10.1007/s10967-008-0728-1

Stone, C.A., Kawai, K., Kupka, R., Fawzi, W.W., 2010. Role of selenium in HIV infection. Nutrition Reviews 68, 671–681. https://doi.org/10.1111/j.1753-4887.2010.00337.x

Stork, A., Jury, W.A., Frankenberger, W.T., 1999. Accelerated volatilization rates of selenium from different soils. Biol Trace Elem Res 69, 217–234. https://doi.org/10.1007/BF02783874

Stroud, J.L., McGrath, S.P., Zhao, F.-J., 2012. Selenium speciation in soil extracts using LC-ICP-MS. J. Environ. Anal. Chem. 92, 222–236. https://doi.org/10.1080/03067310903111661

Suess, E., Aemisegger, F., Sonke, J.E., Sprenger, M., Wernli, H., Winkel, L.H.E., 2019. Marine versus Continental Sources of Iodine and Selenium in Rainfall at Two European High-Altitude Locations. Environ Sci Technol 53, 1905–1917. https://doi.org/10.1021/acs.est.8b05533

Sun, J., Yang, R., Zhu, J., Pan, Y., Yang, M., Zhang, Z., 2019. Can the increase of irrigation frequency improve the rate of water and salt migration in biochar-amended saline soil? J Soils Sediments. https://doi.org/10.1007/s11368-019-02357-9

Sun, G.-X., Meharg, A.A., Li, G., Chen, Z., Yang, L., Chen, S.-C., Zhu, Y.-G., 2016. Distribution of soil selenium in China is potentially controlled by deposition and volatilization? Scientific Reports 6. https://doi.org/10.1038/srep20953

Supriatin, S., Weng, L., Comans, R.N.J., 2015. Selenium speciation and extractability in Dutch agricultural soils. Sci. Total Environ. 532, 368–382. https://doi.org/10.1016/j.scitotenv.2015.06.005

-T-

Takeda, A., Tsukada, H., Takahashi, M., Takaku, Y., Hisamatsu, S., 2015. Changes in the chemical form of exogenous iodine in forest soils and their extracts. Radiat. Prot. Dosim. 167, 181–186. https://doi.org/10.1093/rpd/ncv240

Takeda, A., Unno, Y., Tsukada, H., Takaku, Y., Hisamatsu, S., 2019. Speciation of iodine in soil solution in forest and grassland soils in Rokkasho, Japan. Radiat. Prot. Dosim. 184, 368–371. https://doi.org/10.1093/rpd/ncz103

Tanaka, T., Thiry, Y., 2020. Assessing the recycling of chlorine and its long-lived 36Cl isotope in terrestrial ecosystems through dynamic modeling. Sci. Total Environ. 700, 134482. https://doi.org/10.1016/j.scitotenv.2019.134482

Tamm, O., 1922. Um best ämning ow de oorganiska komponenterna i markens gelcomplex. Medd. Statens Skogsförsökanst 19, 385–404.

Taylor, S.R., McLennan, S.M., 1995. The geochemical evolution of the continental crust. Reviews of Geophysics 33, 241–265. https://doi.org/10.1029/95RG00262

Terry, N., Zayed, A.M., De Souza, M.P., Tarun, A.S., 2000. Selenium in higher plants. Annu. Rev. Plant Physiol. Plant Mol. Biol. 51, 401–432. https://doi.org/10.1146/annurev.arplant.51.1.401

Tessier, A., Campbell, P.G.C., Bisson, M., 1979. Sequential extraction procedure for the speciation of particulate trace metals. Anal. Chem. 51, 844–851. https://doi.org/10.1021/ac50043a017

Thiry, Y., Schmidt, P., Van Hees, M., Wannijn, J., Van Bree, P., Rufyikiri, G., Vandenhove, H., 2005. Uranium distribution and cycling in Scots pine (Pinus sylvestris L.) growing on a revegetated U-mining heap. J. Environ. Radioact., 81, 201–219. https://doi.org/10.1016/j.jenvrad.2004.01.036

Thiry, Y., Albrecht, A., Tanaka, T., 2018. Development and assessment of a simple ecological model (TRIPS) for forests contaminated by radiocesium fallout. J. Environ. Radioact. 190–191, 149–159. https://doi.org/10.1016/j.jenvrad.2018.05.009

Tolu, J., 2012. Spéciation et mobilité du sélénium présent dans les sols à l'état de traces : contribution aux prévisions à long terme (thesis). Pau.

Tolu, J., Le Hécho, I., Bueno, M., Thiry, Y., Potin-Gautier, M., 2011. Selenium speciation analysis at trace level in soils. Anal. Chim. Acta 684, 126–133. https://doi.org/10.1016/j.aca.2010.10.044

Tolu, J., Thiry, Y., Bueno, M., Jolivet, C., Potin-Gautier, M., Le Hécho, I., 2014. Distribution and speciation of ambient selenium in contrasted soils, from mineral to organic rich. Sci. Total Environ. 479–480, 93–101. https://doi.org/10.1016/j.scitotenv.2014.01.079

Torres, J., Pintos, V., Domínguez, S., Kremer, C., Kremer, E., 2010. Selenite and Selenate Speciation in Natural Waters: Interaction with Divalent Metal Ions. J Solution Chem 39, 1–10. https://doi.org/10.1007/s10953-009-9491-3

Tschiersch, J., Shinonaga, T., Heuberger, H., 2009. Dry deposition of gaseous radioiodine and particulate radiocaesium onto leafy vegetables. Sci. Total Environ. 407, 5685–5693. https://doi.org/10.1016/j.scitotenv.2009.06.025

Tsukada, H., Takeda, A., Tagami, K., Uchida, S., 2008. Uptake and Distribution of Iodine in Rice Plants. Journal of Environmental Quality 37, 2243–2247. https://doi.org/10.2134/jeq2008.0010

Tuttle, M.L.W., Fahy, J.W., Elliott, J.G., Grauch, R.I., Stillings, L.L., 2014. Contaminants from Cretaceous black shale: I. Natural weathering processes controlling contaminant cycling in Mancos Shale, southwestern United States, with emphasis on salinity and selenium. Appl. Geochem. 46, 57–71. https://doi.org/10.1016/j.apgeochem.2013.12.010

Tyler, G., 2005. Changes in the concentrations of major, minor and rare-earth elements during leaf senescence and decomposition in a Fagus sylvatica forest. For. Ecol. Manag. 206, 167–177. https://doi.org/10.1016/j.foreco.2004.10.065

-U-

Ukonmaanaho, L., Merilä, P., Nöjd, P., Nieminen, T., 2008. Litterfall production and nutrient return to the forest floor in Scots pine and Norway spruce stands in Finland. Boreal Environ. Res. 13, 67–91.

Unit, W.H.O.N., 1996. Recommended iodine levels in salt and guidelines for monitoring their adequacy and effectiveness.

Unno, Y., Tsukada, H., Takeda, A., Takaku, Y., Hisamatsu, S., 2017. Soil-soil solution distribution coefficient of soil organic matter is a key factor for that of radioiodide in surface and subsurface soils. J. Environ. Radioact. 169–170, 131–136. https://doi.org/10.1016/j.jenvrad.2017.01.016

Ulrich, B., 1983. Interaction of forest canopies with atmospheric constituents SO_2, alkali and earth alkali cations and chloride," In B. Ulrich and J. Pankrath, Eds., Effect of accumulation of air pollutants in forest ecosystems, D. Reidel Publishers, Dordrecht, 330-345

Ulrich, E., Coddeville, P., Lanier, M., 2002. Retombées atmosphériques humides en France entre 1993 et 1998. ADEME, Paris.

-V-

Valdez Barillas, J.R., Quinn, C.F., Pilon-Smits, E.A.H., 2011. Selenium accumulation in plants--phytotechnological applications and ecological implications. Int J Phytoremediation 13 Suppl 1, 166–178. https://doi.org/10.1080/15226514.2011.568542

Velinsky, D.J., Cutter, G.A., 1990. Determination of elemental selenium and pyrite-selenium in sediments. Anal. Chim. Acta 235, 419–425. https://doi.org/10.1016/S0003-2670(00)82102-9

Vergutz, L., Manzoni, S., Porporato, A., Novais, R.F., Jackson, R.B., 2012. Global resorption efficiencies and concentrations of carbon and nutrients in leaves of terrestrial plants. Ecol. Monogr. 82, 205–220. https://doi.org/10.1890/11-0416.1

Vives i Batlle, J., Vandenhove, H., Gielen, S., 2014. Modelling water and ^{36}Cl cycling in a Belgian pine forest - Model for ^{36}Cl cycling in a Belgian pine forest.

Vriens, B., Lenz, M., Charlet, L., Berg, M., Winkel, L.H.E., 2014. Natural wetland emissions of methylated trace elements. Nat Commun 5, 3035. https://doi.org/10.1038/ncomms4035

Vriens, B., Ammann, A.A., Hagendorfer, H., Lenz, M., Berg, M., Winkel, L.H.E., 2014b. Quantification of Methylated Selenium, Sulfur, and Arsenic in the Environment. PLOS ONE 9, e102906. https://doi.org/10.1371/journal.pone.0102906

-W-

Wang, S., Liang, D., Wang, D., Wei, W., Fu, D., Lin, Z., 2012. Selenium fractionation and speciation in agriculture soils and accumulation in corn (Zea mays L.) under field conditions in Shaanxi Province, China. Sci. Total Environ. 427–428, 159–164. https://doi.org/10.1016/j.scitotenv.2012.03.091

Watts, M.J., Joy, E.J.M., Young, S.D., Broadley, M.R., Chilimba, A.D.C., Gibson, R.S., Siyame, E.W.P., Kalimbira, A.A., Chilima, B., Ander, E.L., 2015. Iodine source apportionment in the Malawian diet. Sci. Rep. 5, 15251. https://doi.org/10.1038/srep15251

Watts, M.J., Mitchell, C.J., 2009. A pilot study on iodine in soils of Greater Kabul and Nangarhar provinces of Afghanistan. Environ. Geochem. Health 31, 503–509. https://doi.org/10.1007/s10653-008-9202-9

Watts, M.J., Mitchell, C.J., 2008. A pilot study on iodine in soils of Greater Kabul and Nangarhar provinces of Afghanistan. Environ Geochem Health 31, 503. https://doi.org/10.1007/s10653-008-9202-9

Wen, H., Carignan, J., 2007. Reviews on atmospheric selenium: Emissions, speciation and fate. Atmospheric Environment 41, 7151–7165. https://doi.org/10.1016/j.atmosenv.2007.07.035

Weng, L., Vega, F.A., Supriatin, S., Bussink, W., Riemsdijk, W.H.V., 2011. Speciation of Se and DOC in Soil Solution and Their Relation to Se Bioavailability. Environ. Sci. Technol. 45, 262–267. https://doi.org/10.1021/es1016119

Wessjohann, L.A., Schneider, A., Abbas, M., Brandt, W., 2007. Selenium in chemistry and biochemistry in comparison to sulfur. Biol. Chem. 388, 997–1006. https://doi.org/10.1515/BC.2007.138

Whicker, J.J., Pinder, J.E., Ibrahim, S.A., Stone, J.M., Breshears, D.D., Baker, K.N., 2007. Uranium partition coefficients (Kd) in forest surface soil reveal long equilibrium times and vary by site and soil size fraction. Health Phys 93, 36–46. https://doi.org/10.1097/01.HP.0000258924.55225.cd

White, P.J., 2016. Selenium accumulation by plants. Annals of Botany 117, 217–235. https://doi.org/10.1093/aob/mcv180

Winkel, L.H.E., Vriens, B., Jones, G.D., Schneider, L.S., Pilon-Smits, E., Bañuelos, G.S., 2015. Selenium Cycling Across Soil-Plant-Atmosphere Interfaces: A Critical Review. Nutrients 7, 4199–4239. https://doi.org/10.3390/nu7064199

Wu, T.-J., Chiu, H.-Y., Yu, J., Cautela, M.P., Sarmento, B., das Neves, J., Catala, C., Pazos-Perez, N., Guerrini, L., Alvarez-Puebla, R.A., Vranješ-Đurić, S., Ignjatović, N.L., 2018. Chapter 1 - Nanotechnologies for early diagnosis, in situ disease monitoring, and prevention, in: Uskoković, V., Uskoković, D.P. (Eds.), Nanotechnologies in Preventive and Regenerative Medicine, Micro and Nano Technologies. Elsevier, pp. 1–92. https://doi.org/10.1016/B978-0-323-48063-5.00001-0

-X-

Xu, C., Chen, H., Sugiyama, Y., Zhang, S., Li, H.-P., Ho, Y.-F., Chuang, C., Schwehr, K.A., Kaplan, D.I., Yeager, C., Roberts, K.A., Hatcher, P.G., Santschi, P.H., 2013. Novel molecular-level evidence of iodine binding to natural organic matter from Fourier transform ion cyclotron resonance mass spectrometry. Sci. Total Environ. 449, 244–252. https://doi.org/10.1016/j.scitotenv.2013.01.064

Xu, C., Miller, E.J., Zhang, S., Li, H.-P., Ho, Y.-F., Schwehr, K.A., Kaplan, D.I., Otosaka, S., Roberts, K.A., Brinkmeyer, R., Yeager, C.M., Santschi, P.H., 2011. Sequestration and remobilization of radioiodine (129I) by soil organic matter and possible consequences of the remedial action at Savannah River Site. Environ. Sci. Technol. 45, 9975–9983. https://doi.org/10.1021/es201343d

Xu, C., Zhang, S., Sugiyama, Y., Ohte, N., Ho, Y.-F., Fujitake, N., Kaplan, D.I., Yeager, C.M., Schwehr, K., Santschi, P.H., 2016. Role of natural organic matter on iodine and 239,240Pu distribution and mobility in environmental samples from the northwestern Fukushima Prefecture, Japan. J. Environ. Radioact. 153, 156–166. https://doi.org/10.1016/j.jenvrad.2015.12.022

Xu, C., Zhong, J., Hatcher, P.G., Zhang, S., Li, H.-P., Ho, Y.-F., Schwehr, K.A., Kaplan, D.I., Roberts, K.A., Brinkmeyer, R., Yeager, C.M., Santschi, P.H., 2012. Molecular environment of stable iodine and radioiodine (129I) in natural organic matter: Evidence inferred from NMR and binding experiments at environmentally relevant concentrations. Geochim. Cosmochim. Acta 97, 166–182. https://doi.org/10.1016/j.gca.2012.08.030

-Y-

Yamada, H., Hisamori, I., Yonebayashi, K., 2002. Identification of organically bound iodine in soil humic substances by size exclusion chromatography / inductively coupled plasma mass spectrometry (SEC / ICP-MS). Soil Sci. Plant Nutr. 48, 379–385. https://doi.org/10.1080/00380768.2002.10409215

Yamada, H., Kiriyama, T., Yonebayashi, K., 1996. Determination of Total Iodine in Soils by Inductively Coupled Plasma Mass Spectrometry. Soil Sci. Plant Nutr.42, 859–866. https://doi.org/10.1080/00380768.1996.10416633

Yamaguchi, N., Nakano, M., Takamatsu, R., Tanida, H., 2010. Inorganic iodine incorporation into soil organic matter: evidence from iodine K-edge X-ray absorption near-edge structure. J. Environ. Radioact. 101, 451–457. https://doi.org/10.1016/j.jenvrad.2008.06.003

Yeager, C.M., Amachi, S., Grandbois, R., Kaplan, D.I., Xu, C., Schwehr, K.A., Santschi, P.H., 2017. Chapter Three - Microbial Transformation of Iodine: From Radioisotopes to Iodine Deficiency, in: Sariaslani, S., Gadd, G.M. (Eds.), Adv. Appl.Microbiol. Academic Press, pp. 83–136. https://doi.org/10.1016/bs.aambs.2017.07.002

Younes, K., Laduranty, J., Descostes, M., Grasset, L., 2017a. Molecular biomarkers study of an ombrotrophic peatland impacted by an anthropogenic clay deposit. Organic Geochemistry 105, 20–32. https://doi.org/10.1016/j.orggeochem.2016.12.005

Yuita, K., Kihou, N., 2005. Behavior of Iodine in a Forest Plot, an Upland Field, and a Paddy Field in the Upland Area of Tsukuba, Japan: Vertical Distribution of Iodine in Soil Horizons and Layers to a Depth of 50 m. Soil Sci. Plant Nutr. 51, 455–467. https://doi.org/10.1111/j.1747-0765.2005.tb00053.x

-Z-

Zanella, A., Ponge, J.-F., de Waal, R., Ferronato, C., De Nobili, M., Juilleret, J., 2018. Humusica 1, article 3: Essential bases – Quick look at the classification. Applied Soil Ecology, HUMUSICA 1 - Terrestrial Natural Humipedons 122, 42–55. https://doi.org/10.1016/j.apsoil.2017.05.025

Zhang, Y., Moore, J.N., 1996. Selenium Fractionation and Speciation in a Wetland System. Environ. Sci. Technol. 30, 2613–2619. https://doi.org/10.1021/es960046l

Zhao, X., Hou, X., Zhou, W., 2019. Atmospheric Iodine (127I and 129I) Record in Spruce Tree Rings in the Northeast Qinghai-Tibet Plateau. Environ. Sci. Technol. 53, 8706–8714. https://doi.org/10.1021/acs.est.9b01160

Zhao, X.Q., Mitani, N., Yamaji, N., Shen, R.F., Ma, J.F., 2010. Involvement of Silicon Influx Transporter OsNIP2;1 in Selenite Uptake in Rice. Plant Physiology 153, 1871–1877. https://doi.org/10.1104/pp.110.157867

Zheng, J., Takata, H., Tagami, K., Aono, T., Fujita, K., Uchida, S., 2012. Rapid determination of total iodine in Japanese coastal seawater using SF-ICP-MS. Microchemical Journal 100, 42–47. https://doi.org/10.1016/j.microc.2011.08.007

Zhou, L.J., Rao, R., Corcoran, E., Kelly, D., 2016. Distribution of radionuclides between atmosphere and ash during combustion of contaminated vegetation. J Environ Radioact 165, 159–167. https://doi.org/10.1016/j.jenvrad.2016.09.017

Zhu, Y.-G., Huang, Y.-Z., Hu, Y., Liu, Y.-X., 2003. Iodine uptake by spinach (Spinacia oleracea L.) plants grown in solution culture: effects of iodine species and solution concentrations. Environ Int 29, 33–37. https://doi.org/10.1016/S0160-4120(02)00129-0